



City Research Online

City, University of London Institutional Repository

Citation: AL-Azawi, Z. M. (1990). The response of reinforced concrete slabs to hard missile impact. (Unpublished Doctoral thesis, City University London)

This is the accepted version of the paper.

This version of the publication may differ from the final published version.

Permanent repository link: <https://openaccess.city.ac.uk/id/eprint/8296/>

Link to published version:

Copyright: City Research Online aims to make research outputs of City, University of London available to a wider audience. Copyright and Moral Rights remain with the author(s) and/or copyright holders. URLs from City Research Online may be freely distributed and linked to.

Reuse: Copies of full items can be used for personal research or study, educational, or not-for-profit purposes without prior permission or charge. Provided that the authors, title and full bibliographic details are credited, a hyperlink and/or URL is given for the original metadata page and the content is not changed in any way.

*THE RESPONSE OF REINFORCED CONCRETE SLABS
TO HARD MISSILE IMPACT*

by

Z.M. AL-AZAWI

B.Sc., M.Sc. Civil Engineering

Thesis presented for the Degree of
Doctor of Philosophy in the
Faculty of Engineering

Department of Civil Engineering
The City University (U.K.)

January, 1990

SUMMARY

Impact loads result when a structure is hit by a missile. The two major considerations in designing for impact are the limitation of local damage and the control of the overall response of the target structural element. Local damage may include penetration, perforation, scabbing and/or punching shear in the region of the impact on the structure. Overall response includes flexure and reaction shear in the structure.

Since the analytical prediction of local damage effects is extremely difficult, damage formulae have been developed on an empirical basis. These formulae depend on many parameters which may be classified into two groups, either missile parameters or target parameters. Two of the target parameters, the amount of reinforcing steel and maximum size of aggregate are not considered in the existing empirical formulae to determine critical perforation and scabbing velocities. The principle aim of the research reported in this thesis is, therefore, to find a term accounting for the level of reinforcement to be included in the formulae and to establish the influence of the maximum size of aggregate on the value of missile impact velocity causing scabbing or perforation.

The research undertaken involved an experimental programme of sixty-four individual tests. The tests were concerned with the influence of the two parameters previously mentioned upon the perforation and scabbing of model, steel reinforced concrete targets. The test rig was especially designed using high pressure compressed air to accelerate a steel missile

along a barrel to impact upon the target. This system can produce a variety of impact forces by either varying the applied pressure or the mass of the missile.

Chapter One discusses the local effects and the overall dynamic response caused by high velocity impact upon reinforced concrete targets. The evaluation of the yield-line method of analysis for design to resist high velocity impact is mentioned. The objectives and scope of the proposed research are also discussed. Chapter Two contains a literature review on procedures for determining local missile effects. The chapter considers and compares the existing empirical formulae. Also mentioned in Chapter Two are the experimental investigations into the effects of reinforcement and the associated model similarity requirements for impact conditions. The design and construction of a high velocity impact testing facility and the instrumentation associated with the facility are described in Chapter Three. Chapter Four discusses the fabrication of specimens and the test procedure. An account of the results obtained from the experimental programme is given in Chapter Five and Chapter Six discusses the development and application of the new perforation and scabbing formulae. Empirical formulae have been proposed to account for the amount of reinforcement. A general discussion of the results and the conclusions drawn from the experimental results and some recommendations for future research work are given in Chapter Seven and Eight respectively.

ACKNOWLEDGEMENTS

The author wishes to thank his supervisor, Dr L.F. Boswell, for his assistance during the experimental work and for his guidance in the preparation of this thesis.

The author also wishes to acknowledge the support of the technical staff in the Department of Civil Engineering, in particular, Mr J. Rose, Mr J. Fenton, Mr P. Mennell, Mr A. Bonomini, Mr V. Bullemor, Mr L. Ansdell and Mr R. Counsell, who helped in this project with advice and practical assistance. Appreciation is also given to Mr G. Kupferblum, Department of Mechanical Engineering who assisted during the design of the missile launcher.

Miss V. Mauree is commended for her careful and patient typing of this thesis.

Finally, and most importantly, I am indebted to Iraqi Government for their financial support, and to my wife for her continuous encouragement and assistance throughout the period of this research work.

CONTENTS

	<u>PAGE</u>
SUMMARY	i
ACKNOWLEDGEMENTS	iii
CONTENTS	iv
NOTATIONS	vii
LIST OF FIGURES	ix
LIST OF TABLES	xi
LIST OF PLATES	xiii
CHAPTER 1 INTRODUCTION	
1.1 General Introduction	1
1.2 The Objectives of the Proposed Research Programme	2
1.3 Scope of Research	5
1.4 Arrangement of Thesis	6
CHAPTER 2 LITERATURE REVIEW	
2.1 General Introduction	9
2.2 Review of Commonly Used Procedures for Determining Local Missile Effects	10
2.3 A Review of Formulae for the Prediction of Local Concrete Damage	12
2.3.1 Modified Petry Formula	16
2.3.2 Army Corps of Engineers Formula ..	17
2.3.3 Modified National Defence Research Committee Formula	20
2.3.4 Ammann and Whitney Formula	23
2.3.5 The Ballistic Research Laboratory Formula	24
2.3.6 Bechtel Corporation Formula	25
2.3.7 Stone and Webster Corporation Formula	28
2.3.8 Commissariat a L'Energie Atomique- Electricite de France Formula	28
2.3.9 Kar Formula	32
2.3.10 Degen Formula	36
2.3.11 Chang Formula	37
2.3.12 Haldar and Miller Formula	39
2.3.13 Hughes Formula	42
2.3.14 Adeli and Amin Formula	45
2.4 Comparison of Impact Formulae	47
2.4.1 Comparison of Penetration Formulae	47
2.4.2 Comparison of Scabbing Formulae ..	53
2.4.3 Comparison of Perforation Formulae	57
2.4.4 Comments on the Performance of Previous Work	61
2.5 Previous Experimental Investigations into the Effect of Reinforcement Quantity for Rigid Missile Impact	62

2.6	Similarity and Scaling Relationships for Impact Conditions	67
CHAPTER 3	THE DESIGN, CONSTRUCTION AND OPERATION OF THE HIGH VELOCITY IMPACT APPARATUS AND ASSOCIATED INSTRUMENTATION	
3.1	Introduction	71
3.2	The High Velocity Impact Facility	71
3.3	Instrumentation	74
3.3.1	Missile Impact Velocity Measurement	74
3.3.2	Slab Reaction Load Cells	78
3.3.3	Linear Variable Differential Transformer	79
3.3.4	High Speed Camera	79
CHAPTER 4	THE FABRICATION OF THE TARGET SPECIMENS AND THE EXPERIMENTAL PROCEDURE	
4.1	Introduction	89
4.2	The Test Specimens	89
4.2.1	Model Slab	89
4.2.2	Model Materials	90
4.2.2.1	Reinforcement	90
4.2.2.2	Model Concrete	93
4.2.3	Experimental Programme	93
4.3	Specimen Fabrication	96
4.3.1	Reinforcement Cages	96
4.3.2	Micro-Concrete Mix	99
4.3.3	Concrete Casting and Curing of Specimens	99
4.3.4	Concrete Control Specimens	101
4.4	Test Procedure	102
CHAPTER 5	EXPERIMENTAL RESULTS	
5.1	Introduction	107
5.2	The Perforation Resistance of the Model Concrete Slabs	107
5.2.1	Critical Perforation Velocity	107
5.2.2	The Measurement of Transient Load at the Critical Perforation Velocity	109
5.2.3	The Transient Target Displacement at the Critical Perforation Velocity	109
5.2.4	General Panel Damage Caused by the Missile at the Perforation Velocity	109
5.3	The Scabbing Resistance of the Model Concrete Slabs	134
5.3.1	Critical Scabbing Velocity	134
5.3.2	The Measurement of Transient Load at the Critical Scabbing Velocity	134
5.3.3	The Transient Target Displacement at the Critical Scabbing Velocity	135
5.3.4	General Panel Damage Caused by the Missile at the Scabbing Velocity	135

CHAPTER 6	DEVELOPMENT AND APPLICATION OF NEW AND EXISTING FORMULAE FOR THE DETERMINATION OF CRITICAL PERFORATION AND SCABBING VELOCITIES	
6.1	Introduction	155
6.2	The Development and Application of the Proposed New Perforation Formula	156
6.2.1	Evaluation of Existing Empirical Formulae to Predict Critical Perforation Velocity	163
6.3.	The Development and Application of the Proposed New Scabbing Formula	183
6.3.1	Evaluation of Existing Empirical Formulae to Predict Critical Scabbing Velocity	194
CHAPTER 7	DISCUSSION	
7.1	Perforation and Scabbing Resistance of the Target	216
7.2	Procedures Used for Determining the New Formulae	217
7.3	Limitations of the Proposed Perforation and Scabbing Formulae	217
7.4	The Mechanisms of Scabbing and Perforation Damage Caused by the Missile Impact	218
7.5	Comments on the Transient Displacement and Reaction Load Measurements	220
CHAPTER 8	CONCLUSIONS AND RECOMMENDATIONS FOR FUTURE WORK	
8.1	Conclusions	224
8.2	Recommendations for Future Work	228
REFERENCE	230
APPENDIX A	239
APPENDIX B	247

NOTATION

a	Half size of the concrete aggregate.
A_p	Weight of the missile per unit projected area.
C	Coefficient used in the Stone and Webster Corporation formula for scabbing thickness.
c_1, c_2, c_3, c_4, c_5	Constants in equation (6.2)
d	Target thickness.
d_p	Perforation target thickness.
d_s	Scabbing target thickness.
D	Diameter of the missile.
D_1	Outside diameter of the missile in the case of a hollow circular section.
e, e_2, e_3, e_4, e_5	Constants in equation (6.12).
E	Modulus of elastisity of material of the missile.
E_c	Concrete strain modulus.
E_m	Modulus of elastisity of mild steel.
f'_c	Concrete compressive strength.
fr	Concrete tensile strength (modulus of rupture).
I	Impact factor (dimensionless parameter) proposed by Haldar & Miller = $\frac{(12)k.W.V^2}{(32.2)D^3.f'_c}$.
I'	Impact factor (dimension parameter) proposed by Hughes = $\frac{M.V^2}{fr.D^3}$.
K	Missile nose shape factor.
K'	Missile nose shape factor used in Hughes formula.
K_1	Concrete penetrability factor = $\frac{180}{\sqrt{f'_c}}$.
K_p	Penetration coefficient used in modified Petry formula.
M	Mass of the missile.
m_c	Mass of concrete ejected by the impact.
r	Flexural reinforcement ratio (ratio between bending steel mass and concrete volume).
r_1	The bending reinforcement quantity in % each way, each face.
S	Strain rate factor.
t	Missile wall thickness.
V	Velocity of the missile.
V_{cp}	Critical perforation velocity of the missile.
V_{cs}	Critical scabbing velocity of the missile.
V_f	Formula velocity of the missile.
V_i	Incident velocity of the missile.
V_r	Exit velocity of the missile.

V_t	Test velocity of the missile.
W	Weight of the missile.
X	Observed penetration depth.
X_p	Calculated penetration depth.
σ_c	Concrete compressive strength (Pa).
ρ	Density of concrete.

LIST OF FIGURES

<u>FIGURE</u>		<u>PAGE</u>
1.1	Shear-failure Due to Hard Missile Impact on Reinforced Concrete Target	4
2.1	Missile Impact Phenomena	14
2.2	Values of Penetration Coefficient (K_p) for Reinforced Concrete	18
2.3	Coefficient "C" for Scabbing Thickness	29
2.4	Shape Effects of Solid Projectiles with Closed Ends	35
2.5	Different Diameters of Projectiles	35
2.6	Test "CEA-EDF" Formula Comparison	65
2.7	Test "CEA-EDF" Formula Comparison	65
2.8	The Variations of Critical Perforation Velocity for Hard Missile Impacted Upon Reinforced Concrete Target	66
3.1	Schematic Diagram of Missile Launcher	73
3.2	The Missile Launcher	76
3.3	Electric Circuitry for Missile Impact Velocity Measurement	81
3.4	Strain Gauge Arrangements on Load Cells	83
4.1	The Model Slab Dimensions	91
4.2	Stress-Strain Characteristics of Wire Reinforcement	92
4.3	Sieve Analysis of River Gravel Sand and Aggregate Grading for Microconcrete	94
5.1(a)-(k)	Measured Transient Load at Critical Perforation Velocity	112-117
5.2(a)-(k)	Transient Displacement of Target at Four Different Positions from the Center	119-129
5.3(a)-(j)	Measured Transient Load at Critical Scabbing Velocity	137-141
5.4(a)-(j)	Transient Displacement of Target at Four Different Positions from the Center	143-152
6.1	Comparison of the Test and Proposed Perforation Velocity	162
6.2(a)-(j)	Test Velocity/Formula Velocity Ratios (perforation resistance)	168-177
6.3	Comparison of the Test and Predicted Perforation Velocity (modified Petry formula)	179
6.4	Comparison of the Test and Predicted Perforation Velocity (CED-EDF formula)	181
6.5	Comparison of the Test and Predicted Perforation Velocity (Chang formula)	184
6.6	Comparison of the Test and Predicted Perforation Velocity (Halдар & Miller formula)	186
6.7	Comparison of the Test and Predicted Perforation Velocity (Adeli & Amin formula)	188

6.8	Comparison of the Test and Proposed Scabbing Velocity	196
6.9(a)-(j)	Test Velocity/Formula Velocity Ratios (scabbing resistance)	202-211
6.10	Comparison of the Test and Predicted Scabbing Velocity (Chang formula)	212
6.11	Comparison of the Test and Predicted Scabbing Velocity (Halдар & Miller formula)	214

LIST OF TABLES

<u>TABLE</u>		<u>PAGE</u>
2.1	A Summary of Concrete Penetration Formula	49
2.2	A Summary of Scabbing Formulae	54
2.3	A Summary of Perforation Formulae	58
2.4	Scaling Relationships Associated with Impact Studies	70
4.1	Details of Experimental Programme	95
5.1	The Results for Perforation Resistance Tests ...	111
5.2	The Maximum Reaction Loads of the Targets at Critical Perforation Velocity	118
5.3	The Maximum Transient Deflection at Critical Perforation Velocity	130
5.4	The Results for Scabbing Resistance Tests	136
5.5	The Maximum Reaction Loads of the Targets at Critical Scabbing Velocity	142
5.6	The Maximum Transient Deflection at Critical Scabbing Velocity	153
6.1	Experimental Test Results (perforation resistance)	157
6.2	Comparison of Test and Proposed Formula Velocities (perforation resistance)	161
6.3	Comparison of Experimental Results with the Proposed Formula Predictions (perforation resistance)	164
6.4	Measured and Calculated Critical Perforation Velocities	166
6.5	Test Velocity/Formula Velocity Ratios (perforation resistance)	167
6.6	Comparison of Experimental Results with the Corrected Modified Petry Formula (perforation resistance)	180
6.7	Comparison of Experimental Results with the Corrected "CEA-EDF" Formula (perforation resistance)	182
6.8	Comparison of Experimental Results with the Corrected Chang Formula (perforation resistance)	185
6.9	Comparison of Experimental Results with Corrected Haldar & Miller Formula (perforation resistance)	187
6.10	Comparison of Experimental Results with Corrected Adeli & Amin Formula (perforation resistance)	189
6.11	Experimental Test Results (scabbing resistance)	190
6.12	Comparison of Test and Proposed Formula velocities (scabbing resistance)	195
6.13	Comparison of Experimental Results with the Proposed Formula Predictions (scabbing resistance)	197
6.14	Measured and Calculated Critical Scabbing Velocities	200
6.15	Test Velocity/Formula Velocity Ratios (scabbing resistance)	201

6.16	Comparison of Experimental Results with Corrected Chang Formula (scabbing resistance)	213
6.17	Comparison of Experimental Results with Corrected Haldar & Miller Formula (scabbing resistance)	215

LIST OF PLATES

<u>PLATE</u>		<u>PAGE</u>
3.1	The Missiles Showing the Air Seals	75
3.2	The Testing Frame	77
3.3	Measuring Device for Determination of Missile Velocity	80
3.4	The Load Cell	82
3.5	The Recording System Used Throughout the Experiments	84
3.6	Arrangement and Method of Fixing of LVDT's to the Test Frame	85
3.7	High Speed Camera	87
3.8	Film Analysis System	88
4.1	Specimen Manufacture Showing Welding of the Mesh	97
4.2	Reinforcement Showing the Edge Beams	98
4.3	Reinforcement and Mould Prior to Casting	100
4.4	Wooden Form for Casting Slabs	100
4.5	Compression Testing Machine	103
4.6	Indirect Testing of Concrete for Determination of Tensile Splitting Strength	104
4.7	Arrangement of the Load Cells	105
5.1	Front Face Damage of Target (Perforation)	131
5.2	Rear Face Damage of Target (Perforation)	132
5.3	Rear Face Damage of Plain Concrete Target (Perforation)	133
5.4	Rear Face Damage of Target (Scabbing)	154

CHAPTER ONE

INTRODUCTION

1.1 General Introduction

Nuclear power plants and many other structures need protection against impact from sources such as missiles and aircraft. A missile impact results in both local wall damage and overall dynamic response of the target wall and supporting structure. The response of the structure depends on the material properties of both the impacting object and the structure. The weight, size and velocity of the impacting object also effect response.

The characteristics of the impacted loads which control the overall response of the target are governed by the absorption of kinetic energy from the missile at acceptable target deflections. These loads are limited, however, by the yield, buckling, crushing or local destruction of the impacting object. The overall dynamic response of the target consists of shear and flexural deformations. A potential flexural or shear failure of the target will occur if the strain energy capacity of the wall and the supports is smaller than that part of the kinetic energy which has been transmitted from the zone of penetration or perforation into the wall.

Local damage consists of spalling of concrete from the impacted area and scabbing of concrete from the back face of the target. If the kinetic energy of the missile is sufficient the missile may perforate the wall. The local effects depend largely on the relative properties of the missile and the impacted object. For concrete barriers, local damage in the form of scabbing and penetration into or

perforation of the barrier are generally characteristic of impact by a hard missile. Soft missile impact rarely causes penetration or perforation except at extremely high and unlikely velocities. They may, however, cause backface cracking and scabbing. The effects of impact of a flexible missile such as an aircraft are intermediate between those caused by hard and soft missiles.

Conventionally, a yield-line analysis is made to evaluate the possibility of a flexural failure caused by a concentrated load. Tests have shown, however, that before yield-lines can occur under a dynamic loading condition there will be scabbing of concrete from the rear surface of the barrier. This is true for both uniform and concentrated loads and brings into question the applicability of the yield-line method of analysis for design against missile impact when the ductility ratio of the steel is small (15). The ductility ratio is normally defined as the ratio of displacement under load to the displacement when the steel first reaches its yield stress (17). Thus, the yield-line theory may not provide a suitable basis for assessing the behaviour of the structure when the ductility ratio is small.

In recognition of the complex nature of hard missile impact upon reinforced concrete, empirical formulae have been developed to determine the local effects of missiles on targets or barriers.

1.2 The objectives of The Proposed Research Programme

Due to the complex physical process associated with missile impact, local effects are evaluated primarily by application

of empirical relationships which are based on missile impact test results. All of these relationships, which were basically developed empirically or semi-empirically for concrete impact problems, are restricted in their range of application.

The local effect may be classified into perforation, penetration and scabbing or spalling or both depending on many parameters. These parameters can be classified into two groups. Firstly, those associated with the missile such as the weight, size, velocity, nose shape, deformability and inclination of the missile with respect to the target surface. Secondly, parameters associated with the target such as thickness, concrete compressive strength, amount of reinforcing steel and size of aggregate. Only the target thickness and concrete compressive strength have been included in the empirical formulae reported in the literature. The effects of the amount of reinforcing steel and the aggregate size have not been previously considered. This is probably due in part to the fact that most of the investigated targets were under-reinforced (0.3% - 1% each way) with respect to the applied dynamic loading. These values represent the percentage of the cross-sectional area of reinforcement divided by the cross-sectional area of the concrete. It was considered, therefore, that specific tests should be carried out to determine the effects of varying the amount of reinforcement and aggregate size upon the critical perforation and scabbing velocities. The critical perforation velocity is defined as the velocity necessary to just cause perforation. The critical scabbing velocity is defined as the velocity necessary to just cause scabbing of

concrete from the back face of the concrete target.

Experimental and numerical investigations by Süper on thick plate impact, which have been reported by Eibl (1) show that when the first diagonal crack occurs fig. (1.1), a very high proportion of the initial kinetic energy of the missile is transferred from the concrete to the reinforcing steel (both stirrups and longitudinal reinforcement). This is a significant mechanism of energy absorption and demonstrates the importance of the amount of reinforcing steel upon impact effects. The amount of reinforcing steel seems to have a considerable influence on the perforation of concrete walls (7).

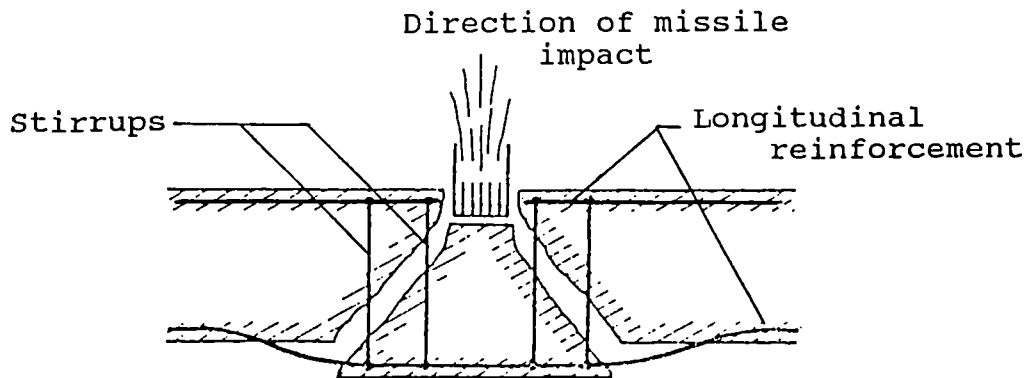


FIG. (1.1)

SHEAR-FAILURE DUE TO HARD MISSILE IMPACT
ON REINFORCED CONCRETE TARGET AFTER EIBL (1)

A review of the literature indicates that further experiments are needed to be conducted with high amounts of reinforcement (1% - 3% each way) ref.(7). Also, since the effect of different sizes of aggregate has not been investigated these should also be included in a further investigation. The effect of these parameters upon scabbing and perforation can then be evaluated. It is to be expected that the application of the existing empirical formulae to predict local effects for heavily reinforced targets would give an overestimate of these effects.

The principal objectives of the proposed experimental programme were to determine the influence of the amount of reinforcing steel in a reinforced concrete slab specimen as well as determining the influence of the maximum size of aggregate in the concrete.

1.3 Scope of Research

i) The research undertaken consisted of an experimental programme. The experiments were concerned with determining the influence of high amounts of reinforcement and the maximum aggregate size of concrete upon the perforation and scabbing of model steel reinforced concrete targets. The targets were of dimensions 1150 mm × 1150 mm square and 150 mm thick with a circular part having a constant thickness which varied between specimens and has the value of 120 mm, 100 mm or 80 mm. The targets were subjected to impact at the center point of the circular part of the target. The impact load was produced by a very hard steel missile of 49.8 mm diameter with a variable length depending on the mass required. The magnitudes of the masses used were, 3.69 kg, 3.2 kg, 2.7 kg and 2.2 kg and these travelled at different velocities ranging from 37 m/sec. to 118 m/sec. The test rig was specially designed and constructed to produce a high velocity impact load using compressed air acting on the hard missile and accelerating it inside a long barrel fig. (3.2).

A total of 64 slabs were tested with fully fixed supports, 30 slabs were tested to study the scabbing

resistance and 34 slabs tested to study perforation resistance. The percentage of the flexural steel reinforcement has been varied between 0% and 1.55% each way each face and the maximum aggregate size used in the manufacture of the concrete was either 4 mm or 2 mm. In all cases three targets of identical construction were tested each time for each of the chosen independent test variables i.e. weight of the missile, circular slab thickness, amount of steel and aggregate size. The impact velocity was adjusted in successive shots to approach the critical value which can cause either just scabbing or just perforation. The details of the experimental programme are shown in table (4.1).

- ii) It was intended to develop new empirical relationships from the results of the experimental programme to determine the scabbing and perforation velocities of a hard missile impact acting upon reinforced concrete model slabs.
- iii) Comparisons between the measured and calculated critical scabbing and critical perforation velocities using the existing empirical formulae were to be made.
- iv) An attempt was made to improve existing formulae by including factors which account for variations in the level of reinforcement and the size of aggregate.

1.4 Arrangement of Thesis

Chapter 1 provides an introduction to the subject matter contained within the thesis.

The literature survey which is carried out in Chapter 2

covers the following aspects:

- i - A review of commonly used procedures for determining local missile effects.
- ii - A study of available formulae for local concrete damage prediction.
- iii - A comparison of the available formulae.
- iv - A study of available experimental investigations into the effects of reinforcement and
- v - A study of similarity and scaling relationships for impact conditions.

Chapter 3 describes the design and construction of high velocity impact testing facility. The instrumentation associated with the test facility are also described. Chapter 4 discusses the fabrication of the specimens and test procedure.

During each impact test the critical missile velocity for scabbing or perforation, the reaction-time histories and the dynamic transient deflections at four points on the slab were measured. The velocity of the ejected concrete during the impact was also obtained from the use of high speed filming. The experimental results for all the test series are presented in Chapter 5.

Chapter 6 discusses the development and application of the new perforation and scabbing formula. Empirical relationships have been proposed to determine the critical perforation and the critical scabbing velocity of hard

missile impacted upon concrete targets. Modification factors have been proposed to account for the amount of reinforcement.

Finally, Chapter 7 and Chapter 8 discusses the result, and considers the conclusions that may be deduced from the research work presented and suggests recommendations for further work.

CHAPTER TWO

LITERATURE REVIEW

2.1 General Introduction

To design a concrete structure to resist impact loading it is necessary to limit the extent of local damage and to determine the overall response of the associated structural element. Local damage around the impacted area may include penetration, perforation, scabbing or punching shear. Sometimes a combination of these effects may occur. Overall response includes shear and flexural effects.

The analytical prediction of local damage effects is extremely difficult and is due to the complex nature of the transient stress state and the reinforced concrete target. Damage criteria have been developed on an empirical basis by correlating and evaluating available data obtained from small scale tests. These empirical formulae are considered valid for small missiles with limited deformation upon impact. For such missiles satisfaction of specified perforation criteria automatically implies satisfaction of criteria for punching shear. Large deformable missiles such as automobiles do not penetrate the target structure and the previously mentioned empirical formulae do not apply.

The prediction of overall response is generally based on an energy momentum relationship or on a derivation of an impact forcing function which is dependent upon the type of missile and target involved. The prediction of overall response however, is outside the scope of the research project described in this thesis.

2.2 Review of Commonly Used Procedures for Determining Local Missile Effects

Several techniques with various degrees of complexity are available to study the local effects due to impact loading upon concrete structures. To study these effects it is necessary to know the damage criteria as well as the damage prediction equations which correlate the impact load and the structural strength. The impact mechanism is very complicated and cannot be easily determined mathematically. Therefore, an empirical or approximate solution is necessary. The design criterion for preventing concrete structures from experiencing unacceptable local effects is generally expressed in terms of the structure thickness to prevent backface scabbing and/or perforation. The penetration depth estimation may or may not be directly involved in this type of study. Conceptually, an empirical or approximate solution to estimate backface scabbing or perforation depth could be developed in the following three ways (2,3):

- (i) The penetration depth may be estimated for the known missile properties disregarding the target thickness. The penetration depth thus obtained can then be correlated with the target scabbing or perforation thickness.
- (ii) The scabbing or perforation thickness may be empirically correlated with the missile properties provided reliable and sufficient experimental results are available.

(iii) A semi-analytical relationship between scabbing and/or perforation thickness and the missile properties may be developed. This semi-analytical formulation may then be modified using reliable test data.

The Modified Petry formula (4,5), Army Corps of Engineers formula "ACE" (4,5), Modified National Defence Research Committee formula "NDRC" (6), Ammann and Whitney formula (4,5), Kar formula (7), Degen formula (19), Haldar and Miller formula (2, 22, 3, 21) and the new quadratic formula proposed by Adeli and Amin (5) are based on the first concept described above.

The Ballistic Research Laboratory formula "BRL" (4,5), the Bechtel formula (9), Stone and Webster formula (10) and the Commissariat al Energie Atomique - Electricite de France formula "CEA-EDF" (11) are based on the second concept.

The Chang (20) and Hughes formulae (24) are based on the third concept.

2.3 A Review of Formulae for The Prediction of Local Concrete Damage

Local effects can be defined as occurring in the vicinity of the missile impact. These local effects might be the ejection of concrete pieces from the impacted face, ejection of concrete from the rear face or the missile passing through the target thickness. A discussion of terms and symbols which are used in the local damage prediction formulae now follows:

- (i) Penetration is the depth to which a projectile enters a concrete target without passing through. The concrete is assumed not scab on the back face and thus the penetration depth is independent of the thickness of the target. The observed penetration depth is defined by the term, X and the calculated penetration depth by X_p .
- (ii) Scabbing consists of the ejection of pieces of concrete from the back of the slab opposite to the impacted area thus leaving a back crater after impact. The scabbing thickness is the minimum thickness to prevent scabbing and is defined by d_s .
- (iii) Spalling is the ejection of pieces of concrete from the front face region surrounding the area of impact thus leaving a crater.

(iv) Perforation is the depth required by the projectile to pass just through the slab. The exit velocity of the projectile after it passes through the slab is, therefore, zero. The perforation thickness is defined by the term d_p .

Figure (2.1) shows schematically the type of local effects caused by impacting missiles

X = observed penetration depth.

X_p = calculated penetration depth.

d_s = scabbing thickness which is the target thickness just enough to prevent scabbing and

d_p = perforation thickness which is the target thickness just enough to prevent perforation.

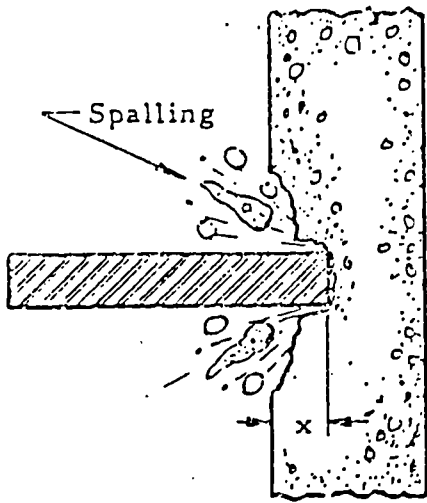
The parameters which influence local effects may be divided into missile and target parameters and are listed as follows:

a) Missile Parameters

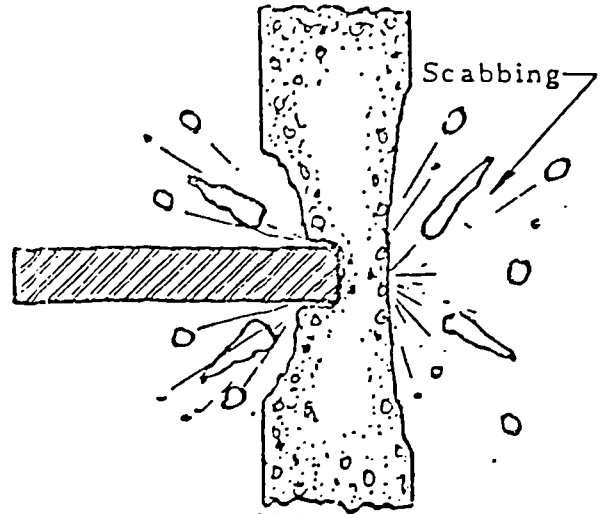
- weight of the missile, W
- size of the missile, e.g. the diameter if it is cylindrical, D
- velocity of the missile, V
- nose shape of the missile, K
- deformability of the missile
- inclination of missile with respect to the target surface.

b) Target Parameters

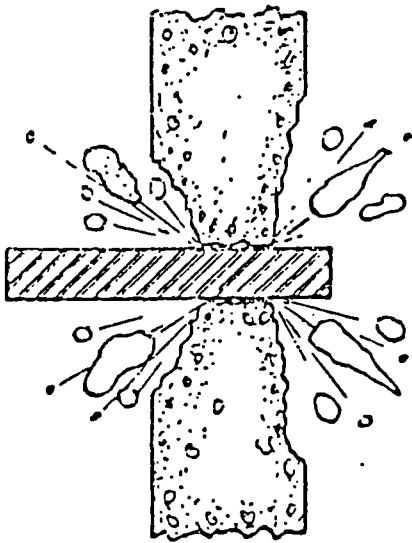
- target thickness, d
- concrete strength (compressive f_c' or tensile f_r)
- size of aggregate
- amount of reinforcing steel.



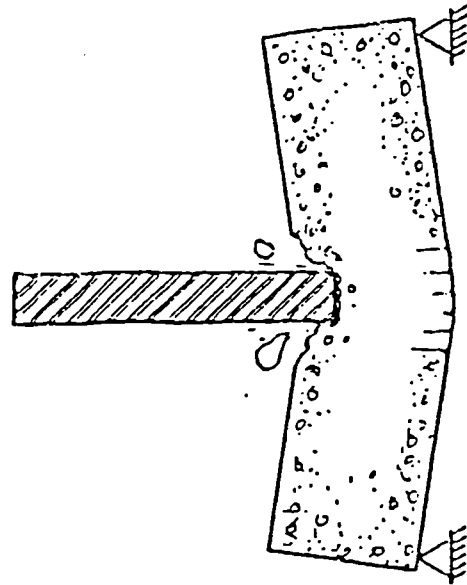
a) Missile Penetration and Spalling



b) Target Scabbing



c) Perforation



d) Overall Target Response

FIG. (2.1)

MISSILE IMPACT PHENOMENA

The impacting missile can be classified as either hard or soft depending upon whether the deformation of the missile is small or large relative to the target deformation. The missile is considered to be hard when it is so stiff that its deformation is small when compared with that of the target. Soft missiles are those with a moderate or large amount of deformation compared with the target deformation.

Until 1975 local missile impact effects for hard missiles on concrete targets had been determined using empirical formulae (some of which possess a partial theoretical basis). These formulae were based upon experimental results obtained prior to 1946 for concrete slabs that were perforated by projectiles and bombs to define the penetration depth and the perforation and scabbing thicknesses.

The most commonly used formulae were the Modified Petry formula (4,5), the Army Corps of Engineers formula (4,5), the Modified National Defence Research Committee formula (6), the Ammann and Whitney formula (4,5) and the Ballistic Research Laboratory formula (4,5). These formulae, however, are based upon limited test data. In nearly all of the tests the striking missile was an essentially non-deformable projectile or bomb often made of armour-piercing steel, whilst the target was a massive non-deformable concrete target. These formulae, therefore, are applicable only to this conditions and should not be applied elsewhere.

The empirical formulae are applicable to missile impact normal to the target. The angle of strike has a substantial influence on penetration depth (6), particularly for angles

greater than 20° from the normal.

The formulae are based upon limited parameter variation. Until 1979, the parametric range of available test data was limited to:

$$d/D \geq 3$$

$$D \leq 16 \text{ in} \quad (1 \text{ in} = 25.4 \text{ mm})$$

$$0.2 \text{ lb/in}^3 \leq W/D^3 \leq 0.8 \text{ lb/in}^3 \quad (1 \text{ lb/in}^3 = 0.02768 \text{ kg/m}^3)$$

$$500 \text{ ft/sec.} \leq V \leq 3000 \text{ ft/sec.} \quad (1 \text{ ft/sec.} = 0.3048 \text{ m/sec.})$$

$$3 \leq \frac{d_s}{D} \leq 18$$

$$3 \leq \frac{d_p}{D} \leq 18$$

Some of these formulae, however, are based upon a narrower range of test parameters than those quoted (4).

2.3.1 Modified Petry Formula

According to Kennedy (4,5), the modified Petry formula was originally developed in 1910 and predicts the penetration depth as follows:

$$X_p = 12 K_p A_p \log_{10} \left(1 + \frac{v^2}{215000} \right) \quad (2.1)$$

where K_p is a coefficient which is dependent upon the reinforcing details. The coefficient has the value of 0.00799 for massive concrete, 0.00426 for normal reinforced concrete and 0.00284 for specially reinforced concrete. The coefficient has been modified to account for the effect of concrete strength by Amirkian (4,5). The modified value of

K_p is a function of concrete strength f'_c , figure (2.2).

There are two versions of the modified Petry formula, the modified Petry 1 formula which uses the original value of K_p whilst the modified Petry 2 formula use the values given in Figure (2.2). For both formula the weight

A_p = the weight of missile per unit projected area (lb/ft²) and

V = the velocity of missile (ft/sec.).

Amirkan (4,5) has suggested that the perforation thickness will be determined by:

$$d_p = 2 X_p \quad (2.2)$$

and the scabbing thickness by:

$$d_s = 2.2 X_p \quad (2.3)$$

2.3.2 Army Corps of Engineers Formula

In 1946 the Army Corps of Engineers (4,5) developed the following formula for the calculation of missile penetration

$$\frac{X_p}{D} = \frac{282 W V^{1.5}}{D^{2.785} f'_c{}^{0.5} 1000^{1.5}} + 0.5 \quad (2.4)$$

where X_p and D are expressed in inches, W is expressed in lbs, V is expressed in ft/sec. and f'_c is expressed in psi.

Equation (2.4) has been commonly referred to as the Army Corps of Engineers - ACE - formula and this equation is based exclusively upon a statistical fitting of the

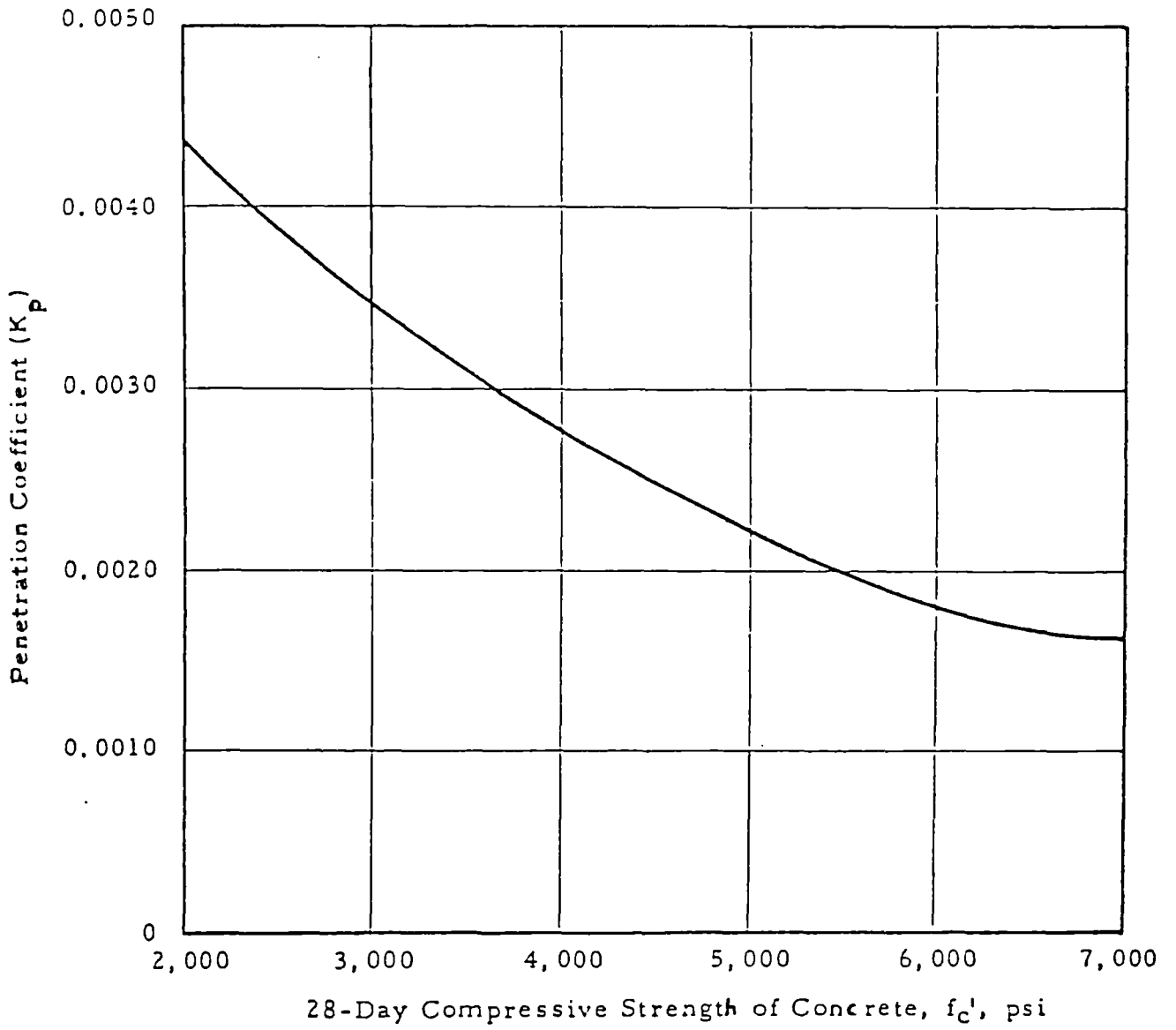


FIG. (2.2)

VALUES OF PENETRATION COEFFICIENT (K_p) FOR
REINFORCED CONCRETE

experimental data. It has been found (4) that when this formula is extrapolated beyond the previously defined range of the test data it can lead to error.

In 1943 high velocity ballistic tests were carried out on 38, 76 and 155 mm steel cylindrical missiles and the following relationships for predicting scabbing and perforation thickness were obtained using regression analysis:

$$\frac{d_s}{D} = 2.12 + 1.36 \left(\frac{x_p}{D} \right) \quad 3 \leq \frac{d_s}{D} \leq 18 \quad (2.5)$$

$$0.65 \leq \frac{x_p}{D} \leq 11.75$$

$$\frac{d_p}{D} = 1.32 + 1.24 \left(\frac{x_p}{D} \right) \quad 3 \leq \frac{d_p}{D} \leq 18 \quad (2.6)$$

$$1.35 \leq \frac{x_p}{D} \leq 13.5$$

The equations (2.5) and (2.6) are commonly known as the Army Corps of Engineers formula for perforation and scabbing.

These relationships are applicable only within the penetration depth to projectile diameter ratios indicated. For ratios not within this limit, these equations will lead to increasingly conservative results (4).

Perforation tests were also reported in 1944 on 133 concrete slabs (6) for 0.5 calibre bullets, where the slab thickness was varied from 3 to 18 times the projectile diameter. The strength of concrete used in these tests varied from 1500 to 7000 pounds per square inch.

These more extensive tests yielded regression equations for perforation and scabbing thickness which differ only very

slightly (less than 10 percent) from equations (2.5) and (2.6).

It is considered that equations (2.5) and (2.6) are more appropriate for missile impact related to nuclear facilities (4) since large projectile diameters were used in the original tests.

2.3.3 Modified National Defence Research Committee Formula

In 1946 the National Defence Research Committee "NDRC" (6) proposed a theory of penetration for a non-deforming projectile penetrating a massive concrete target. This theory of penetration enables the calculation of the total depth of penetration, the impact force - time history and the penetration - depth time history. The NDRC theory propose the following formula:

$$\frac{X_p}{D} = \left[\frac{4 K \cdot K_1 \cdot W \cdot V^{1.8}}{D (1000 D)^{1.8}} \right]^{0.5} \quad \frac{X_p}{D} \leq 2.0 \quad (2.7)$$

$$\frac{X_p}{D} = 1 + \frac{K \cdot K_1 \cdot W \cdot V^{1.8}}{D (1000 D)^{1.8}} \quad \frac{X_p}{D} > 2.0 \quad (2.8)$$

where X_p and D are expressed in inches, W is expressed in lbs and V is expressed in ft/sec.

In these formulae K is a missile nose shape factor in which

- $K = 0.72$ for flat nosed bodies.
- $= 0.84$ for blunt nosed bodies.
- $= 1.0$ for average bullet nose (spherical end)
- $= 1.14$ for very sharp nose.

K_1 is a concrete penetrability factor which is a function of the concrete strength. Unfortunately, after 1946 there was a lack of interest in investigating projectile penetration of concrete and the NDRC effort was stopped without completely defining the factor K_1 . Until recently, therefore, the NDRC formula had not been used extensively for missile impact problems in the nuclear industry. According to reference (6) the factor K_1 should lie between 2 and 5 depending upon the concrete strength to fit the available test data. Kennedy (4) suggested in 1966 that the concrete penetrability factor K_1 is proportional to the reciprocal of the ultimate concrete tensile strength, which in turn was taken to be proportional to the square root of the ultimate concrete compressive strength f'_c (psi). This suggestion was based upon theoretical and experimental considerations.

The following relationship for K_1 was obtained by fitting this relationship to the experimental data available for the larger missile diameters

$$K_1 = \frac{180}{\sqrt{f'_c}} \quad . \quad (2.9)$$

The combination of equations (2.7), (2.8) and (2.9) is defined as the Modified NDRC formula for penetration.

The primary advantage of the Modified NDRC formula is that since it is based upon a theory of penetration, it can be extrapolated beyond the range of available test data with some confidence. A nondeformable cylindrical missile penetrating a massive reinforced concrete target would be the ideal condition for the application of the Modified NDRC

equations. Essentially, this formulation neglects the rear boundary effects, they cannot be used if scabbing develops on the rear side of the target or a moveable conical plug is formed during impact.

The concrete property that is explicitly included in the modified NDRC equations is the concrete compressive strength. The size of the aggregate and the amount of reinforcing steel are not considered. However, Slitter (7) commented that the effects of these parameters on the penetration depth may not be significant. The equations however can be used for normal reinforced concrete targets. For over - reinforced concrete structures, they would probably over predict the penetration depth. Also, these formulae were derived solely from impact data for missile velocities greater than 500 ft/sec.

From this discussion, it is clear that the NDRC equations are developed using the information on penetration depth for small diameter, light weight and high impact velocity projectiles. In general these equations give the upper bound estimate of the penetration depth for large missiles. This over prediction (sometimes by a factor of eight or nine) is particularly noticeable when $\left(\frac{x_p}{D}\right)$, the ratio of penetration depth to missile diameter is less than 0.6 (7). For slab thickness to projectile diameter ratio greater than 3, equations (2.7) and (2.8) can be used in conjunction with equations (2.5) and (2.6) for predicting the perforation and scabbing thicknesses (4). For many impact problems, however, the slab thickness to projectile diameter is substantially less than three.

Chelapati and Kennedy (8) have proposed parabolic curve fitting passing through the origin and having the same slope as equations (2.5) and (2.6). This parabolic fit for small penetration thickness to projectile diameter ratios leads to the following equations

$$\frac{d_p}{D} = 3.19\left(\frac{x_p}{D}\right) - 0.718\left(\frac{x_p}{D}\right)^2 \quad \begin{array}{l} \frac{x_p}{D} < 1.35 \\ \frac{d_p}{D} < 3 \end{array} \quad (2.10)$$

$$\frac{d_s}{D} = 7.91\left(\frac{x_p}{D}\right) - 5.06\left(\frac{x_p}{D}\right)^2 \quad \begin{array}{l} \frac{x_p}{D} < 0.65 \\ \frac{d_s}{D} < 3 \end{array} \quad (2.11)$$

The use of this modification together with equations (2.7), (2.8) and (2.9) is known as the modified NDRC formula for perforation and scabbing.

2.3.4 Ammann and Whitney Formula

The following formula has been developed to predict the penetration depth of small explosively generated fragments travelling over 1000 ft/sec. (4,5)

$$\frac{x_p}{D} = \frac{282 K W V^{1.8}}{D(f'_c)^{0.5} (1000D)^{1.8}} \quad (2.12)$$

where this formula is expressed in imperial units. This formula is not intended for use with the lower velocity missiles of primary interest to nuclear facilities (4).

2.3.5 The Ballistic Research Laboratory (BRL) Formula

The previously mentioned formula for the calculation of perforation and scabbing thickness relate the calculated thickness to the calculated penetration depth, X_p . The BRL formula directly predicts the perforation thickness for a concrete wall having an ultimate compressive strength of 3000 p.s.i (4,5) in the following way:

$$\frac{d_p}{D} = 7.8 \frac{W V^{1.33}}{D^{2.8} (1000)^{1.33}} \quad (2.13)$$

where d_p and D are expressed in inches, W is expressed in lbs and V is expressed in ft/sec. This equation has been extended for other values of the ultimate compressive strength in which it is assumed that the perforation thickness is inversely proportional to the square root of f'_c (p.s.i) as follows

$$\frac{d_p}{D} = \frac{427 W V^{1.33}}{D^{2.8} (f'_c)^{0.5} 1000^{1.33}} \quad (2.14)$$

This formula is known as the modified BRL formula for perforation.

It has been recommended that the scabbing thickness can be estimated from

$$d_s = 2 d_p \quad (2.15)$$

where d_p is defined by equations (2.13) or (2.14). This relationship is defined, herein, as the modified BRL formula for scabbing.

2.3.6 Bechtel Corporation Formula

Although relationships have been developed for predicting damage to reinforced concrete panels from non-deformable military type projectiles with velocities typically exceeding (1000 ft/sec.), these relationships have questionable validity in the velocity range of missiles postulated in nuclear power plant design (typically below 500 ft/sec.).

They are also considered inapplicable for the prediction of damage from softer (more deformable) missiles, such as steel pipes. Full-scale tests were, therefore, conducted by the Bechtel Corporation to obtain more applicable information on the damage capability of these postulated missiles (9). The first part of these tests involved impacting (6 in) and (9 in) thick reinforced concrete panels with (1 in) steel rod missiles weighing up to (8 lbs) and having impact velocities between 150 and 322 ft/sec. The test panels were 4 ft square simply supported on four edges with a free span of 3.875 ft. The second part of these tests involved impacting (12 in), (18 in) and (24 in) thick reinforced concrete panels with (8 in) nominal diameter steel pipes (schedule 40), wood poles and solid steel slugs weighing up to 215 lbs, and having impact velocities between 122 and 490 ft/sec. The test panels were 9 ft square, simply supported on four edges with a free span of 8 ft. The (8 in) missile tests revealed a significant variation of damage with respect to missile type. The wood poles produced no local damage (impact velocities between 300 and 490 ft/sec.) and only minor structural response. These missiles exhibited gross deformability with

2 ft to 4.5 ft of the length of the missile disintegrating upon impact.

The steel pipes penetrated deeper, but produced less spall damage than the steel slugs at comparable velocities. The pipe missiles also exhibited significant deformation (shortening) on impact which increased with missile velocity. The steel slugs (and rods) sustained little or no general permanent deformation.

The damage (penetration and scabbing) produced by the solid (1 in) rods was comparable to that of the (8 in) solid steel slugs.

The difference in local damage caused by the different missile types is primarily due to the difference in the combined effects of missile deformation and penetration, which determines the missile stopping time and the magnitude of the interface force developed between the missile and the target. A variation in the characteristics of the interface force-time function is also observed to be significant in determining the magnitude of the structural response. At comparable impact velocities missiles with the shorter stopping time (higher interface forces) produced more severe local damage and greater structural response.

Based upon these full-scale test results the Bechtel Corporation has developed an empirical formula for predicting the scabbing thickness of concrete targets struck by non-deformable solid steel slugs and rods and moderately hollow steel pipes as follows.

For solid steel missiles

$$d_s = 15.5 \frac{W^{0.4} V^{0.5}}{(f'_c)^{0.5} D^{0.2}} \quad (2.16)$$

For steel pipe missiles

$$d_s = 5.42 \frac{W^{0.4} V^{0.65}}{(f'_c)^{0.5} D^{0.2}} \quad (2.17)$$

where d_s and D are expressed in inches, W is expressed in lbs, V is expressed in ft/sec, and f'_c is expressed in p.s.i. The application of eq. (2.17) to steel pipe missiles automatically accounts for the influence of moderate missile deformability. This formula was specifically developed for (8 in) diameter (schedule 40) pipes, but it has also been compared with test results for (3 in) and (12 in) diameter (schedule 40) pipes (10) and has been found to be adequate for these cases. The formula does not account for a variation in pipe thickness to diameter ratio and is based upon results for (schedule 40) pipes only.

To ensure that scabbing will not occur, the design thickness of a reinforced concrete element must be greater than that determined by these equations.

An increase in thickness of 25% (which need not exceed 10 in) is recommended.

Insufficient data were acquired to establish or verify relationships for the threshold of perforation.

2.3.7 Stone and Webster Corporation Formula

Stone and Webster have developed an empirical formula for predicting the scabbing thickness of concrete targets struck by steel missiles with velocities typical of nuclear plant applications. The formula has been derived from the results of test conducted upon quarter scale specimens. This formula accounts for the influence of the wall thickness (t) to outside diameter (D) ratio and the deformability of hollow steel pipes missiles. The formula is given (10) as,

$$d_s = \left(\frac{W V^2}{C} \right)^{1/3} \quad (2.18)$$

where d_s and D are expressed in inches, W is expressed in lbs and V is expressed in ft/sec.

C is a coefficient defined by figure (2.3) for various $2t/D$ ratios, t is the missile wall thickness and D is the outside missile diameter. The range of test parameters for the application of this formula is

$$3000 \text{ psi} \leq f'_c \leq 4500 \text{ psi} \quad (\text{psi} = 6.89476 \text{ Kpa})$$

$$1.5 \leq \frac{d_s}{D} \leq 3.0$$

$$0.06 \leq \frac{2t}{D} \leq 1.0$$

$$75 \text{ ft/sec.} \leq V \leq 250 \text{ ft/sec.} \quad (\text{ft/sec.} = 0.3048 \text{ m/sec.})$$

The ratio $2t/D$ equal to unity corresponds to a solid steel missile.

2.3.8 Commissariat a L'Energie Atomique - Electricite de France (CEA - EDF) Formula

Since 1974 a large program has been undertaken in France to develop a method of computation to describe the behaviour of

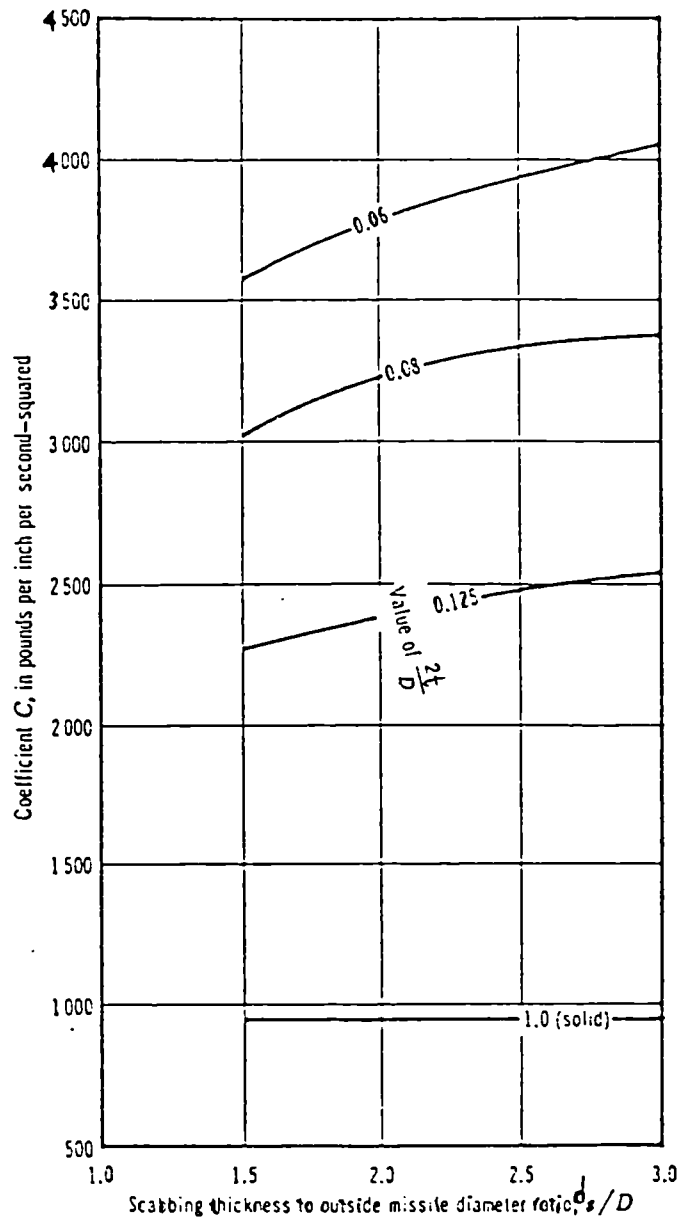


FIG. (2.3)

COEFFICIENT C FOR SCABBING THICKNESS

reinforced concrete walls subjected to rigid missile impacts. The program is now described briefly:

i) An initial series of tests have been performed on behalf of Electricite de France "EDF" and of the Experimental Center of Research on Building and Public work "CEBTP" at Saint - Remy - Les Chevreuse (11). Thirteen perforation tests of concrete slabs were conducted in this series with a missile striking at a speed of about (28.5 m/sec.) The missile consisted of a steel cylinder bolted to a cylindrical nose piece. Three such pieces were used during the testing and are described as follows,

- A nose of 110 mm diameter with a hemispherical end, total mass of the missile with nose 334 kg.
- A nose of 110 mm diameter with a nearly flat end, total mass of the missile with nose 343 kg.
- A nose of 155 mm diameter with a nearly flat end, total mass of the missile with nose 340 kg.

The missile was allowed to fall from a height of about 47 m and was guided by three 12 mm diameter rods, the concrete slabs were square (150 x 150 cm) and of variable thickness (17.5 - 40 cm). These slabs were reinforced in different ways and the total weight of reinforcement steel per cubic meter varied from (108 to 346 kg) with a concrete strength of 38 N/mm².

These tests represented a preliminary study in which a quick, qualitative indication of the form of the failure and perforation was required. It should be

noted, however, that during these tests the velocity of the missile was relatively low. It should be noted also that similitude in impact experimentation requires identical velocities between the model and the prototype.

ii) In the second series of tests for "EDF" carried out by the Central Direction of Public Work (12) a 305 mm diameter naval gun fired missiles masses 160 to 227 kg with flat ends at concrete slabs measuring 5 x 5 m. The velocities varied from 77.5 to 160.4 m/sec. Fifteen missiles were fired into 40 cm thick slabs and ten into 50 cm thick slabs. These concrete slabs were reinforced with four layers, each steel layer included horizontal and vertical bars of 16 mm diameter at a spacing of 8 per meter. The total mass of reinforcement steel per cubic meter was 265 and 220 kg respectively.

iii) A third series of tests was performed at Aquitaine Scientific and Technical Research Center "CESTA" of the French Atomic Energy Commission "CEA" (13) with a 300 mm air gun and 1.46 x 1.46 m slabs. The missile had a variable diameter between 50 and 300 mm with corresponding masses between 5 and 300 kg.

The specimens had a constant thickness of 26 cm and an identical arrangement of reinforcement except for a single unreinforced specimen. Two different mass of reinforcement per cubic meter were used and these were 160 and 260 kg respectively.

These experiments were performed at one fifth scale to examine the laws of similarity. Recent tests have been performed in France since 1979 and their main characteristics are summarized in ref. (14). The results of these tests can be presented in a homogeneous perforation formula referred to as the "CEA - EDF" formula given by

$$d_p = 0.82 (\sigma_c)^{-0.375} \rho^{-0.125} V^{0.75} \left(\frac{M}{D}\right)^{0.5} \quad (2.19)$$

where

σ_c = ultimate compressive strength of concrete (Pa)

ρ = density of concrete (kg/m³)

V = missile perforation velocity (m/sec.)

M = mass of missile (kg)

D = missile diameter (m)

d_p = target perforation thickness (m).

The validity of this formula for a cylindrical flat nose missile is given by the following ranges.

$$20 \text{ m/sec.} \leq V \leq 200 \text{ m/sec.}$$

$$0.3 \leq d_p/D \leq 4$$

$$10 \text{ MPa} \leq \sigma_c \leq 45 \text{ MPa}$$

$$75 \text{ kg/m}^3 \leq \text{reinforcing steel with four layers} \leq 300 \text{ kg/m}^3$$

2.3.9 Kar Formula

Recent tests indicate the limitation of the modified Petry, Ballistic Research Laboratory, Ammann and Whitney and the modified NDRC formula to predict the local effects of concrete barriers subjected to impact by missiles. Kar (15,

16, 17, 18, 19, 20) has proposed a set of modified formulae for calculating the local impact effects of missiles on concrete barriers.

The formula for penetration was originally developed for missile penetration into earth. A constant coefficient has been introduced for concrete barriers to account for the different material and is based upon the test results. The different formulae take into consideration the cross-sectional area as well as the outside dimension and shape of the missiles. They also consider the weight, impacting velocity, nose shape factor and material properties of the missiles, the size of coarse aggregate and the material properties of concrete. The proposed formulae have been developed by a spatial curve fitting of results (20). The depth of penetration X_p (measured in inches) is given

by

$$\frac{X_p}{D} = \left[\frac{4 K.K_1}{D_1} \left(\frac{E}{E_m}\right)^{1.25} \frac{W.V^{1.8}}{(1000 D)^{1.8}} \right]^{0.5} \quad \frac{X_p}{D} \leq 2 \quad (2.20)$$

$$\frac{X_p}{D} = \frac{K.K_1}{D_1} \left(\frac{E}{E_m}\right)^{1.25} \frac{W.V^{1.8}}{(1000 D)^{1.8}} + 1 \quad \frac{X_p}{D} > 2 \quad (2.21)$$

where E and E_m are the modulus of elasticity of material of the missile and mild steel respectively and are expressed in the same units.

K_1 is the concrete penetrability factor and is given as a function of the concrete ultimate compressive strength (f'_c) It is assumed that K_1 equals $\frac{180}{\sqrt{f'_c}}$, in which (f'_c) has the units of pounds per square inch obtained from the concrete

cylinder test. For specimens other than cylinder of suitable modified valued of f'_c should be used.

K is the missile nose shape factor fig. (2.4).

For practical cases the following values may be used.

K = 0.72 for flat nosed solid bodies or

$$K = 0.72 + (0.0306) \left[\left(\frac{D_1}{D} \right)^2 - 1 \right] \leq 1 \text{ for hollow circular}$$

sections (pipe) or irregular sections fig. (2.5) where

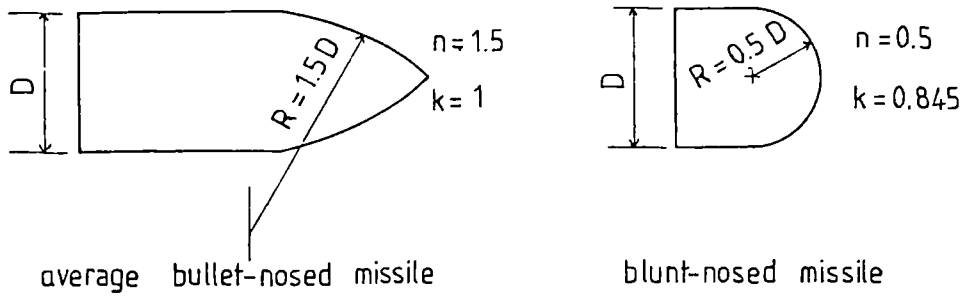
D_1 = the outside diameter of the missile in the case of a hollow circular section and is equal to (D) in the case of a solid rectangular section.

D = the diameter of missile that has the same contact surface area as that of the actual solid missile.

$K = 0.72 + 0.25 (n - 0.25)^{0.5} \leq 1.17$ for missiles with a special nose in which n = the ratio of the radius of the nose to the diameter of the missile.

X_p , D and D_1 are expressed in inches, W is expressed in lbs and V is expressed in ft/sec.

Kar stated that the factor $(E/E_m)^{1.25}$ is approximate and its use is recommended only until sufficient test data is available for improvement. For most practical cases $E = E_m$ and in this case the Kar penetration equation for flat nosed solid cylindrical missiles becomes identical to the NDRC formula. Kar also proposed the following scabbing and perforation equations.



n = caliber radius of the missile nose
 $= R/D$

k = nose shape factor
 $= 0.72 + 0.25 \sqrt{n - 0.25}$ for solid missiles with closed ends

FIG. (2.4)

SHAPE EFFECTS OF SOLID PROJECTILES WITH CLOSED ENDS

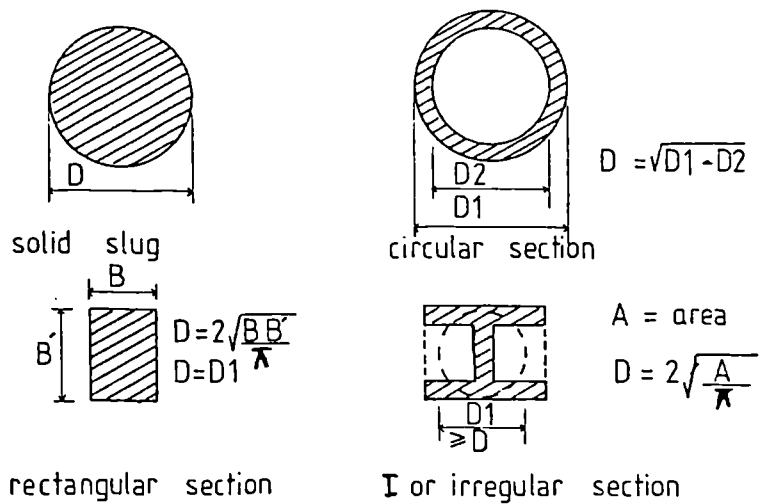


FIG. (2.5)

DIFFERENT DIAMETERS OF PROJECTILES

$$b\left(\frac{d_s - a}{D}\right) = 7.91 \left(\frac{X_p}{D}\right) - 5.06 \left(\frac{X_p}{D}\right)^2 \quad \frac{X_p}{D} \leq 0.65 \quad (2.22)$$

$$b\left(\frac{d_s - a}{D}\right) = 2.12 + 1.36 \left(\frac{X_p}{D}\right) \quad (2.23)$$

$$3 \leq \frac{d_s}{D} \leq 18$$

$$0.65 \leq \frac{X_p}{D} \leq 11.75$$

$$\frac{d_p - a}{D} = 3.19 \left(\frac{X_p}{D}\right) - 0.718 \left(\frac{X_p}{D}\right)^2 \quad \frac{X_p}{D} \leq 1.35 \quad (2.24)$$

$$\frac{d_p - a}{D} = 1.32 + 1.24 \left(\frac{X_p}{D}\right) \quad (2.25)$$

$$3 \leq \frac{d_p}{D} \leq 18$$

$$1.35 \leq \frac{X_p}{D} \leq 13.5$$

where $b = (E_m/E)^{0.2}$ and a is half the concrete aggregate size. The terms d_s , d_p and a are expressed in inches.

A discussion of the Kar formulae has been given by Burdette (21).

2.3.10 Degen Formula

A statistical analysis of the experimental data given in ref. (12, 13, 22, 23) has been undertaken by Degen (24) who has proposed the following formulae:

$$\frac{d_p}{D} = 0.69 + 1.29 \left(\frac{X_p}{D}\right) \quad 2.65 \leq \frac{d_p}{D} \leq 18 \quad (2.26)$$

$$\frac{d_p}{D} = 2.2 \left(\frac{X_p}{D}\right) - 0.3 \left(\frac{X_p}{D}\right)^2 \quad \frac{X_p}{D} \leq 1.52 \quad (2.27)$$

where d_p , X_p and D are expressed in inches and the experimental data include the following ranges of variables

$$89 \text{ ft/sec.} \leq V \leq 1013 \text{ ft/sec.} \quad (1 \text{ fps} = 0.3048 \text{ m/sec.})$$

$$0.7 \leq d/D \leq 3$$

$$38.5 \text{ lb} \leq W \leq 756 \text{ lb} \quad (1 \text{ lb} = 0.453592 \text{ kg})$$

$$4860 \text{ psi} \leq f_c' \leq 6450 \text{ psi} \quad (1 \text{ psi} = 6.89476 \text{ kPa})$$

$$4.3 \text{ in} \leq D \leq 11.8 \text{ in} \quad (1 \text{ in} = 25.4 \text{ mm})$$

$$6.9 \text{ in} \leq d \leq 23.6 \text{ in}$$

Reinforcement 0, 10 to 21.84 lb/ft³ (1 lb/ft³ = 16.0185 kg/m³)

2.3.11 Chang Formula (semi-analytical formula)

Most of the early studies of missile impact problems were developed empirically for high velocity projectiles (velocity > 500 ft/sec.). Their application, therefore, to the low velocity regime is questionable. Recently, impact tests were conducted for lower velocity missiles and several empirical formulae were developed. In 1981 Chang (25) proposed a semi-analytical formula for evaluating the scabbing and perforation thickness of concrete panels. These formulae are given as follows:

$$d_s = Y \left(\frac{u}{v}\right)^{0.4a} \frac{(Mv^2)^{0.4}}{D^{0.2} (f_c')^{0.4}}$$

$$d_p = Z \left(\frac{u}{v}\right)^{0.5b} \left(\frac{Mv^2}{Df_c'}\right)^{0.5}$$

where

M = the mass of missile.

v = the impact velocity.

D = the missile diameter and

u = a reference velocity.

The symbols a and b are numerical constants and y and z are assumed to be normal random variables, the mean and variance of each will be determined. Due to the limited amount of available test data Chang used the Bayesian (25) approach rather than more conventional means of statistical analysis in his work.

Chang's theory assumes that the kinetic energy of the missile exceeds the flexural strain energy of the concrete barriers and initiates cracking and scabbing.

The scabbing thickness is calculated by equating the kinetic energy and strain energy capacity. A reference velocity, u, was chosen to be 200 ft/sec. The constant, a, was chosen to be 0.325 by comparing the calculated, Y, values from test data. The random variable, Y, was determined by the Bayesian statistical method and the scabbing thickness of a concrete barrier subject to a cylindrical solid steel missile may be given by equation

$$d_s = 1.84 \left(\frac{200}{v}\right)^{0.13} \frac{(Mv^2)^{0.4}}{D^{0.2} (f'_c)^{0.4}} \quad (2.28)$$

A barrier develops resistance as a missile penetrates. Chang makes the assumption that the maximum resistance occurs upon striking and decreases parabolically to zero when penetration occurs. Once more Chang uses an energy relationship to determine the perforation thickness.

The numerical constant, b, was chosen to be equal to 0.5. The random variable, Z, which is equal to unity is determined by a Bayesian statistical method. The perforation thickness

of a concrete barrier subject to a cylindrical solid steel missile can be calculated by

$$d_p = \left(\frac{200}{v}\right)^{0.25} \left(\frac{Mv^2}{Df'_c}\right)^{0.5} \quad (2.29)$$

The test data from which Chang developed his equations cover the following ranges:

$$\begin{aligned} 55 \text{ ft/sec.} &\leq V \leq 1023 \text{ ft/sec.} && (1 \text{ fps} = 0.3048 \text{ m/sec.}) \\ 0.24 \text{ lb} &\leq W \leq 756 \text{ lb} && (1 \text{ lb} = 0.453592 \text{ kg}) \\ 2 \text{ in} &\leq d \leq 24 \text{ in} && (1 \text{ in} = 25.4 \text{ mm}) \\ 0.79 \text{ in} &\leq D \leq 12 \text{ in} \\ 3300 \text{ psi} &\leq f'_c \leq 6600 \text{ psi} && (1 \text{ psi} = 6.89476 \text{ kPa}). \end{aligned}$$

Haldar (26) discuss Chang's formula and mentions some shortcomings. For instance, experimental observation demonstrates extensive cracking throughout specimens. The Chang assumption of peripheral cracks only, gives an incorrect strain energy capacity. Also, Chang ignores the effect of missile penetration in the calculation of scabbing and perforation thicknesses.

2.3.12 Haldar and Miller Formula

Closer examination of the NDRC equations (eqs. 2.7 and 2.8) reveals that the left hand sides of these equations are dimensionless, but the right hand sides are not. Thus, the functional form of the NDRC equations may not be ideal with some parameters in the NDRC equations receiving undue importance compared with other parameters.

Observing this, Haldar (2, 27, 3, 28) introduced a new dimensionless parameter (I) called the impact factor which is defined as:

$$I = \frac{w k v^2}{gD^3 f'_c} \quad (2.30)$$

All the parameters in equation (2.30) are identical to the parameters in the NDRC equations. To be consistent with respect to units, equation (2.30) can be rewritten as:

$$I = \frac{12 k w v^2}{32.2D^3 f'_c} \quad (2.31)$$

The impact factor indicates the damage potential of a missile and the damage potential is expected to be large when the value of I is large. This suggests that if a missile has a high impact energy, or small impact area, or if it is going to hit a weak concrete structure it has a greater damage potential.

Haldar and Miller identified a total of 625 tests for penetration in which the impact factor varied within the range of 0.3 - 455. The results were plotted as the ratio of the observed penetration depth to the missile diameter against the impact factor I . Due to the vary wide range of impact, the factor has different statistical characteristics in the various ranges of the values of I . Three equations for the calculation of the penetration depth corresponding to the three ranges of impact factor gave the best fit for the data points. These equations are,

$$\frac{x_p}{D} = -0.0308 + 0.2251 I \quad 0.3 \leq I \leq 4.0 \quad (2.32)$$

$$\frac{x_p}{D} = 0.6740 + 0.0567 I \quad 4.0 \leq I \leq 21.0 \quad (2.33)$$

and

$$\frac{x_p}{D} = 1.1875 + 0.0299 I \quad 21 \leq I \leq 455 \quad (2.34)$$

Of the 625 examples that were considered by Haldar and Miller, nine are described by equation (2.32), ninety four by equation (2.33) and five hundred and twenty two by equation (2.34). The coefficients of determination of equations (2.32), (2.33) and (2.34) are 0.95, 0.70 and 0.9, respectively. Haldar mentioned also that these new relationship should be used in the future to predict the penetration depths in concrete structures due to non-deformable missile impact. Equations (2.32), (2.33) and (2.34) will be denoted as the Haldar penetration equations.

The scabbing thickness of a concrete structure subjected to non-deformable missile impact can be estimated by the impact factor concept. From an extensive literature survey a total of 176 cases were found by Haldar and Miller in which scabbing was observed. Out of 176 cases, 129 are for bullets and 47 are for large missiles. For 89 cases, backface crater depths are reported. For the remaining 87 cases, however, backface crater information is not available and for this reason these cases are not considered by the authors.

For the 89 cases, a scatter diagram of the ratio of observed scabbing depth to missile diameter d_s/D is plotted against the impact factor, I , which vary from 21 to 385. A linear regression analysis was carried out between the d_s/D and I parameters. The following equation resulted:

$$\frac{d_s}{D} = 3.3437 + 0.0342 I \quad 21 \leq I \leq 385 \quad (2.35)$$

The corresponding value of coefficient of determination is found to be 0.8 and equation (2.35) will be denoted as the Haldar scabbing equation.

2.3.13 Hughes Formula

The NDRC penetration formula is based on a physical model of the impact process in which it is assumed that the contact force increases linearly to a constant maximum value.

Degen (24) has shown that this assumption was incorrect and he suggested an alternative model in which the force was maximum at the beginning of the impact and decreased to zero at maximum penetration.

Chang (25) used a similar model in his work.

In 1983 Hughes (29) used a force penetration model, which is essentially a combination of those used by the NDRC and Chang. The force is assumed to increase linearly to a maximum (when concrete spalls in the contact zone), after which it falls parabolically to zero at maximum penetration. He also assumed that the penetration depth (X_p) depends on the missile diameter (D), impact velocity (V), concrete strain modulus (E_c) and the concrete tensile strength (modulus of rupture) (f_r). Dimensional analysis as detailed in the reference (29) gives

$$\frac{X_p}{D} = J_1[Mv^2/(f_r D^3), E_c/f_r] \quad (2.36)$$

where J_1 is some unknown function which relates the three dimensionless parameters, X_p/D , $Mv^2/(f_r D^3)$ and E_c/f_r .

Equation (2.36) can be simplified for normal weight concrete because with sufficient accuracy, $E_c/fr = 7600 = \text{constant}$. This particular parameter can thus be considered invariant and may be eliminated from equation (2.36) so that

$$\frac{X_p}{D} = J_2[I'] \quad (2.37)$$

where $I' = Mv^2/(frD^3)$.

The impact parameter I' is similar to that of Haldar and Miller (2, 27, 3, 28) and is a measure of the damage potential of the missile.

By the same method it can be shown that the scabbing thickness d_s and the perforation thickness d_p are given by

$$\frac{d_s}{D} = J_3[I'] \quad (2.38)$$

$$\frac{d_p}{D} = J_4[I'] \quad (2.39)$$

Hughes used Williams conclusion (30) that the bearing strength of concrete is proportional to the strain rate factor S . Hughes concluded that the depth of penetration, X_p , is inversely proportional to the strain rate factor, S . Thus equation (2.37) can be written as

$$\frac{X_p}{D} = h I'/S \quad (2.40)$$

where $h = \text{constant coefficient}$ and S is a function of I' .

By using the least square fit technique and using various forms for the unknown function S , Hughes found the following formula for predicting the penetration depth X_p

$$\frac{X_p}{D} = 0.19 K' I'/S \quad (2.41)$$

where

- K' = is the nose shape factor.
- = 1.0 for flat nosed missiles.
- = 1.12 for blunt nosed missiles.
- = 1.26 for average bullet nose (spherical end) and
- = 1.39 for very sharp nose.

- S = strain rate factor
- = $1.0 + 12.3 \text{ Ln } (1.0 + 0.03 I')$.

Note that the impact parameter I' is dimensionless.

Hughes equations for scabbing and perforation are as follows:

$$\frac{d_s}{D} = 1.74 \left(\frac{X_p}{D}\right) + 2.3 \quad \frac{X_p}{D} > 0.7 \quad (2.42)$$

$$\frac{d_s}{D} = 5.0 \left(\frac{X_p}{D}\right) \quad \frac{X_p}{D} < 0.7 \quad (2.43)$$

$$\frac{d_p}{D} = 1.58 \left(\frac{X_p}{D}\right) + 1.4 \quad \frac{d}{D} > 3.5 \quad (2.44)$$

$$\frac{d_p}{D} = 3.6 \left(\frac{X_p}{D}\right) \quad \frac{d}{D} < 3.5 \quad (2.45)$$

The formulae are valid in the range $I' < 3500$, which is the range of available test data, but will be conservative in the range $I' < 40$ and $d/D < 3.5$. This is because the theory

which has been used neglects both elastic and global effects, which tend to reduce the severity of local damage.

The formula refer to hard cylindrical missiles at normal incidence and barriers of normal weight concrete. The barriers are reinforced with 0% - 1.5% each way, front face bending reinforcement and 0.3% - 1.7% each way back face bending reinforcement with no shear reinforcement.

2.3.14 Adeli and Amin Formula

Adeli and Amin observed a proportional relationship between the observed penetration depth, X_p , and the dimensionless impact factor I defined as follows:

$$I = \frac{K W V^2}{g D^3 f'_c} \quad (2.46)$$

Quadratic and cubic polynomials were found (5) to best fit to the test data. Test results from the programs conducted in Europe and USA (7) were used. The following two equations for estimating the penetration depth of concrete are proposed:

$$\frac{X_p}{D} = 0.0416 + 0.1698 I - 0.0045 I^2 \quad (2.47)$$

$$\frac{X_p}{D} = 0.0123 + 0.196 I - 0.008 I^2 + 0.0001 I^3 \quad (2.48)$$

New formula for predicting the scabbing and perforation thickness were also proposed as follows:

$$\frac{d_s}{D} = 1.8685 + 0.40351 I - 0.0114 I^2 \quad (2.49)$$

$$\frac{d_p}{D} = 0.906 + 0.3214 I - 0.0106 I^2 \quad (2.50)$$

These formulae have been developed within the following range of applicability

$$89 \text{ ft/sec.} \leq V \leq 1023 \text{ fps} \quad (\text{fps} = 0.3048 \text{ m/sec.})$$

$$0.7 \leq \frac{d}{D} \leq 18$$

$$0.24 \text{ lb} \leq W \leq 756 \text{ lb} \quad (\text{lb} = 0.453592 \text{ kg})$$

$$0.3 \leq I \leq 21$$

$$0.8 \text{ in} \leq D \leq 12 \text{ in} \quad (\text{in} = 25.4 \text{ mm})$$

$$\frac{x_p}{D} \leq 2.0$$

2.4 Comparison of Impact Formula

2.4.1 Comparison of Penetration Formulae

Eight different formula varying in their theoretical basis and ranges of applicability are available to predict the penetration depth in reinforced concrete panels under the impact of non-deformable missiles. Table (2.1) summarizes these formulae. In 1976 Kennedy (4) compared the four available equations at that time using the experimental results carried out in the USA and Europe. Kennedy concluded that the modified NDRC formula was the best among the first four formulas for calculating the penetration depth of non-deformable missiles in a massive concrete target.

In 1984 the eight penetration formulae were re-evaluated by Adeli and Amin (5) using the updated test data summarized by Slitter (7). Most of these data were obtained during the last decade. These test results are used to evaluate the formula for predicting local effects caused by hard missiles upon concrete structures. The following observations have been made by Adeli and Amin (5).

- (i) For $\frac{X}{D} \geq 0.6$, the modified NDRC, Haldar and Miller, Hughes and the quadratic and cubic formulae proposed by Adeli and Amin produced results within the range $\pm 25\%$ when compared with experimental results.
- (ii) For $\frac{X}{D} < 0.6$, the modified Petry 2, Haldar and Miller and the quadratic and cubic formulae compare favourably with experimental results.

(iii) The ACE formula and the modified Petry 1 formula over-predict the penetration depth by a large margin.

Generally, Hughes, Haldar and Miller and the quadratic and cubic formulae of Adeli and Amin provided the best prediction of penetration depth.

Table (2.1): A summary of concrete penetration formulae

No.	Name of formula	Formula	Theoretical basis	Limitations of applicability
1	Modified Petry (1910)	$X_p = 12 K_p A_p \log_{10} \left(1 + \frac{v^2}{215000} \right)$ $K_p = 0.00799 \text{ massive concrete}$ $= 0.00426 \text{ normal reinforcement}$ $= 0.00284 \text{ special reinforcement}$ = function of (f_c') as shown in fig. 2.2	Empirical	
2	ACE (1946)	$\frac{X_p}{D} = \frac{282 W V^{1.5}}{D^{2.785} f_c' 0.5^{1.5} 1000^{1.5}} + 0.5$	Statistical fitting of experimental data	$d/D \geq 3$ $D < 16 \text{ in}$ $0.2 \leq W/D^3 \leq 0.8 \text{ lb/in}^3$ $500 \leq V \leq 3000 \text{ ft/sec.}$
3	Modified NDRC (1946)	i) $\frac{X_p}{D} = \left[\frac{4K K_1 W V^{1.8}}{D(10000)^{1.8}} \right]^{0.5} \frac{X_p}{D} \leq 2.0$ ii) $\frac{X_p}{D} = 1 + \frac{K K_1 W V^{1.8}}{D(10000)^{1.8}} \frac{X_p}{D} > 2.0$ $K = 0.72 \text{ flat nosed missile}$ $= 0.84 \text{ blunt nosed missile}$ $= 1.00 \text{ spherical end missile}$ $= 1.14 \text{ very sharp nose missile}$ $K_1 = 180/\sqrt{f_c'}$	Penetration theory and experimental considerations	$3 \leq d/D \leq 18$ $V \geq 500 \text{ ft/sec.}$ $2 \leq K_1 \leq 5$

Table (2.1): A summary of concrete penetration formulae (continued)

No	Name of formula	Formula	Theoretical basis	Limitations of applicability
4	Ammann & Whitney	$\frac{X_p}{D} = \frac{282 K W V^{1.8}}{D(f_c')^{0.5} (10000)^{1.8}}$		$V > 1000$ ft/sec.
5	Kar (1978)	<p>i) $\frac{X_p}{D} = \left[\frac{4 K K_1}{D_1} \left(\frac{E}{E_m} \right)^{1.25} \frac{W V^{1.8}}{10000^{1.8}} \right]^{0.5} \frac{X_p}{D} \leq 2$</p> <p>ii) $\frac{X_p}{D} = \frac{K K_1}{D_1} \left(\frac{E}{E_m} \right)^{1.25} \frac{W V^{1.8}}{(10000)^{1.8}} + 1 \frac{X_p}{D} > 2$</p> <p>$K = 0.72$ for flat nosed missile</p> <p>$= 0.72 + (0.0306) \left[\left(\frac{D_1}{D} \right)^2 - 1 \right] \leq 1$ for hollow circular section (pipe) or irregular section</p> <p>D_1 = the outside diameter of missile</p> <p>D = the diameter of missile has the same contact area as that of actual solid missile</p> <p>$K = 0.72 + 0.25(n - 0.25)^{0.5} \leq 1.17$ for special nose missile</p> <p>n = the ratio of the radius of the nose to the diameter of the missile</p>	Regression analysis	Same as modified NDRC formulas

Table (2.1): A summary of concrete penetration formulae (continued)

No	Name of formula	Formula	Theoretical basis	Limitations of applicability
6	Haldar & Miller (1982)	i) $\frac{X_p}{D} = -0.0308 + 0.2251I$ $0.3 \leq I \leq 4.0$ ii) $\frac{X_p}{D} = 0.6740 + 0.0567I$ $4.0 \leq I \leq 2.10$ iii) $\frac{X_p}{D} = 1.1875 + 0.0299I$ $21 \leq I \leq 455$ $I = \frac{12}{32.2} \frac{K W V^2}{D^3 f'_c}$	Regression analysis	$89 \leq V \leq 1023$ ft/sec. $0.7 \leq d/D \leq 18$ $0.24 \leq W \leq 756$ lb $0.3 \leq I \leq 455$ $0.8 \leq D \leq 12$ in $X_p/D \leq 2.0$
7	Hughes (1983)	$\frac{X_p}{D} = 0.19K' I'/S$ $I' = \frac{12}{32.2} \frac{W V^2}{\text{fr.} D^3}$ $S = 1.0 + 12.3 \ln(1.0 + 0.031I')$ $K' = 1.0$ for flat nosed missile $= 1.12$ for blunt nosed missile $= 1.26$ for spherical end missile $= 1.39$ for very sharp nose	Physical model of the impact process and regression analysis	$I' < 3500$ $89 \leq V \leq 1023$ ft/sec. $0.7 \leq d/D \leq 18$ $0.8 \leq D \leq 12$ in $0.24 \leq W \leq 756$ lb

Table (2.1): A summary of concrete penetration formulae (continued)

No	Name of formula	Formula	Theoretical basis	Limitations of applicability
8	Adeli & Amin (9184)	$i) \quad \frac{X_p}{D} = 0.0416 + 0.1698I - 0.0045I^2$ $ii) \quad \frac{X_p}{D} = 0.0123 + 0.196I - 0.008I^2 + 0.0001I^3$ $I = \frac{12}{32.2 D} \frac{K W V^2}{f'_c}$	Quadratic and cubic regression analysis	$89 \leq V \leq 955$ ft/sec. $4.5 \leq d \leq 18$ in $0.26 \leq W \leq 213$ lb $0.3 \leq I \leq 21.0$ $3210 \leq f'_c \leq 6131$ psi $0.79 \leq D \leq 8$ in $X_p/D \leq 2.0$

in = 25.4 mm
 psi = 6.89476 kpa
 fps = 0.3048 m/sec
 lb/ft³ = 16.0185 kg/m³
 lb/in³ = 0.0276 kg/m³

2.4.2 Comparison of Scabbing Formulas

Table (2.2) shows the available formulae for the calculation of the scabbing thickness, their basis, and range of applicability.

These formulae have been re-evaluated by Adeli and Amin (5) using the experimental results in which scabbing occurred (7). The Stone and Webster and Kar formulae were not included. In the former case the range of applicable concrete compressive strength (f'_c) was limited to only three specimens and was, therefore, insufficient for comparison. In the latter case insufficient information regarding the aggregate size was given. Also, if the aggregate size is neglected in the Kar formula for scabbing and perforation it becomes the same as the modified NDRC formula. The following observations can be made regarding the calculation of scabbing thickness.

- (i) The Adeli and Amin, Chang and Bechtel formulae predict the scabbing thickness more accurately than the other formulae. They are, in general, the least conservative. The modified NDRC and ACE formulae compare favourably with the experimental data, but they are somewhat more conservative than the Chang and Bechtel formulae.
- (ii) The Hughes formula is the most conservative in predicting the scabbing thickness.
- (iii) The modified Petry 1, 2 and BRL formulae are the least accurate in predicting the scabbing thickness.

Table (2.2): A summary of scabbing formulae for Non-deformable missile

No	Name of formula	Formula	Theoretical basis	Limitations of applicability
1	Modified Petry (1910)	$d_s = 2.2 X_p$	Empirical	
2	ACE (1946)	$\frac{d_s}{D} = 2.12 + 1.36 \left(\frac{X_p}{D}\right)$ $3 \leq \frac{d_s}{D} \leq 18$ $0.65 \leq \frac{X_p}{D} \leq 11.75$	Statistical fitting of experimental data	$\frac{d}{D} \geq 3$ $D \leq 16$ in $0.2 \leq W/D \leq 0.8$ lb/in ³ $500 \leq V \leq 3000$ ft/sec.
3	Modified NDRC (1946) (1966)	i) $\frac{d_s}{D} = 2.12 + 1.36 \left(\frac{X_p}{D}\right)$ ii) $\frac{d_s}{D} = 7.91 \left(\frac{X_p}{D}\right) - 5.06 \left(\frac{X_p}{D}\right)^2$	Penetration theory and experimental consideration	$3 \leq \frac{d}{D} \leq 18$ $V \geq 500$ ft/sec.
4	Modified BRL (1968)	$d_s = 2 d_p$		
5	Bechtel Corporation formula (1975)	$d_s = 15.5 \frac{W^{0.4} V^{0.5}}{(f_c)^{0.5} D^{0.2}}$	Empirical	$6 \leq d \leq 24$ in $1 \leq D \leq 8$ in $4500 \leq f_c \leq 5940$ psi $8 \leq W \leq 213$ lb $100 \leq V \leq 350$ ft/sec.

Table (2.2): A summary of scabbing formulae for Non-deformable missile (continued)

No	Name of formula	Formula	Theoretical basis	Limitations of applicability
6	Stone & Webster (1976)	$d_s = \left(\frac{W V^2}{C} \right)^{1/3}$	Empirical	$3000 \leq f'_c \leq 4500$ psi $1.5 \leq \frac{d_s}{D} \leq 3.0$ $0.06 \leq \frac{2t}{D} \leq 1.0$ $75 \leq V \leq 250$ ft/sec.
7	Kar (1978)	i) $b \left(\frac{d_s - a}{D} \right) = 7.91 \frac{X_P}{D} - 5.06 \left(\frac{X_P}{D} \right)^2$ ii) $b \left(\frac{d_s - a}{D} \right) = 2.12 + 1.36 \left(\frac{X_P}{D} \right)^3$ $b = (E_m/E)$ and a half of aggregate size	Regression analysis	Same as modified NDRC form
8	Chang (1981)	$d_s = 1.84 \left(\frac{200}{V} \right)^{0.13} \frac{(MV^2)^{0.4}}{D^{0.2} (f'_c)^{0.4}}$	Bayesian analysis and some principles of mechanics	$55 \leq V \leq 1023$ ft/sec. $0.24 \leq W \leq 756$ lb $5 \leq d \leq 24$ lb $0.79 \leq D \leq 12$ in $3300 \leq f'_c \leq 6600$ psi

Table (2.2): A summary of scabbing formulae for Non-deformable missile (continued)

No	Name of formula	Formula	Theoretical basis	Limitations of applicability
9	Halder and Miller (1982)	$\frac{d^s}{D} = 3.3437 + 0.0342I \quad 21 \leq I \leq 385$ $I = \frac{12}{32.2} \frac{K W V^2}{D^3 f'_c}$	Regression analysis	$89 \leq V \leq 1023 \text{ ft/sec.}$ $0.7 \leq \frac{d}{D} \leq 18$ $0.24 \leq W \leq 756 \text{ lb}$ $21 \leq I \leq 385$ $0.8 \leq D \leq 12 \text{ in}$ $X_{p/D} \leq 2.0$
10	Hughes (1983)	$i) \quad \frac{d^s}{D} = 5.0 \frac{X_p}{D}$ $ii) \quad \frac{d^s}{D} = 1.74 \frac{X_p}{D} + 2.3$	Physical model of the impact process and Regression analysis	$I' < 3500$ $89 \leq V \leq 1023 \text{ ft/sec.}$ $0.7 \leq \frac{d}{D} \leq 18$ $0.2 \leq D \leq 12 \text{ in}$ $0.24 \leq W \leq 756 \text{ lb}$
11	Adeli & Amin (1984)	$\frac{d^s}{D} = 1.8685 + 0.40351I - 0.0114I^2$	Quadratic regression analysis	$96 \leq V \leq 1023 \text{ ft/sec.}$ $6.0 \leq d \leq 24 \text{ in}$ $4.96 \leq W \leq 749.58 \text{ lb}$ $0.3 \leq I \leq 21.0$ $3820 \leq f'_c \leq 6825 \text{ psi}$ $1.77 \leq D \leq 12 \text{ in}$

2.4.3 Comparison of Perforation Formulae

Table (2.3) shows the available formulae for estimating the perforation thickness, their theoretical basis and ranges of applicability. Also, these formulae have been re-evaluated by Adeli and Amin (5) using experimental results in which perforation occurred (7). The following observations can be made.

- (i) The Adeli and Amin, Chang, Degen and CEA-EDF perforation formulae predict the most accurate perforation thickness.
- (ii) The NDRC and Petry 1 formulae also show good agreement with the experimental results, but are not as good as those four formulae mentioned in (i) above.
- (iii) The Hughes formula predicted that perforation occurred in some tests when it was not observed (41 out of 87 tests). It is, therefore, conservative in predicting the perforation thickness.
- (iv) In most of the tests in which perforation occurred the Petry 2 and the BRL formulae predicted no perforation. They are not, therefore, recommended to be used to calculate the perforation thickness for situations similar to those of the tests.
- (v) The ACE formula has the smallest range of applicability and does not show good agreement with the experimental results.

Table (2.3): A summary of perforation formulae for non-deformable missile

No	Name of formula	Formula	Theoretical basis	Limitations of applicability
1	Modified Petry (1910)	$d_p = 2 X_p$	Empirical	
2	ACE (1946)	$d_p = 1.32 + 1.24 \frac{X_p}{D}$ $3 \leq \frac{d_p}{D} \leq 18$ $1.35 \leq \frac{X_p}{D} \leq 13.5$	Statistical fitting experimental data	$\frac{d}{D} > 3$, $D \leq 16$ in $0.2 \leq \frac{W}{D^3} \leq 0.8$ lb/in ³ $500 \leq V \leq 3000$ ft./sec.
3	Modified NDRC (1946) (1966)	i) $\frac{d_p}{D} = 1.32 + 1.24 \frac{X_p}{D}$ $3 \leq \frac{d_p}{D} \leq 18$ $1.35 \leq \frac{X_p}{D} \leq 13.5$ ii) $\frac{d_p}{D} = 3.19 \left(\frac{X_p}{D}\right) - 0.718 \left(\frac{X_p}{D}\right)^2$ $\frac{d_p}{D} \leq 3$ $X_p/D \leq 1.35$	Penetration theory and experimental considerations	$3 \leq \frac{d}{D} \leq 18$ $V > 500$ ft./sec.
4	Modified BRL (1968)	i) $\frac{d_p}{D} = 7.8 \frac{W^{1.33}}{D^{2.8} (1000)^{1.33}}$ $f_c = 3000$ psi ii) $\frac{d_p}{D} = \frac{427 W^{1.33}}{D^{2.8} (f_c)^{0.5} (1000)^{1.33}}$		

Table (2.3): A summary of perforation formulae for non-deformable missiles (continued)

No	Name of formula	Formula	Theoretical basis	Limitations of applicability
5	CEA - EDF (1977)	$d_p = 0.82(\sigma_c)^{-0.375} 0.125 v^{0.75} \left(\frac{M}{D}\right)^{0.5}$	Least squares	$20 \leq v \leq 200$ m/sec. $0.3 \leq \frac{d_p}{D} \leq 4$ $30 \leq \sigma_c \leq 45$ MPa $75 \leq 4$ layers ≤ 300 kg/m cylindrical flat nose
6	Kar (1978)	$i) \frac{d_p^{-a}}{D} = 1.32 + 1.24 \frac{X_p}{D}$ $ii) \frac{d_p^{-a}}{D} = 3.19 \frac{X_p}{D} - 0.718 \left(\frac{X_p}{D}\right)^2$	Regression analysis	$3 \leq \frac{d_p}{D} \leq 18$ $v \geq 500$ ft/sec.
7	Degen (1980)	$i) \frac{d_p}{D} = 0.69 + 1.29 \left(\frac{X_p}{D}\right)$ $ii) \frac{d_p}{D} = 2.2 \frac{X_p}{D} - 0.3 \left(\frac{X_p}{D}\right)^2$	Statistical analysis	$89 \leq v \leq 1013$ ft/sec $0.7 \leq \frac{d_p}{D} \leq 3$ $38.5 \leq W \leq 756$ lb $4860 \leq f_c \leq 6450$ psi $4.3 \leq D \leq 11.8$ in $6.9 \leq d \leq 23.6$ in Reinforcement, 0, 10-21.84

Table (2.3): A summary of perforation formulae for non-deformable missile (continued)

No	Name of formula	Formula	Theoretical basis	Limitations of applicability
8	Cheng (1981)	$d_p = \left(\frac{200}{V}\right)^{0.25} \left(\frac{MV^2}{Df'_c}\right)^{0.5}$	Bayesian analysis and some principles of mechanics	$55 \leq V \leq 1023$ ft/sec $0.24 \leq W \leq 756$ lb $3300 \leq f'_c \leq 6600$ psi $0.79 \leq D \leq 12$ in $2 \leq d \leq 24$ in
9	Hughes (1983)	i) $\frac{d_p}{D} = 3.6 \frac{X_p}{D}$ ii) $\frac{d_p}{D} = 1.58 \frac{X_p}{D} + 1.4$	Physical model of the impact process and Regression analysis	$I' < 3500$ $89 \leq V \leq 1023$ ft/sec. $0.7 \leq \frac{d}{D} \leq 18$ $0.2 \leq D \leq 12$ in $0.24 \leq W \leq 756$ lb
10	Adeli & Amin (1984)	$\frac{d_p}{D} = 0.906 + 0.3214I - 0.0106I^2$	Quadratic regression analysis	$89 \leq V \leq 1023$ $3 \leq d \leq 23.6$ in $1.77 \leq D \leq 12$ in $4.96 \leq W \leq 756.19$ lb $4550 \leq f'_c \leq 7130$ psi $0.3 \leq I \leq 21$

2.4.4 Comments on the Performance of Previous Work

Adeli and Amin (5) suggested the following recommendations.

- (i) For non-deformable missiles with velocities lower than 475 ft/sec., the quadratic formula found by Adeli and Amin is recommended for calculating the penetration depth.
- (ii) For a non-deformable missile having a velocity higher than 475 ft/sec. and lower than 1000 ft/sec., the Adeli quadratic or modified NDRC formulae are recommended for calculating the penetration depth.
- (iii) For non-deformable missiles of velocity less than 1020 ft/sec., the Adeli quadratic, Chang or Bechtel formulae are recommended for computing the scabbing thickness.
- (iv) For non-deformable missiles having a velocity of less than 1020 ft/sec., the Adeli quadratic, Chang, Degen or CEA-EDF formulae are recommended for computing the perforation thickness.

2.5 Previous Experimental Investigations into the Effect of Reinforcement Quantity for Rigid Missile Impact

A number of formulae which have been developed from experimental impact studies are in use for assessing the performance of reinforced concrete. In general a term involving the level of reinforcement is not included in these formulae. A homogeneous perforation formula known as the "CEA-EDF" formula has been obtained (14) and is given as follows:

$$v_c = 1.3(\sigma_c)^{1/2} \rho^{1/6} \left(\frac{D \cdot d_p^2}{M}\right)^{2/3}$$

where V_c = critical perforation velocity (m/sec.)

σ_c = ultimate compressive strength of concrete (P_a)

ρ = density of concrete (kg/m^3)

D = missile diameter (m)

M = missile mass (kg)

and d_p = perforation target thickness (m).

The formula has been developed from experiments (11, 12, 13, 14). This formula determines the velocity of a missile required to just achieve perforation. It contains no reinforcement quantity dependent term, but it is valid for four symmetrical layers of reinforcement of between 75 and 300 kg/π^3 . No difference in behaviour was found for equally or unequally spaced reinforcement through the concrete thickness, figure (2.6).

The formula is always valid when there are only 2 layers close to the rear surface figure (2.6), but it is not exact when there is only one layer close to each face. In this case the perforation velocity given by the formula should

be corrected by the coefficient $\frac{1}{3}(2 + \frac{r}{250})$ where r is the reinforcement ratio in kg/m^3 (ratio between bending steel mass and concrete volume) reference (14) and figure (2.7). Also, when there is no reinforcement, the perforation velocity is $\frac{2}{3}$ of that given by the formula.

The reinforced concrete construction techniques used in Europe require a relatively large quantity of reinforcing steel together with a relatively thin overall wall thickness. British reactor construction practice generally follows the converse arrangement with a minimum steel reinforcement being complemented with a thick wall (31). For that reason a series of experiments has been conducted at the Atomic Energy Establishment - Winfrith, to study the effects of variations in the amount of bending reinforcement in a concrete slab and also the effects of introducing shear stirrups between the bending meshes. These experiments have been carried out on concrete targets approximately representative of good quality reactor concrete, at about 1/8 scale.

The bending reinforcement amounts used were 0 - 0.5% each way, each face with shear reinforcement amounts from 0 - 0.5% of the plan area. The test results are shown graphically in figure (2.8) (31). The critical velocity for perforation shown for each level of reinforcement is the average of several measured values in each case. The error bars indicate the overall spread in measured values as well as the assumed uncertainties in precision of the measuring systems. The inclusion of shear stirrups increased the critical perforation velocity by providing additional

resistance to the formation of the conical crack surface. It can be seen that 0.125% shear steel with 0.125% each way, each face (EWEF) bending steel gives a similar perforation resistance as 0.1875% bending steel only. Also 0.5% shear with 0.5% bending are equivalent to little more than 0.625% bending reinforcement alone. Previous experimental work at Winfrith provides further justification for the suggestion that the CEA-EDF formula could be modified (32) to include a bending reinforcement quantity dependent term by including an additional factor $(r_1^{0.27})$ to become

$$v_c = 1.3 (\sigma_c)^{1/2} \rho^{1/6} \left[\frac{D \cdot d_p^2}{M} \right]^{2/3} r_1^{0.27}$$

where r_1 is the bending reinforcement quantity in % each way, each face ($0.125\% \leq r_1 \leq 0.5\%$).

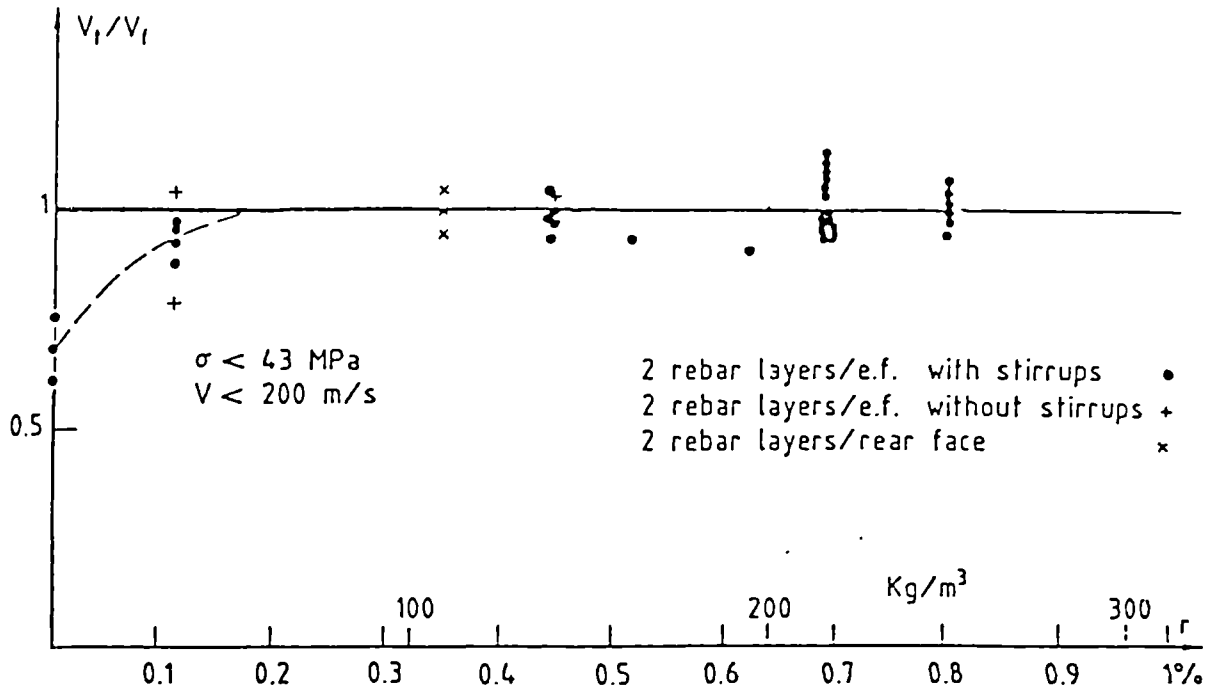


FIG. (2.6)

TEST - CEA EDF FORMULA COMPARISON

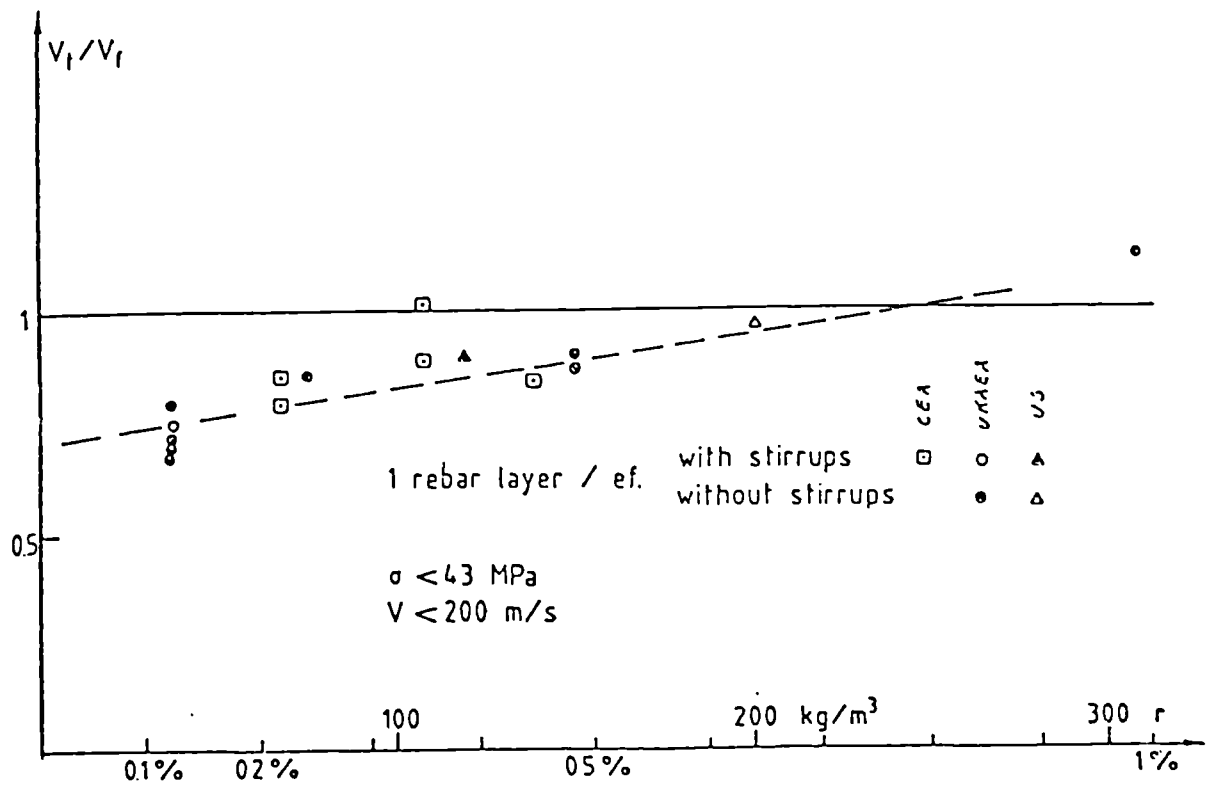


FIG. (2.7)

TESTS - CEA EDF FORMULA COMPARISON

diameter of the target = 2.3 m
 thickness of the target = 0.246 m
 diameter of the missile = 0.12 m
 mass of the missile = 27 kg

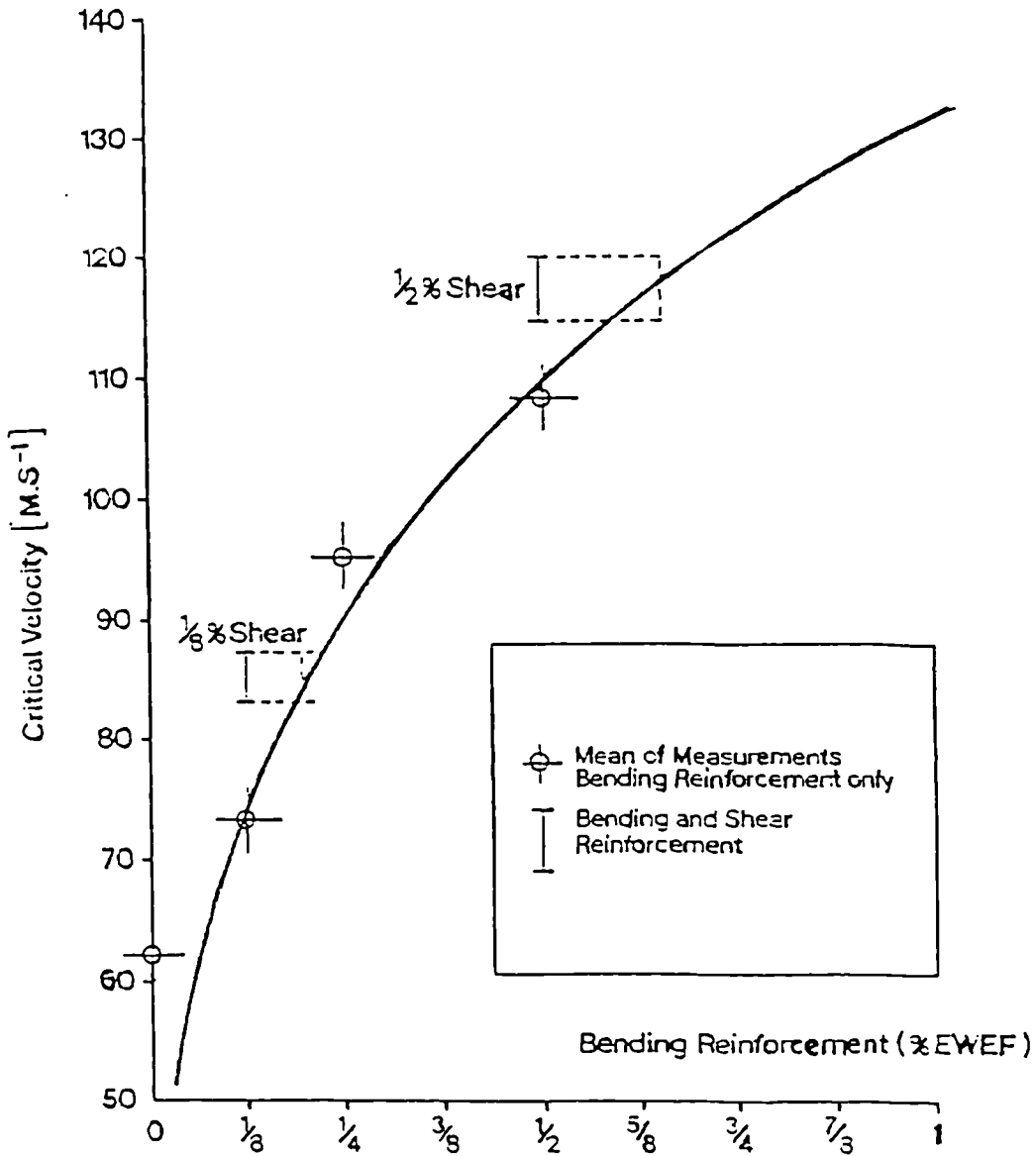


FIG. (2.8)

THE VARIATIONS OF CRITICAL PERFORATION VELOCITY FOR HARD MISSILE IMPACTED UPON REINFORCED CONCRETE TARGET

2.6 Similarity and Scaling Relationships for Impact Conditions

Although modern analytical techniques are very powerful and all types of loading and structures can be analysed in principle, there is still a need for experimental testing of complete structures or parts of a structure. This is particularly the case for dynamic loading in which the behaviour of a structure is very complex and verification of analysis under laboratory or under field conditions may be necessary. Such tests can be performed at reduced or full scale using the same or different materials as the prototype. In the planning of experiments and the subsequent analysis of results, the laws of similitude must be satisfied. The prediction of prototype performance from observations of model behaviour under homologous load may be achieved if the concepts of similarity are applied. It is recognized that the locations, times and forces in one system may be homologous with locations, times and forces in a corresponding system.

In static problems there are two fundamental dimensions to consider and these are length and mass (or force). In dynamic problems a third dimension, the time, is also considered. In order to produce a true model, therefore, three independent scale factors should be chosen, s_L , s_m and s_t relating to length, mass and time, respectively. All other scale factors follow from the governing differential equations, if available, or from dimensional analysis (33).

The scale factor is so conceived that s_i denotes the ratio between the quantity i in the model and an identical quantity in the prototype, i.e. $s_h = h_m/h_p$ for the depth of a beam (subscript m stands for model, p for prototype). A model is said to be geometrically similar to the prototype if all its dimensions are scaled by the same factor. Corresponding points or time which do not necessarily have equal values are called homologous. Generally there is similarity if a function m has a constant ratio to a function p evaluated for a homologous point and a homologous time. In regard to a stress-strain diagram this means that the modulus of elasticity, yield stress and failure stress must be similar in the prototype and model. Also, the dimensionless strain is the same in the prototype and model.

The problem considered in reinforced concrete structures can be assumed to be independent of temperature effects so the relevant fundamental dimensions are mass, length and time. In most impact situations the materials in the missile and target structure are stressed well beyond the linear elastic limit into the range of nonlinear behaviour. To achieve the necessary similitude between the various constitutive relationships for such composites as reinforced concrete, identical material scaling was used in which the aggregate particles may be scaled and the reinforcing bars may be replaced by suitable wire (33). By such an approach identity of stress-strain curves for the model and prototype materials can be achieved. The selection of "replica" scaling for materials immediately sets to unity the scaling relationships for density, stress, strain and velocity.

Using the scaling factor for linear dimensions defines all the other scaling relationships (34). This is shown in column five table (2.4), where it can be seen that the scaling law is now extremely simple. Experimental investigation (32) have been carried out using "replica" scaling at three different linear scales which were 1.0, 0.37 and 0.12 scale models. It was found that the response and general behaviour of the model followed very closely that of the prototype.

The specific application of similarity and scaling to the experimental work reported in this thesis will be given in Chapter 4.

Table (2.4): Scaling relationships associated with impact studies

Parameter	Dimensions	Full scale value	General model value	Model value using REPLICA modelling	Typical quantities
Length	L	d	$s_L d$	sd	Missile dimensions Target dimensions
Mass*	M	m	$s_m^* m$	s_m^3	Missile mass Target weight
Time	T	t	$s_t t$	st	Duration of load Natural period of target
Density	ML^{-3}	ρ	$s_\rho \rho$	ρ	Densities of materials in structure and missile
Strain	-	ϵ	$s_\epsilon \epsilon$	ϵ	
Stress	$ML^{-1}T^{-2}$	σ	$s_\sigma \sigma$	σ	Includes pressure and material moduli
Velocity*	LT^{-1}	v	$s_v v^*$	v	Missile velocity Stress wave velocities Ejecta velocity
Acceleration	LT^{-2}	a	$s_a a$	$s^{-1} a$	(Except gravity)
Rate of strain	T^{-1}	r	$s_r r$	$s^{-1} r$	
Force*	MLT^{-2}	w	$s_w w^*$	s_w^2	Applied load Structural reactions
Energy*	ML^2T^{-2}	E	$s_E E^*$	$s^3 E$	Kinetic energy of missile

The scale factor is defined as $s = f_m / f_p$

Parameters marked * are not independent quantities.

CHAPTER THREE

THE DESIGN, CONSTRUCTION AND OPERATION OF THE HIGH VELOCITY IMPACT APPARATUS AND ASSOCIATED INSTRUMENTATION

3.1 Introduction

The review of the literature that has been undertaken does not include specific reference to the effects of varying the high amounts of reinforcement (1% to 3% each way) and the influence of maximum aggregate size upon the local damage which arises as a result of high velocity impact.

It has been stated that the objectives of the work reported herein are to investigate the effect of varying the amount of reinforcement and the influence of the maximum size of aggregate upon the scabbing and perforation damage of reinforced concrete slabs. In order to carry out a relevant experimental programme a high velocity impact facility was required to be constructed. This apparatus is capable of firing missiles up to 4 kg mass at velocities of the order of 150 m/sec. Thus the apparatus is capable of operating over a significant range for current purposes.

This chapter describes the design and construction of an impact testing facility situated within the heavy structures laboratory of the Department of Civil Engineering together with a description of the instrumentation necessary to measure and record the impact event.

3.2 The High Velocity Impact Facility

A variety of methods may be employed to produce an impact load (35). The method adopted by the author used a high pressure source to accelerate a missile along a barrel to

impact upon a target. The air pressure method offers good control of missile speed. The use of a gravity method of impact required prohibitive headroom if the apparatus was to be capable of operating over a significant range of impact velocity.

The pressure chamber used as the compressed air reservoir had a volume of 0.4 m^3 and the air was released by a rapid release valve. The system was designed to operate at a maximum pressure of 4.55 N/mm^2 . The maximum operating pressure for the valve and chamber were 4.6 N/mm^2 and 6.9 N/mm^2 respectively.

The pressurised air for the chamber was provided by compressed air cylinders (size J, British Oxygen Company) at a pressure of 13.7 N/mm^2 . A regulator controlled the pressure transferred to the pressure vessel such that the latter operated at 4.55 N/mm^2 .

The barrel within which the missile travelled was 4.5 m long and had an internal diameter of 50 mm . This length is sufficient to enable a 4 Kg mass to reach a velocity of 150 m/sec . The barrel was constructed from grade A carbon steel and was honed to H8 specification, B.S. 5242, Part 1, 1987 (36).

Fig. (3.1) shows the schematic arrangement of the impact apparatus. The pressure vessel was equipped with an automatic safety air-relief valve to limit the maximum pressure in the reservoir to 4.55 N/mm^2 . The outlet from the reservoir was 50 mm nominal bore pipe leading to the barrel. A rapid release valve which was activated electrically was situated between the pressure vessel and the barrel. The

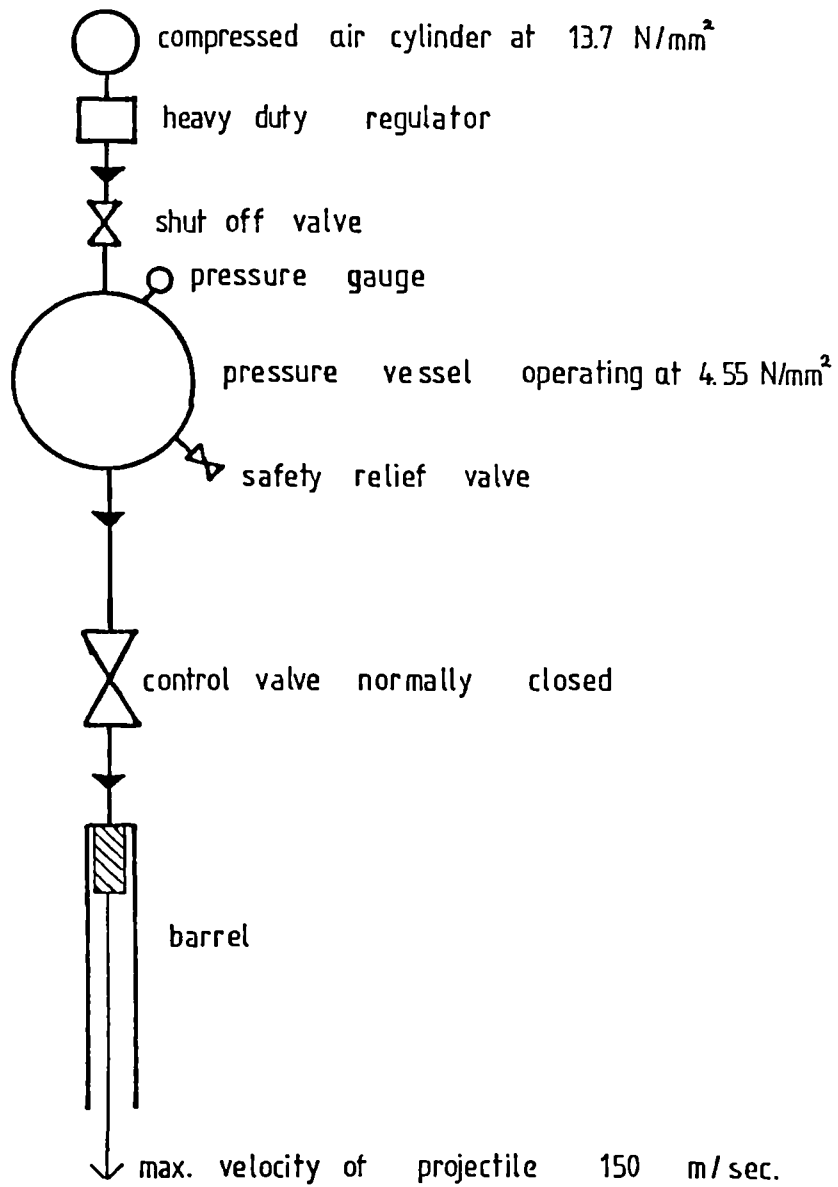


FIG. (3.1) SCHEMATIC DIAGRAM OF MISSILE LAUNCHER

characteristics of this valve were, maximum inlet pressure 4.6 N/mm², maximum pressure drop 0.07 N/mm², and maximum flow rate 1.37 m³/sec.

The length of the missile was variable depending upon the required mass. Its diameter, however, was a constant 49.8 mm and it was made from EN24T steel. Two seals were fitted around the circumference of the missiles to contain the pressure causing motion, plate (3.1). In all tests the missiles were located at a fixed position inside the barrel and when the solenoid valve was opened the air pressure from the reservoir acted on the missile and accelerated it along the barrel. This system can produce a variety of impact forces by either varying the applied pressure or the mass of the missile. The barrel was situated in an under ground chamber with concrete walls about 32 cm thick for safety, fig. (3.2).

The test slab specimen was supported on eight load cells which were precompressed by eight tension rods such that all stages of the impact process the load cells were in compression. The cells were fixed to a rigid steel frame and this frame was connected to a very rigid massive concrete floor, plate (3.2).

3.3 Instrumentation

3.3.1 Missile Impact Velocity Measurement

The missile impact velocity was measured in each test. The measurement device obtained the time of travel of the missile over a distance of 500 mm which was assumed to provide an accurate missile velocity measurement. This device consisted of two sets of photodiodes with 12V light

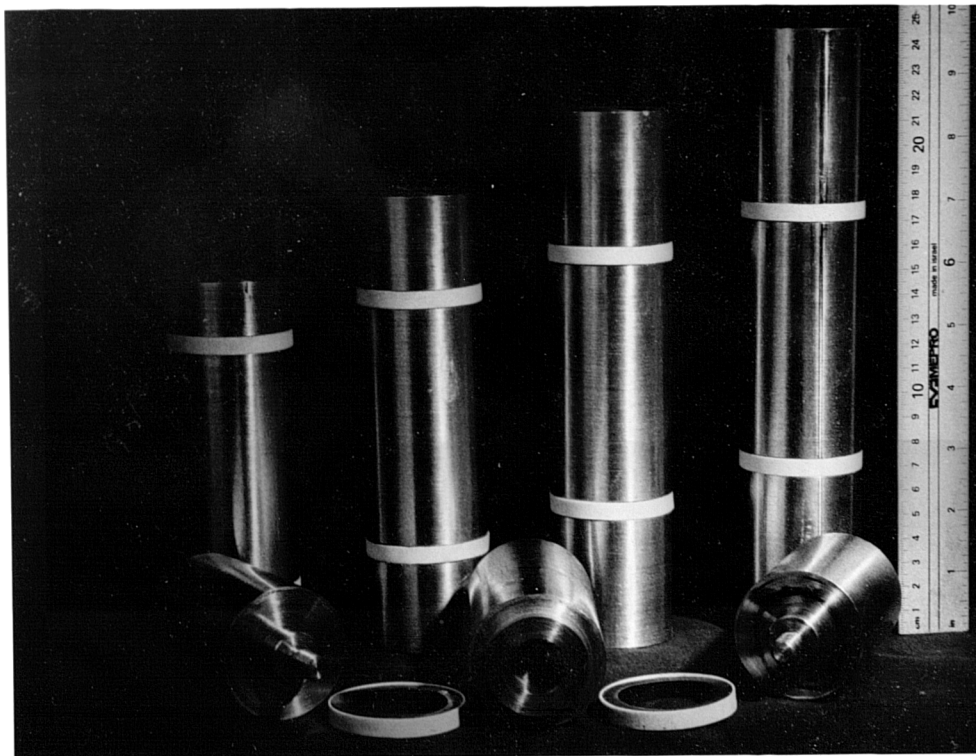
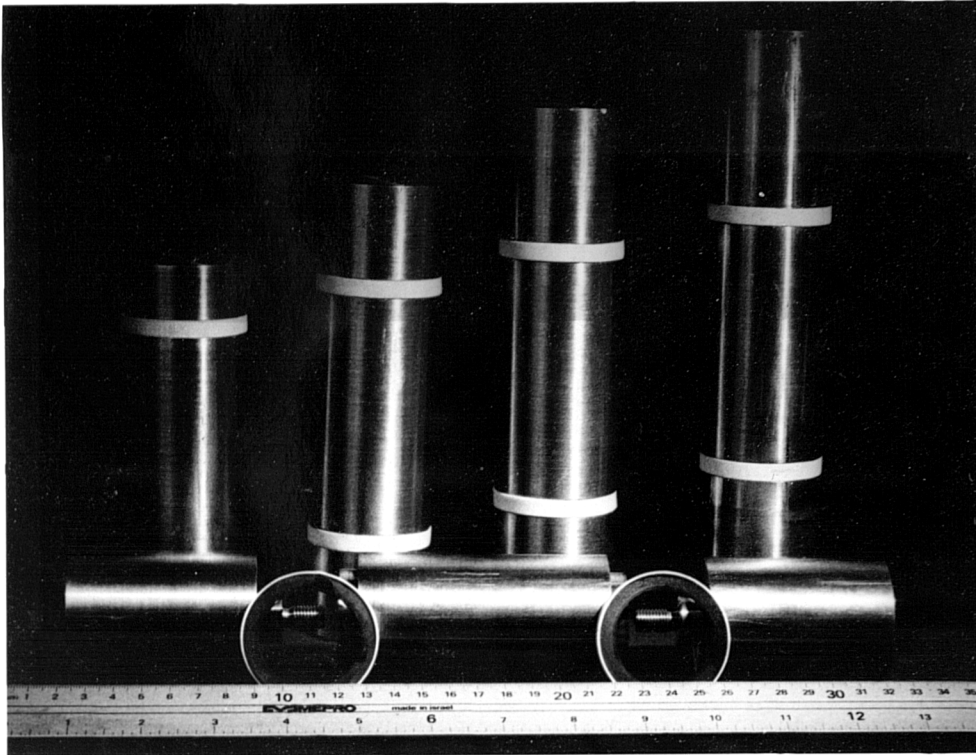


PLATE (3.1)

THE MISSILES SHOWING THE AIR SEALS

ITEM NO.	DESCRIPTION	air cylinder size J (BOC LTD)
1	compressed air regulator	model M 600
2	heavy duty hose	
3	long pressure vessel	0.4 m ³ capacity
4	pressure relief valve	
5	safety direct mounting	pressure gauge
6	shutt-off valve	
7	barrel	
8	pipe support	
9	2" nominal bore control valve	
10		

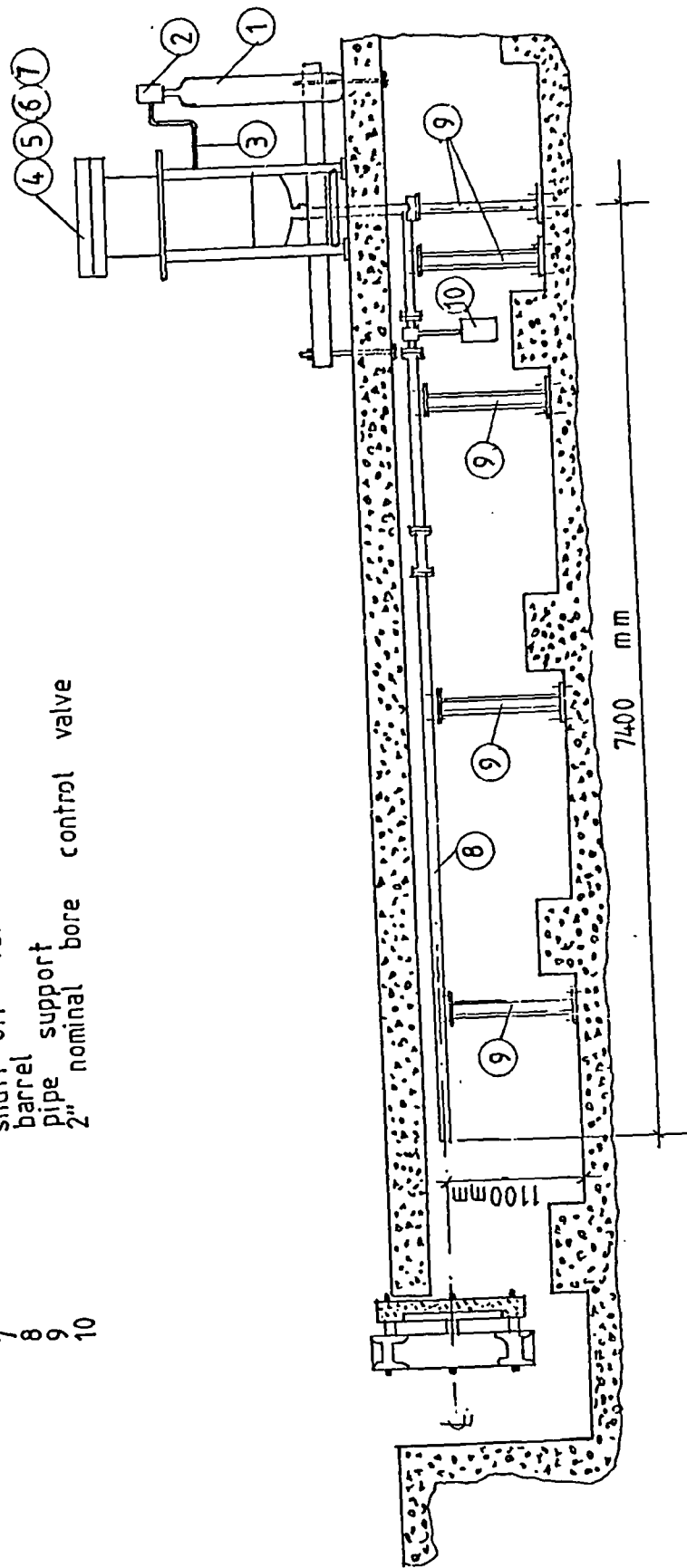


FIG. (3.2) THE MISSILE LAUNCHER

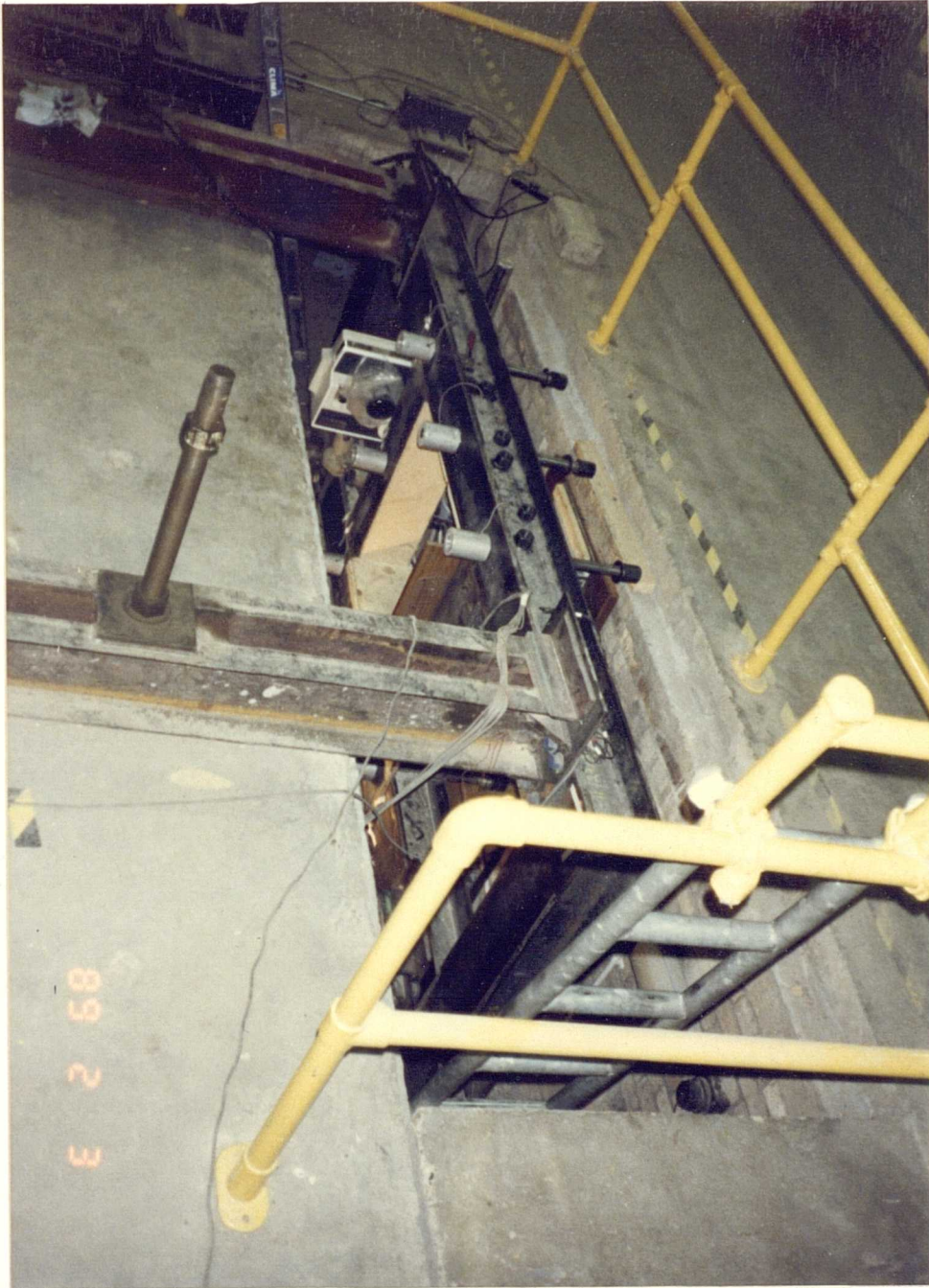


PLATE (3.2)
THE TESTING FRAME

bulbs set at 500 mm apart plate (3.3). The device was mounted in a fixed position on the end of the barrel in line with the barrel longitudinal axes within the space available between the end of the barrel and the impacted slab face so that the photodiodes were placed at 1300 mm and 800 mm from the impacted slab face. The electric circuit for start-stop switching signals is shown in fig. (3.3). Just before impact the missile cut the two light beams of the photodiodes and triggered the start and stop signals in an advance timer counter via the photo-electric switches. The time interval was then registered and the velocity of the missile calculated.

3.3.2 Slab Reaction Load Cells

Eight load cells were used to measure the time history of the reaction force of the slabs,. The load cells consisted of aluminium hollow cylinders having a wall thickness of 5.15 mm and a length of 113 mm, plate (3.4). The walls were accurately machined, each having twelve electrical resistance strain gauges (FLA-6-11) fixed to the surface. Fig. (3.4) shows the arrangement of gauges for maximum sensitivity. This arrangement eliminated bending strain and thus measures only axial strain. All the load cells were calibrated to a maximum force of 2.5 ton (24.91 KN) in increments of 0.5 ton (4.98 KN) using a testing machine with a 5 ton (49.82 KN) proof ring capacity to measure the applied load. The strain gauge signals were amplified using a model S.E 429 type amplifier, the amplified output being recorded on an oscillograph type S.E 6012 (U.V. recorder) set at a rate of 0.5 m/sec paper speed. The output from the load cells was recorded for two seconds. Plate (3.5) shows the recording

system.

3.3.3 Linear Variable Differential Transformer

Electrical transducers are commonly employed in dynamic measurement since they can provide a continuous recording of the mode of deformation at specific points on a specimens. Since the impacted slab has a circular central part with constant thickness which simulated the boundary conditions and give symmetrical deformation of a specimens, four linear variable differential transformers over the radius were used in all the tests to measure the dynamic displacement. These points were at distance of 205 mm, 270 mm, 335 mm and 400 mm from the slab center. The transducers were fixed to the test frame as shown in plate (3.6). The LVDTs were calibrated using a laboratory made tool consisting of a V-block and a digimatic micrometer head capable of indicating up to 0.001 mm. The block and micrometer were mounted in line on a flat steel plate. The probe was adjusted so that the signal from the LVDT was zero. Calibration took place about this point for a deflection of ± 48 mm. The signal from the LVDT was reproduced on a U.V. recorder and was proportional to deflection enabling the direct measurement of the displacement. During a test the recorder ran for two second with a paper print out speed of 0.5 m/sec.

3.3.4 High Speed Camera

The velocity of the ejected concrete from the back of the slab opposite to the impacted area was obtained using a Hadland high speed rotating prism camera capable of filming at speed up to 10000 frames per second. To film the ejected concrete the camera was set up in relation to the slab,

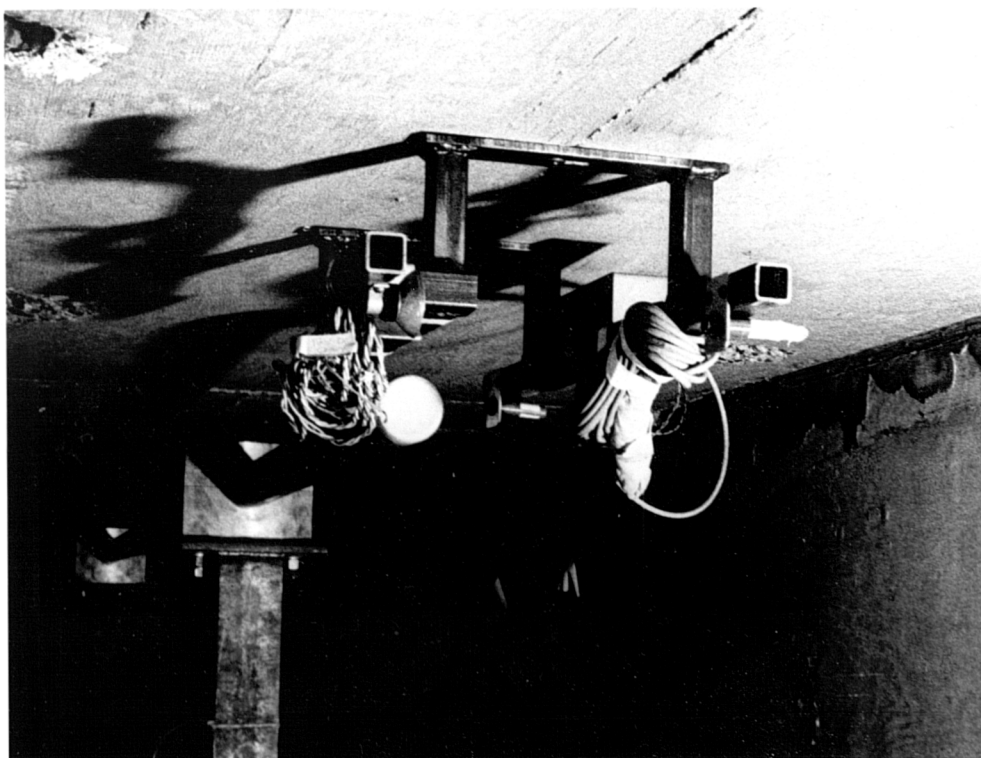
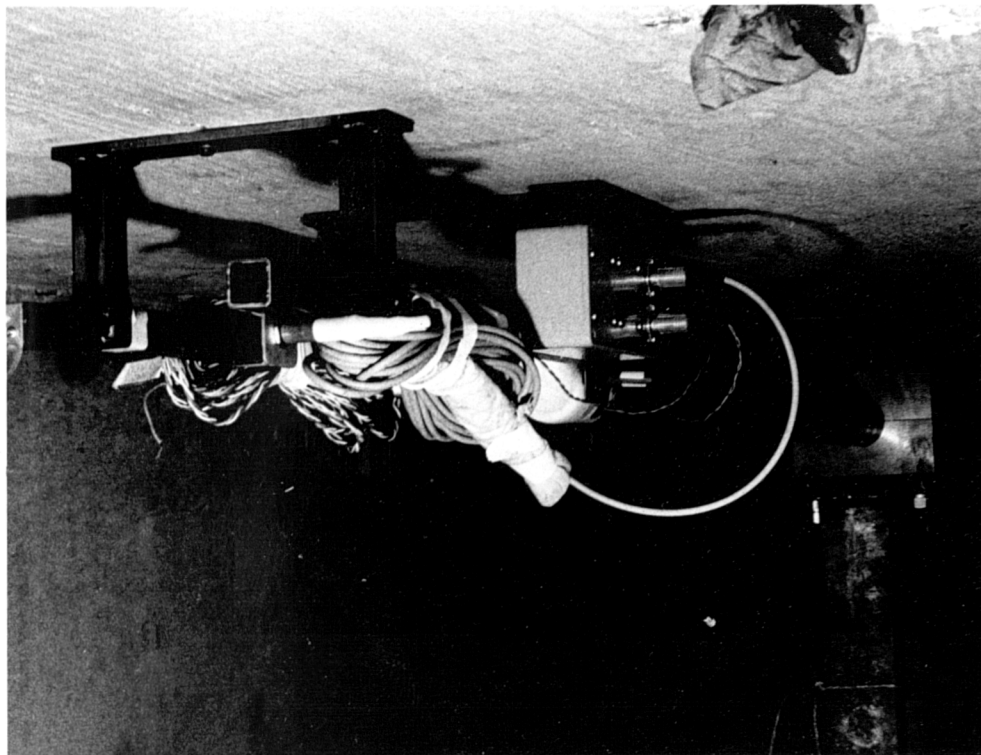


PLATE (3.3)

MEASURING DEVICE FOR DETERMINATION
OF MISSILE VELOCITY

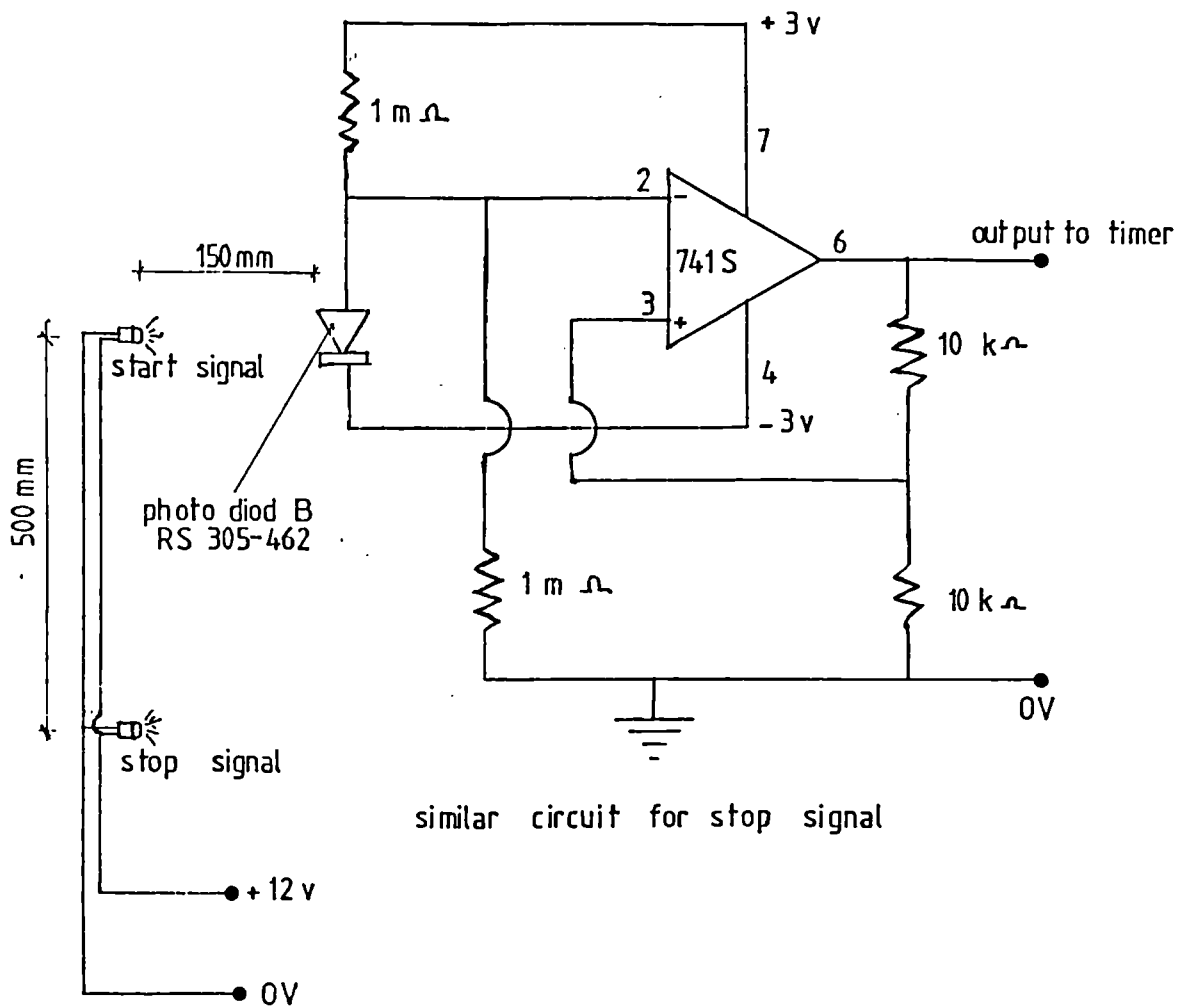


FIG. (3.3) ELECTRIC CIRCUITRY FOR MISSILE IMPACT VELOCITY MEASUREMENT

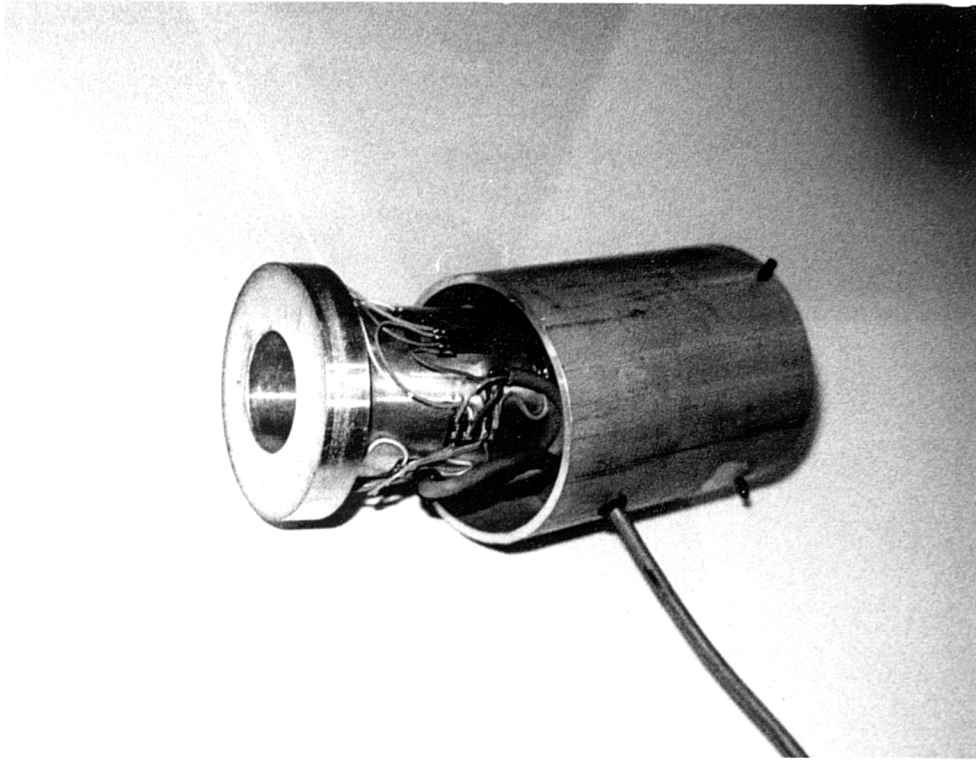


PLATE (3.4)
THE LOAD CELL

NOTE

A = active strain gauge
 D = dummy strain gauge

STRAIN
 GAUGE CIRCUIT

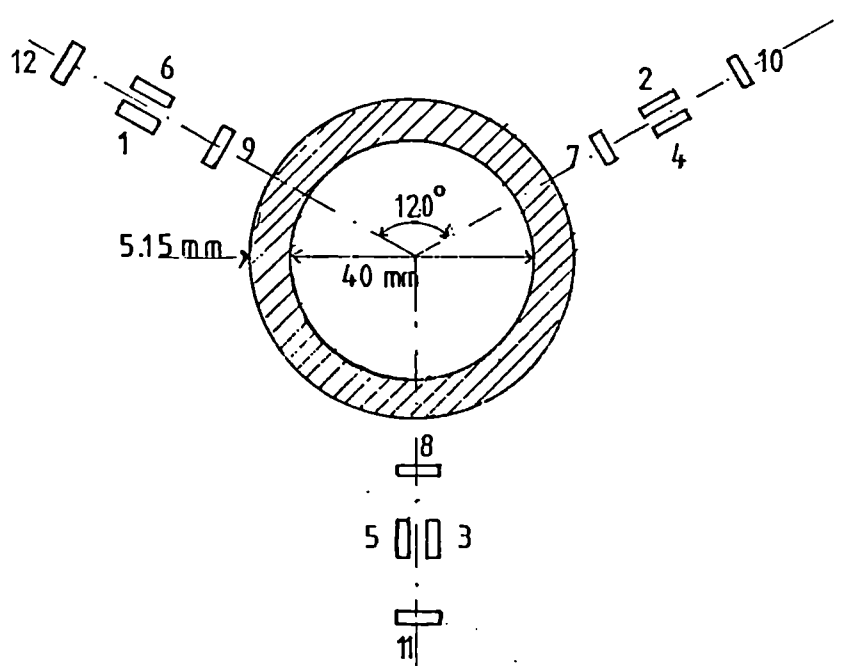
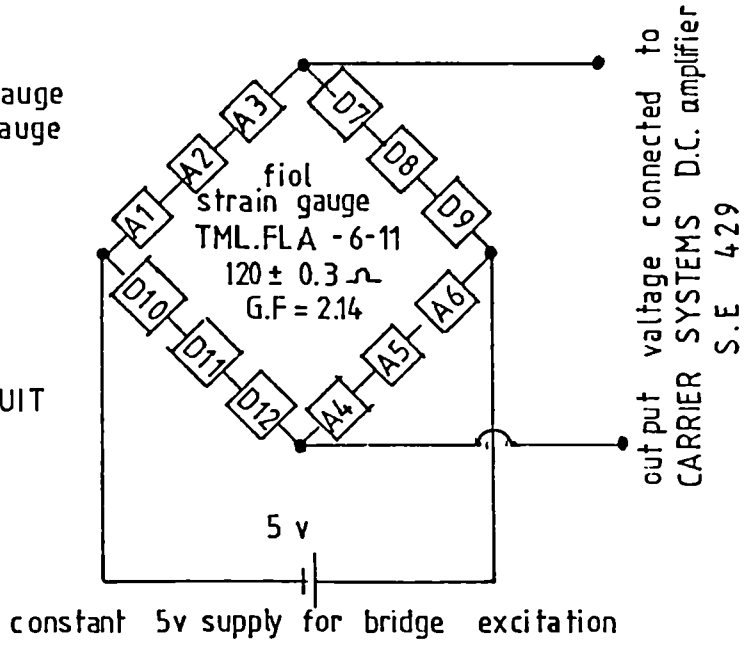


FIG.(3.4) STRAIN GAUGE ARRANGEMENTS ON LOAD CELL

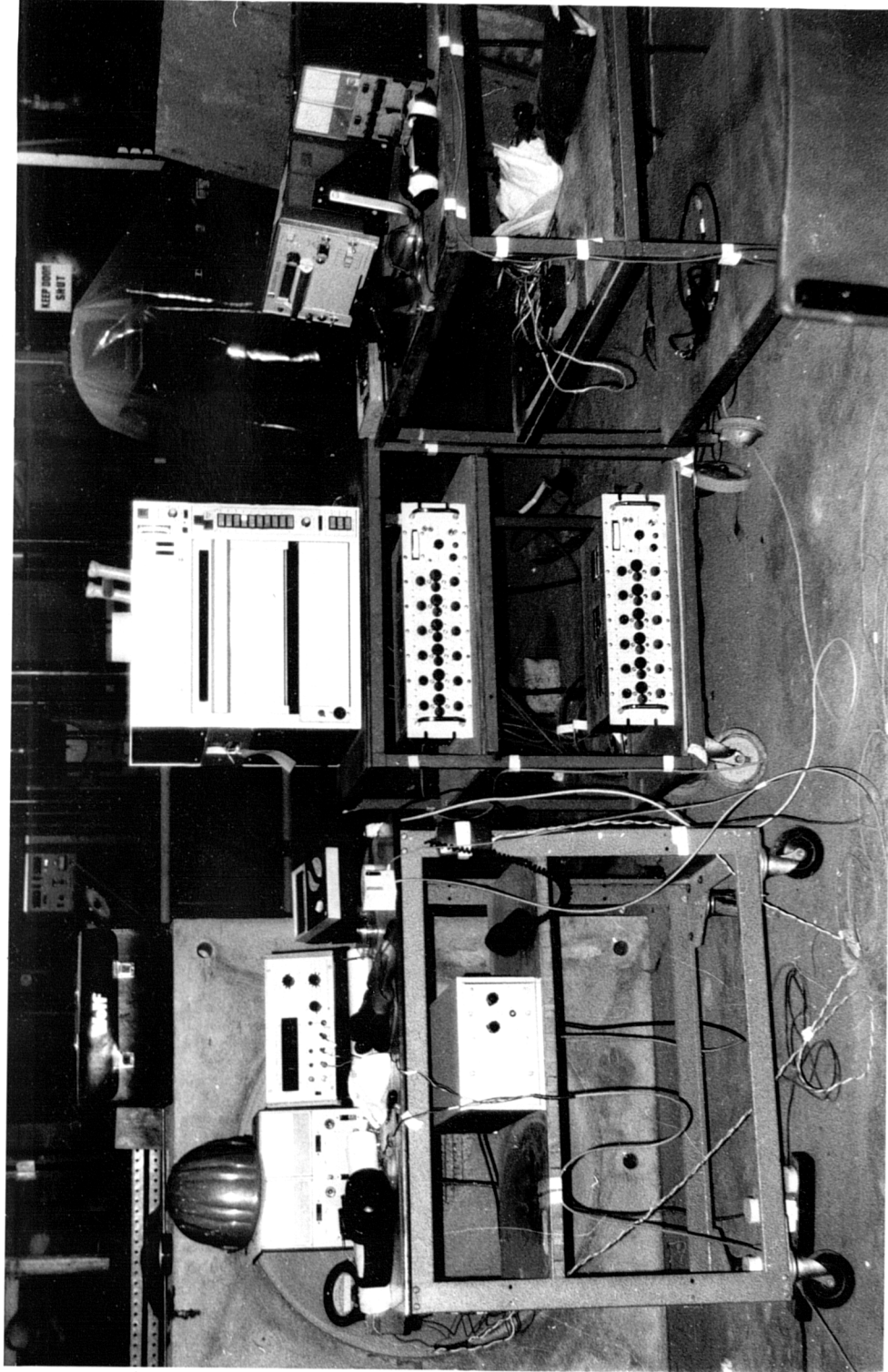


PLATE (3.5)

THE RECORDING SYSTEM USED
THROUGHOUT THE EXPERIMENTS

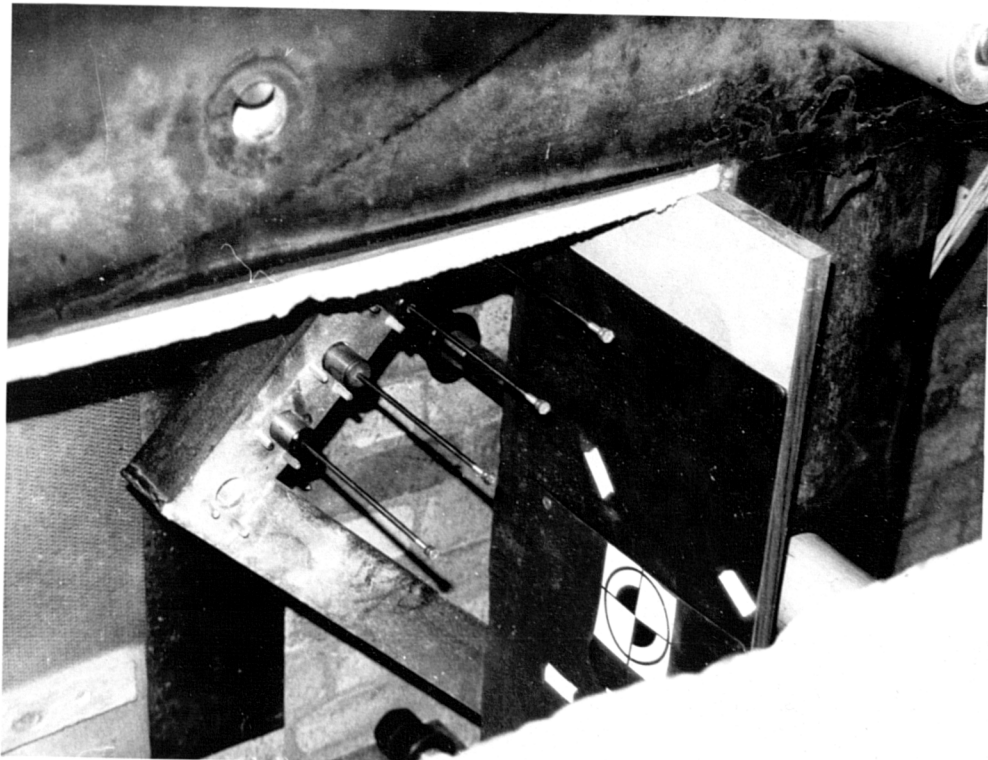
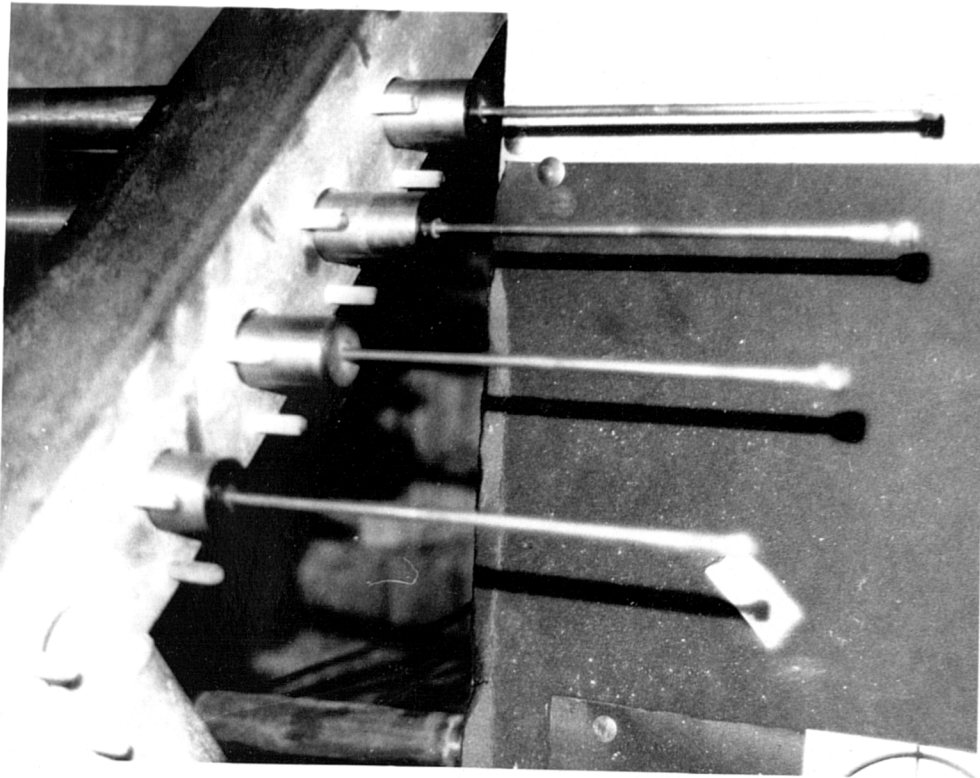


PLATE (3.6)

ARRANGEMENT AND METHOD OF FIXING
OF LVDT'S TO THE TEST FRAME

plate (3.7). A Kodak type 7224 Eastman 4-X negative film of standard 100 ft (30.48 m) length was used for each test. To make sure that the event was recorded on the film at a constant film speed (5000 frames per second) the camera was required to trigger the control valve to release the pressurised air after 9 m of the film went through the camera. This procedure gave enough time for the camera to reach the required film speed to capture the event. For real time correlation of the film an electronic pulse generator deposited timing marks on the film at a pre-set rate of 1000 marks per second.

For subsequent analysis of each film, an x-y scale reference was placed on the rig. The system shown in plate (3.8) was used as a film analysis facility to obtain accurate information from the high speed film. The apparatus consisted of a pin registered analysis projector with a frame counter and single frame advance operator. The film was projected onto a screen above which a sonic digitiser was situated. The digitiser measured coordinates and positions anywhere on the screen and was interfaced with a BBC microcomputer to give a graphical output of the ejected concrete particle velocity.



PLATE (3.7)

HIGH SPEED CAMERA

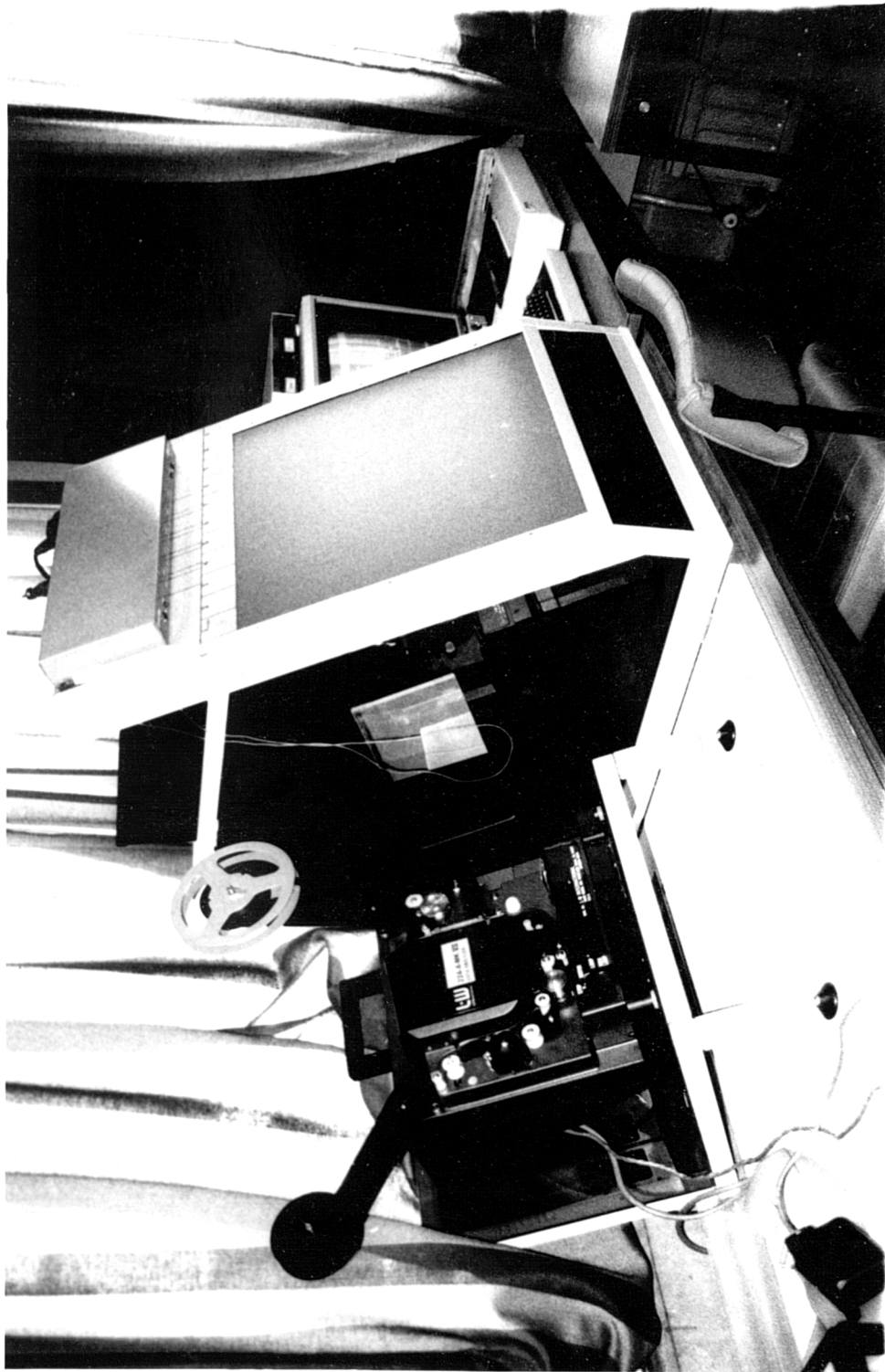


PLATE (3.8)

FILM ANALYSIS SYSTEM

CHAPTER FOUR

THE FABRICATION OF THE TARGET SPECIMENS AND THE EXPERIMENTAL PROCEDURE

4.1 Introduction

The experimental programme consisted of sixty-four impact tests on model reinforced concrete slabs with fixed supports. Thirty-four tests were conducted to study perforation resistance and the remaining thirty were used to study scabbing resistance. In these tests the quantity of bending reinforcement in the targets was varied between 0% and 1.55% of the cross-section area of concrete each way for each face. The targets were impacted by a solid flat faced steel missile. The perforation and scabbing resistance have been quantified in terms of the velocity at which the missile causes either just perforation or just scabbing. The missile impact velocities for the tests on the models were ranged from 42 m/sec to 123 m/sec for perforation tests and 40 m/sec to 62 m/sec for scabbing tests. This chapter describes the fabrication of the specimens as well as the experimental procedure.

4.2 The Test Specimens

4.2.1 Model Slab

For practical convenience the slabs were identical square targets 1150 mm × 1150 mm and 150 mm thick. A circular central part with a reduced thickness of 120 mm, 100 mm or 80 mm was formed within the square. This arrangement allowed appropriate boundary conditions and provided a containing restraint for the area impacted by the missile. These conditions were similar to those provided by parts of a

prototype structure surrounding an impacted zone fig. (4.1). The target thickness to diameter ratio was chosen on the assumption that although missile perforation or penetration is a local phenomenon, some bending of the impacted structure should be allowed around the impact zone (32). The reduced circular area within the square provided appropriate boundary conditions allowing symmetrical bending. The measured transient deflection of the target are shown in fig. (5.2) and fig. (5.4) and confirm the validity of this assumption.

4.2.2 Model Materials

4.2.2.1 Reinforcement

Black Annealed Mild steel plain wire, 4 mm diameter was used as the model reinforcement. This wire was used as the longitudinal main reinforcement. The two way spanning slabs were reinforced in two perpendicular directions, each face, to give the same resistance bending moment per unit width in both directions. The quantity of this reinforcement varied between 0% and 1.55% of the cross-section area of concrete, each way, each face. The 4 mm wires were cold worked using a twisting machine which applied a constant force for a fixed time (12 sec) to straighten the wires. The bond between the wire and concrete was improved by increasing the roughness of the wire surface. The original low yield stress of 139 N/mm^2 was increased to 453 N/mm^2 at 0.2% plastic strain proof stress. This gave the model wire reinforcement a stress scale factor of unity compared to the prototype reinforcement. A typical stress-strain curve for wire used is shown in fig. (4.2). The tensile test was carried out in accordance with the recommendations of B.S. 18: 1987 (37). In general the stress-strain characteristics of the model

tests series NO.	thicknss (t) mm	diameter (2R) mm
S1,S2,S3,S4,S5,S8 S9,S10 and S11	100	860
S6	80	690
S7	120	860

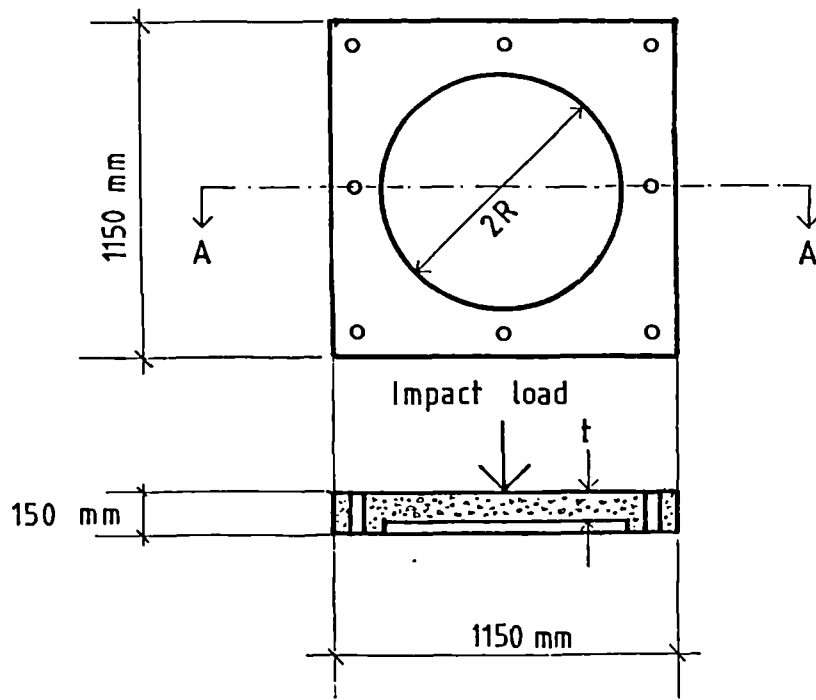
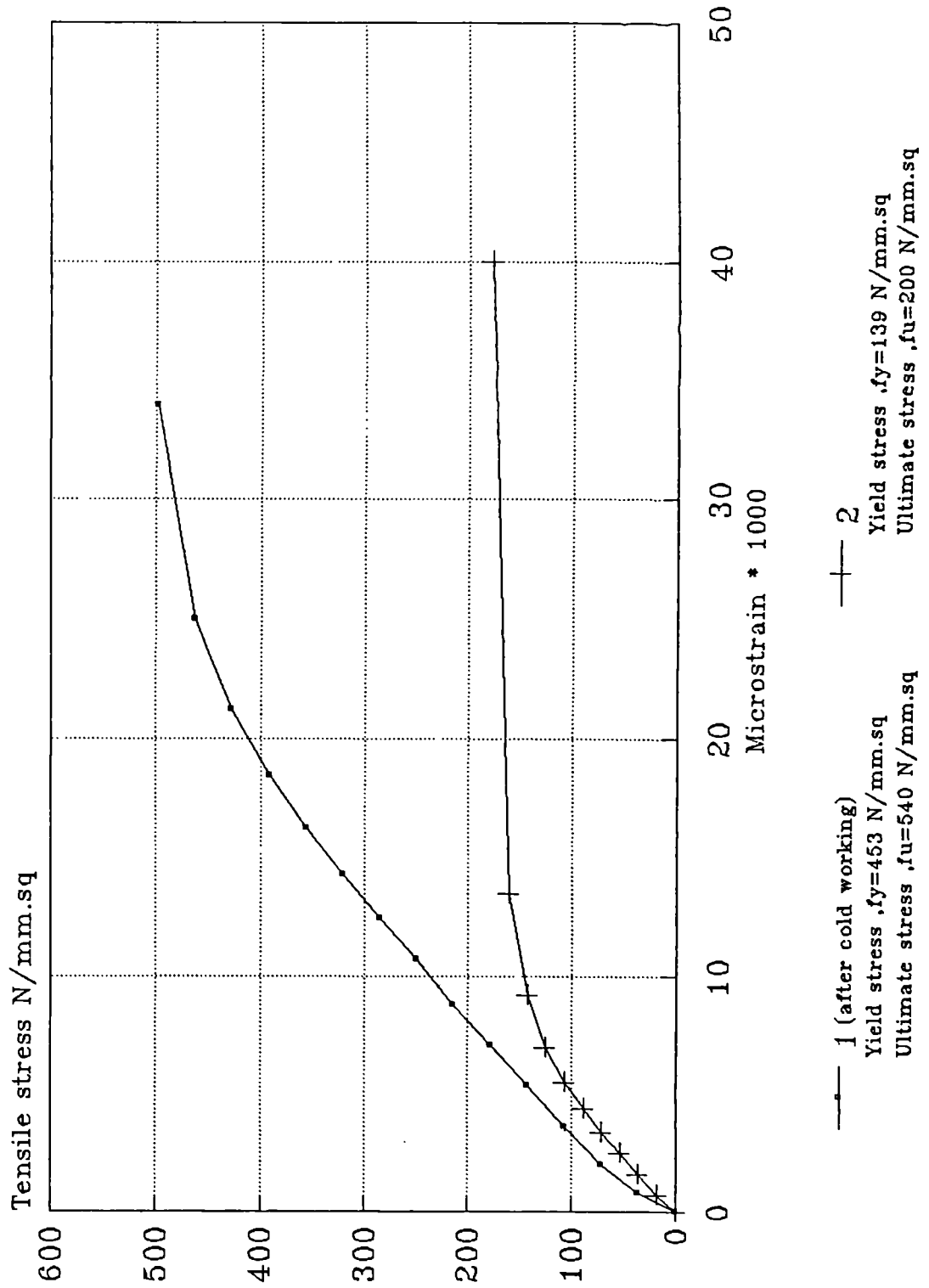


FIG.(4.1) THE MODEL SLAB DIMENSIONS

FIG. (4.2) STRESS-STRAIN CHARACTERISTICS OF WIRE REINFORCEMENT



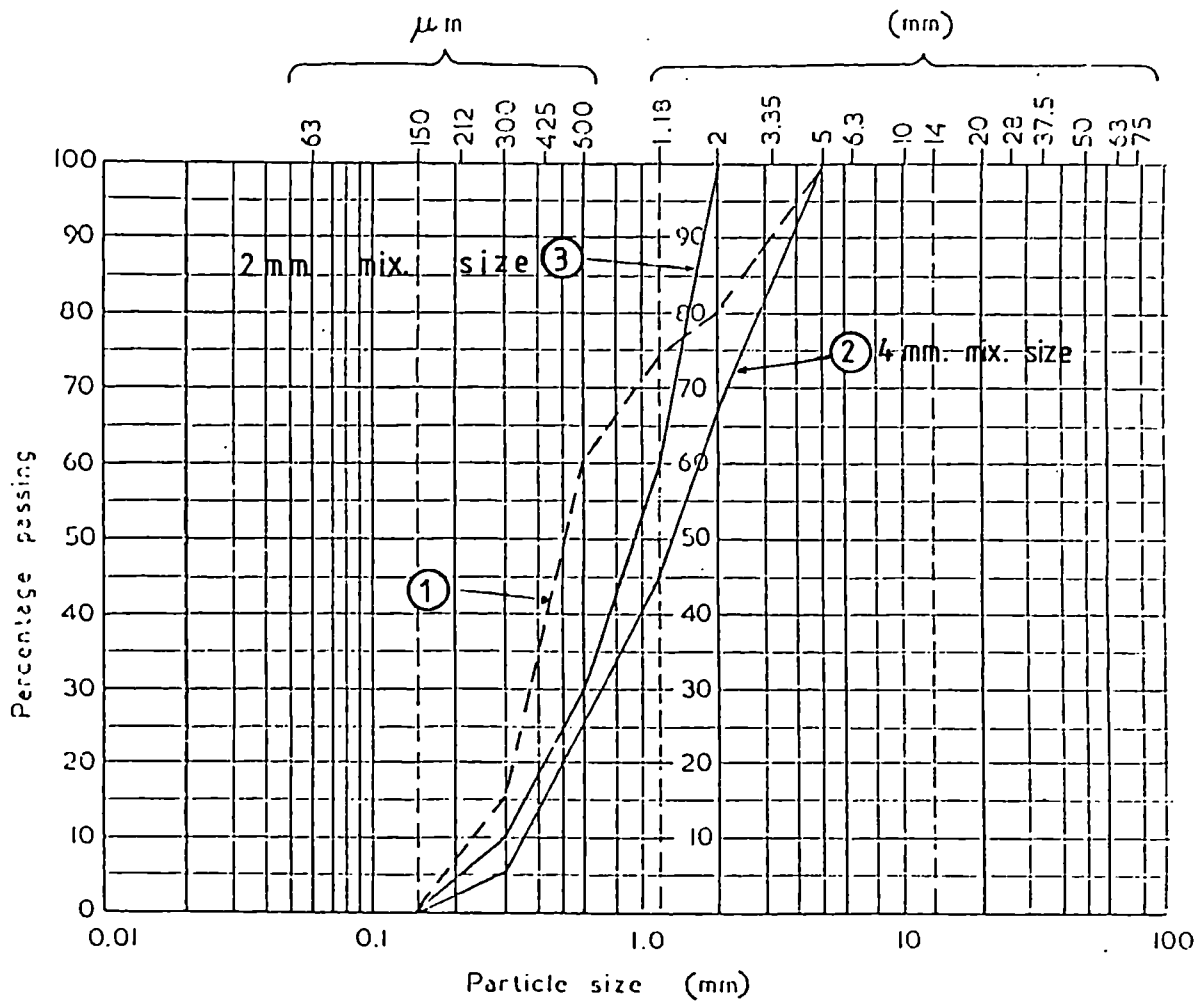
wire reinforcement are typical of the prototype steel reinforcement.

4.2.2.2 Model Concrete

The properties of micro-concrete are such that the material is ideal for modelling prototype concrete. The maximum aggregate size used in the research described here in did not exceed 4 mm. To satisfy similitude conditions the grading of concrete constituents should also be scaled. A more finely ground cement was not available so Ordinary Portland cement was used throughout the experimental programme. The cement used was supplied in a single batch. The chemical composition, fineness and test methods of material properties for this cement are given in B.S. 12: 1978 (38). River gravel sand was used as the micro-concrete aggregate and fig. (4.3) provides details of the grading. The sieve analysis complied with B.S. 410: 1986 (39) and the aggregate grading for the micro-concrete was found to be within zone 1, B.S. 882: 1983 (40).

4.2.3 Experimental Programme

The details of the experimental programme are shown in table (4.1). A series of ten experiments were conducted, each series having six identical slabs. A further series consisting of four slabs only were also conducted. For the first ten series, three slabs were tested to study the perforation resistance and the second three were tested to study the scabbing resistance. In the eleventh series, four slabs were tested to study the perforation resistance with no reinforcement. The boundary conditions were kept the same for all the slabs and the missiles used were flat faced right



ASTM sieve No.	4	5 - 8	8 - 16	16 - 30	30 - 50	50 - 100	100 - 200
nomina aperture size (mm)	4.75	4 - 2.36	2.36 - 1.18	1.18 - 0.6	0.6 - 0.3	0.3 - 0.15	0.15 - 0.075
① actual grading of river gravel sand	1.2%	18.7 %	6.1 %	13 %	45.3 %	14.6 %	1.1 %
② agg. grading for microconcrete	1.1%	31.7 %	21.3 %	21.2 %	18.6 %	6.1 %	—
③ agg. grading for microconcrete	—	—	40 %	30 %	20 %	10 %	—

FIG. (4.3) SIEVE ANALYSIS OF RIVER GRAVEL SAND AND AGGREGATE GRADING FOR MICROCONCRETE

Table (4.1) : Details of Experimental Programme

Series No.	Maximum size of aggregate (mm)	Mass of missile (kg)	Reinforced ratio kg/m ³	Percentage of reinforcement	Total No. of slabs
S1	4	3.7	160	1%(1 layer each face 4 mm ϕ at 24 mm c/c each way)	6
S2	4	3.7	390	2.5%(2 layers each face, 4 mm ϕ at 20 mm c/c each way)	6
S3	4	3.2	390	2.5%(2 layers each face, 4 mm ϕ at 20 mm c/c each way)	6
S4	4	2.6	390	2.5%(2 layers each face, 4 mm ϕ at 20 mm c/c each way)	6
S5	4	2.2	390	2.5%(2 layers each face, 4 mm ϕ at 20 mm c/c each way)	6
S6	4	3.7	390	2.5%(1 layer each face, 4 mm ϕ at 12.5 mm c/c each way)	6
S7	4	3.7	400	2.5%(2 layers each face, 4 mm ϕ at 16 mm c/c each way)	6
S8	4	3.7	490	3.1%(2 layers each face, 4 mm ϕ at 16 mm c/c each way)	6
S9	4	3.7	320	2%(2 layers each face, 4 mm ϕ at 24 mm c/c each way)	6
S10	2	3.7	390	2.5%(2 layers each face, 4 mm ϕ at 20 mm c/c each way)	6
S11	4	3.7	0	0	4

cylinders made of very high strength steel (EN24T) having an ultimate tensile stress within the range (850-1000 N/mm²).

The independent test variables were

1. The mass of the missile, four different masses were used, 3.7 kg, 3.2 kg, 2.7 kg and 2.2 kg.
2. The missile impact velocity which varied between 40 m/sec to 123 m/sec.
3. The slab thickness, three values were used, 80 mm, 100 mm and 120 mm.
4. The concrete compressive strength which varied between 44 N/mm² and 57 N/mm².
5. The maximum aggregate size which was either 4 mm or 2 mm.
6. The percentage of the bending steel reinforcement, which was varied between 0% and 1.55% of the cross-section area of concrete each way, each face.

4.3 Specimen Fabrication

4.3.1 Reinforcement Cages

The reinforcing bars were first twisted and then cut to the required length before welding. The welding was conducted along the edge of the mesh only and a special wooden mould was used to fix the specific bar spacing required. Plate (4.1) shows a typical reinforcing cage being made. Single or double layers of reinforcement, each face were used depending upon the area of steel required. Plate (4.2) shows details of a finished cage. In particular, the reinforcement for the edge beam should be noted. The edge beam provided a suitable



PLATE (4.1)

SPECIMEN MANUFACTURE SHOWING
WELDING OF THE MESH

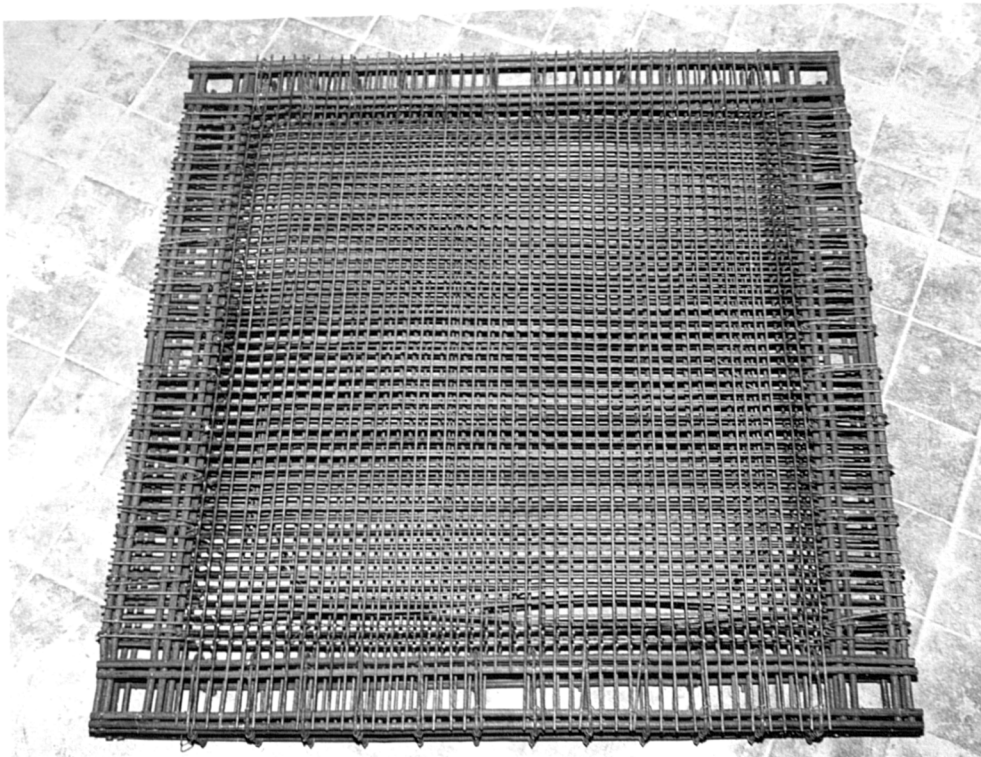
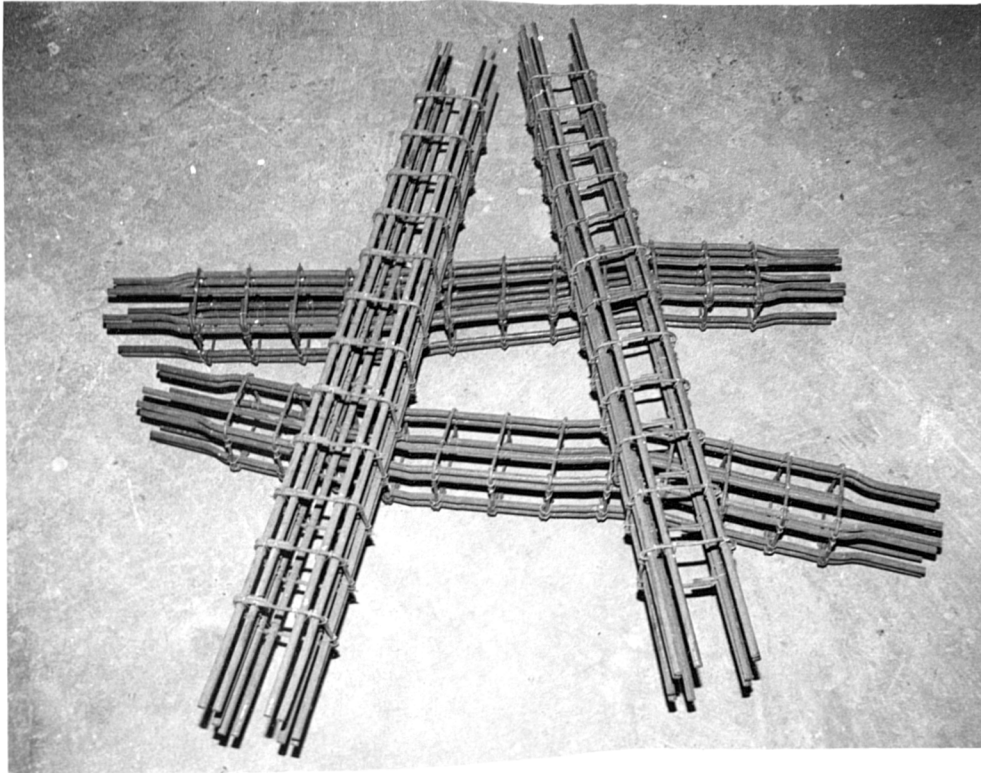


PLATE (4.2)

REINFORCEMENT SHOWING THE
EDGE BEAMS

restraint for the area impacted by the missile. The completed reinforcement cage was placed in an oiled mould and eight plastic pipes were placed within the edge beams at equal distances to make a hole for the tension rod plate (4.3). These tension rods were used to support the slab in the testing frame against a system of load cells, which provided a history of the reaction load during the impact event.

4.3.2 Micro-concrete Mix

The micro-concrete mix produced from the aggregate described in section 4.2.2.2 was designed to produce compressive and tensile strengths which were as close as possible to those expected from the prototype concrete mix used in structures which are generally designed to withstand high velocity impact. This mix had an average 28 days compressive strength of between 44 N/mm^2 and 57 N/mm^2 from 100 mm control cubes and a tensile splitting strength of between 3 N/mm^2 and 4 N/mm^2 . Aggregate/cement and water/cement ratios of 4 and 0.46 by weight, respectively, were chosen for the slabs having a 4 mm maximum size of aggregate. For slabs having a maximum aggregate size of 2 mm the corresponding ratios were 3.53 and 0.46 by weight. Several trial mixes were made before selecting a design that produced good workability and the required compressive strength without excessive shrinkage.

4.3.3 Concrete Casting and Curing of Specimens

Two slabs were cast together with ten 100 mm cube control specimens each time. The wooden form shown in plate (4.4) and the cube moulds were cleaned prior to the application of

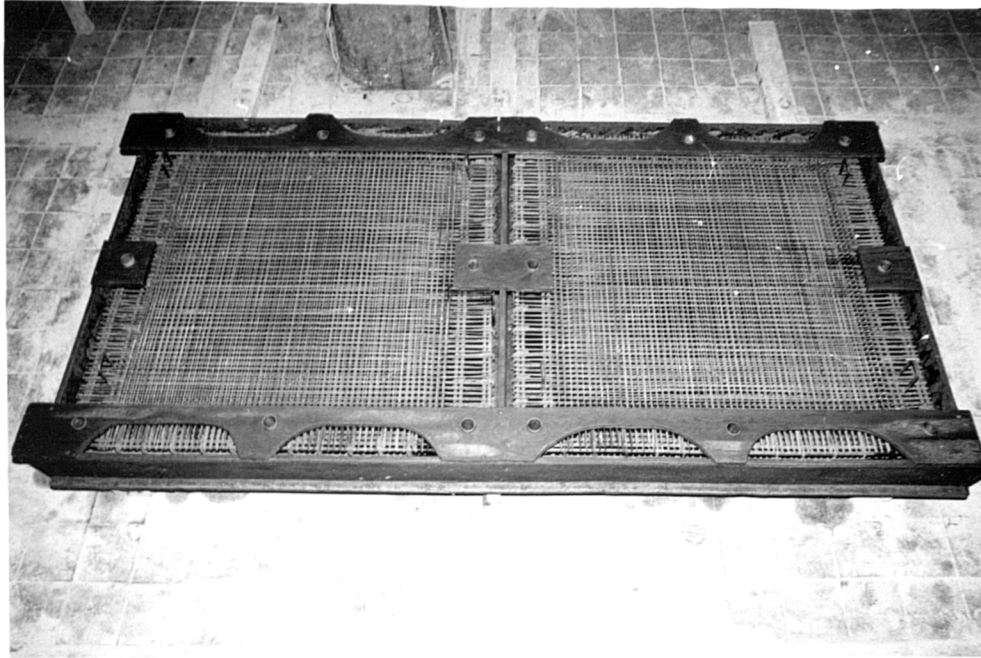


PLATE (4.3)

REINFORCEMENT AND MOULD PRIOR
TO CASTING



PLATE (4.4)

WOODEN FORM FOR CASTING SLABS

a thin film of mould oil. The reinforcing cages were placed in the form with 8 mm cover for the top and bottom face of the slabs. The cover was achieved by using plastic spacers. Four pans of 0.1 m³ capacity each of an electric concrete mixer were used to cast the two slabs and ten cubes. The correct proportion of cement, individual sizes of aggregates, sand and water were accurately weighed. The individual sizes of aggregates were poured into the pan with the cement and were then mixed for a minute, followed by the sand and mixed for a further minute. Water was then added in stages with the mixing pan switched on and the contents were mixed for a further two minutes. The wet concrete was deposited in the slab moulds and cubes in four and three layers, respectively. After each pour the vibration table was switched on and a vibration poker was run along the outside surfaces of the form until the wet concrete began to bleed. The top surfaces of the slabs and cubes were over filled by 1 mm and left for two hours to allow for initial shrinkage before being levelled and trowelled smooth. The slabs and cubes were then left to set normally in the laboratory under an ambient temperature of 18°C for a total of 24 hours after casting. The two slabs were then carefully demoulded and cured for a further four days by covering with wet cloth. The cubes having been removed from the moulds were immersed in a water pan in the laboratory until they were ready for testing.

4.3.4 Concrete Control Specimens

The compressive strength and tensile splitting strength were obtained using 100 mm cubes. According to B.S. 1881 Part 120: 1983 (41) the strength of a cylinder is equal to four-fifths of the strength of cube. The cylinder strength

can, therefore, be obtained from the cube strength and hence, the cylinder compressive strength of concrete used in slabs can be obtained. Three cubes were used to determine the compressive strength of each slab and the tests were carried out using an Avery-Denison crushing machine, plate (4.5). The loading rate was 150 KN/minute in accordance with B.S. 1881, Part 116: 1983 (42). To check the tensile splitting strength, two cubes were tested for each slab using the same crushing machine at a loading rate of 30 KN/minute according to B.S. 1881 Part 117: 1983 (43). Plate (4.6) shows the testing arrangement.

4.4 Test Procedure

In all tests the targets were vertically suspended on the testing frame which rested against a massive concrete abutment. A total of 8 load cells around the edge of the slab were interposed between the slab and the testing frame, plate (4.7), to measure the reaction load during the impact event. The slab was held against the load cells by 8 bolts, which were sufficiently preloaded to ensure slab - load cell contact at all stages of the missile - target interaction. The solid steel missile was projected at the target using the compressed air gun as described in section (3.2). The principal objective of the experiments was to derive a value of missile impact velocity which would result in the target being just perforated or just scabbed. This velocity is designated the critical velocity (V_c) for perforation or scabbing and on the basis of a balance of the energy of the system before and after impact (32) and is given by

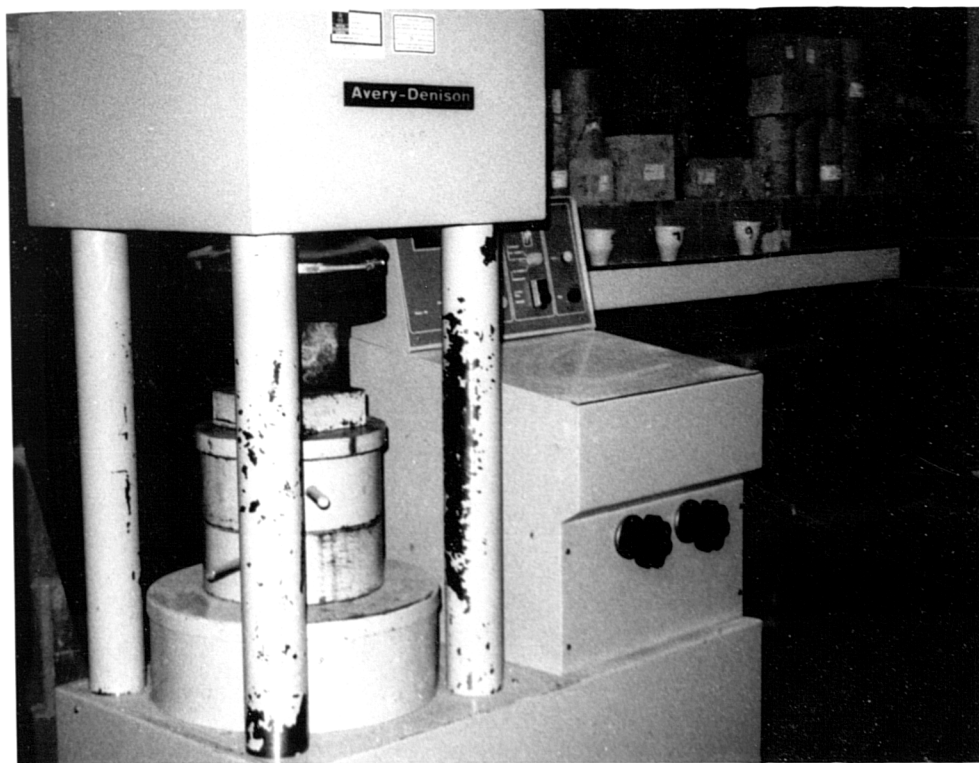
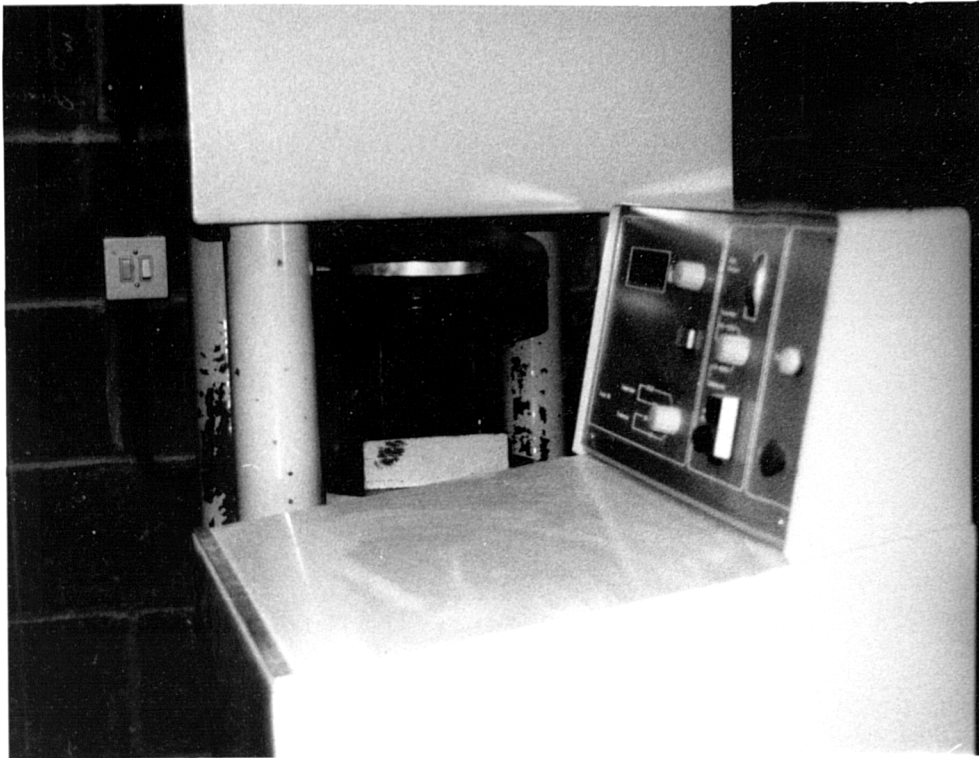


PLATE (4.5)

COMPRESSION TESTING MACHINE

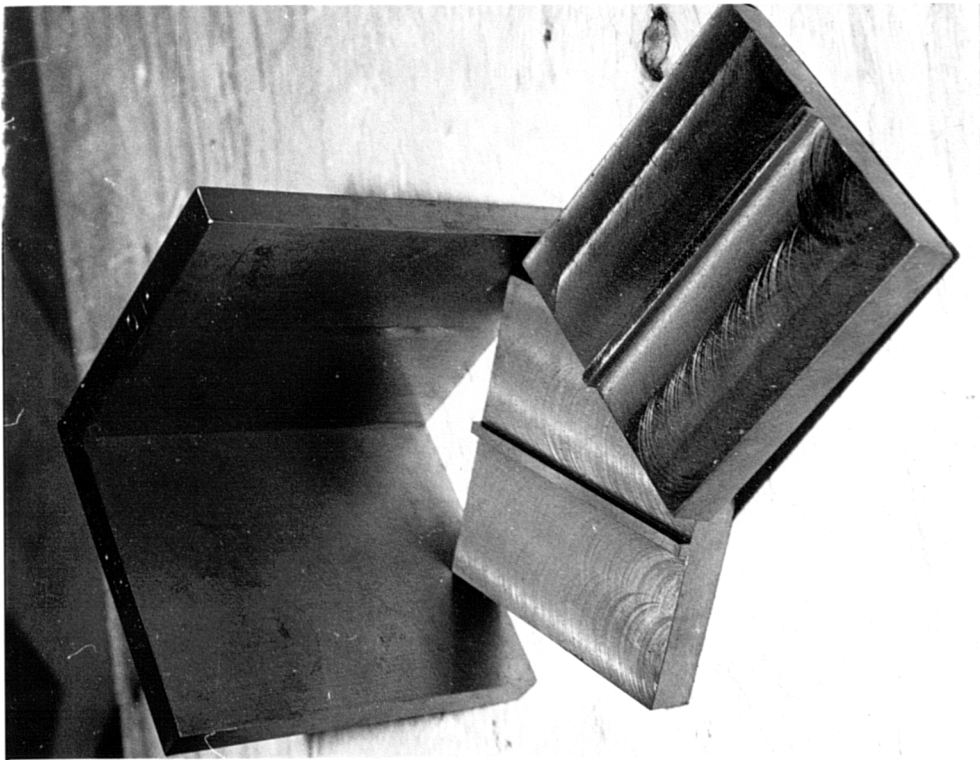
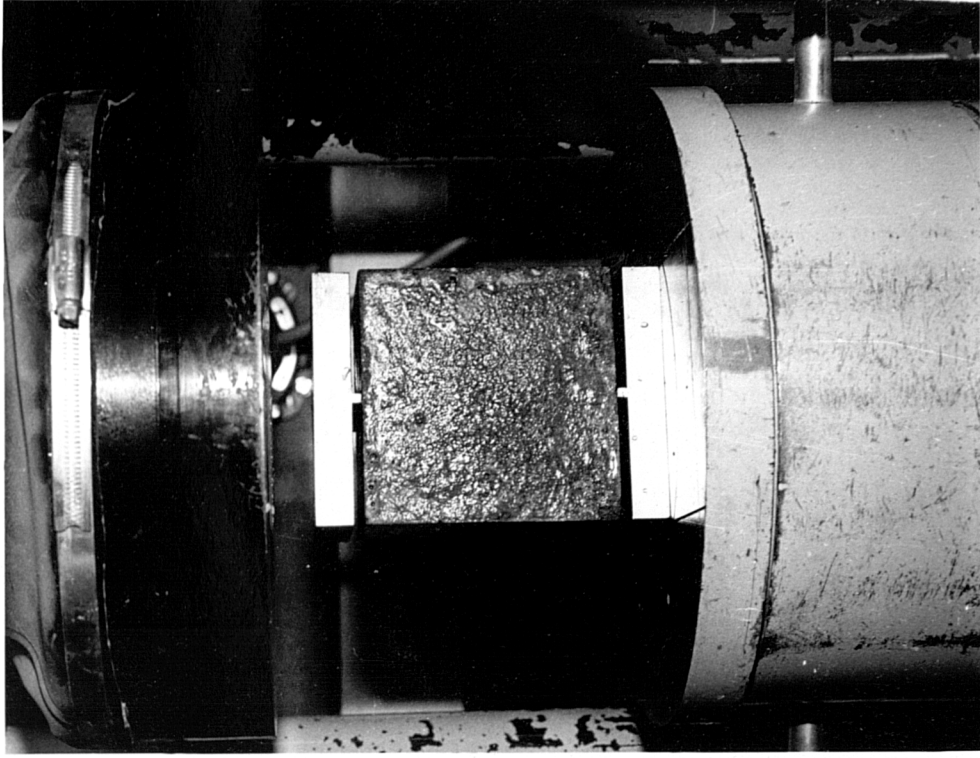


PLATE (4.6)

INDIRECT TESTING OF CONCRETE FOR
DETERMINATION OF TENSILE SPLITTING
STRENGTH

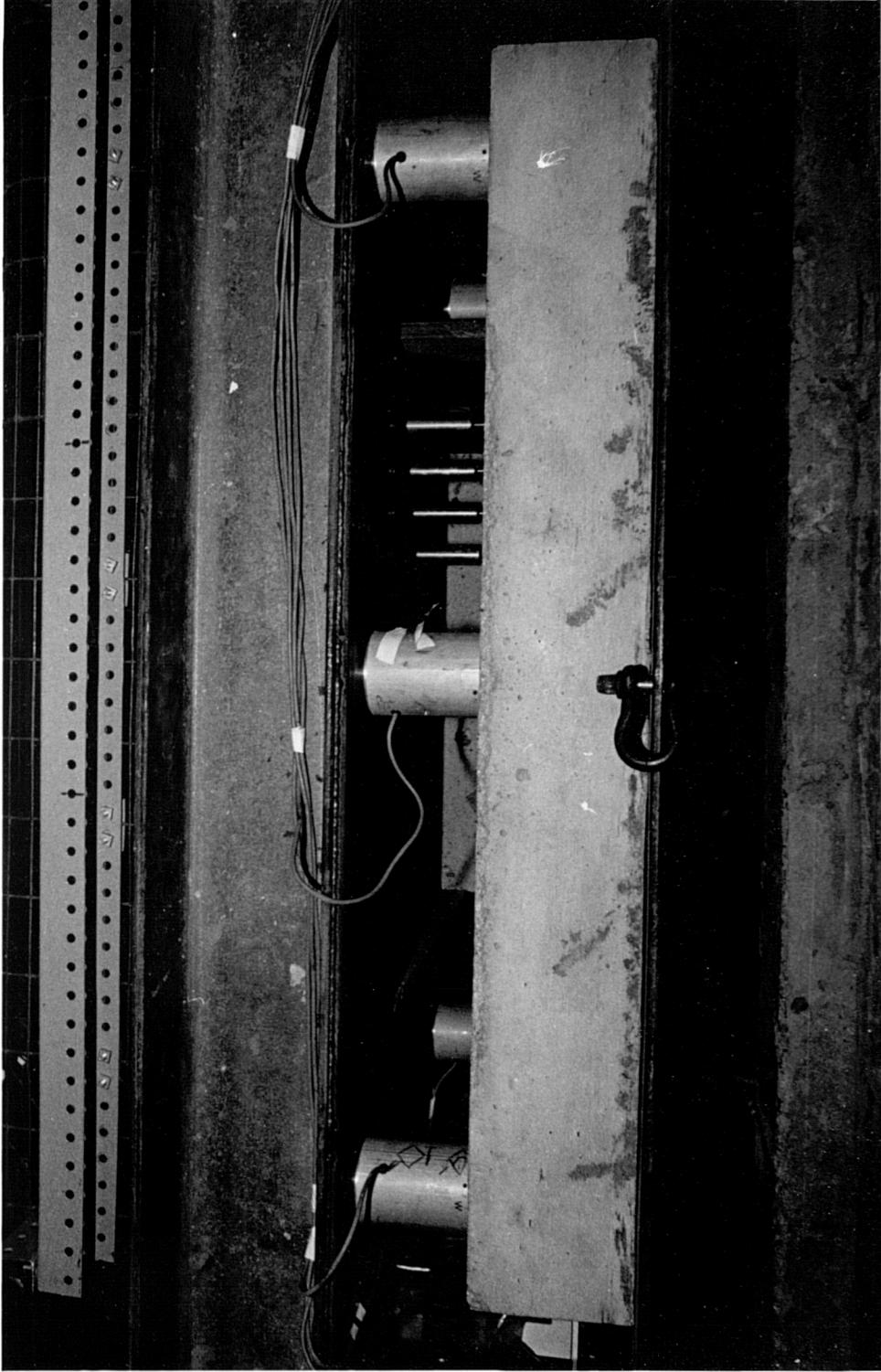


PLATE (4.7)
ARRANGEMENT OF THE LOAD CELLS

$$V_i^2 = V_c^2 + V_r^2 \left(1 + \frac{m_c}{M}\right)$$

where V_i = incident velocity of the missile.

V_r = exit velocity of the missile.

m_c = mass of concrete ejected by the impact and

M = mass of the missile.

This energy balance assumes that the ejected concrete travels at the same velocity as the exit velocity of the missile. Normally three targets of identical construction were tested for each of the chosen independent test variables and the impact velocity adjusted in successive shots to approach the critical value. Transient deflections of the targets and the reaction load imposed by the target on the testing steel frame were measured during the impact process. High speed cinephotography recorded the impact event from the back of the slab opposite to the impact area to obtain the velocity of the ejected concrete. Missile impact velocity was measured by the method described in section (3.3.1). A preliminary period of 15 minutes was allowed before each test to enable the electrical apparatus to stabilize and for the necessary safety checks to be conducted on the complete experimental system.

CHAPTER FIVE
EXPERIMENTAL RESULTS

5.1 Introduction

This chapter presents the experimental high velocity impact test results for the model concrete slabs. The results of experiments are described in which rigid faced steel missiles have been impacted upon concrete model slabs to study the perforation resistance or the scabbing resistance of the slab. These two resistances have been quantified in terms of the velocity at which the missile just perforates the slab, or the face opposite impact is just scabbed. In addition to this velocity, transient deflections of the target and the magnitude of the load imposed by the target on the testing frame were measured for each test. A high speed camera recorded the impact event from the back of the slab opposite to the impacted area to obtain the velocity of the ejected concrete.

5.2 The Perforation Resistance of The Model Concrete Slabs

5.2.1 Critical Perforation Velocity V_{cp}

The results of experiments are described in which rigid flat faced steel missiles have been impacted upon thirty-four concrete targets to study the perforation resistance of the targets. The quantity of flexural steel in these slabs was varied between 0% and 1.55% each way, each face. The concrete panel under test was supported on eight load cells against a massive abutment as shown in plate (3.2).

A solid steel missile was projected by compressed air at the centre point of the target. The impact force was controlled

by varying the missile mass or the pressure causing motion.

The principal objective of the experiments was to derive a value of missile impact velocity which would result in the target being just perforated. This velocity is designated the critical velocity for perforation V_{cp} , and is derived on the basis of a balance of the energy of the system before and after impact (32).

Thus

$$V_i^2 = V_{cp}^2 + V_r^2 \left(1 + \frac{m_c}{M}\right)$$

where

V_i = incident velocity of the missile.

V_r = exit velocity of the missile.

m_c = mass of concrete ejected by the impact and

M = mass of the missile.

This energy balance assumes that the ejected concrete travels at the same velocity as the exit velocity of the missile (31) and the ejected mass of concrete is equivalent to the mass of concrete contained in a cylinder of diameter 1.7 times the missile diameter and of height equal to the target thickness (32).

The details of the experimental programme are shown in table (4.1). Normally three targets of identical construction were tested to study the perforation resistance for each series. The impact velocity was adjusted in successive shots to achieve the critical value. The instrumentation and the test procedures have been described in Chapters 3 and 4 respectively. The impact test results relating to the

perforation resistance of concrete slabs are presented in table (5.1).

5.2.2 The Measurement of Transient Load at The Critical Perforation Velocity

The magnitude of the reaction upon the loading frame caused by the impacting missile was also measured during the perforation tests. The addition of the results obtained from eight load cells provided the total reaction. Fig. (5.1) shows the measurement of load-time history. The time and magnitudes of the peak reaction loads are shown in table (5.2).

5.2.3 The Transient Target Displacement at The Critical Perforation Velocity

Fig. (5.2) shows the measured transient displacements of the target at four different positions from the centre of the target at the critical perforation velocity using the linear variable differential transformer described in section 3.3.3. The time and the maximum transient deflection are shown in table (5.3).

5.2.4 General Panel Damage Caused by The Missile at The Perforation Velocity

The front and rear face damage of the target which occurred during the perforation test are shown in plates (5.1) and (5.2) respectively. When the missile passes completely through the slab, a neat round hole is noticed where the nose struck. The target rear face then shows spalling on the free surface between supports. The front and rear reinforcement mesh is deformed and in some parts broken at the place of impact. It can be seen that the concrete is shattered within

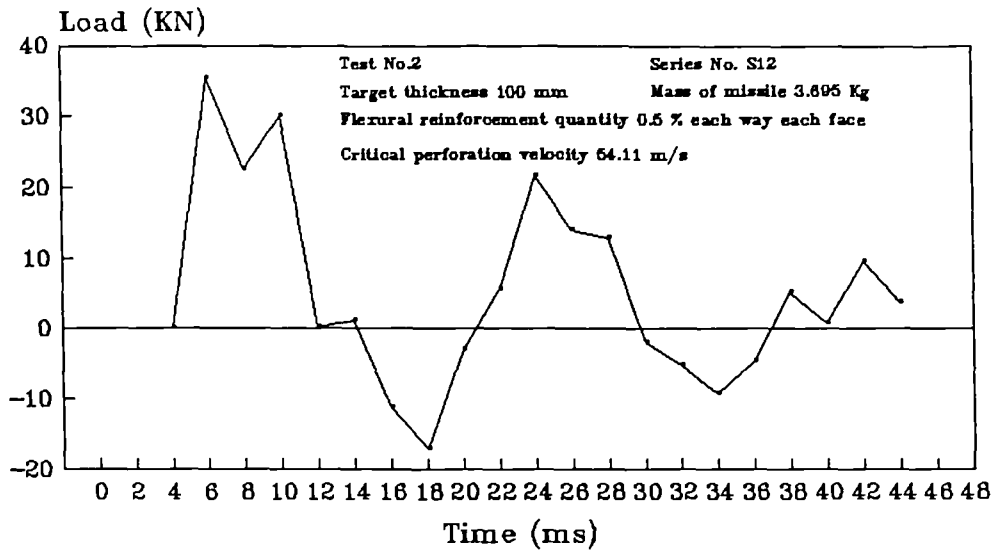
this conical plug and many concrete pieces fall from the rear face of the slab. Plate (5.3) shows the damage caused at perforation to a plain concrete specimen. In general, similar damage was evident for all the slabs tested at the perforation velocity.

Table (5.1): The results for perforation resistance tests

Test No.	Series No.	Total percentage of reinforcement	Mass of missile (kg)	Target thickness (mm)	Concrete density (kg/m ³)	Concrete compressive strength f_c' (cube) (N/mm ²)	Concrete tensile splitting strength σ_{ct} (cube) (N/mm ²)	Missile velocities (m/sec.)		
								Impact	Exit	Critical
2	S1	1%	3.695	100	2284	56.53	3.85	61.72	25.68	54.11
6	S2	2.5%	3.689	100	2257	56.0	3.57	86.76	23.01	82.56
9	S3	2.5%	3.2	100	2302	54.4	3.45	92.87	15.0	91.15
12	S4	2.5%	2.719	100	2271.75	52.93	3.40	110.85	34.37	102.7
17	S5	2.5%	2.23	100	2295	52.36	3.47	122.99	26.76	118.3
14	S6	2.5%	3.698	80	2250.6	45.66	3.31	66.75	12.12	65.33
21	S7	2.5%	3.698	120	2261	44.16	3.10	108	29.58	102.1
24	S8	3.1%	3.685	100	2269.4	48.5	3.20	96.42	30.33	89.76
27	S9	2%	3.694	100	2278.2	45.46	3.54	80.0	20.0	76.55
26	S10	2.5%	3.695	100	2246.2	46.63	3.12	84.89	18.54	82.12
62	S11	0%	3.644	100	2274.6	44.36	3.22	41.66	13.9	37.37

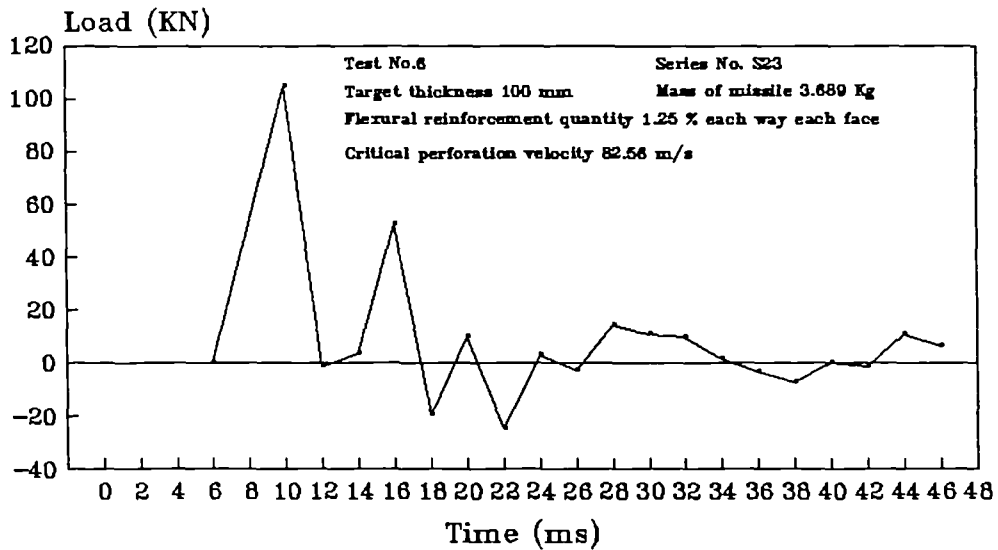
All the series have 4mm max. agg. size except S10 which had 2mm max. agg. size

FIG. (5.1a) MEASURED TRANSIENT LOAD AT CRITICAL PERFORATION VELOCITY



— S12

FIG. (5.1b) MEASURED TRANSIENT LOAD AT CRITICAL PERFORATION VELOCITY



— S23

FIG. (5.1e) MEASURED TRANSIENT LOAD AT CRITICAL PERFORATION VELOCITY

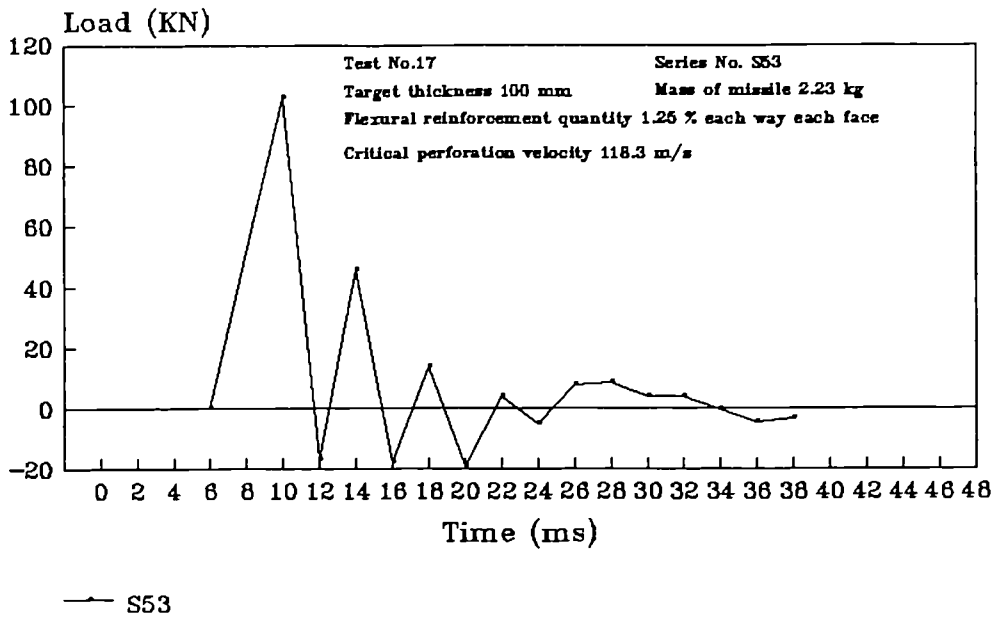


FIG. (5.1f) MEASURED TRANSIENT LOAD AT CRITICAL PERFORATION VELOCITY

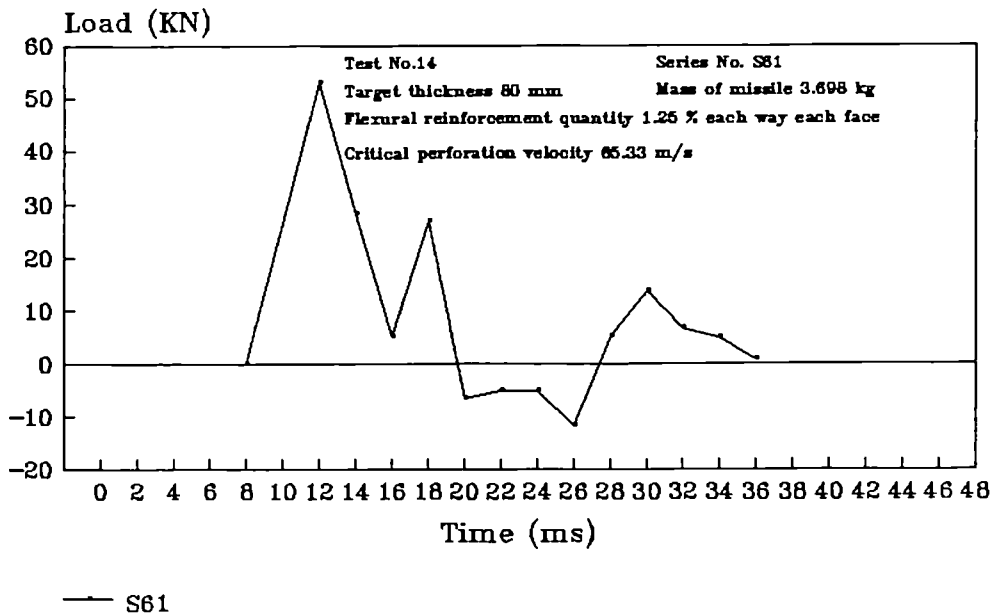


FIG. (5.1g) MEASURED TRANSIENT LOAD AT CRITICAL PERFORATION VELOCITY

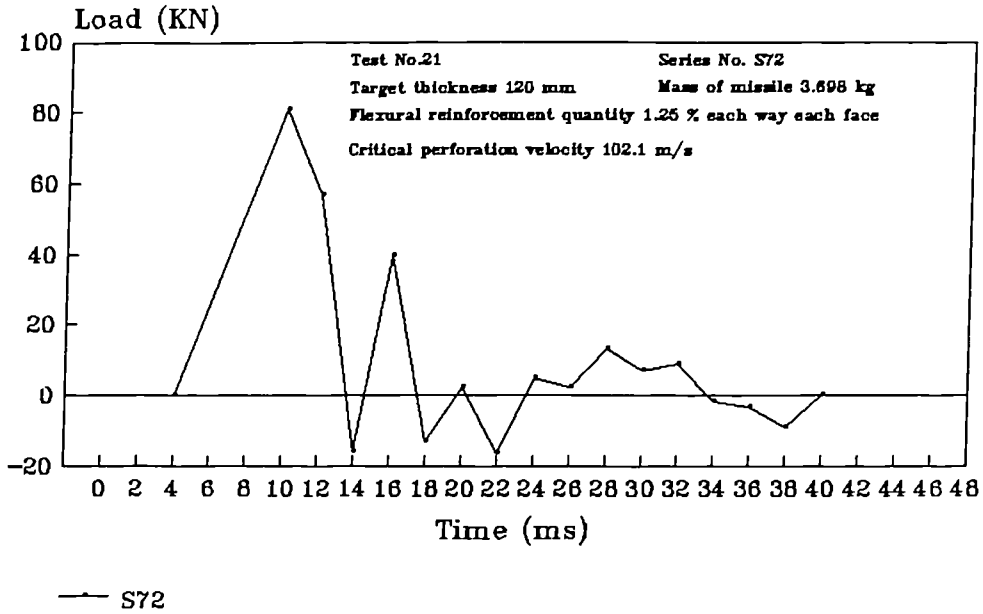


FIG. (5.1h) MEASURED TRANSIENT LOAD AT CRITICAL PERFORATION VELOCITY

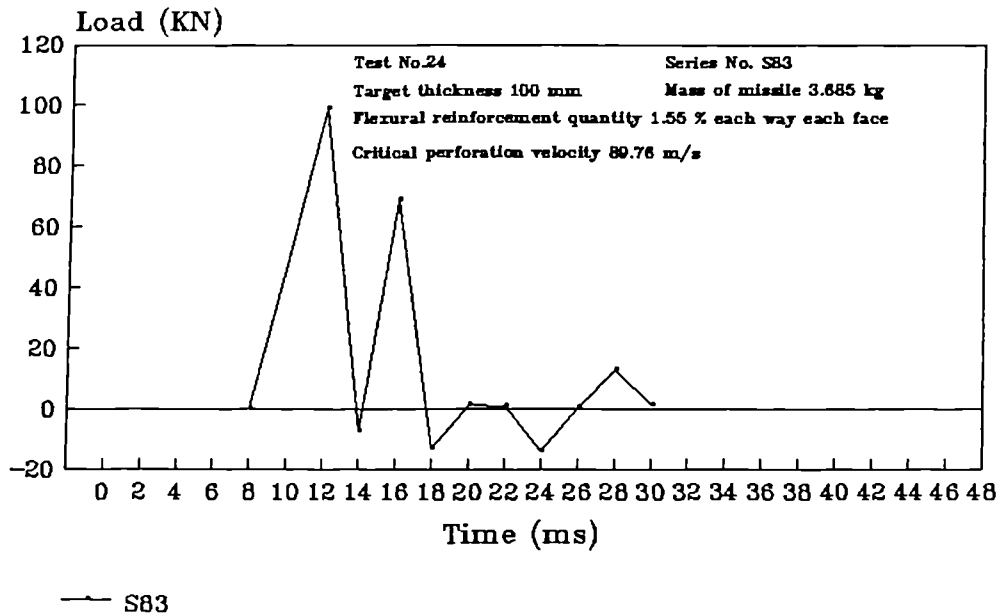


FIG. (5.1i) MEASURED TRANSIENT LOAD AT CRITICAL PERFORATION VELOCITY

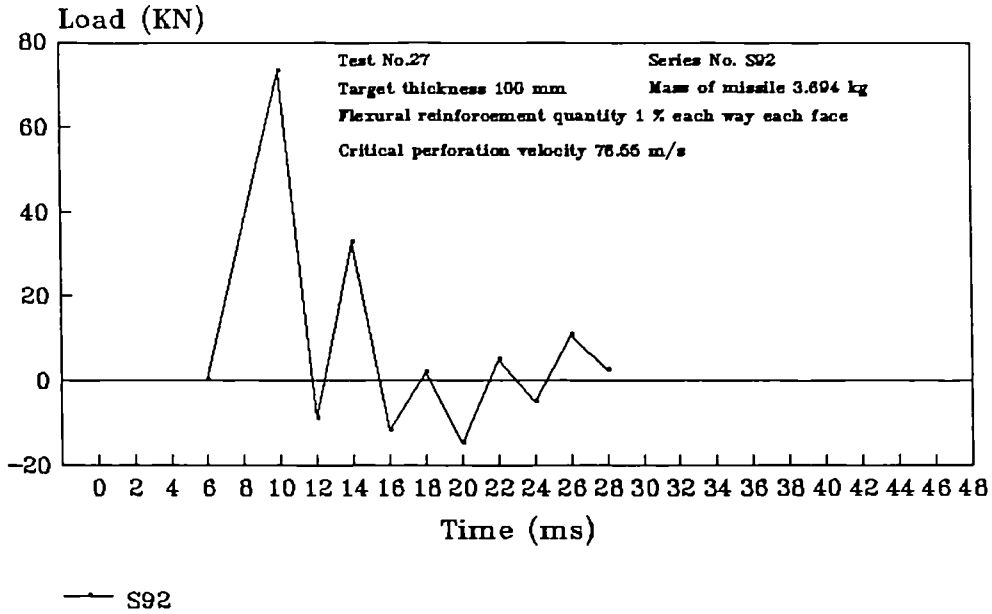


FIG. (5.1j) MEASURED TRANSIENT LOAD AT CRITICAL PERFORATION VELOCITY

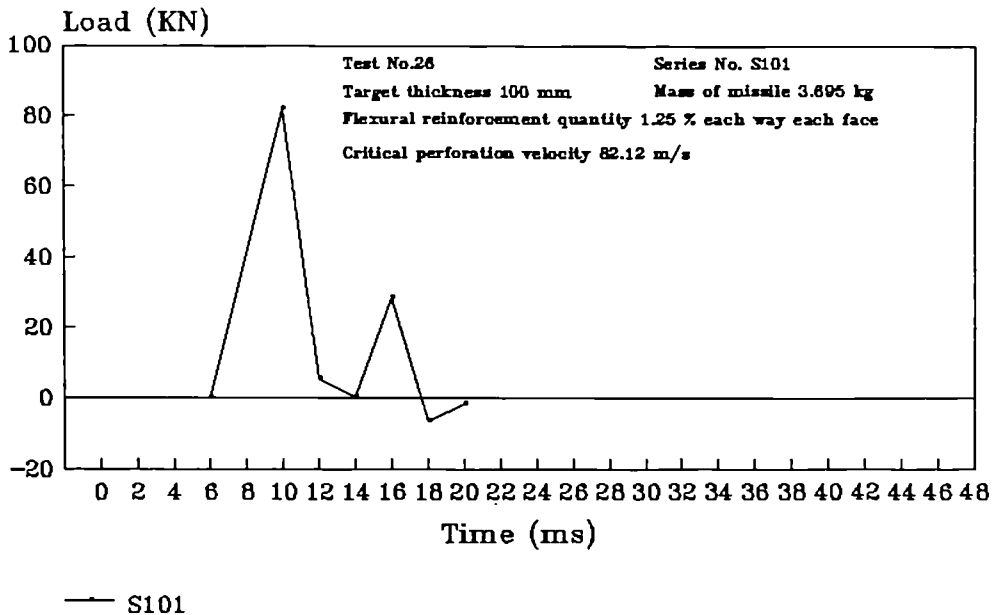
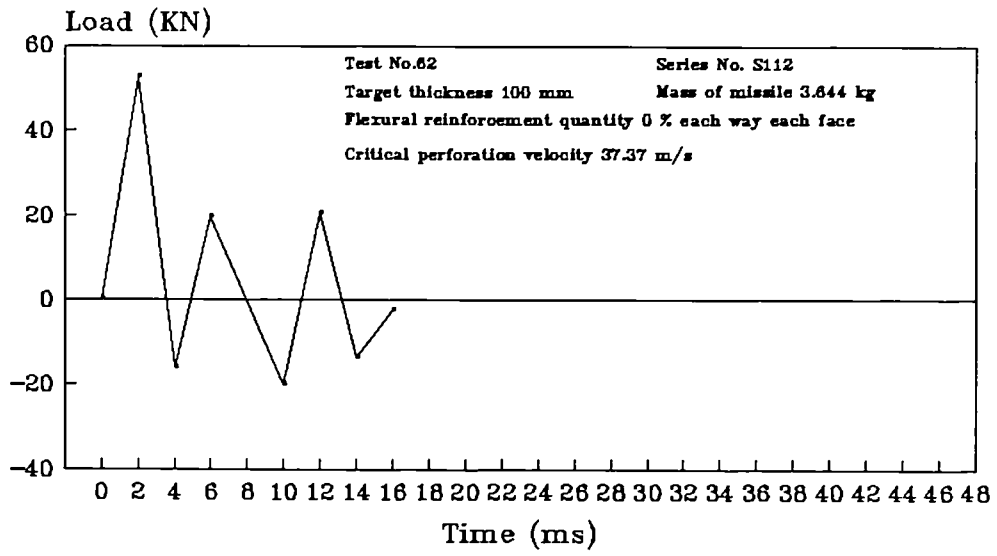


FIG. (5.1k) MEASURED TRANSIENT LOAD AT
CRITICAL PERFORATION VELOCITY



— S112

Table (5.2): The maximum reaction loads of the targets at critical perforation velocity.

Test No.	Series No.	Total percentage of reinforcement	Target thickness (mm)	Reinforcement ratio (kg/m ³)	Maximum reaction load (KN)	At time (ms)
2	S1	1%	100	160	35.35	6
6	S2	2.5%	100	390	104.7	10
9	S3	2.5%	100	390	104.6	10
12	S4	2.5%	100	390	106.09	10
17	S5	2.5%	100	390	102.61	10
14	S6	2.5%	80	390	52.73	12
21	S7	2.5%	120	400	80.91	10
24	S8	3.1%	100	490	99.03	12
27	S9	2%	100	320	73.2	10
26	S10	2.5%	100	390	81.94	10
62	S11	0%	100	0	52.0	2

All the series have 4mm max. agg. size except S10 which had 2mm max. agg. size

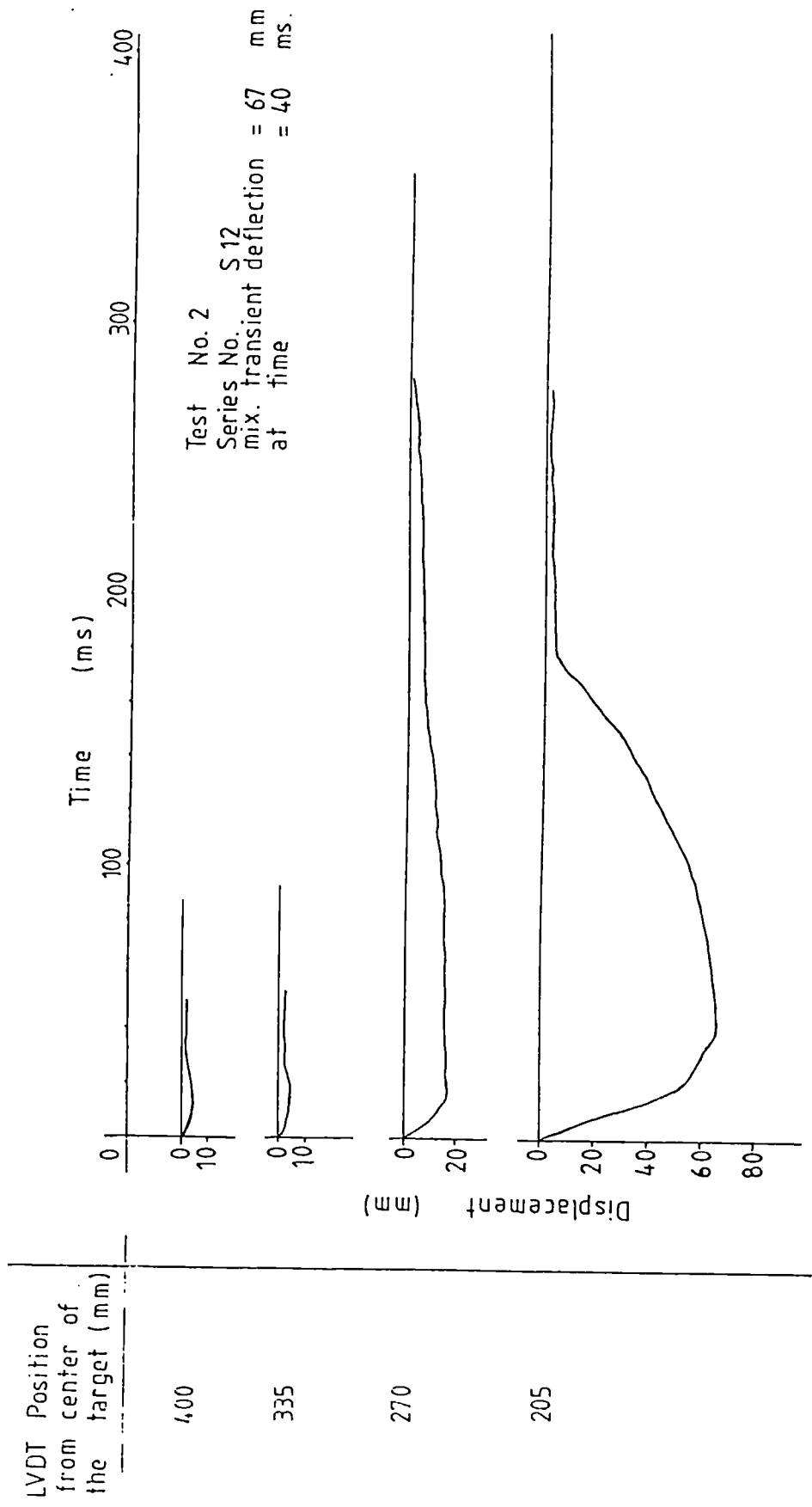


FIG. (5.2a) TRANSIENT DISPLACEMENT OF TARGET AT FOUR DIFFERENT POSITIONS FROM THE CENTER

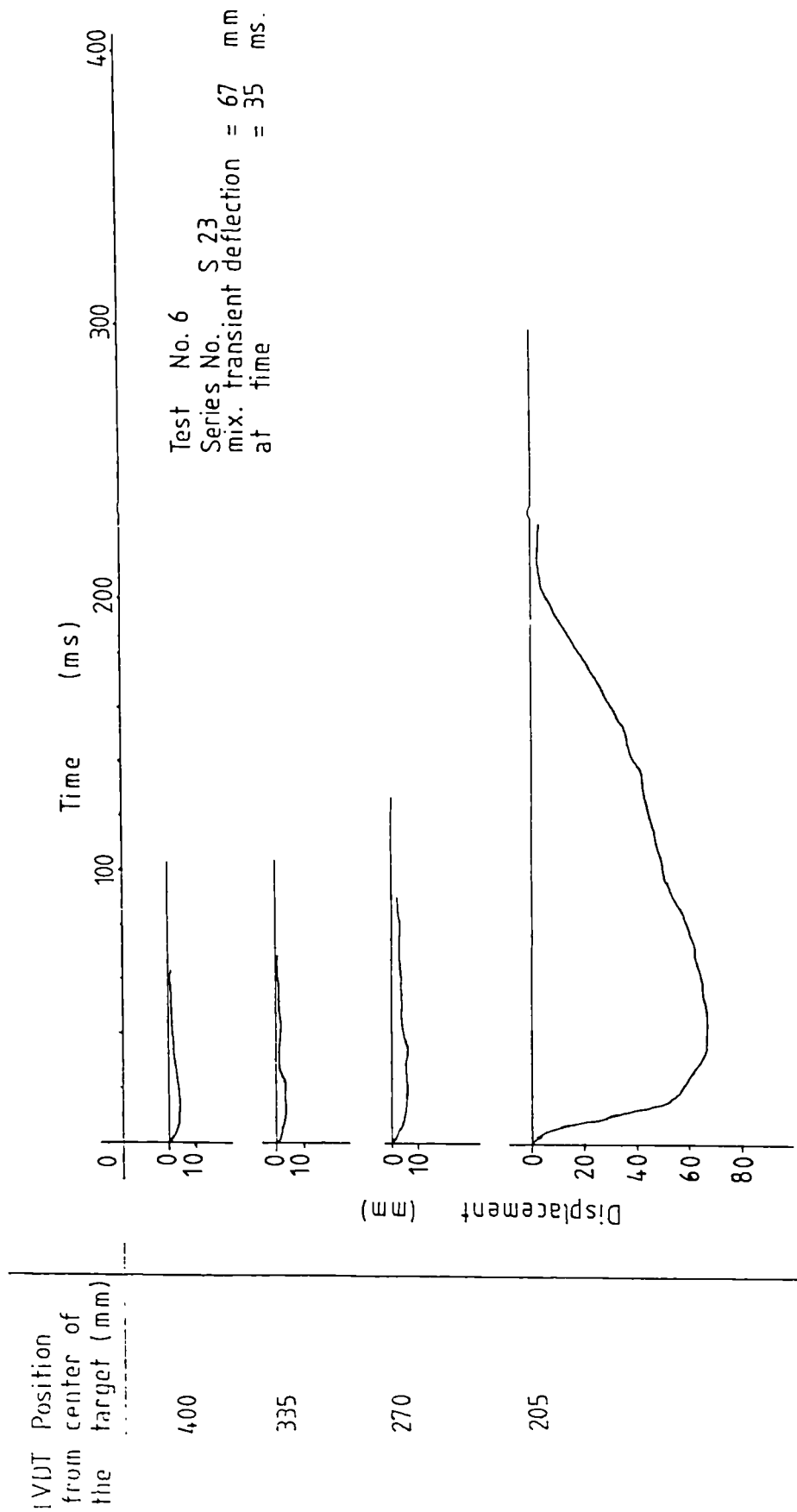


FIG. (5.2b) TRANSIENT DISPLACEMENT OF TARGET AT FOUR DIFFERENT POSITIONS FROM THE CENTER

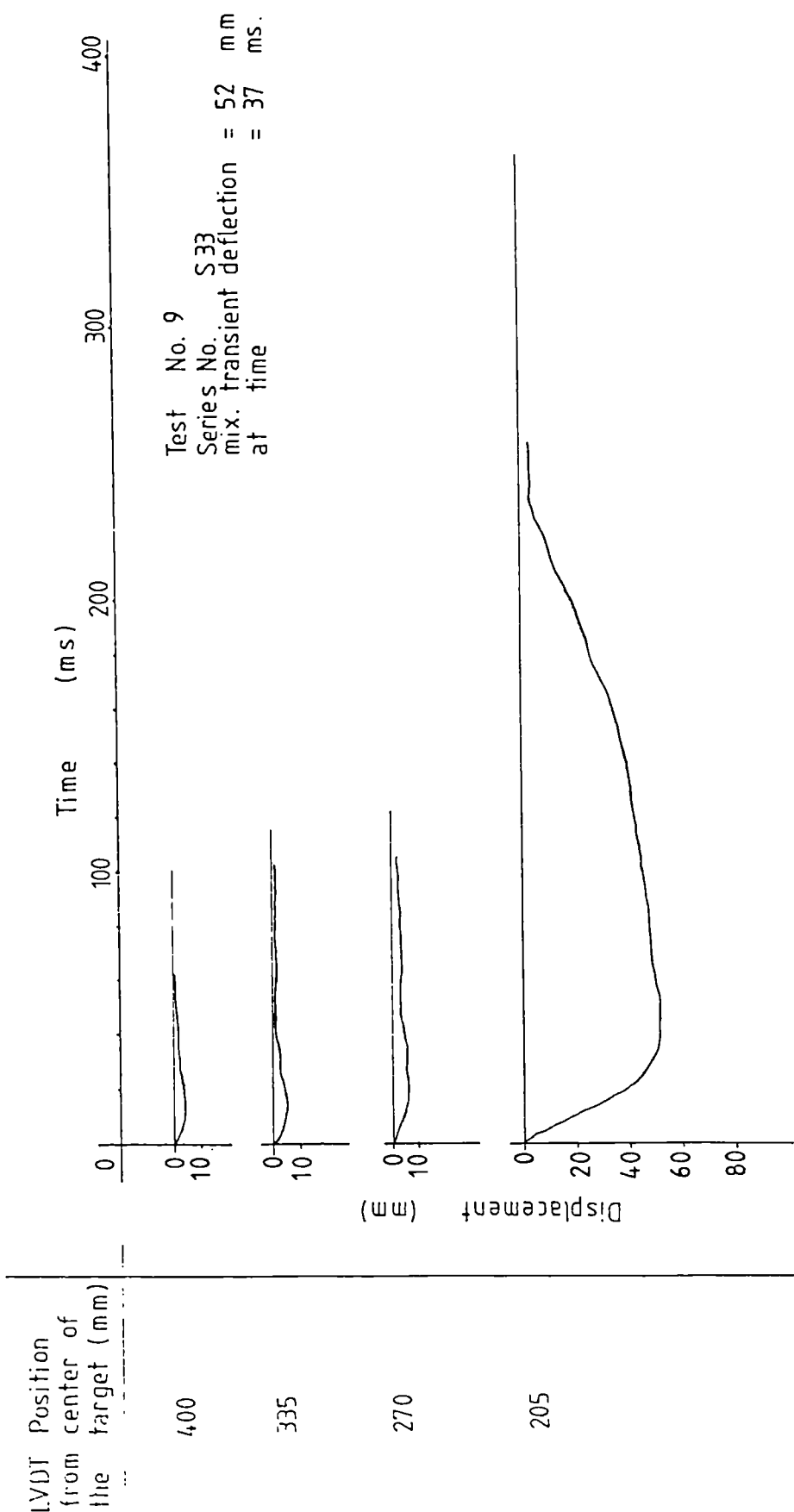


FIG. (5.2c) TRANSIENT DISPLACEMENT OF TARGET AT FOUR DIFFERENT POSITIONS FROM THE CENTER

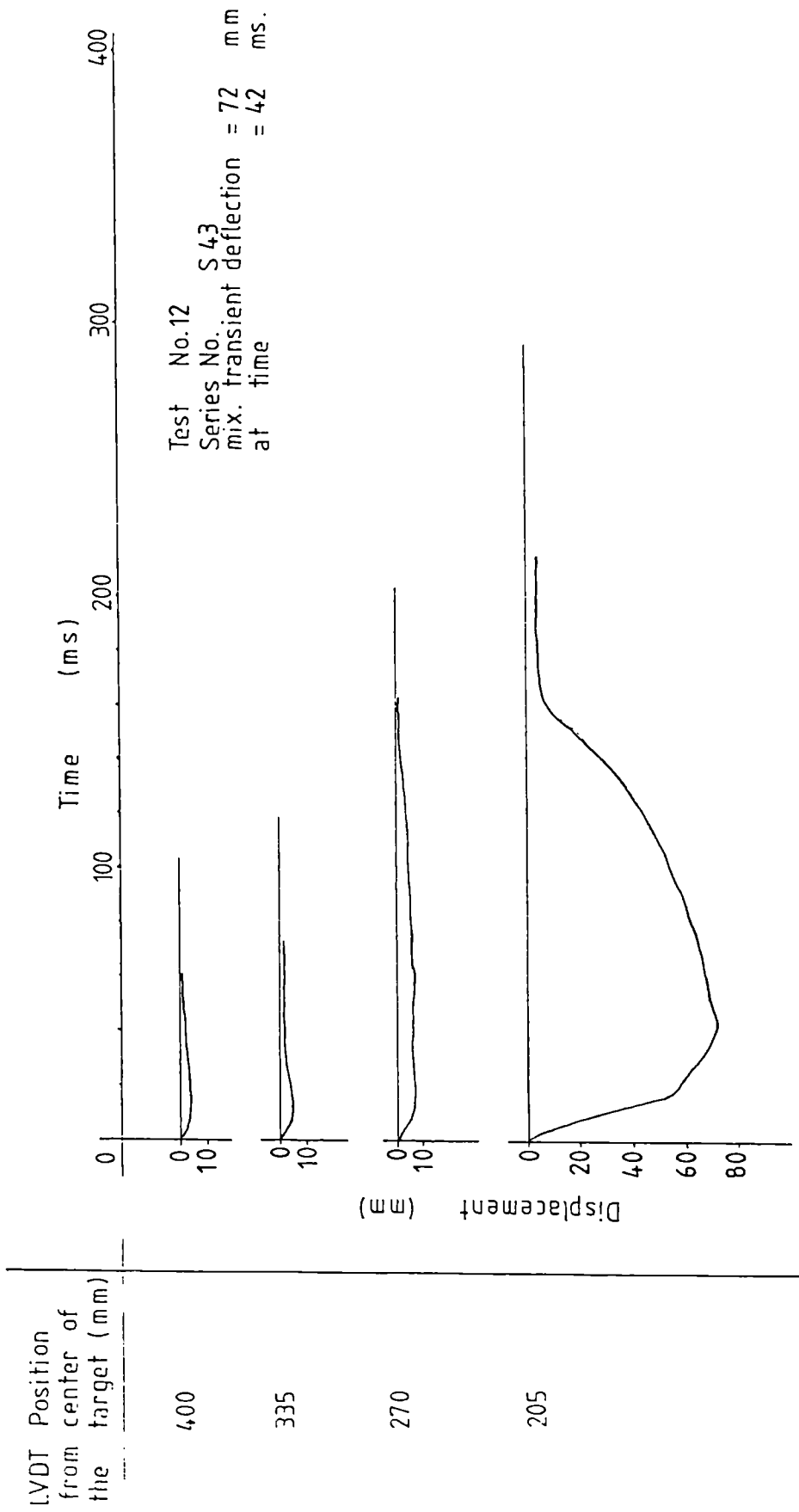


FIG. (5.2d) TRANSIENT DISPLACEMENT OF TARGET AT FOUR DIFFERENT POSITIONS FROM THE CENTER

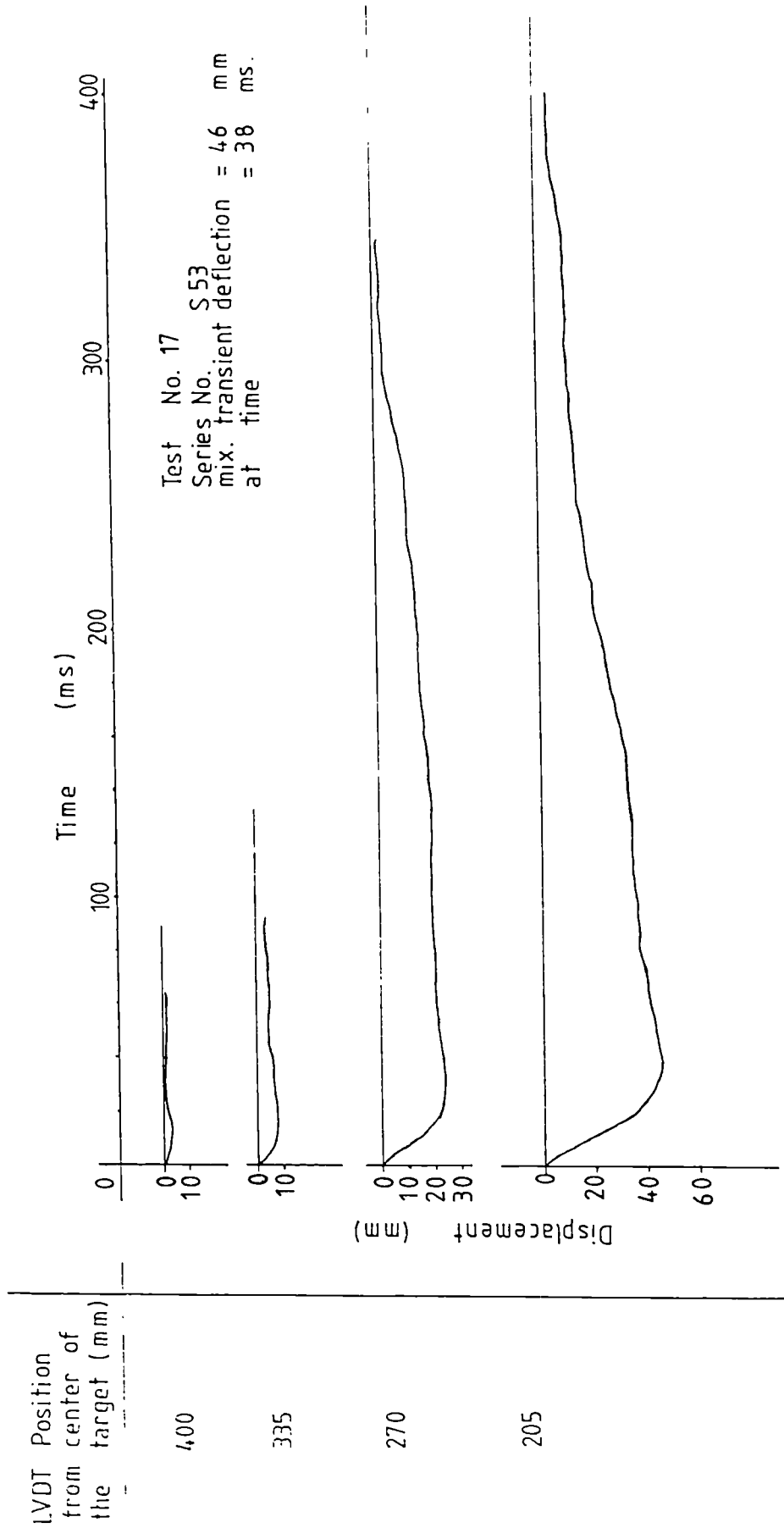


FIG. (5.2e) TRANSIENT DISPLACEMENT OF TARGET AT FOUR DIFFERENT POSITIONS FROM THE CENTER

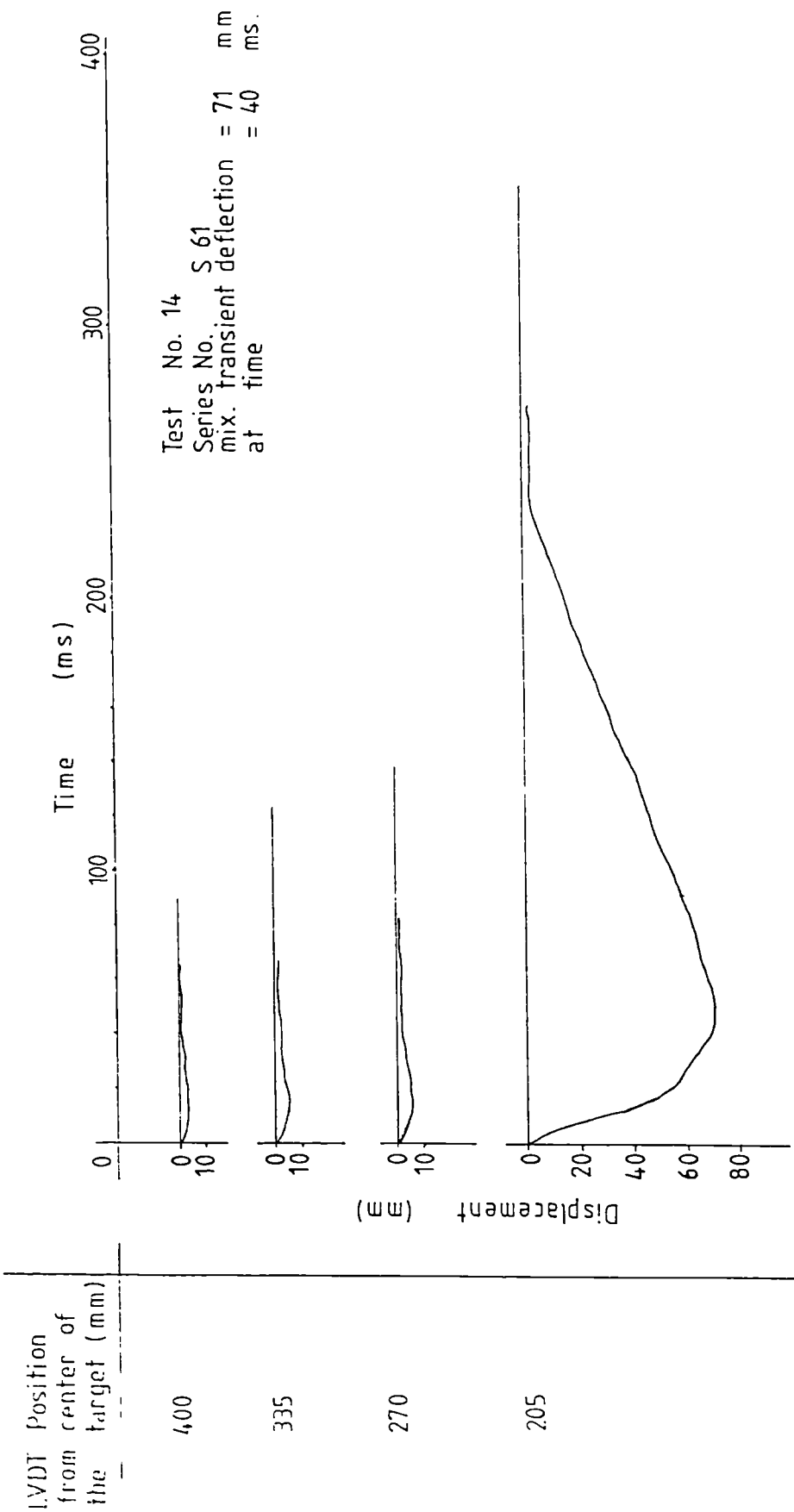


FIG. (5.2f) TRANSIENT DISPLACEMENT OF TARGET AT FOUR DIFFERENT POSITIONS FROM THE CENTER

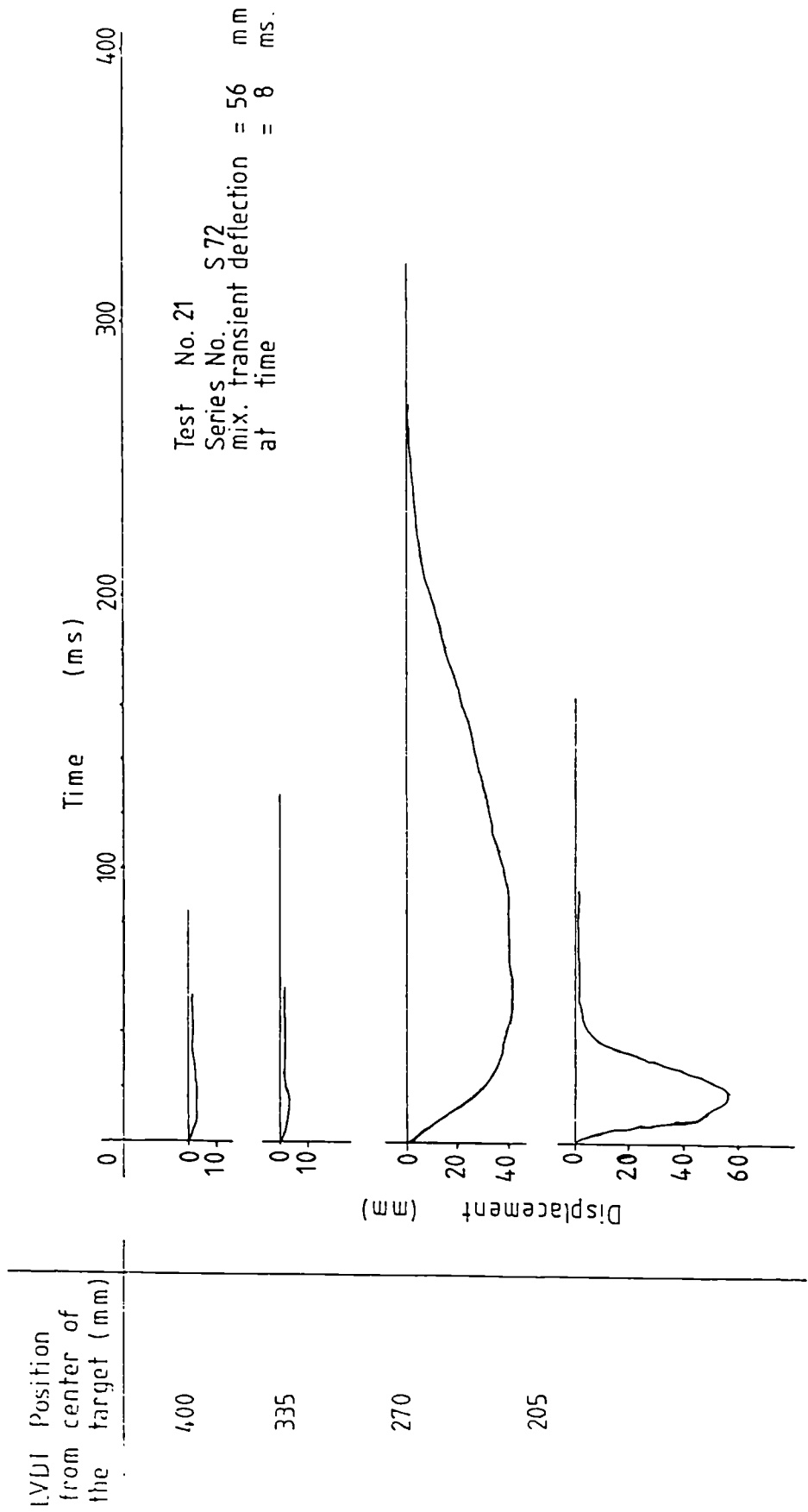


FIG. (5.2g) TRANSIENT DISPLACEMENT OF TARGET AT FOUR DIFFERENT POSITIONS FROM THE CENTER

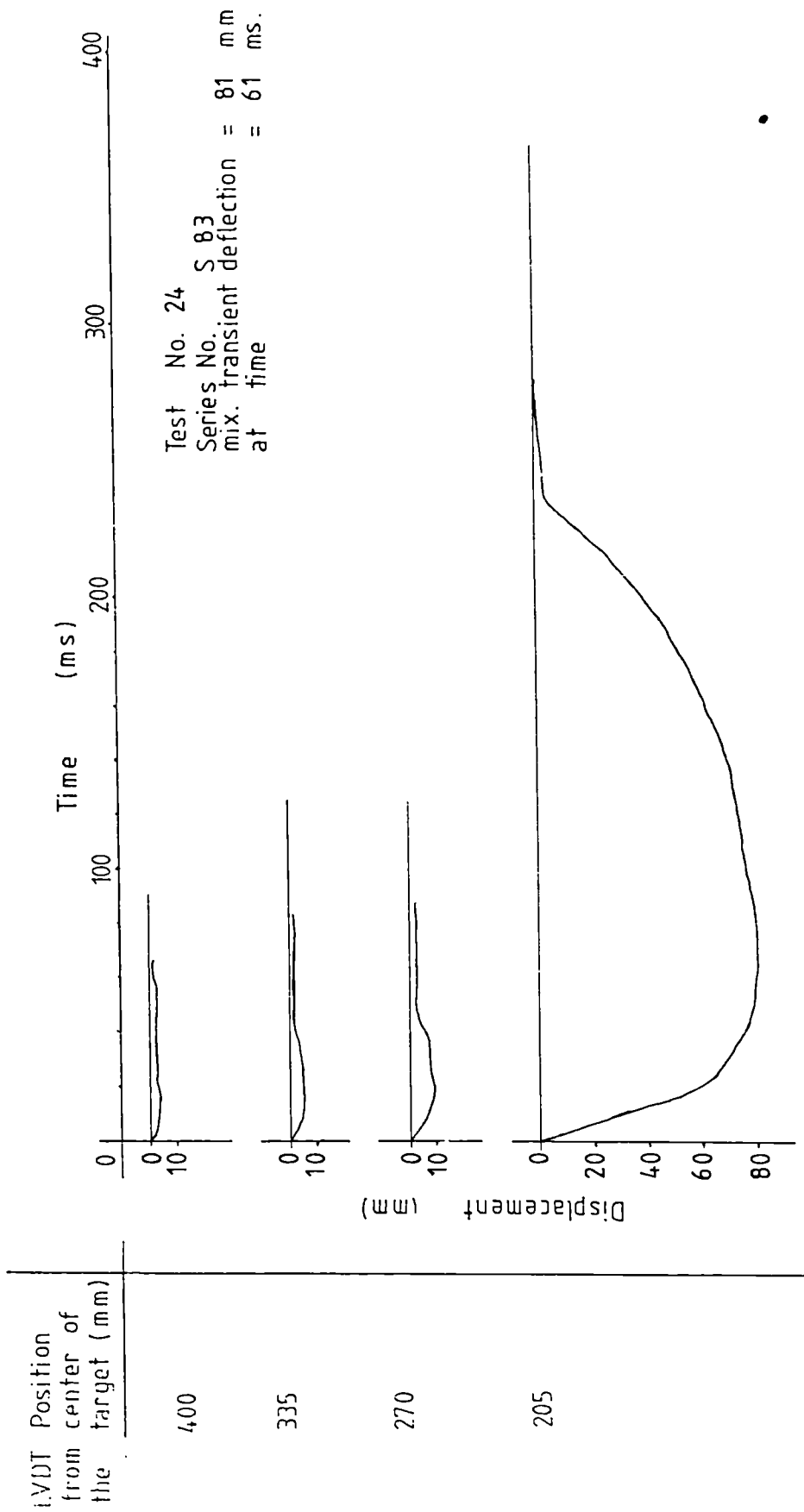


FIG. (5.2h) TRANSIENT DISPLACEMENT OF TARGET AT FOUR DIFFERENT POSITIONS FROM THE CENTER

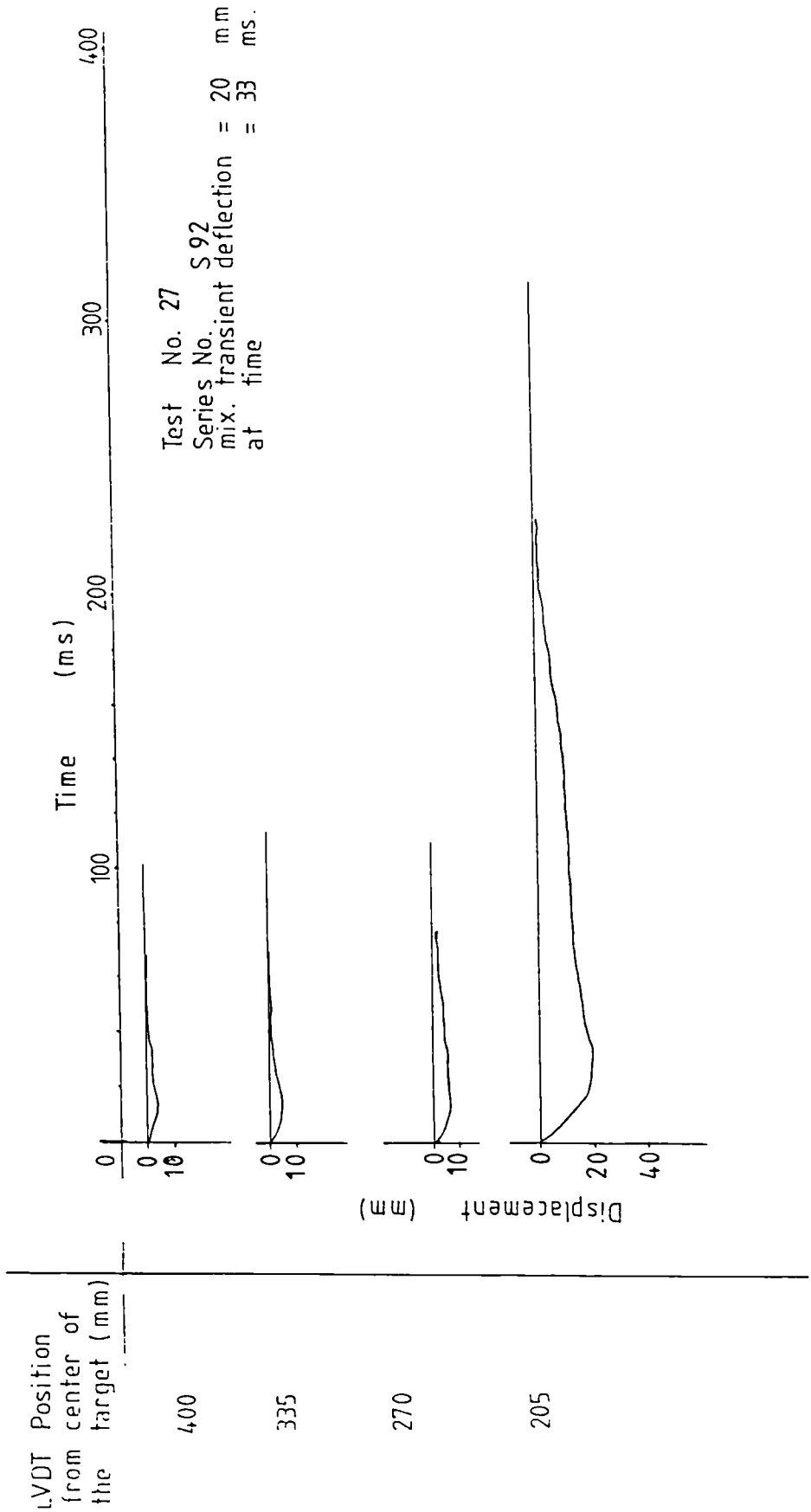


FIG.(5.2i) TRANSIENT DISPLACEMENT OF TARGET AT FOUR DIFFERENT POSITION FROM THE CENTER

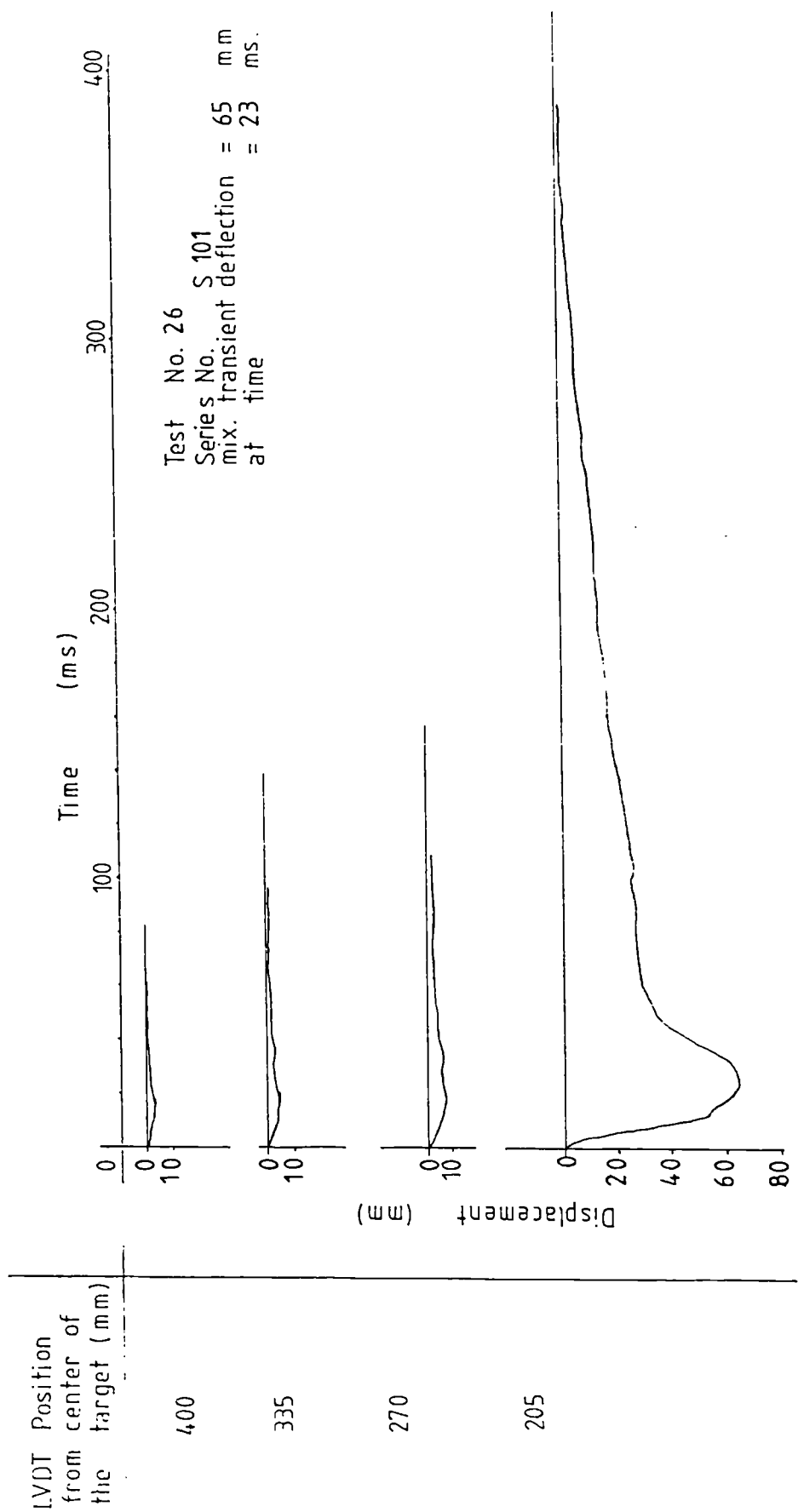


FIG.(5.2j) TRANSIENT DISPLACEMENT OF TARGET AT FOUR DIFFERENT POSITIONS FROM THE CENTER

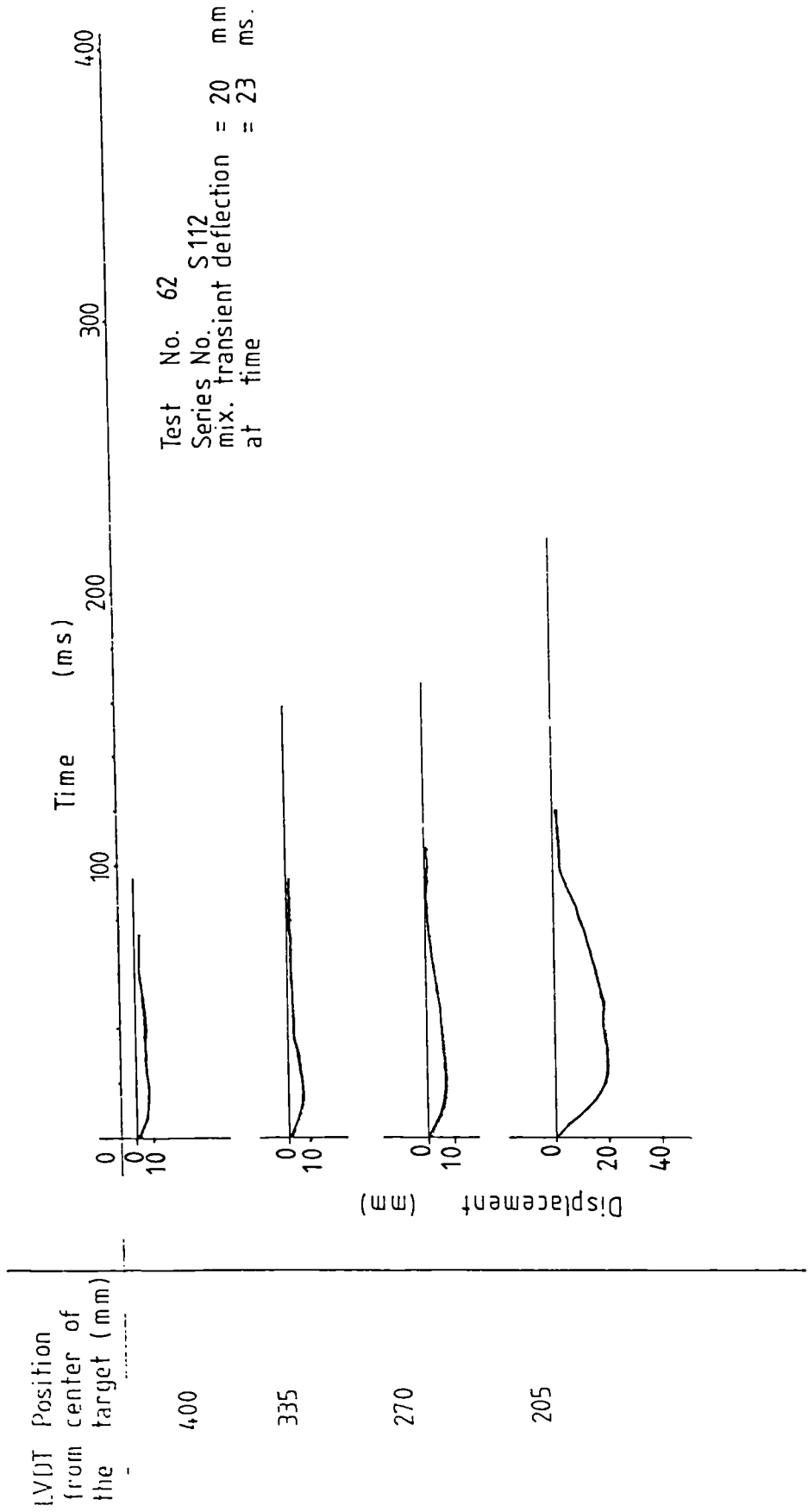


FIG. (5.2k) TRANSIENT DISPLACEMENT OF TARGET AT FOUR DIFFERENT POSITIONS FROM THE CENTER

Table (5.3): The maximum transient deflection at critical perforation velocity.

Test No.	Series No.	Total percentage of reinforcement	Target thickness (mm)	Reinforcement ratio (kg/m ³)	Maximum transient deflection (mm)	At time (ms)
2	S1	1%	100	160	67	40
6	S2	2.5%	100	390	67	35
9	S3	2.5%	100	390	52	37
12	S4	2.5%	100	390	72	42
17	S5	2.5%	100	390	46	38
14	S6	2.5%	80	390	71	40
21	S7	2.5%	120	400	56	8
24	S8	3.1%	100	490	81	61
27	S9	2%	100	320	20	33
26	S10	2.5%	100	390	65	23
62	S11	0%	100	0	20	23

All the series have 4mm max. agg. size except S10 which had 2mm max. agg. size

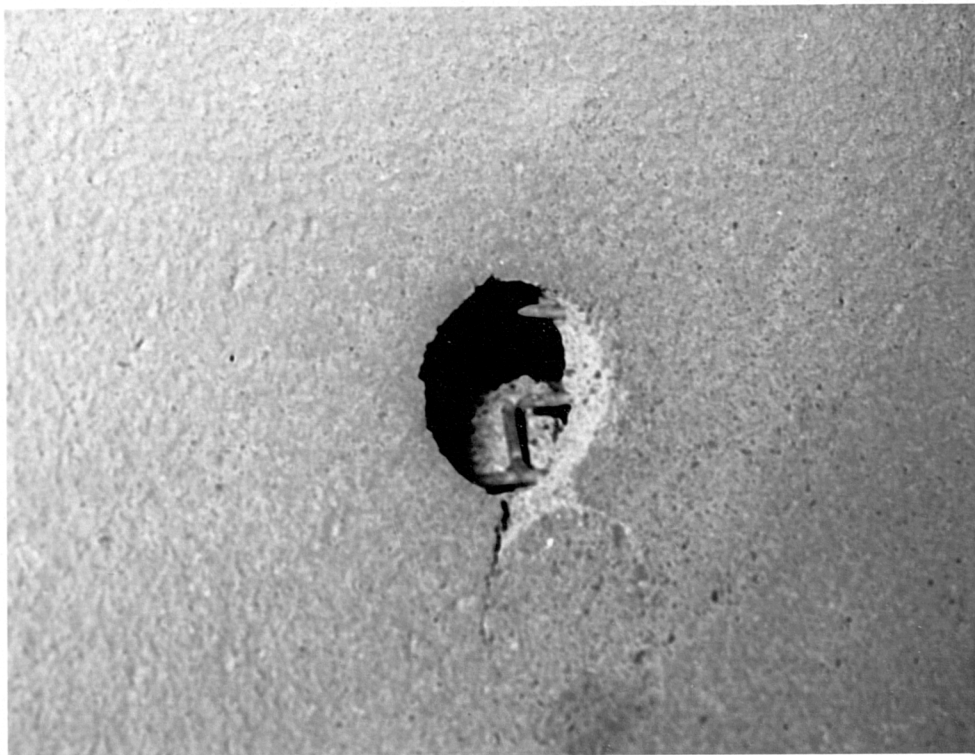
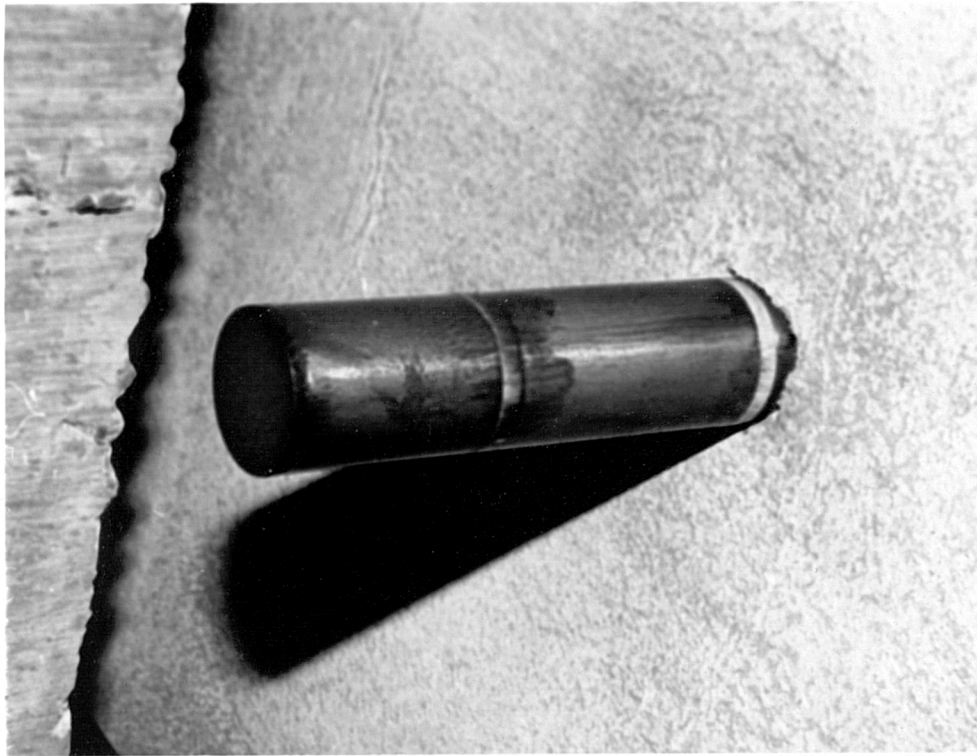


PLATE (5.1)
FRONT FACE DAMAGE OF TARGET
(PERFORATION)

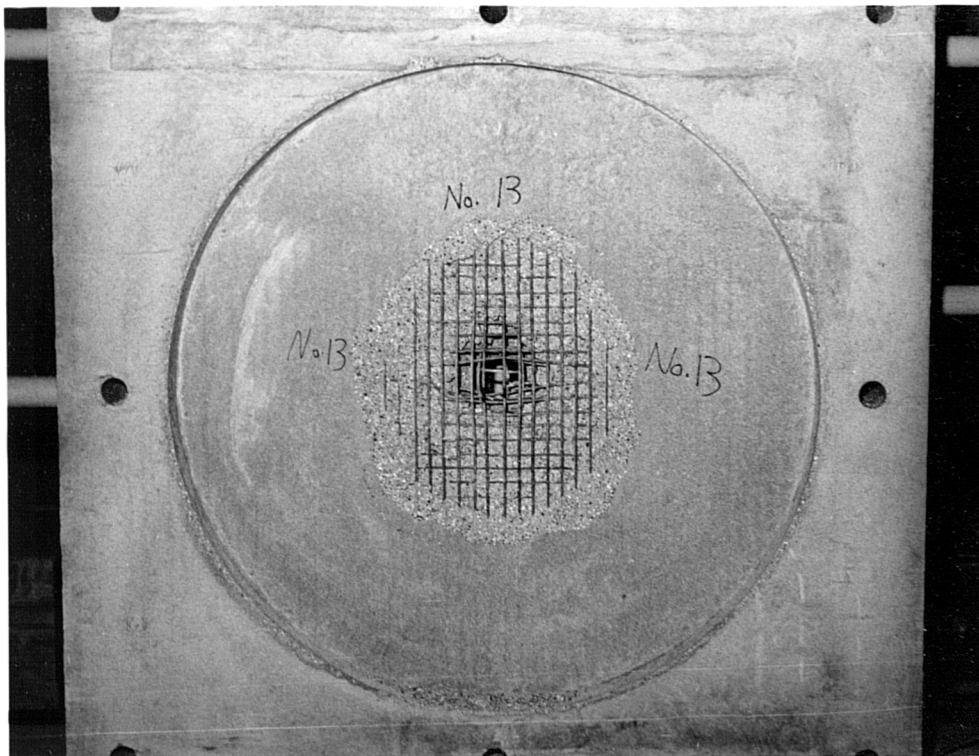
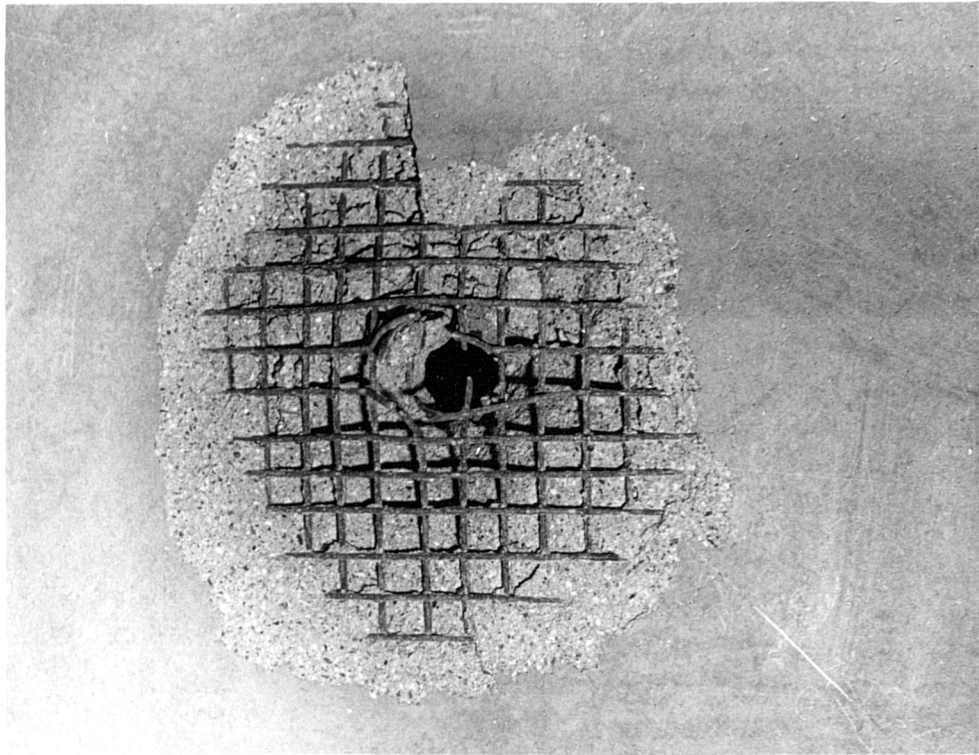


PLATE (5.2)
REAR FACE DAMAGE OF TARGET
(PERFORATION)

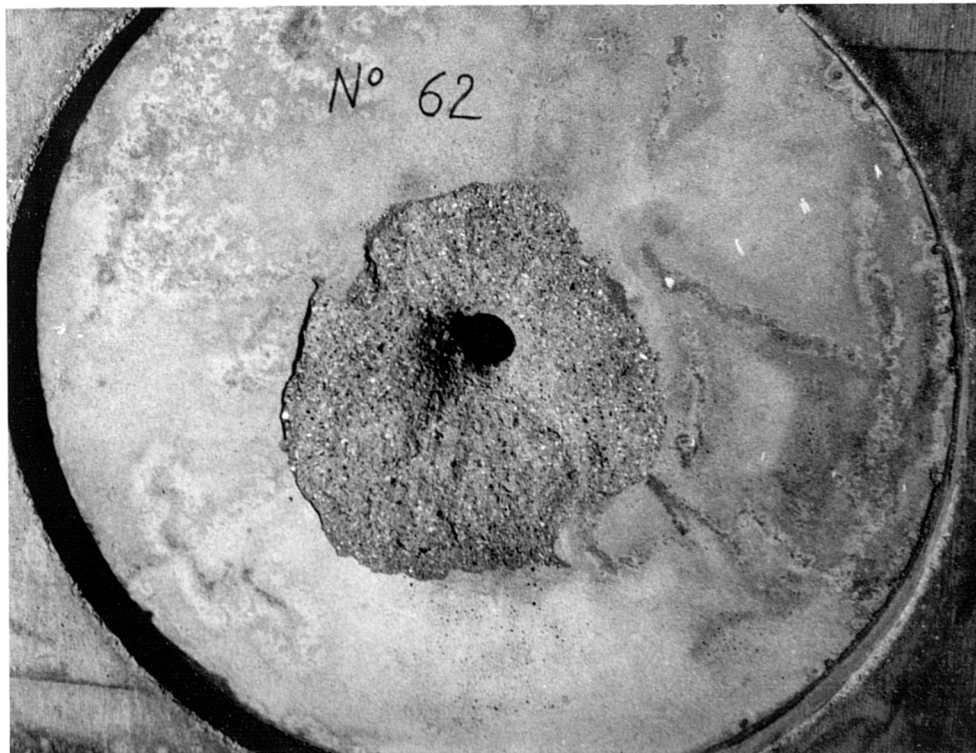
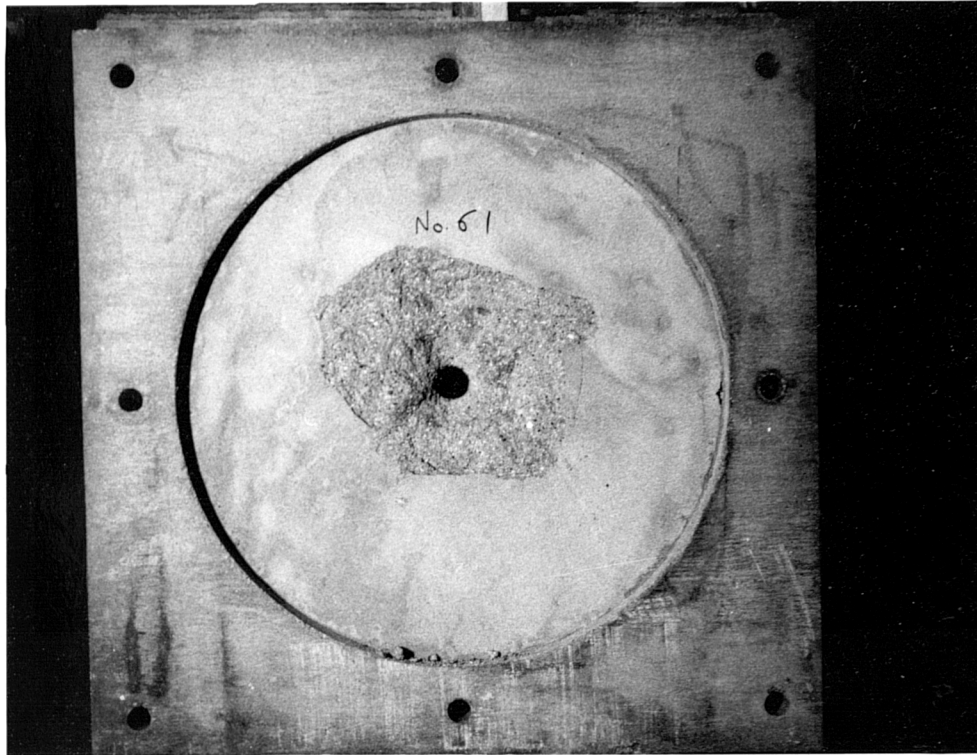


PLATE (5.3)

REAR FACE DAMAGE OF PLAN CONCRETE
TARGET (PERFORATION)

5.3 The Scabbing Resistance of The Model Concrete Slabs

5.3.1 Critical Scabbing Velocity V_{CS}

Experiments were performed using the thirty slabs reported in table (4.1). The test procedure used has been described in section 4.4. Normally three targets of identical construction were tested and the critical scabbing velocity V_{CS} achieved in successive shots. This velocity was related to the incident, V_i and exit, V_r velocities by equating energies before and after impact using the same equation which has been described in section 5.2.1.

The ejected mass of concrete was based on measurements after each test and was taken as 0.71 ± 0.01 kg for all the targets. This mass was equivalent to the mass of the concrete scab on the target rear face. The average diameter of the scab from all the tests was found to be 200 mm and thickness equal to the concrete cover. Also, it is assumed that the ejected concrete cover travels at the same velocity as the exit velocity of the missile (an assumption which has been shown to be generally true in practice). The test results show that the missile penetrates the target front face a distance of 9.0 ± 1.0 mm. The test results for the determination of the scabbing resistance are given in table (5.4).

5.3.2 The Measurement of Transient Load at The Critical Scabbing Velocity

By using the load cells and the procedure described in section 3.3.2, the total reaction loads were measured for the targets when the velocity of the impacted missile just caused scabbing. The total transient reaction loads of all the

series are shown in Fig. (5.3). Each curve represents the sum of the eight load cell signals. The time and magnitudes of the maximum reaction loads are shown in table (5.5).

5.3.3 The Transient Target Displacement at The Critical Scabbing Velocity

Fig. (5.4) shows the measured transient displacements at four different positions from the centre of the target at the critical scabbing velocity. The results were obtained using the procedure described in section 3.3.3. Table (5.6) shows the time of occurrence and the maximum transient deflection of each test.

5.3.4 General Panel Damage Caused by The Missile at The Scabbing Velocity

The rear face damage of the targets tested at the scabbing velocity are shown in plate (5.4). The plate shows stripping of the concrete cover from the rear face. The scab having an average diameter of 200 mm for all the series. The tests also show the missile penetration to be equal to a depth of 9.0 ± 1.0 mm.

Table (5.4): The results for scabbing resistance tests

Test No.	Series No.	Total percentage of reinforcement	Mass of missile (kg)	Target thickness (mm)	Concrete density (kg/m ³)	Concrete compressive strength f_c' (cube) (N/mm ²)	Concrete tensile splitting strength σ_{ct} (cube) (N/mm ²)	Missile velocities (m/sec.)		
								Impact	Exit	Critical
33	S1	1%	3.689	100	2256.5	57.56	3.84	45.83	18.59	41.1
36	S2	2.5%	3.689	100	2268	55.5	3.43	50.05	12.34	48.2
39	S3	2.5%	3.2	100	2267.5	54.53	3.34	56.3	20.75	51.39
42	S4	2.5%	2.695	100	2295	54.8	3.34	57.34	14.7	54.9
45	S5	2.5%	2.21	100	2288.2	53.26	3.44	61.8	18.1	58.2
46	S6	2.5%	3.664	80	2270	48.66	3.41	39.65	15.94	35.62
51	S7	2.5%	3.661	120	2245	45.36	3.18	58.77	5.11	55.86
52	S8	3.1%	3.661	100	2252.2	46.1	3.31	54.83	16.25	51.88
57	S9	2%	3.656	100	2263.8	48.2	3.22	47.32	15.2	44.31
58	S10	2.5%	3.652	100	2242.4	50.23	3.57	47.89	14.41	45.23

All the series have 4mm max. agg. size except S10 which had 2mm max. agg. size

FIG. (5.3a) MEASURED TRANSIENT LOAD AT CRITICAL SCABBING VELOCITY

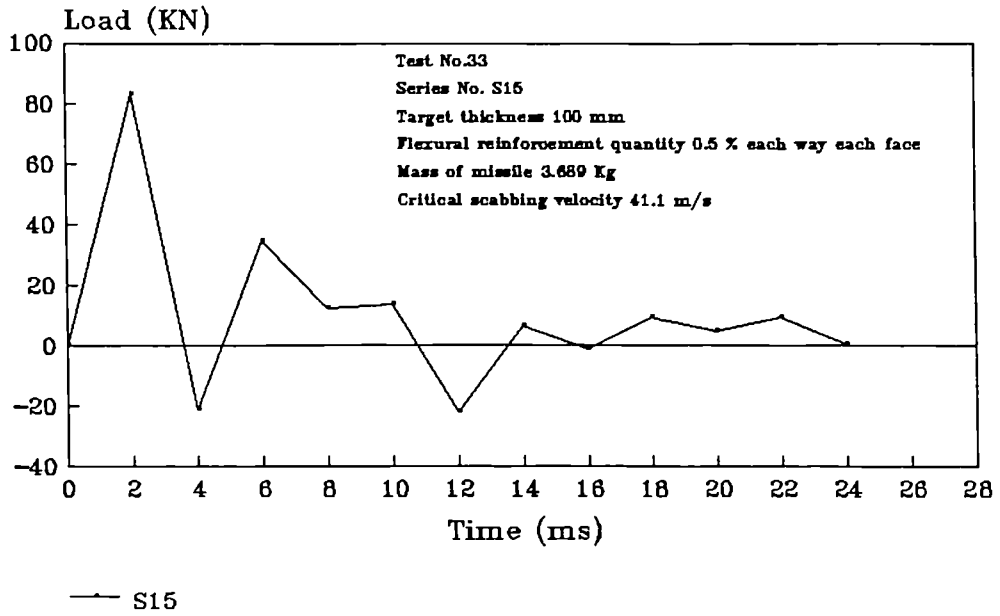


FIG. (5.3b) MEASURED TRANSIENT LOAD AT CRITICAL SCABBING VELOCITY

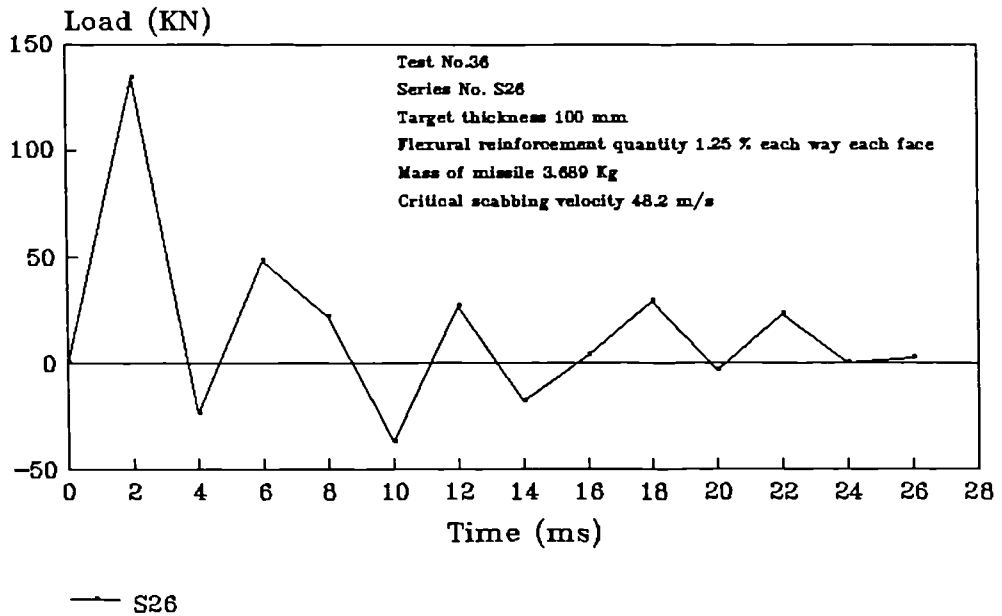


FIG. (5.3c) MEASURED TRANSIENT LOAD AT CRITICAL SCABBING VELOCITY

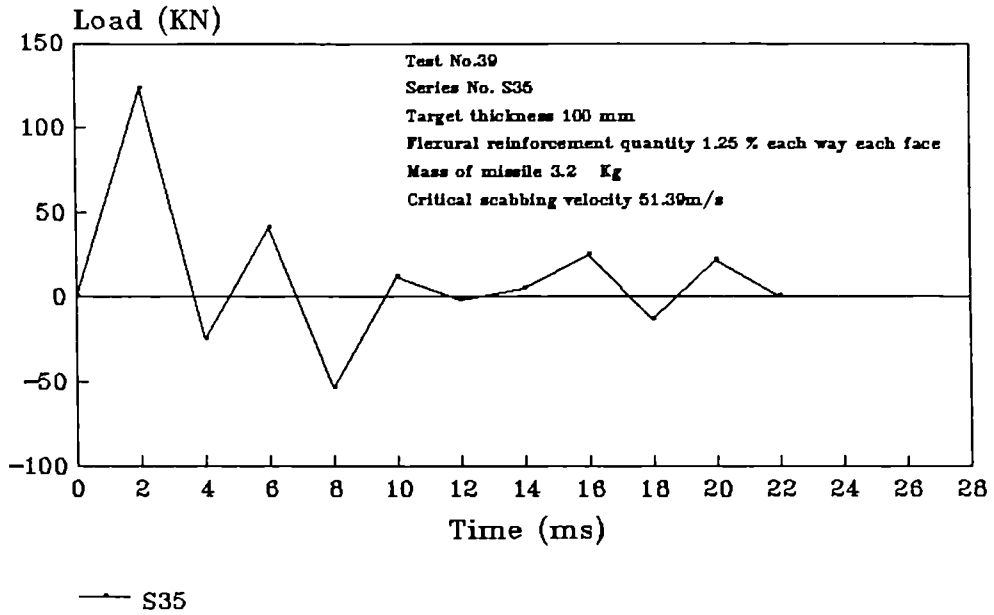


FIG. (5.3d) MEASURED TRANSIENT LOAD AT CRITICAL SCABBING VELOCITY

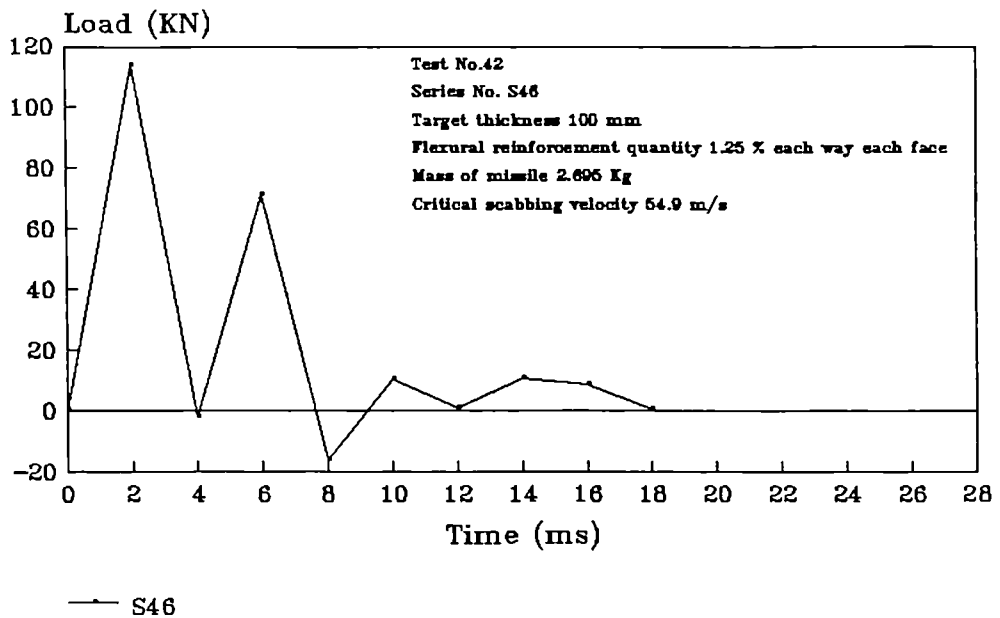


FIG. (5.3e) MEASURED TRANSIENT LOAD AT CRITICAL SCABBING VELOCITY

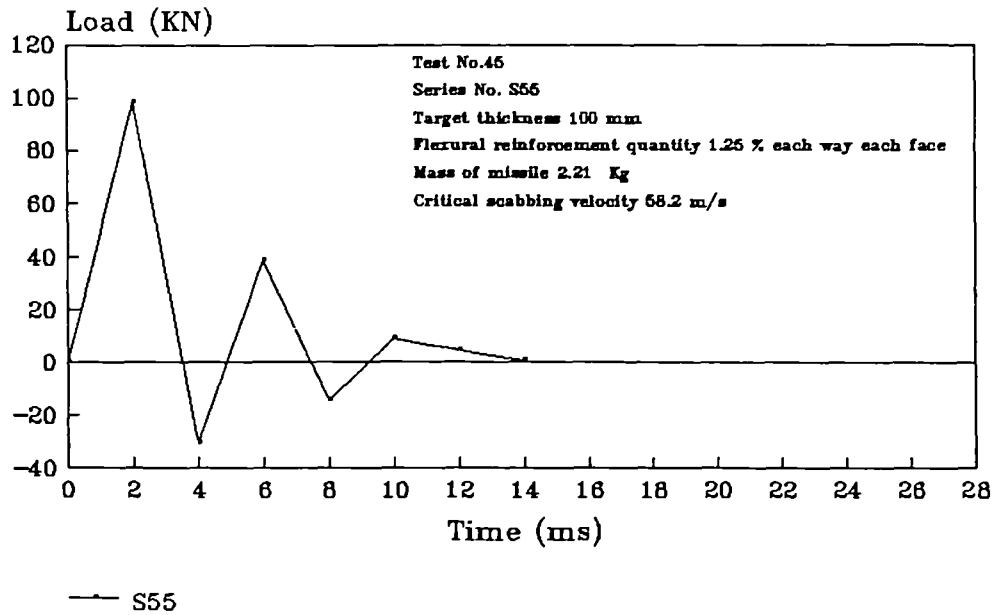


FIG. (5.3f) MEASURED TRANSIENT LOAD AT CRITICAL SCABBING VELOCITY

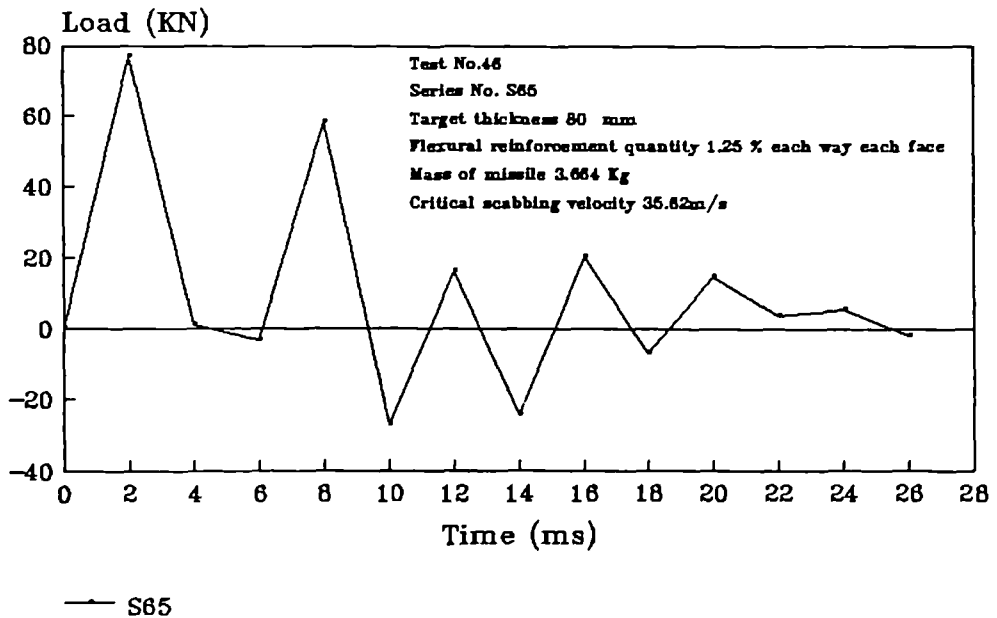


FIG. (5.3g) MEASURED TRANSIENT LOAD AT CRITICAL SCABBING VELOCITY

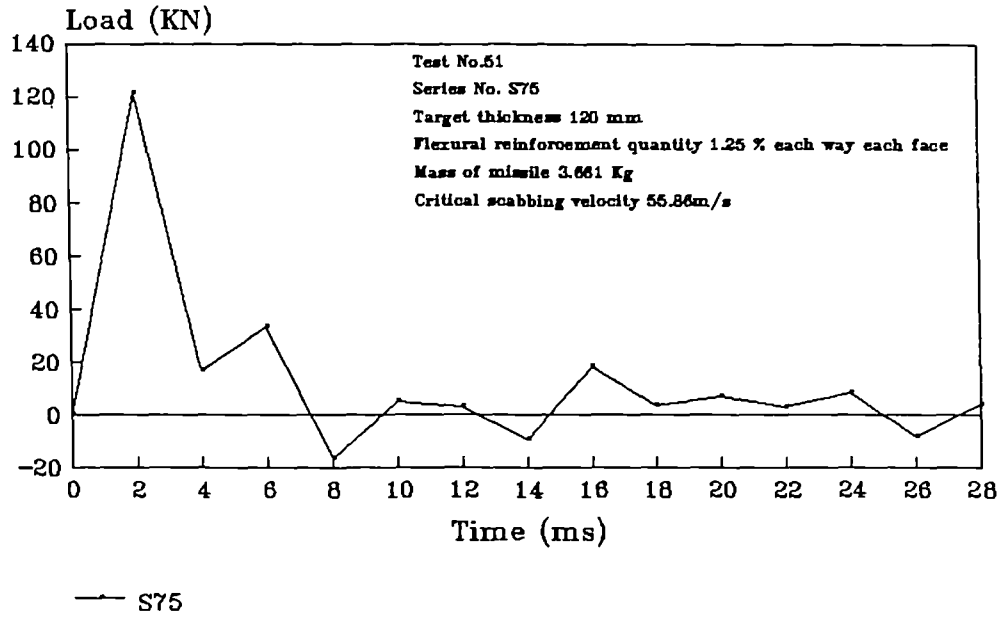


FIG. (5.3h) MEASURED TRANSIENT LOAD AT CRITICAL SCABBING VELOCITY

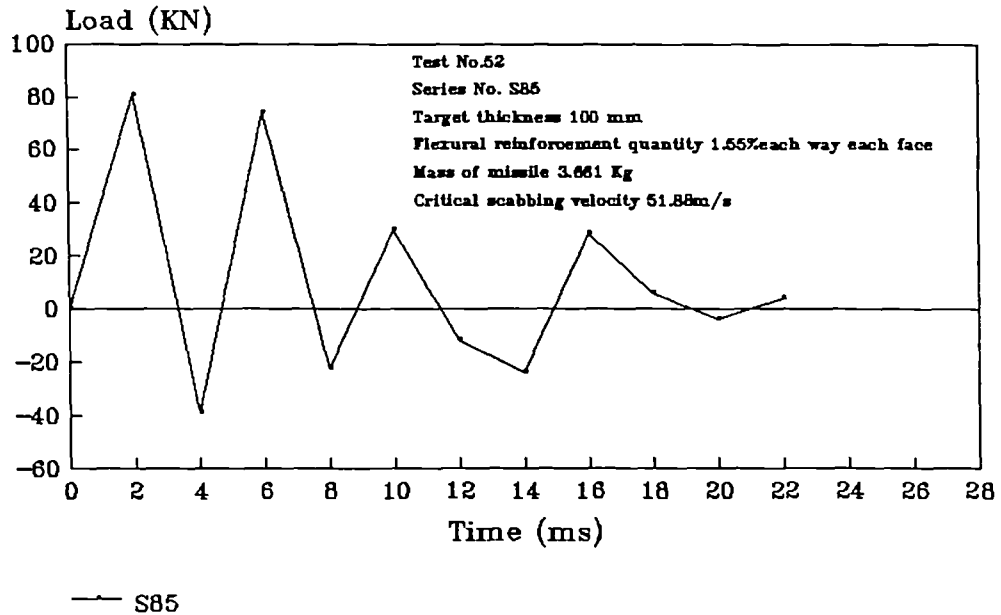


FIG. (5.3i) MEASURED TRANSIENT LOAD AT CRITICAL SCABBING VELOCITY

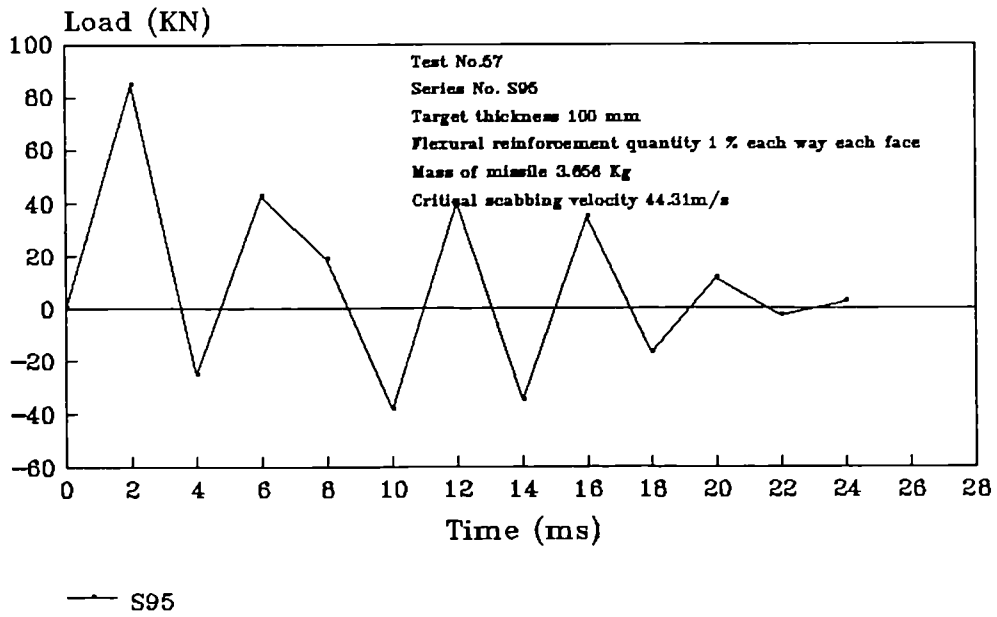


FIG. (5.3j) MEASURED TRANSIENT LOAD AT CRITICAL SCABBING VELOCITY

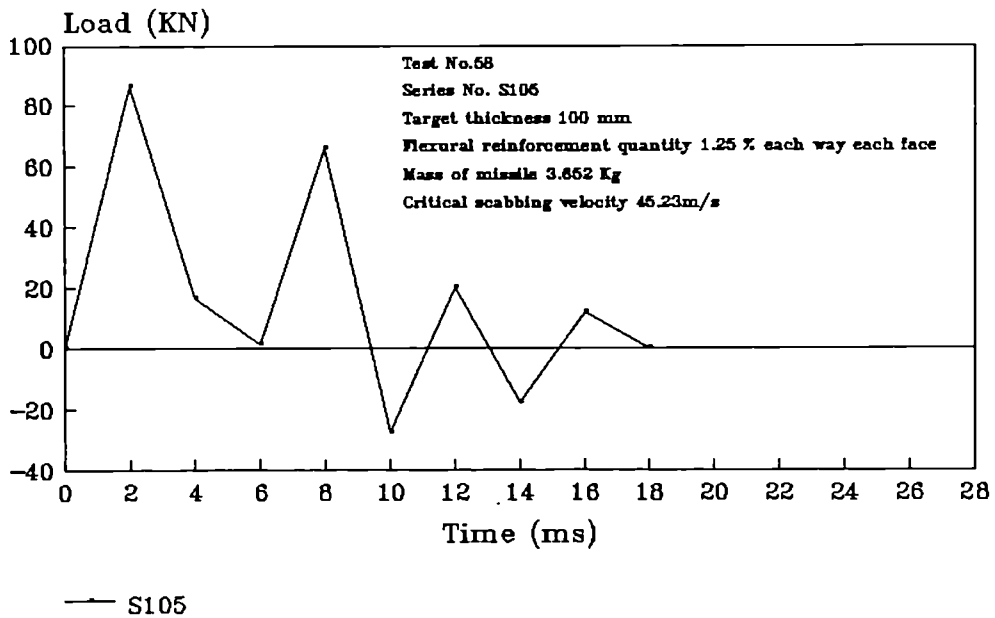


Table (5.5): The maximum reaction loads of the targets at critical scabbing velocity

Test No.	Series No.	Total percentage of reinforcement	Target thickness (mm)	Reinforcement ratio (kg/m ³)	Maximum reaction load (KN)	At time (ms)
33	S1	1%	100	160	83.35	2
36	S2	2.5%	100	390	133.77	2
39	S3	2.5%	100	390	122.75	2
42	S4	2.5%	100	390	113.65	2
45	S5	2.5%	100	390	98.4	2
46	S6	2.5%	80	390	77.02	2
51	S7	2.5%	120	400	121.36	2
52	S8	3.1%	100	490	80.83	2
57	S9	2%	100	320	84.63	2
58	S10	2.5%	100	390	86.51	2

All the series have 4mm max. agg. size except S10 which had 2mm max. agg. size

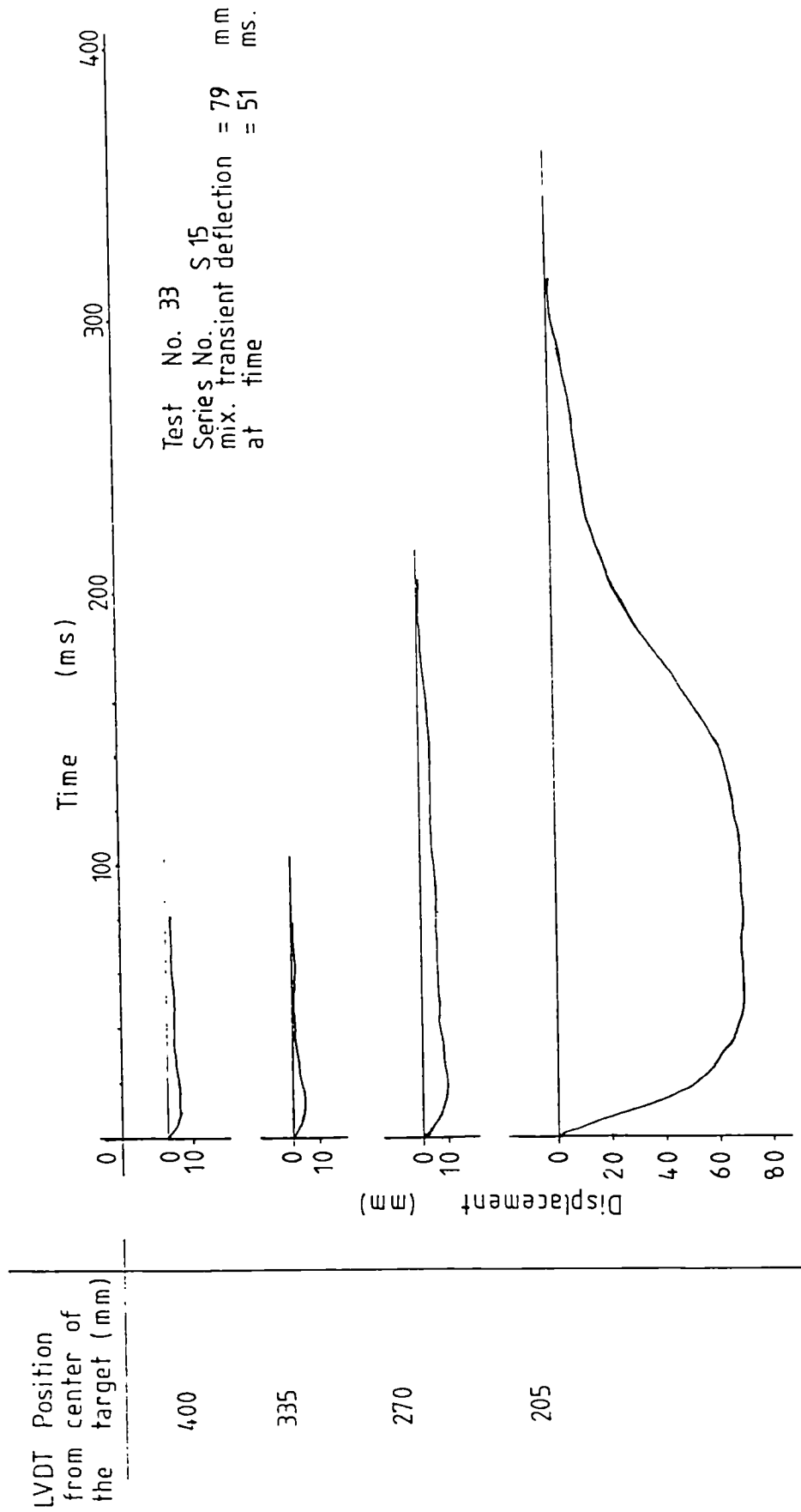


FIG. (5.4a) TRANSIENT DISPLACEMENT OF TARGET AT FOUR DIFFERENT POSITIONS FROM THE CENTER

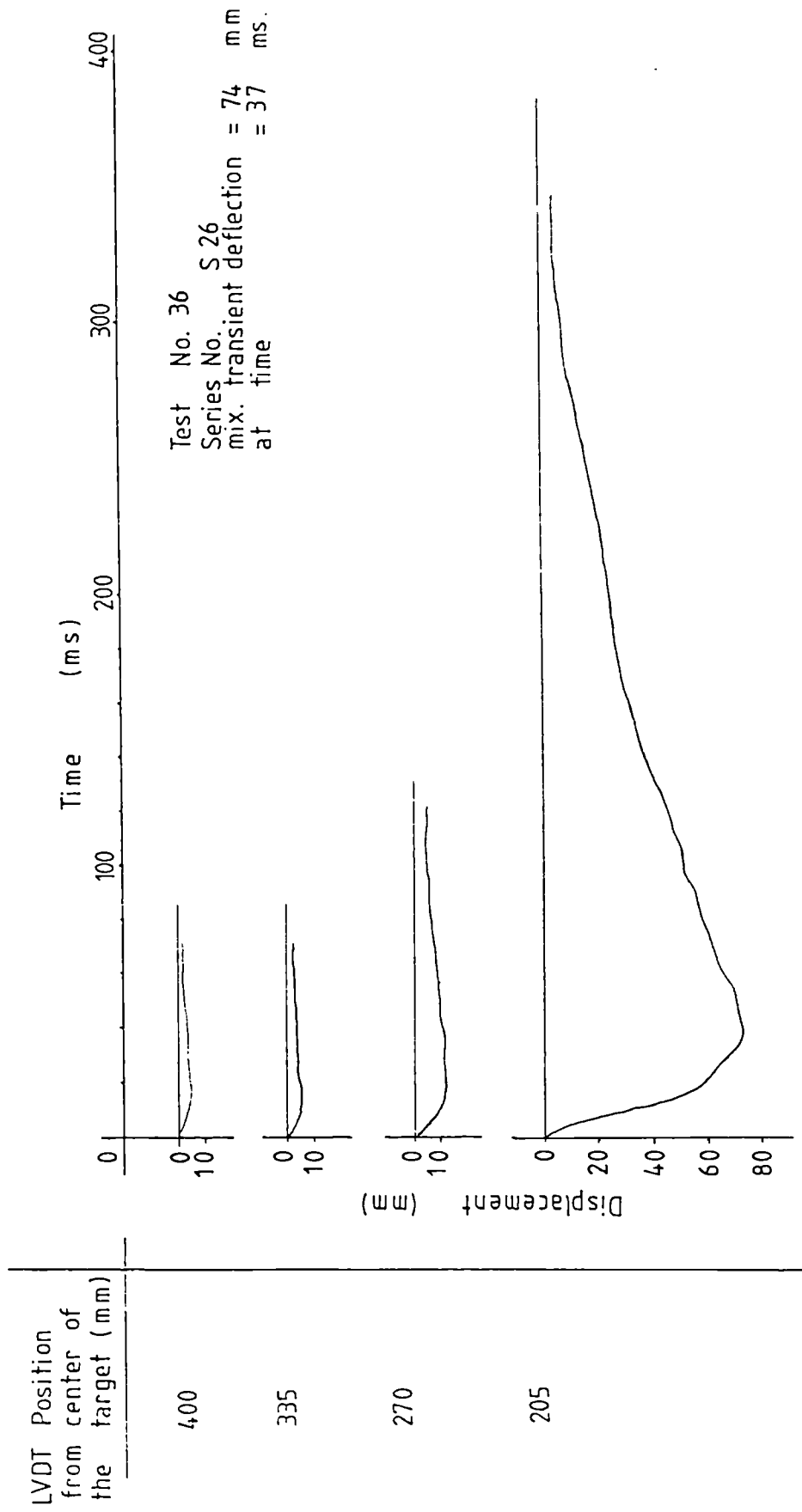


FIG. (5.4b) TRANSIENT DISPLACEMENT OF TARGET AT FOUR DIFFERENT POSITIONS FROM THE CENTER

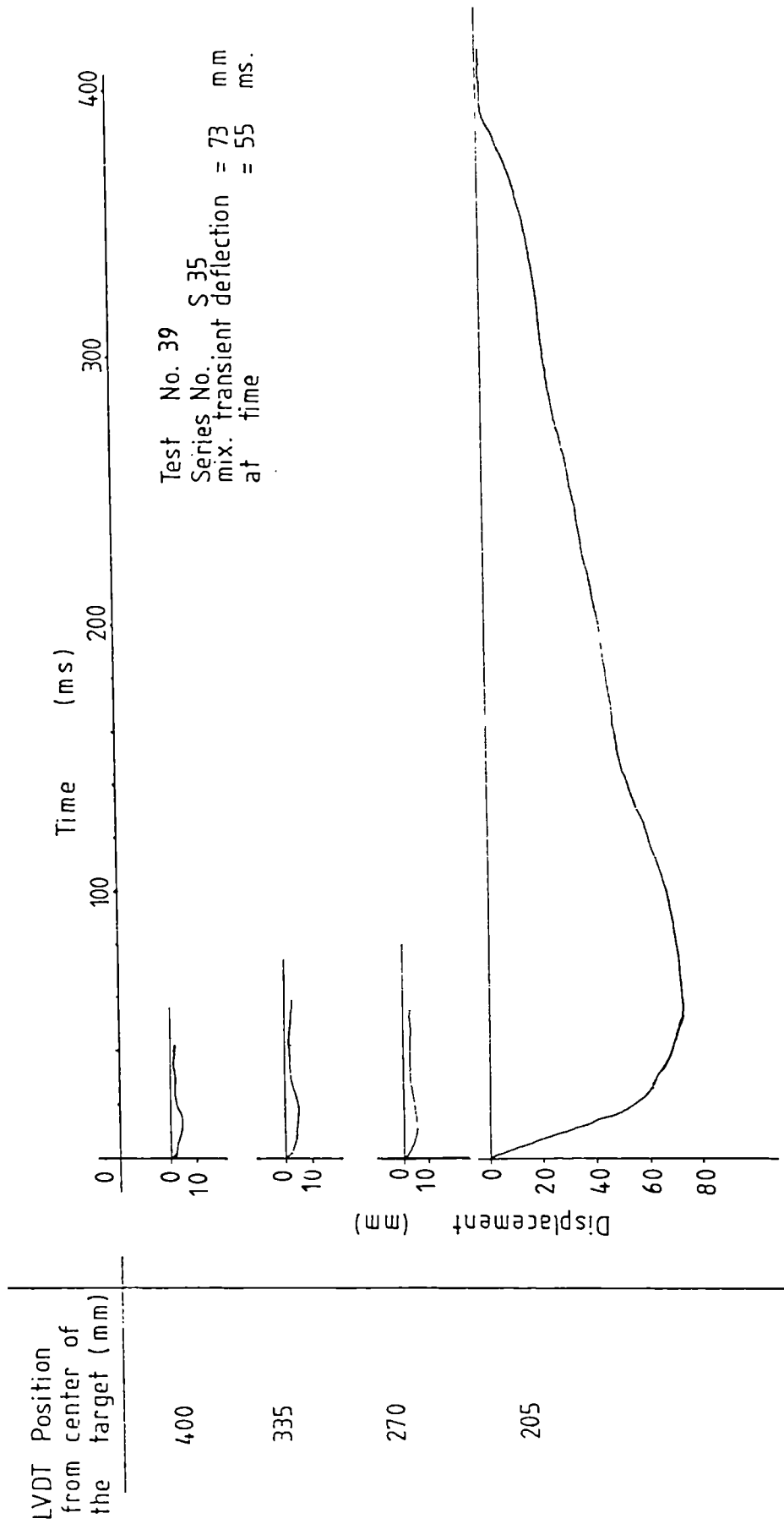


FIG. (5.4c) TRANSIENT DISPLACEMENT OF TARGET AT FOUR DIFFERENT POSITIONS FROM THE CENTER

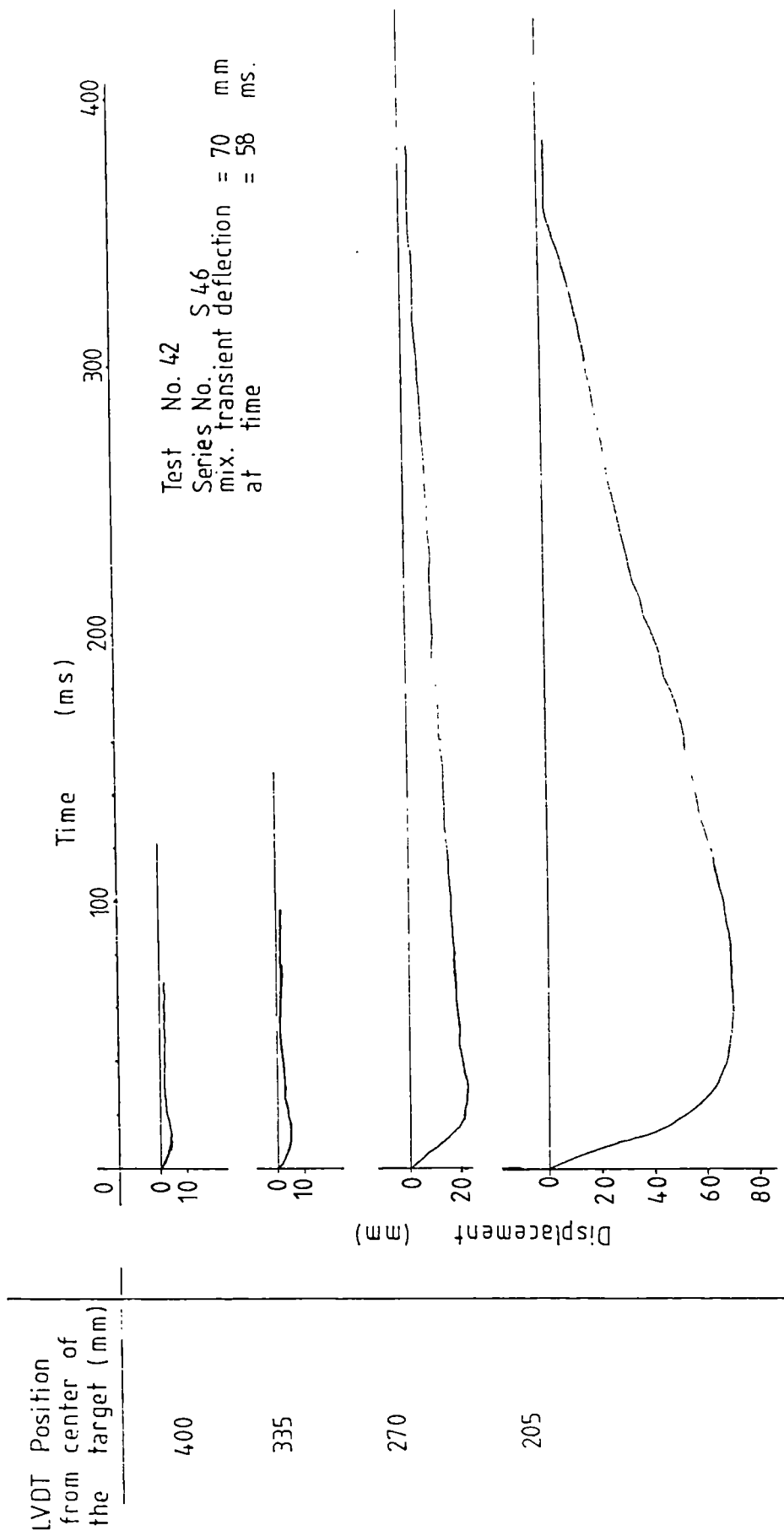


FIG. (5.4d) TRANSIENT DISPLACEMENT OF TARGET AT FOUR DIFFERENT POSITIONS FROM THE CENTER

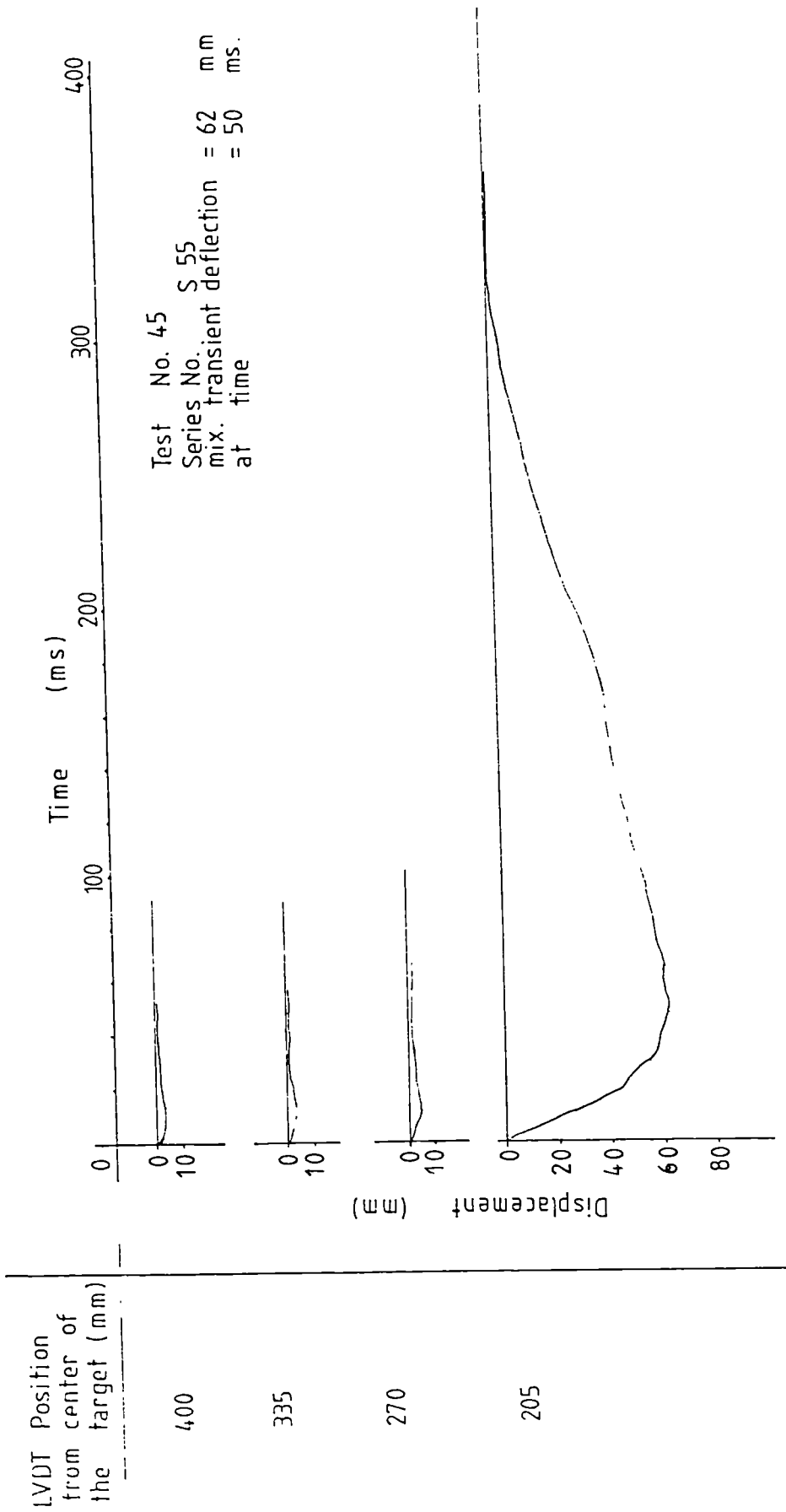


FIG. (5.4e) TRANSIENT DISPLACEMENT OF TARGET AT FOUR DIFFERENT POSITIONS FROM THE CENTER

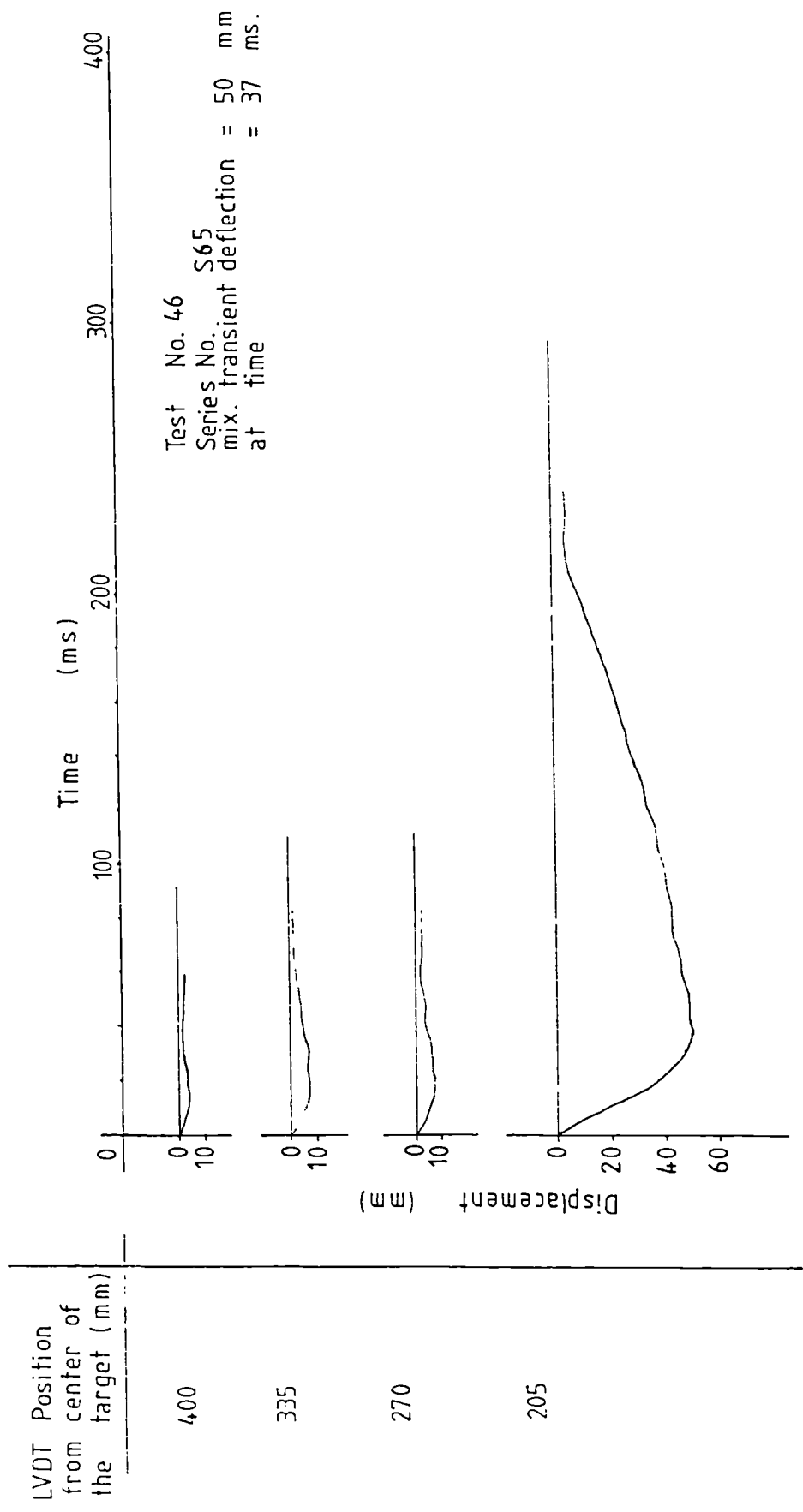


FIG. (5.4f) TRANSIENT DISPLACEMENT OF TARGET AT FOUR DIFFERENT POSITIONS FROM THE CENTER

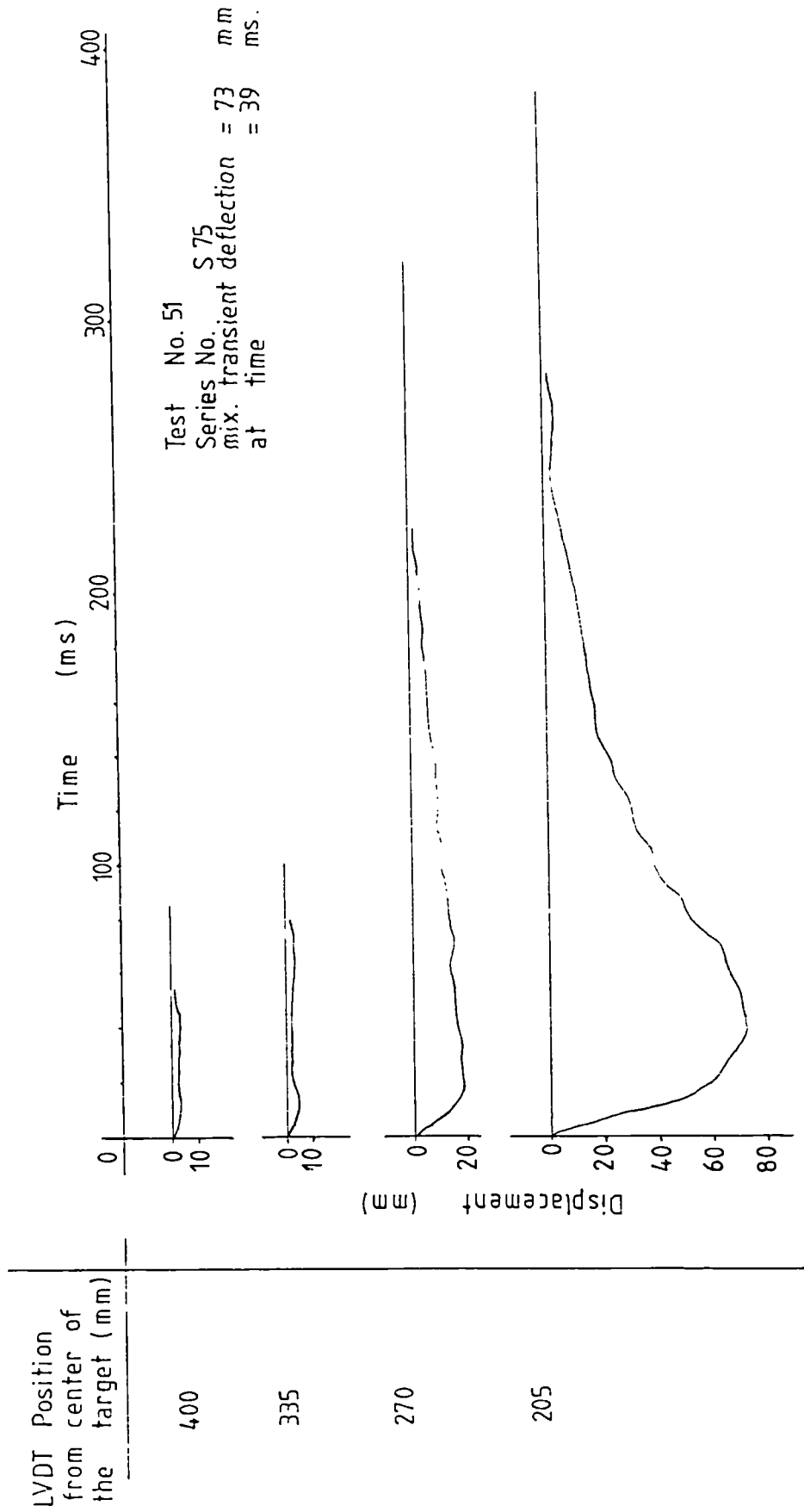


FIG. (5.4g) TRANSIENT DISPLACEMENT OF TARGET AT FOUR DIFFERENT POSITIONS FROM THE CENTER

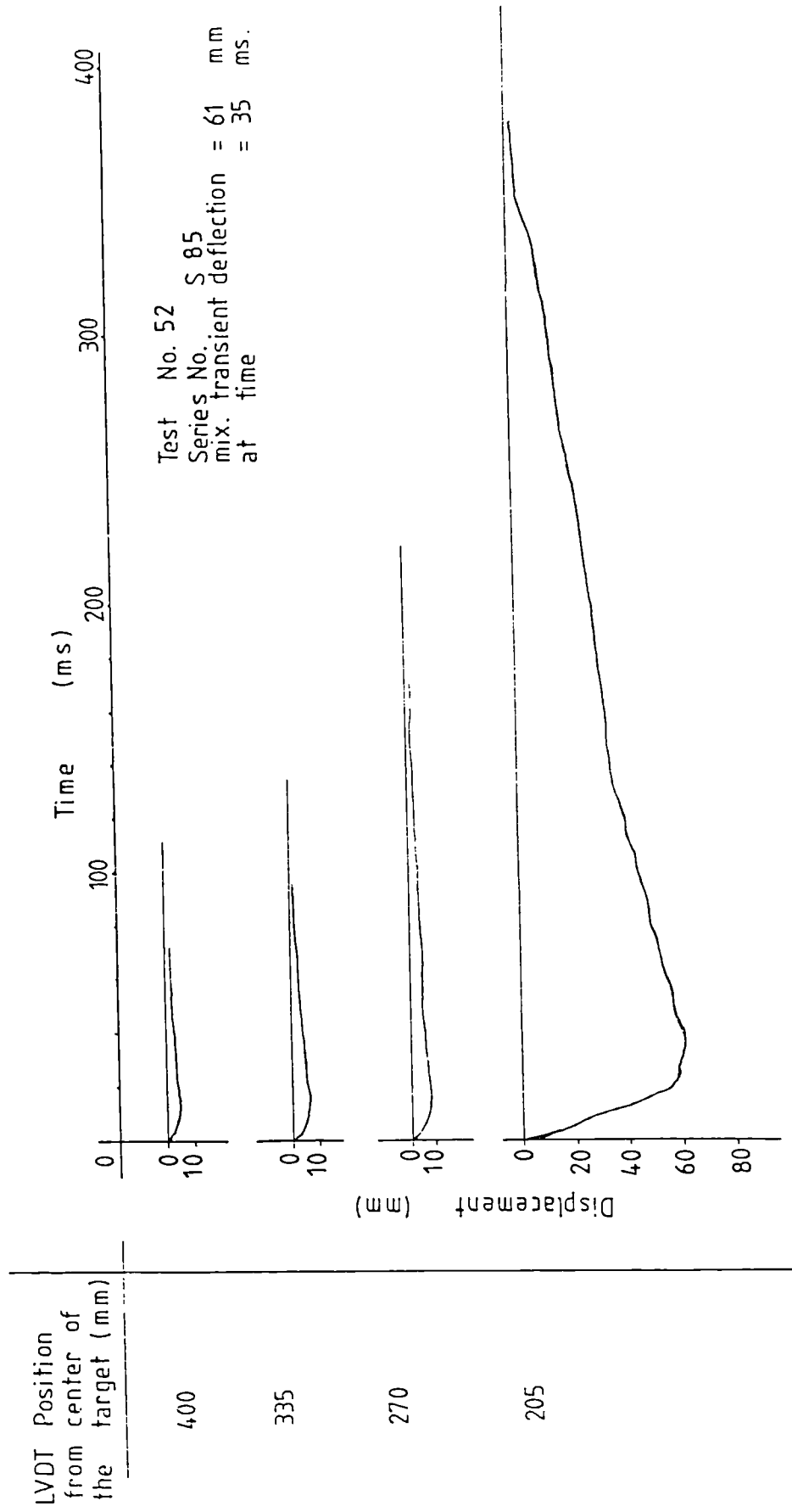


FIG. (5.4h) TRANSIENT DISPLACEMENT OF TARGET AT FOUR DIFFERENT POSITIONS FROM THE CENTER

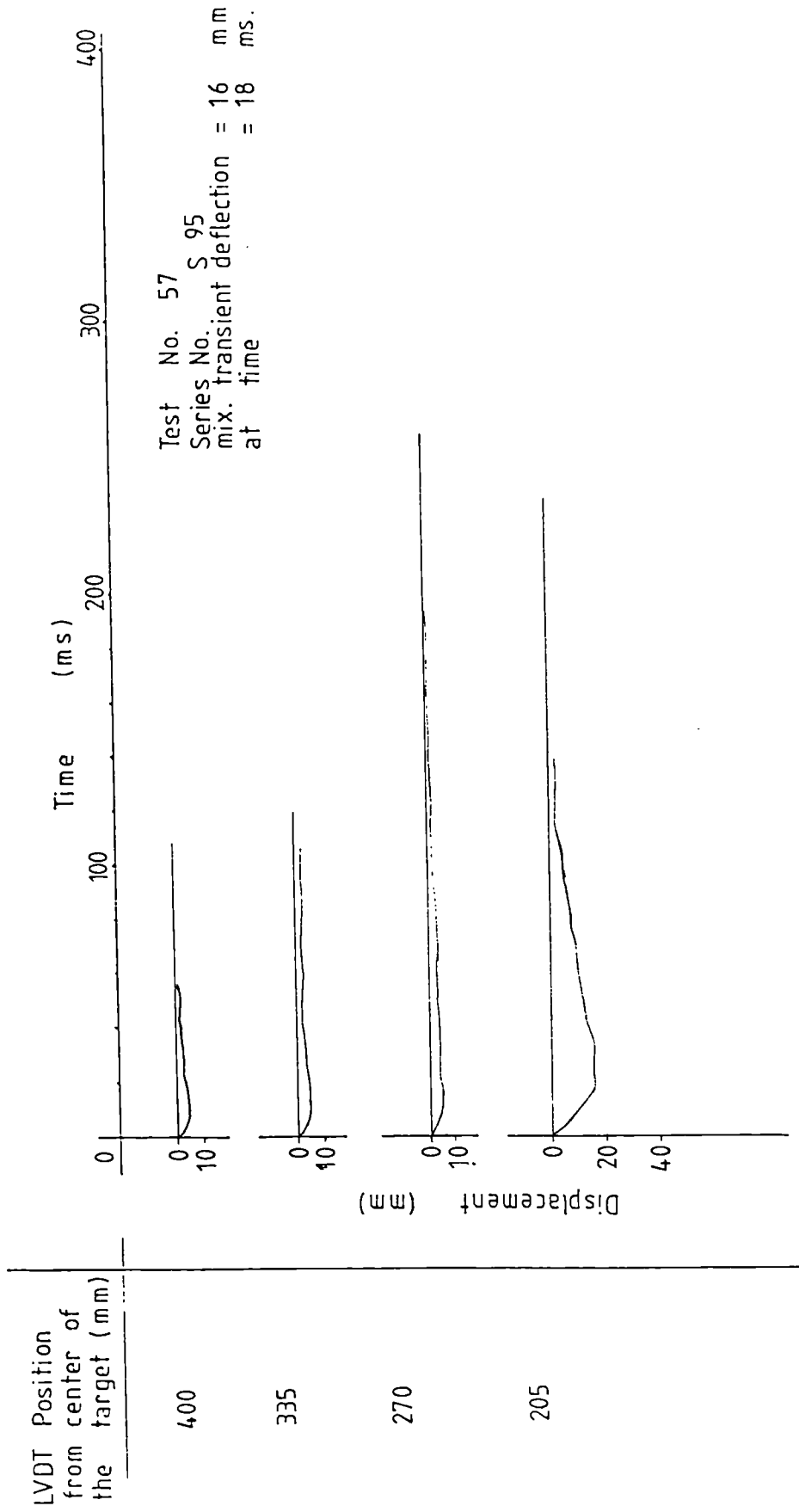


FIG. (5.4 i) TRANSIENT DISPLACEMENT OF TARGET AT FOUR DIFFERENT POSITIONS FROM THE CENTER

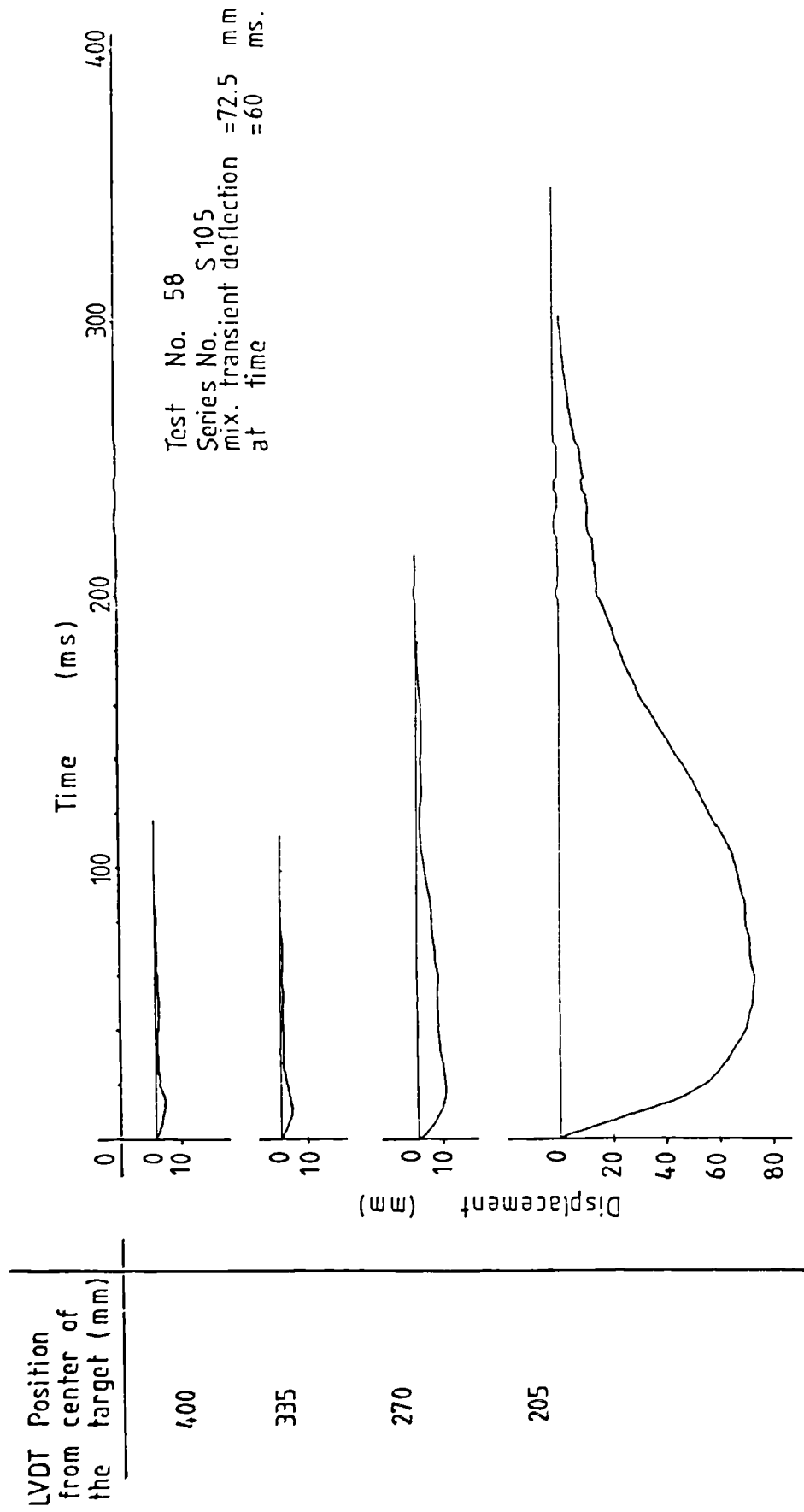


FIG. (5.4j) TRANSIENT DISPLACEMENT OF TARGET AT FOUR DIFFERENT POSITIONS FROM THE CENTER

Table (5.6): The maximum transient deflection at critical scabbing velocity.

Test No.	Series No.	Total percentage of reinforcement	Target thickness (mm)	Reinforcement ratio (kg/m ³)	Maximum transient deflection (mm)	At time (ms)
33	S1	1%	100	160	79	51
36	S2	2.5%	100	390	74	37
39	S3	2.5%	100	390	73	55
42	S4	2.5%	100	390	70	58
45	S5	2.5%	100	390	62	50
46	S6	2.5%	80	390	50	37
51	S7	2.5%	120	400	73	39
52	S8	3.1%	100	490	61	35
57	S9	2%	100	320	16	18
58	S10	2.5%	100	390	72.5	60

All the series have 4mm max. agg. size except S10 which had 2mm max. agg. size

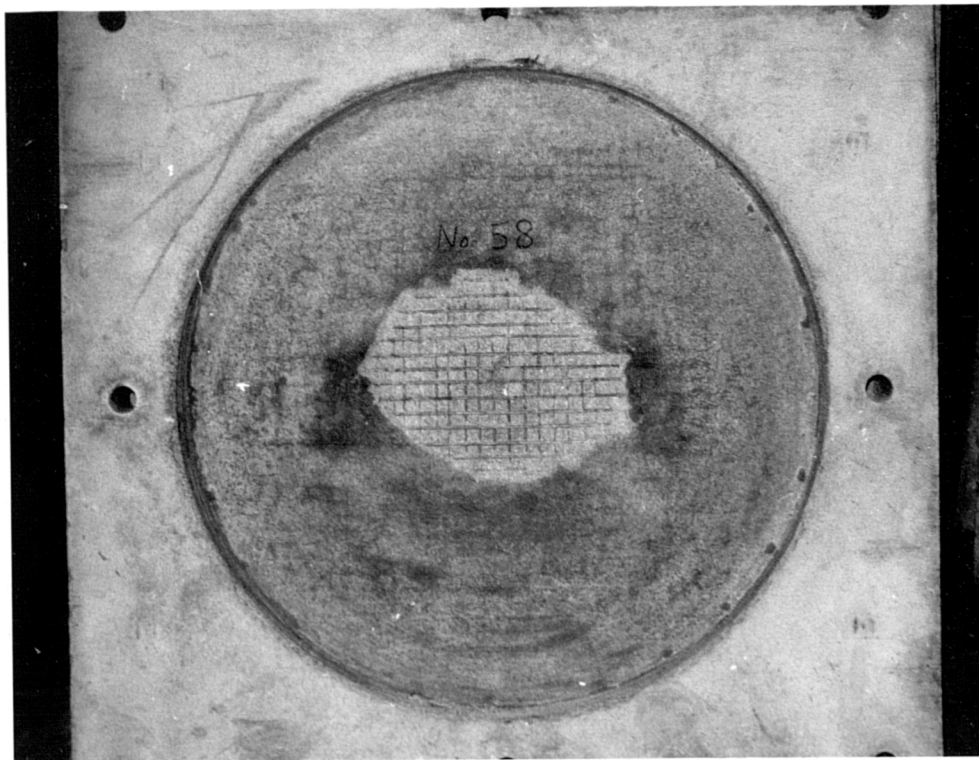
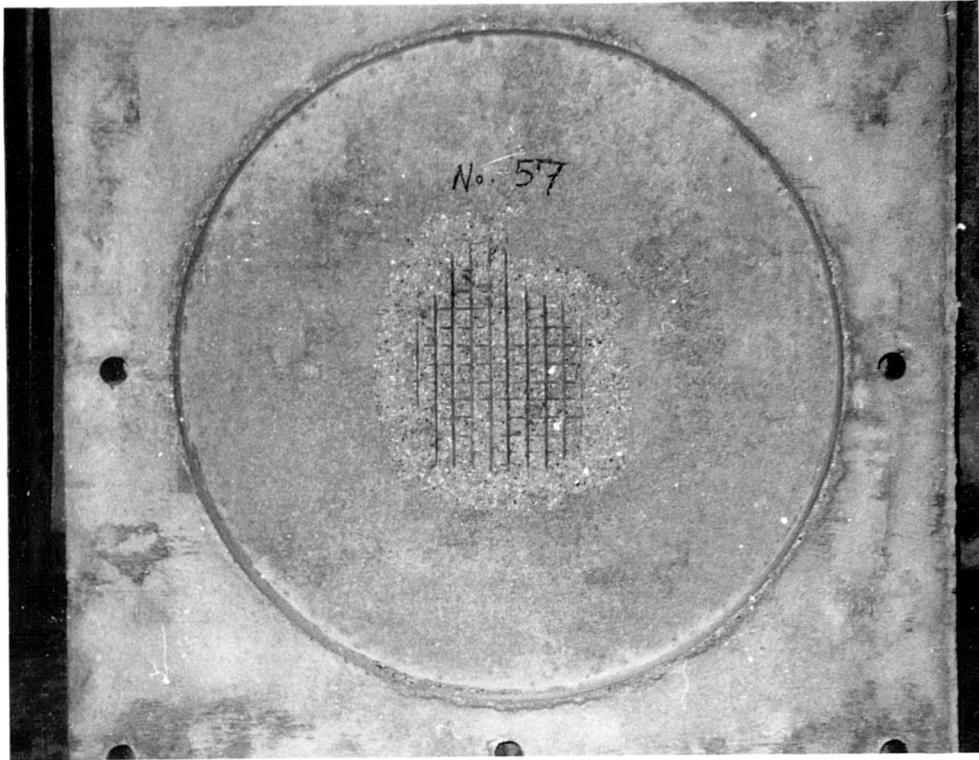


PLATE (5.4)

REAR FACE DAMAGE OF TARGET
(SCABBING)

CHAPTER SIX

DEVELOPMENT AND APPLICATION OF NEW AND EXISTING FORMULAE FOR THE DETERMINATION OF CRITICAL PERFORATION AND SCABBING VELOCITIES

6.1 Introduction

This chapter describes the development of the new empirical relationships for the determination of the critical perforation and the critical scabbing velocities of hard missile impact upon reinforced concrete model slabs. The relationships have been developed as a direct result of the experimental work which has been described. A comparison of the experimental results with the predicted values of the proposed perforation formula, the proposed scabbing formula and the existing empirical formulae which have been described in section 2.3 are also presented. Proposed correction factors to be used with the new relationships and the existing formulae are proposed. These factors make allowance for variations in the amount of flexural reinforcement.

The perforation test observations are presented in section 6.2. This section also includes the development of the proposed perforation formula with the correction factor and the evaluation of the existing perforation formulae with the suggested correction factors. Section 6.3 presents the scabbing test observations. It also includes the development of the proposed scabbing formula with the correction factors and the evaluation of the existing scabbing formulae also with the correction factors to account for variations in the amount of flexural reinforcement.

6.2 The Development and Application Of The Proposed New Perforation Formula

A review of the previously presented test results obtained from the experimental work associated with the determination of the critical perforation velocity is shown in table (6.1). It has been assumed that in the development of an empirical relationship to determine the critical perforation velocity, the perforation thickness varied inversely with the square root of concrete compressive strength f'_c . This assumption has been previously made with respect to high velocity missile impact (6) and enables the experimental results obtained from the tests S2, S6 and S7 series, to be plotted directly on a graph of slab thickness versus missile critical perforation velocity. By using an available computer program "Minitab" (44) to carry out a regression analysis for these test results, the following empirical relationship has been found to define the perforation thickness d_p in terms of the velocity V_{cp}

$$\text{Thus } d_p = 1.778 V_{cp}^{0.909} \quad (6.1)$$

where d_p = target perforation thickness (mm).

V_{cp} = critical perforation velocity (m/sec).

The thickness of the concrete slab to prevent perforation increases as the missile mass increases, and reduces as the concrete compressive strength and missile diameter increases (9). Therefore, the form of a general perforation thickness equation would be

$$d_p = \frac{c_1}{(f'_c)^{c_4}} \cdot \frac{M^{c_2}}{D^{c_3}} \cdot V_{cp}^{c_5} \quad (6.2)$$

Table (6.1) Experimental test results (perforation resistance)

Series No.	Total percentage of reinforcement	Target thickness (mm)	Concrete compressive strength f_c' (cube) (N/mm ²)	Mass of missile (kg)	Diameter of missile (cm)	Critical perforation velocity (m/sec.)
S1	1%	100	56.53	3.695	4.973	54.11
S2	2.5%	100	56.0	3.689	4.972	82.56
S3	2.5%	100	54.4	3.2	4.973	91.15
S4	2.5%	100	52.93	2.719	4.986	102.7
S5	2.5%	100	52.36	2.23	4.983	118.3
S6	2.5%	80	45.66	3.698	4.985	65.33
S7	2.5%	120	44.16	3.698	4.988	102.1
S8	3.1%	100	48.5	3.685	4.974	89.76
S9	2%	100	45.46	3.694	4.985	76.55
S10	2.5%	100	46.63	3.695	4.986	82.12
S11	0%	100	44.36	3.644	4.954	37.37

All the series have 4mm max. agg. size except S10 which had 2mm max. agg. size

where M = missile mass (kg).

D = missile diameter (cm).

f'_c = concrete compressive strength (cube) (N/mm^2).

in which c_1 , c_2 , c_3 , c_4 and c_5 are experimentally determined constants. A value of 0.5 is used for c_4 which is based upon the empirical relationships for higher velocity missiles impact. From eq. (6.1) the value of c_5 is 0.909 and is used in the general perforation thickness equation as follows

$$d_p = \frac{c_1}{(f'_c)^{0.5}} \cdot \frac{M^{c_2}}{D^{c_3}} \cdot V_{cp}^{0.909} \quad (6.3)$$

In order to evaluate the constants in eq. (6.3), the following procedure is adopted. The velocity of the missile of mass 2.719 kg to perforate the slab of thickness 100 mm is 102.7 m/sec (S4 test result from table (6.1)). Using the S4 test result which is substituted into eq.(6.3)

$$100 = \frac{c_1}{(52.93)^{0.5}} \cdot \frac{(2.719)^{c_2}}{(4.986)^{c_3}} \cdot (102.7)^{0.909} \quad (6.4)$$

Also using the S10 test result from table (6.1) and substituting into eq. (6.3)

$$100 = \frac{c_1}{(46.63)^{0.5}} \cdot \frac{(3.695)^{c_2}}{(4.986)^{c_3}} \cdot (82.12)^{0.909} \quad (6.5)$$

Dividing eq. (6.5) by eq. (6.4)

$$c_2 = 0.456$$

With the value of c_2 determined, the value of c_3 can be found by using the S3 and S5 test results from table (6.1) in eq.

(6.3) to give

$$100 = \frac{c_1}{(52.36)^{0.5}} \cdot \frac{(2.23)^{0.456}}{(4.983)^{c_3}} \cdot (118.3)^{0.909} \quad (6.6)$$

and

$$100 = \frac{c_1}{(54.4)^{0.5}} \cdot \frac{(3.2)^{0.456}}{(4.973)^{c_3}} \cdot (91.15)^{0.909} \quad (6.7)$$

Dividing eq. (6.7) by eq. (6.6) the constant

$$c_3 = 45.5$$

By substituting $c_2 = 0.456$ and $c_3 = 45.5$ into eq. (6.3), the value of c_1 can be determined by substituting into eq. (6.1) as follows

$$\frac{c_1}{(f'_C)^{0.5}} \cdot \frac{M^{0.456}}{D^{45.5}} = 1.778$$

$$\therefore c_1 = 1.778 \times (f'_C)^{0.5} \frac{D^{45.5}}{M^{0.456}} \quad (6.8)$$

The test results of series S2, S6 and S7 can be substituted into eq. (6.8) to find the average value of c_1 which is equal to 3.628×10^{32} and the proposed perforation formula becomes

$$d_p = 3.628 \times 10^{32} \frac{M^{0.456}}{(f'_C)^{0.5}} \cdot \frac{V_{cp}^{0.909}}{D^{45.5}} \quad (6.9)$$

The formula is valid only for the experimental conditions which have been previously described.

Table (6.2) shows a comparison of the experimental results with those predicted by the proposed formula. It can be seen that the most accurate prediction of the formula occurs when the flexural reinforcement ratios are 390 kg/m³ which is to be expected. The prediction is not so accurate for other ratios, however, and it is suggested that the formula be corrected by a coefficient which is obtained by plotting the ratio of test velocity to the predicted velocity V_t/V_f against the flexural reinforcement ratio. This coefficient will account for variation in the flexural reinforcement ratio. From fig (6.1) the correction coefficient is obtained in the following way

$$1 = \frac{V_t}{V_f} + Y_1$$

From ΔABC and DBE

$$\frac{Y_1}{0.455} = \frac{408 - r}{408}$$

$$\therefore Y_1 = 0.455 \left(\frac{408 - r}{408} \right)$$

Substituting the value of y_1 into the above equation

$$1 = \frac{V_t}{V_f} + 0.455 \left(\frac{408 - r}{408} \right)$$

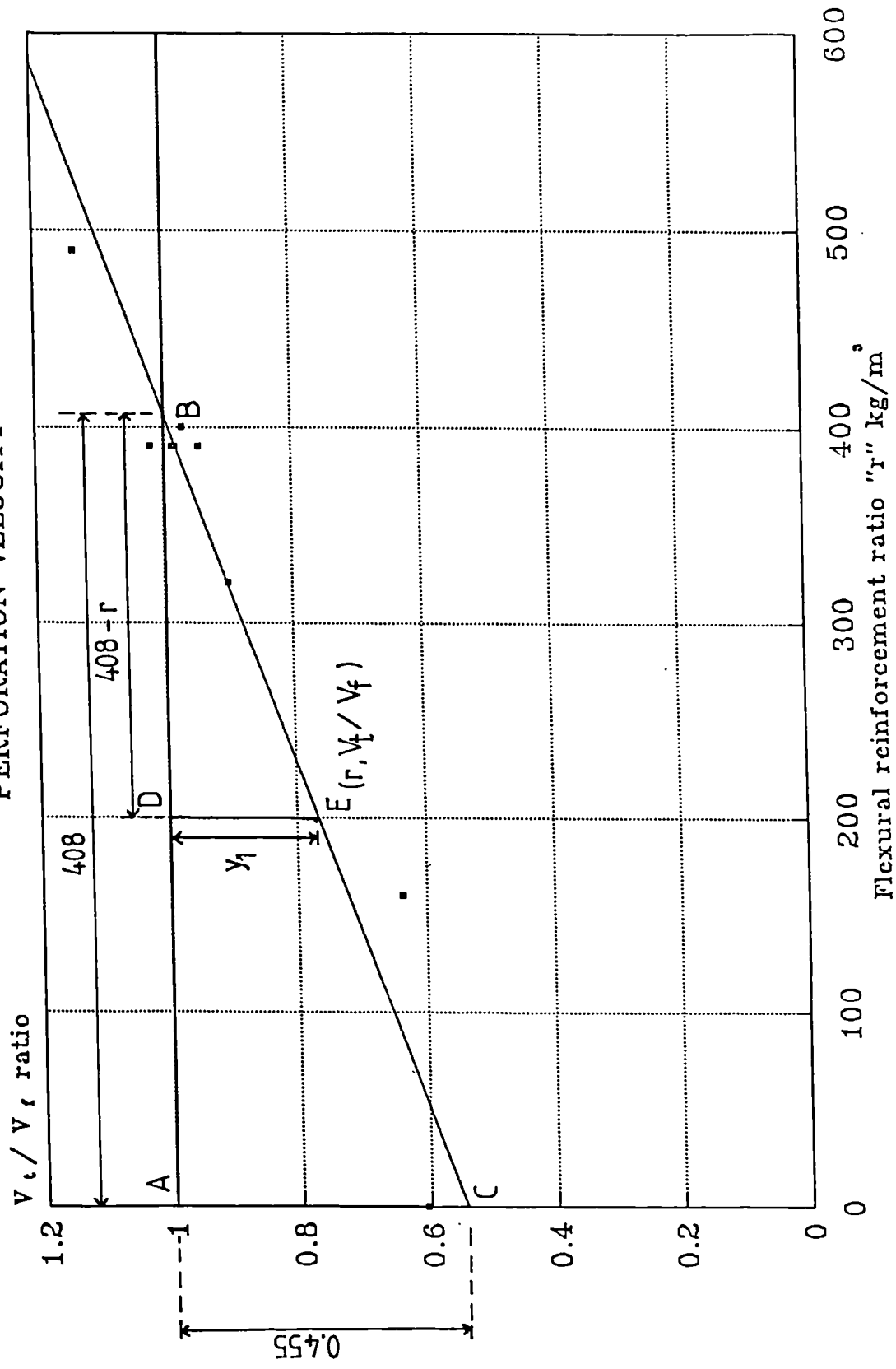
$$\frac{V_t}{V_f} = 1 - 0.455 \left(\frac{408 - r}{408} \right)$$

$$\frac{V_t}{V_f} = 0.455 \left(1.2 + \frac{r}{408} \right)$$

Table (6.2) Comparison of test and proposed formula velocities (perforation resistance)

Series No.	Total percentage of reinforcement	Flexural reinforcement ratio (kg/m ³)	Critical perforation velocity (m/sec.)		Test velocity formula velocity ratio
			Test	Formula	
S1	1%	160	54.11	84.94	0.637
S2	2.5%	390	82.56	83.73	0.986
S3	2.5%	390	91.15	89.39	1.019
S4	2.5%	390	102.7	108.89	0.943
S5	2.5%	390	118.3	116.01	1.019
S6	2.5%	390	65.33	66.64	0.980
S7	2.5%	400	102.1	105.33	0.969
S8	3.1%	490	89.76	78.98	1.136
S9	2%	320	76.55	85	0.9
S10	2.5%	390	82.12	87.08	0.943
S11	0%	0	37.37	61.81	0.604

FIG (6.1) COMPARISON OF THE TEST AND PROPOSED PERFORATION VELOCITY



V_t Test velocity V_f Formula velocity

$$V_t = 0.455 \left(1.2 + \frac{r}{408} \right) V_f \quad (6.10)$$

where V_t = test velocity.

V_f = formula velocity

r = flexural reinforcement ratio (kg/m^3)

For a practical application for a given thickness of target, equation (6.9) will be modified in the following manner. The target thickness to be considered should lie within the range 80-120 mm and the corresponding value of critical perforation velocity V_{cp} obtain from eq. (6.9). The value of V_{cp} is substituted into eq. (6.10) and becomes the term V_f . The quantity r will lie within the range 0-500 Kg/m^3 , hence, V_t is calculated from eq. (6.10) and becomes the corrected critical perforation velocity for the target. Table (6.3) summarises the test velocities and predicted values of the corrected proposed critical perforation velocities.

The test results show the dependence of the critical perforation velocity upon the quantity of flexural reinforcement. There would appear to be no significant influence, however, of the maximum aggregate size upon this velocity.

6.2.1 Evaluation Of Existing Empirical Formulae To Predict Critical Perforation Velocity

The critical perforation velocity of a missile impacting upon a reinforced concrete target can be estimated using the existing empirical formulae described in section 2.3. The data obtained from the current experimental programme can be used with these formulae to determine their accuracy. Table

Table (6.3) Comparison of experimental results with the proposed formula predictions (perforation resistance)

Series No.	Flexural reinforcement ratio (kg/m ³)	Critical perforation velocity (m/sec.)		Test velocity formula velocity ratio
		Test	Formula with correction factor	
S1	160	54.11	61.53	0.88
S2	390	82.56	82.13	1.005
S3	390	91.15	87.68	1.039
S4	390	102.7	106.81	0.961
S5	390	118.3	113.8	1.039
S6	390	65.33	65.37	0.999
S7	400	102.1	104.5	0.977
S8	490	89.76	86.28	1.04
S9	320	76.55	76.74	0.997
S10	390	82.12	85.42	0.961
S11	0	37.37	35.75	1.045

(6.4) summarises the measured and calculated critical perforation velocities using these formulae. Typical calculations of the critical perforation velocity for one of the series are given in appendix A.

It can be seen from table (6.5) and fig (6.2) that the modified Petry 1, "CEA - EDF", Haldar & Miller and Adeli & Amin formulae provide results that are closest to the measured critical perforation velocities defined by the author. The author has ignored others because they are restricted in their range of applicability as follows.

i. The ACE, NDRC, BRL and Kar formulae have been developed for predicting damage to reinforced concrete panels from non-deformable military type projectiles with velocities typically exceeding 150 m/sec.

ii. The mass and the diameter of the missile used to develop the Degen formula was between 17.5 to 343 kg and 100 to 300 mm respectively. The formula was also developed for the prediction of a perforation thickness of concrete target between 0.175 to 0.6 m which is greater than the thickness investigated in this thesis.

iii. The Hughes formula is valid in the range $I' < 3500$ which is the range of available test data, but it will be conservative in the range $I' < 40$ and $d / D < 3.5$ because the theory used to develop this formula neglects both elastic and global effects. These tend to reduce the severity of local damage (29).

It should be noted that the formulae providing results closest to the experimental values do not take into account the variations in the level of flexural reinforcement. Since

Table (6.4) Measured and calculated critical perforation velocities

Series No.	Flexural reinforcement ratio (kg/m ³)	Critical Perforation Velocity (m/sec.)											
		1	2	3	4	5	6	7	8	9	10	11	12
S1	160	54.11	90.09	17.04	71.01	125.3	83.3	71.69	103.83	84.75	85.68	52.57	90.97
S2	390	82.56	79.14	17.0	70.88	125.14	82.84	71.56	103.65	84.6	85.35	52.5	90.62
S3	390	91.15	98.26	18.52	76.11	137.8	90.08	76.86	111.41	90.95	90.35	55.96	95.93
S4	390	102.7	108.9	19.38	82.65	154.64	99.0	83.48	121.01	99.57	96.87	60.23	102.72
S5	390	118.3	123.56	22.24	97.07	178.67	112.52	92.91	134.7	112.8	106.44	66.34	112.73
S6	390	65.33	79.4	-	49.6	98.20	55.53	49.78	73.47	54.57	67.85	35.09	63.36
S7	400	102.1	100.91	54.98	86.61	131.64	93.88	87.59	125.1	91.86	91.5	64.81	97.44
S8	490	89.76	90.32	16.23	68.19	118.74	77.24	68.65	99.72	76.67	79.5	50.65	84.36
S9	320	76.55	90.45	15.08	66.96	116.04	74.82	67.53	97.89	73.41	77.03	49.78	81.68
S10	390	82.12	90.42	15.2	67.43	117.13	75.58	68.0	98.57	74.69	78.04	50.08	82.72
S11	0	37.37	-	-	-	-	-	-	-	-	-	-	-

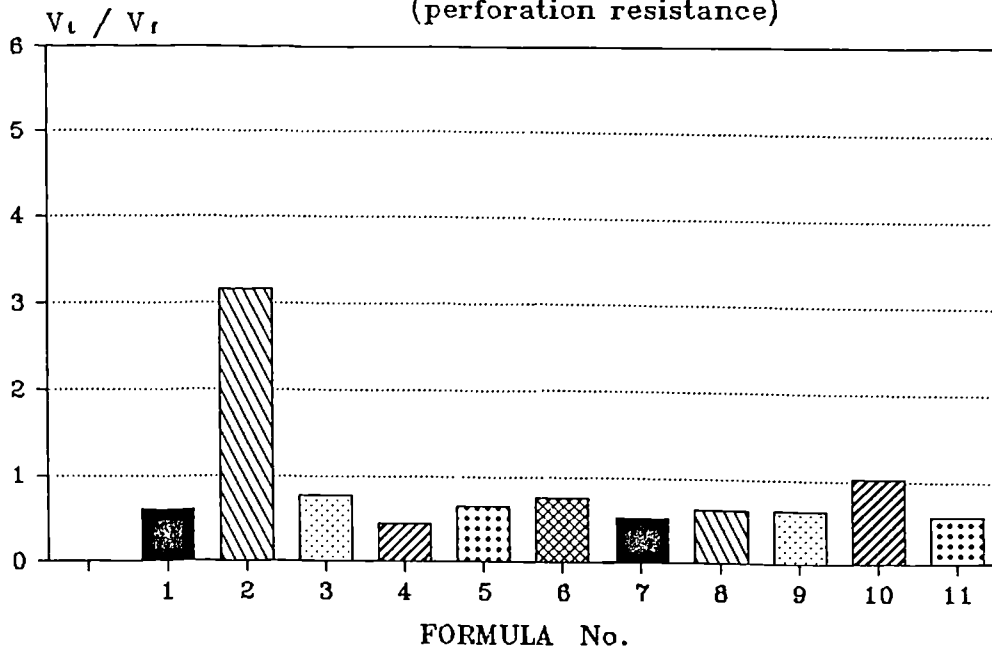
- 1 - Test result
 2 - Modified petry formula
 3 - "ACE" formula
 4 - "NDRC" formula
 5 - "BRL" formula
 6 - "CEA-EDF" formula
 7 - Kar formula
 8 - Degen formula
 9 - Chang formula
 10 - Halder and Miller formula
 11 - Hughes formula
 12 - Adeli and Amin formula

Table (6.5) Test velocity/formula velocity ratios (perforation resistance)

Series No.	Total percentage reinforcement	Flexural reinforcement ratio kg/m ²	measured/calculated critical perforation velocity ratio										
			1	2	3	4	5	6	7	8	9	10	11
S1	1%	160	0.6	3.175	0.762	0.431	0.649	0.754	0.521	0.638	0.63	1.029	0.594
S2	2.5%	390	1.043	4.856	1.164	0.659	0.996	1.153	0.796	0.976	0.967	1.572	0.911
S3	2.5%	390	0.927	4.921	1.197	0.661	1.011	1.186	0.818	1.002	1.008	1.628	0.950
S4	2.5%	390	0.943	5.299	1.242	0.664	1.037	1.230	0.848	1.031	1.06	1.705	1.0
S5	2.5%	390	0.957	5.319	1.218	0.662	1.051	1.273	0.878	1.048	1.111	1.783	1.049
S6	2.5%	390	0.822	-	1.317	0.665	1.176	1.312	0.889	1.197	0.962	1.861	1.031
S7	2.5%	400	1.011	1.857	1.178	0.775	1.087	1.165	0.816	1.111	1.115	1.575	1.047
S8	3.1%	490	0.993	5.53	1.316	0.756	1.162	1.307	0.90	1.170	1.129	1.772	1.064
S9	2%	320	0.846	5.076	1.143	0.659	1.023	1.133	0.782	1.042	0.993	1.537	0.937
S10	2.5%	390	0.908	5.402	1.217	0.701	1.086	1.207	0.833	1.099	1.052	1.639	0.992

- 1 - Modified petry formula
- 2 - "ACE" formula
- 3 - "NDRC" formula
- 4 - "BRL" formula
- 5 - "CEA-EDF" formula
- 6 - Kar formula
- 7 - Degen formula
- 8 - Chang formula
- 9 - Haldar and Miller formula
- 10 - Hughes formula
- 11 - Adeli and Amin formula

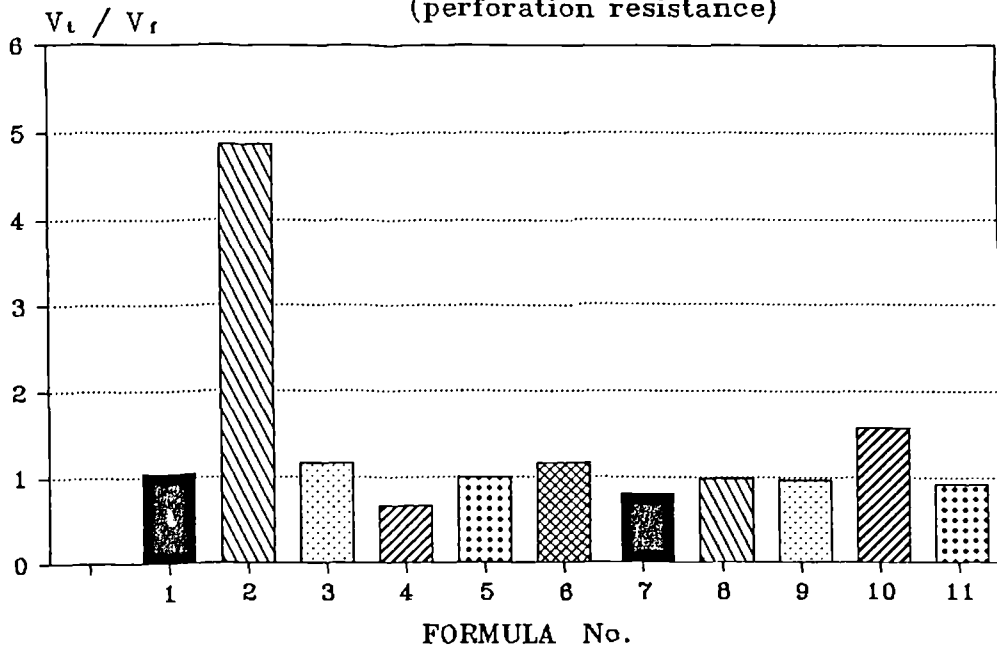
FIG (6.2a) TEST VELOCITY/FORMULA VELOCITY RATIOS
(perforation resistance)



- | | |
|--------------------------|-----------------------------|
| 1-Modified Petry formula | 7-Degen formula |
| 2-ACE formula | 8-Chang formula |
| 3-NDRC formula | 9-Haldar and Miller formula |
| 4-BRL formula | 10-Hughes formula |
| 5-CEA-EDF formula | 11-Adeli and Amin formula |
| 6-Kar formula | |

The calculation uses the experimental data obtained during the S1 series

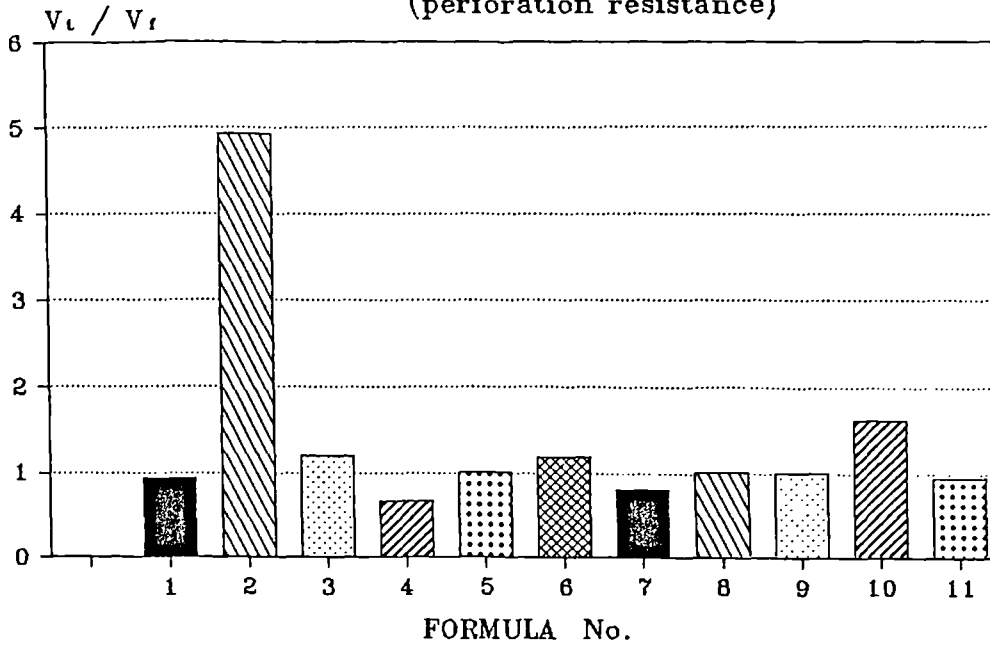
FIG (6.2b) TEST VELOCITY/FORMULA VELOCITY RATIOS
(perforation resistance)



- | | |
|--------------------------|-----------------------------|
| 1-Modified Petry formula | 7-Degen formula |
| 2-ACE formula | 8-Chang formula |
| 3-NDRC formula | 9-Haldar and Miller formula |
| 4-BRL formula | 10-Hughes formula |
| 5-CEA-EDF formula | 11-Adeli and Amin formula |
| 6-Kar formula | |

The calculation uses the experimental data obtained during the S2 series

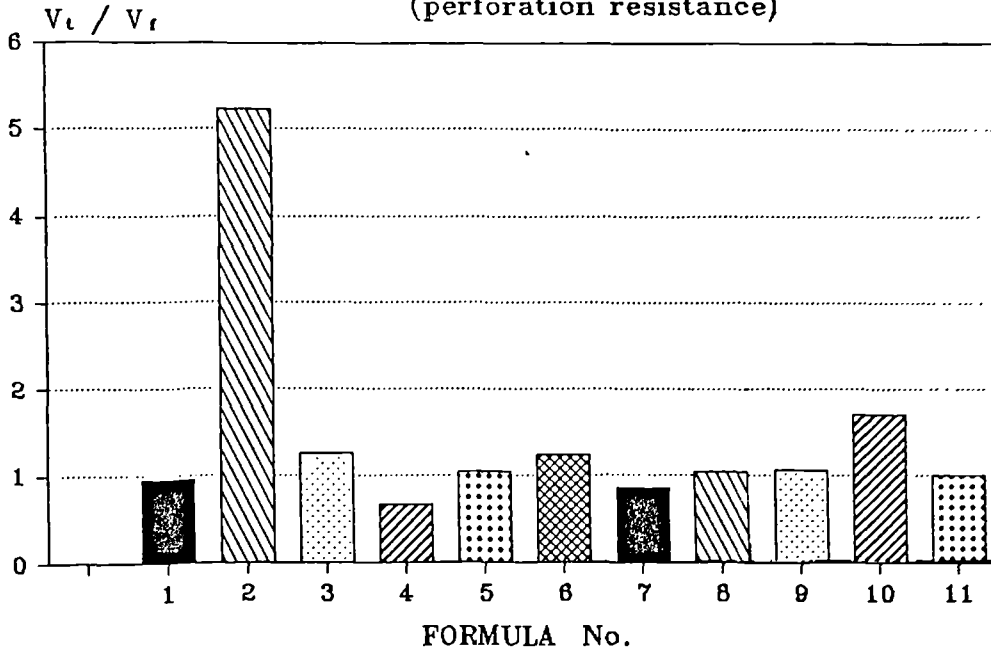
FIG (6.2c) TEST VELOCITY/FORMULA VELOCITY RATIOS
(perforation resistance)



- | | |
|--------------------------|-----------------------------|
| 1-Modified Petry formula | 7-Degen formula |
| 2-ACE formula | 8-Chang formula |
| 3-NDRC formula | 9-Haldar and Miller formula |
| 4-BRL formula | 10-Hughes formula |
| 5-CEA-EDF formula | 11-Adeli and Amin formula |
| 6-Kar formula | |

The calculation uses the experimental data obtained during the S3 series

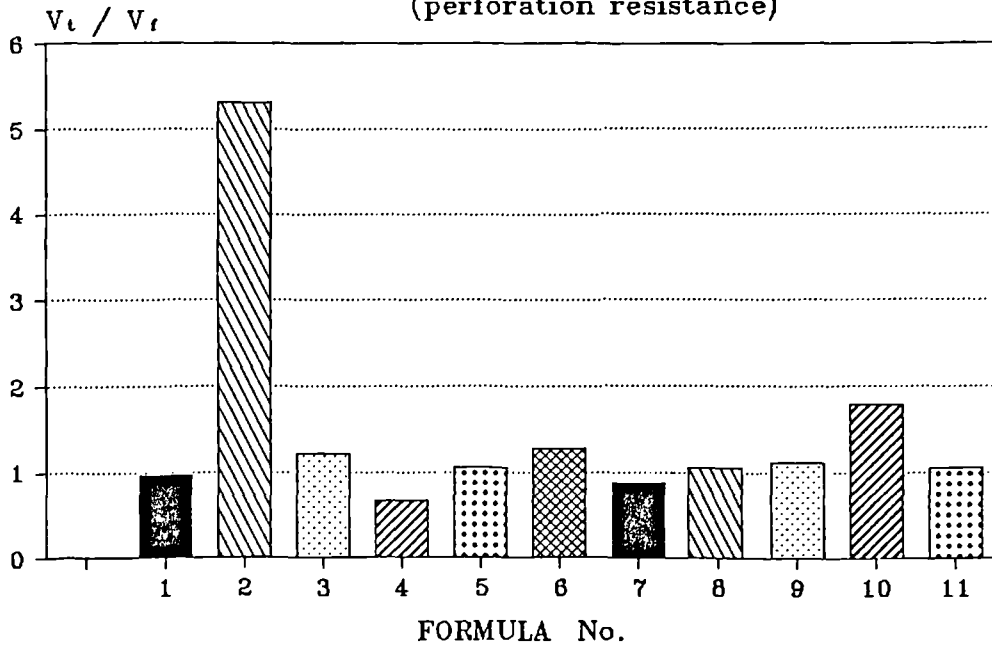
FIG (6.2d) TEST VELOCITY/FORMULA VELOCITY RATIOS
(perforation resistance)



- | | |
|--------------------------|-----------------------------|
| 1-Modified Petry formula | 7-Degen formula |
| 2-ACE formula | 8-Chang formula |
| 3-NDRC formula | 9-Haldar and Miller formula |
| 4-BRL formula | 10-Hughes formula |
| 5-CEA-EDF formula | 11-Adeli and Amin formula |
| 6-Kar formula | |

The calculation uses the experimental data obtained during the S4 series

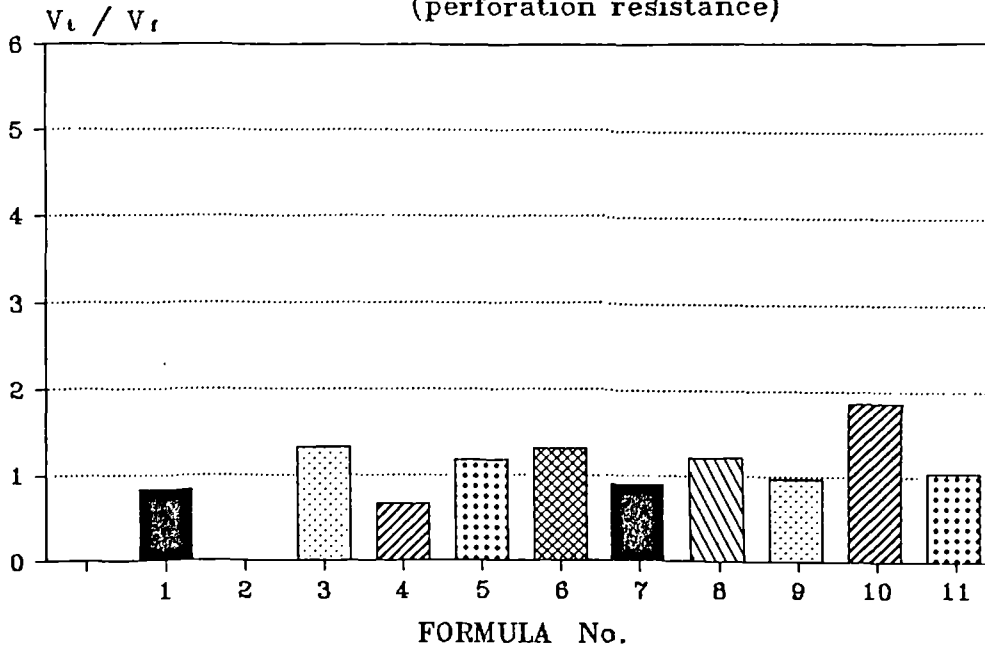
FIG (6.2e) TEST VELOCITY/FORMULA VELOCITY RATIOS
(perforation resistance)



- | | |
|--------------------------|-----------------------------|
| 1-Modified Petry formula | 7-Degen formula |
| 2-ACE formula | 8-Chang formula |
| 3-NDRC formula | 9-Haldar and Miller formula |
| 4-BRL formula | 10-Hughes formula |
| 5-CEA-EDF formula | 11-Adeli and Amin formula |
| 6-Kar formula | |

The calculation uses the experimental data obtained during the S5 series

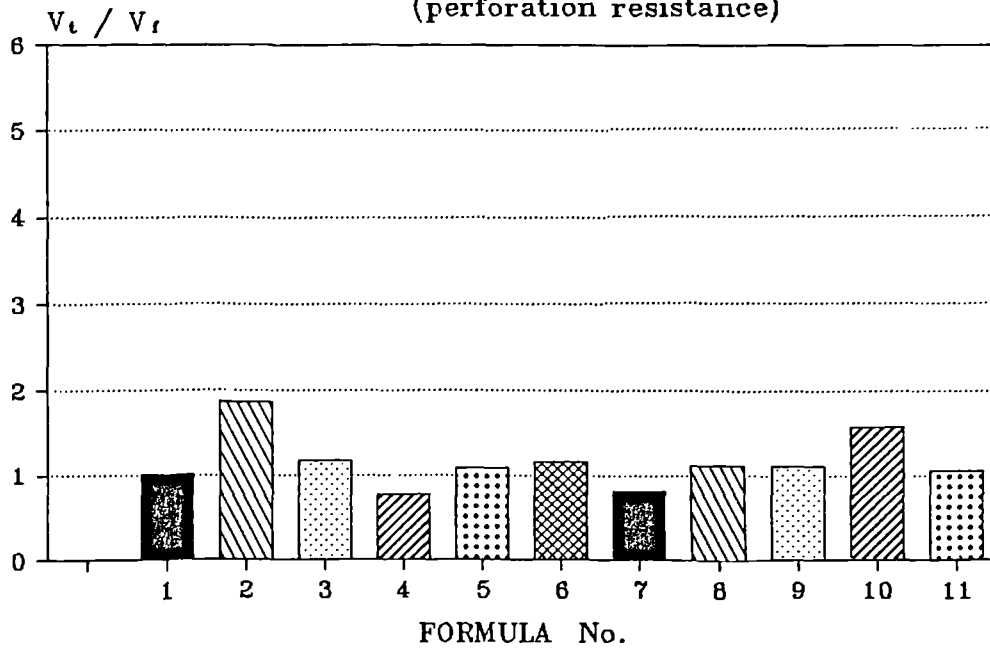
FIG (6.2f) TEST VELOCITY/FORMULA VELOCITY RATIOS
(perforation resistance)



- | | |
|--------------------------|-----------------------------|
| 1-Modified Petry formula | 7-Degen formula |
| 2-ACE formula | 8-Chang formula |
| 3-NDRC formula | 9-Haldar and Miller formula |
| 4-BRL formula | 10-Hughes formula |
| 5-CEA-EDF formula | 11-Adeli and Amin formula |
| 6-Kar formula | |

The calculation uses the experimental data obtained during the S6 series

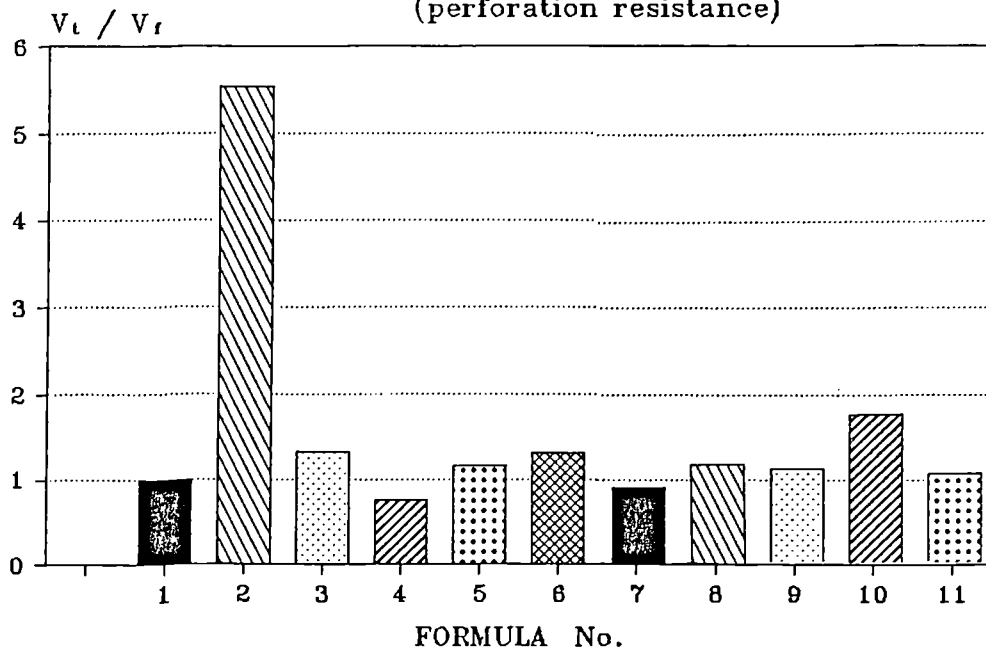
FIG (6.2g) TEST VELOCITY/FORMULA VELOCITY RATIOS
(perforation resistance)



- | | |
|--------------------------|-----------------------------|
| 1-Modified Petry formula | 7-Degen formula |
| 2-ACE formula | 8-Chang formula |
| 3-NDRC formula | 9-Haldar and Miller formula |
| 4-BRL formula | 10-Hughes formula |
| 5-CEA-EDF formula | 11-Adeli and Amin formula |
| 6-Kar formula | |

The calculation uses the experimental data obtained during the S7 series

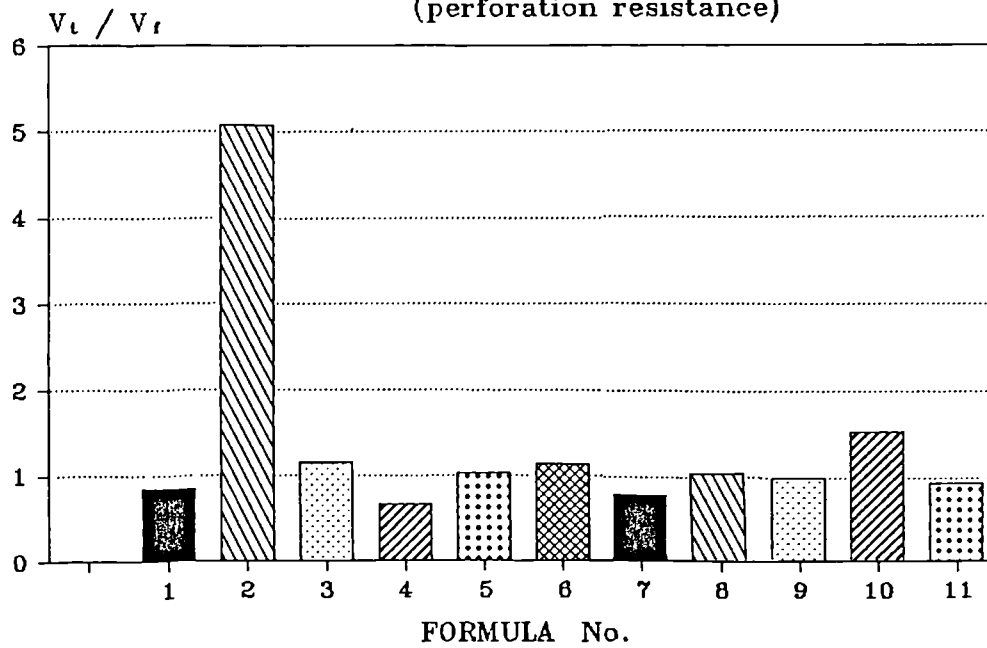
FIG (6.2h) TEST VELOCITY/FORMULA VELOCITY RATIOS
(perforation resistance)



- | | |
|--------------------------|-----------------------------|
| 1-Modified Petry formula | 7-Degen formula |
| 2-ACE formula | 8-Chang formula |
| 3-NDRC formula | 9-Haldar and Miller formula |
| 4-BRL formula | 10-Hughes formula |
| 5-CEA-EDF formula | 11-Adeli and Amin formula |
| 6-Kar formula | |

The calculation uses the experimental data obtained during the S8 series

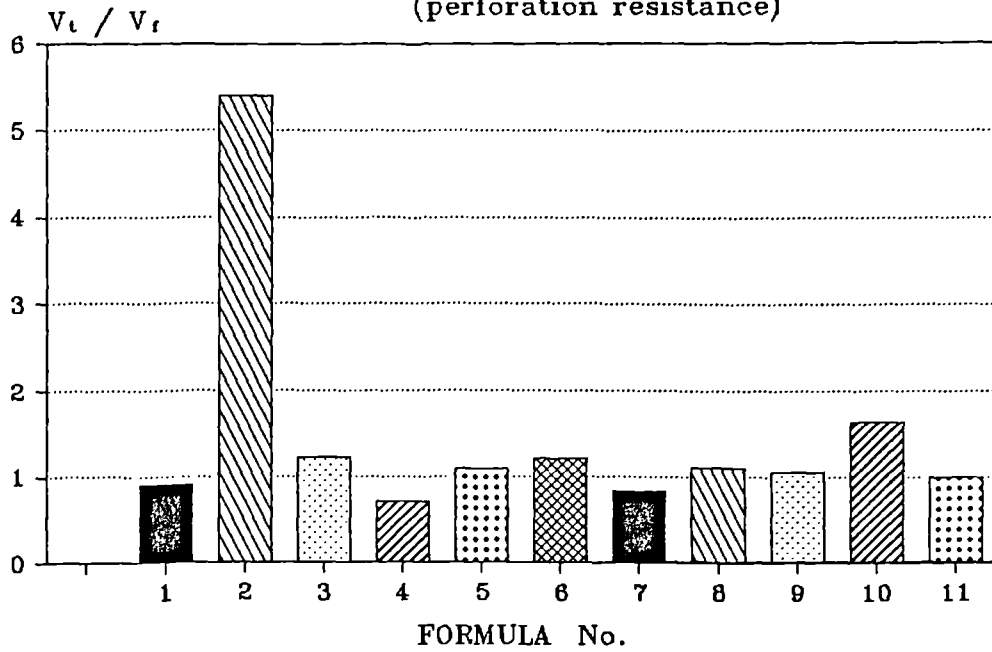
FIG (6.2i) TEST VELOCITY/FORMULA VELOCITY RATIOS
(perforation resistance)



- | | |
|--------------------------|-----------------------------|
| 1-Modified Petry formula | 7-Degen formula |
| 2-ACE formula | 8-Chang formula |
| 3-NDRC formula | 9-Haldar and Miller formula |
| 4-BRL formula | 10-Hughes formula |
| 5-CEA-EDF formula | 11-Adeli and Amin formula |
| 6-Kar formula | |

The calculation uses the experimental data obtained during the S9 series

FIG (6.2j) TEST VELOCITY/FORMULA VELOCITY RATIOS
(perforation resistance)



- | | |
|--------------------------|-----------------------------|
| 1-Modified Petry formula | 7-Degen formula |
| 2-ACE formula | 8-Chang formula |
| 3-NDRC formula | 9-Haldar and Miller formula |
| 4-BRL formula | 10-Hughes formula |
| 5-CEA-EDF formula | 11-Adeli and Amin formula |
| 6-Kar formula | |

The calculation uses the experimental data obtained during the S10 series

the author's opinion is that the level of flexural reinforcement is an important factor, these formulae will be modified by the appropriate factor. The form of the factor is the same, but each formula has its particular numerical values, which are obtained by plotting the ratio of test velocity to the predicted velocity (V_t/V_f) against the flexural reinforcement ratio (r , kg/m^3). From such a graph, the correction factor is obtained using the method described in section 6.2.

The critical perforation velocity given by the Modified Petry 1 formula should be corrected by the coefficient $0.58 (0.724 + \frac{r}{444})$.

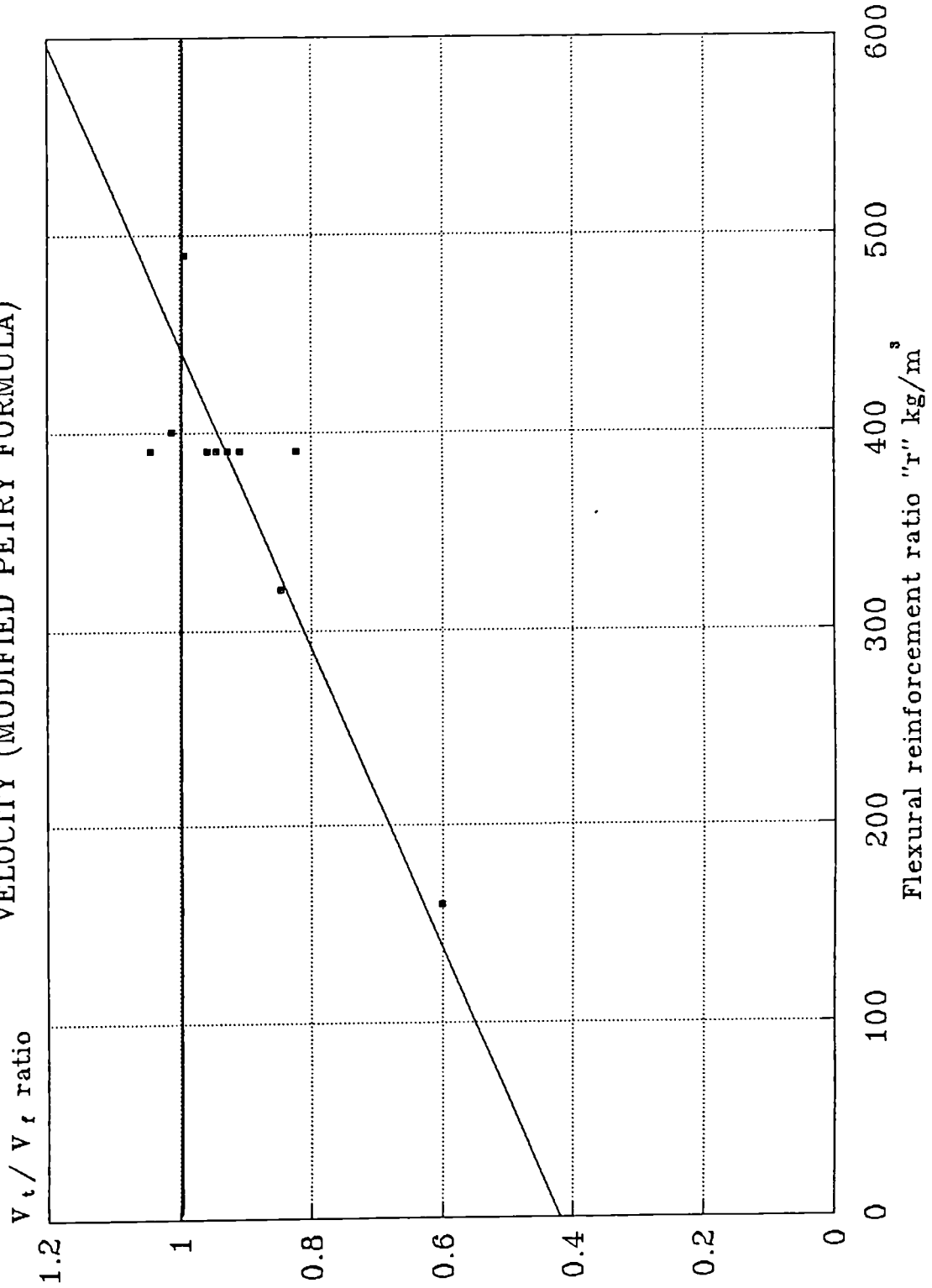
Where r is the flexural reinforcement ratio, kg/m^3 . The coefficient is obtained from a consideration of fig. (6.3). Table (6.6) summarises the measured and the calculated critical perforation velocities using the corrected Modified Petry 1 formula.

The critical perforation velocity given by the "CED - EDF" formula should be modified by including the correction factor, $0.4 (1.5 + \frac{r}{338})$, fig (6.4).

Table (6.7) summarises the measured and the corrected calculated critical perforation velocities. It should be noted that the corrected formula is only valid when there are two layers of reinforcement mesh close to each face. Reference (14) and section 2.5 discuss the limitation of the formula for cases other than two layers of reinforcement close to each face.

The critical perforation velocity given by the Chang formula should be modified by including the correction factor,

FIG (6.3) COMPARISON OF THE TEST AND PREDICTED PERFORATION
 VELOCITY (MODIFIED PETRY FORMULA)



V_t Test velocity V_r Formula velocity

Table (6.6) Comparison of experimental results with the corrected Modified Petry formula (perforation resistance)

Series No.	Flexural reinforcement ratio (kg/m ³)	Critical perforation velocity (m/sec.)		Test velocity formula velocity ratio
		Test	Formula with correction factor	
S1	160	54.11	56.66	0.955
S2	390	82.56	73.55	1.122
S3	390	91.15	91.32	0.998
S4	390	102.7	101.21	1.014
S5	390	118.3	114.83	1.030
S6	390	65.33	73.79	0.885
S7	400	102.1	95.1	1.07
S8	490	89.76	95.74	0.937
S9	320	76.55	75.8	1.01
S10	390	82.12	84.03	0.977

FIG (6.4) COMPARISON OF THE TEST AND PREDICTED PERFORATION

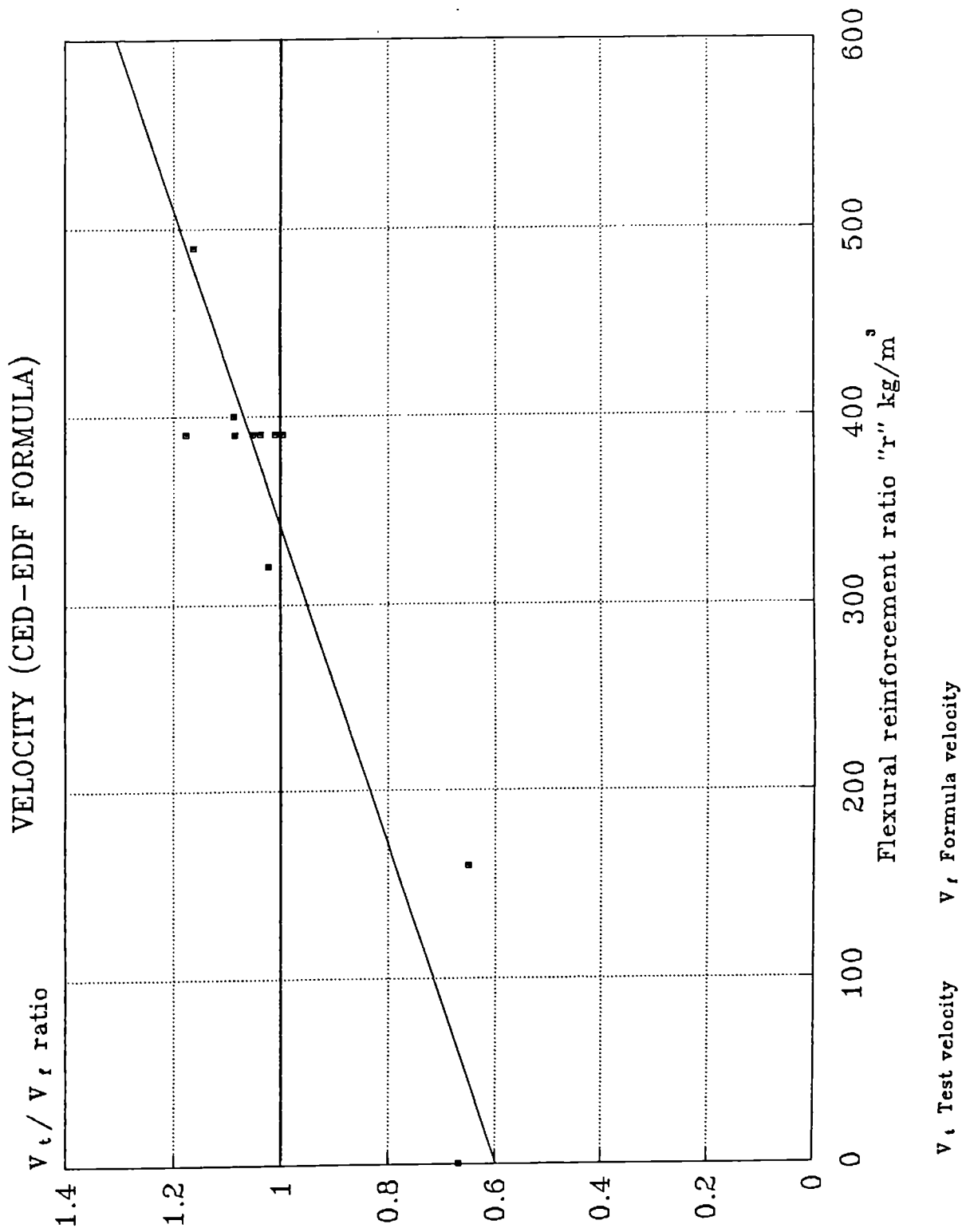


Table (6.7) Comparison of experimental results with the corrected "CEA-EDF" formula (perforation resistance)

Series No.	Flexural reinforcement ratio (kg/m ²)	Critical perforation velocity (m/sec.)		Test velocity formula velocity ratio
		Test	Formula with correction factor	
S1	160	54.11	65.75	0.823
S2	390	82.56	87.93	0.939
S3	390	91.15	95.62	0.953
S4	390	102.7	105.1	0.977
S5	390	118.3	119.44	0.99
S6	390	65.33	58.95	1.108
S7	400	102.1	100.77	1.013
S8	490	89.76	91.13	0.985
S9	320	76.55	73.22	1.045
S10	390	82.12	80.23	1.023

$0.57 (0.75 + \frac{r}{350})$, fig (6.5).

Table (6.8) summarises the results of the measured test velocity to the corrected calculated velocity ratios.

The critical perforation velocity given by the Haldar & Miller formula should be modified by the correction factor, $0.577 (0.733 + \frac{r}{370})$, fig (6.6).

Table (6.9) summarises the results of the measured test velocity to the corrected calculated formula velocity ratios.

Finally the Adeli & Amin formula should be modified by introducing the correction factor, $0.6 (\frac{2}{3} + \frac{r}{400})$, fig (6.7).

Table (6.10) summarises the results for the measured and corrected calculated critical perforation velocities.

6.3 The Development and Application Of The Proposed New Scabbing Formula

The experimental results which have been obtained for the determination of the critical scabbing velocity are presented in table (6.11). It has been assumed that for the development of an empirical formula to determine the critical scabbing velocity, the depth of missile penetration is inversely proportional to the square root of the concrete compressive strength f'_c (6). The results of the current experimental programme demonstrate that for the scabbing tests the missile penetration can be assumed to be equal to one-tenth of the slab thickness - section 5.3.4. Hence, the minimum slab thickness to prevent scabbing may be assumed to be inversely proportional to one-tenth of the square root of the concrete compressive strength f'_c . A plot of the slab thickness versus critical scabbing velocity will enable an empirical relationship to be obtained. For this case the

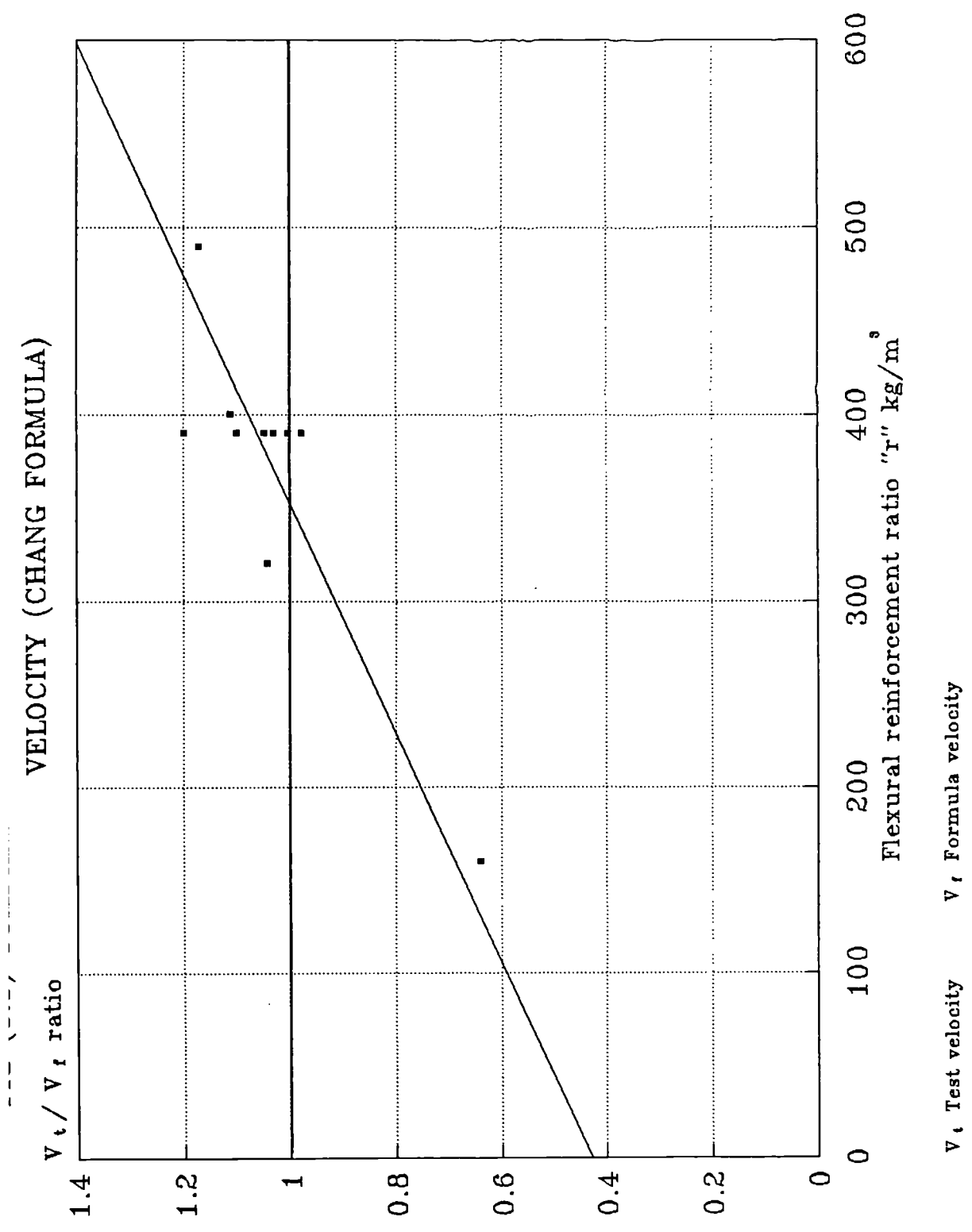


Table (6.8) Comparison of experimental results with the corrected Chang formula (perforation resistance)

Series No.	Flexural reinforcement ratio (kg/m ³)	Critical perforation velocity (m/sec.)		Test velocity formula velocity ratio
		Test	Formula with correction factor	
S1	160	54.11	58.31	0.928
S2	390	82.56	89.9	0.918
S3	390	91.15	96.64	0.943
S4	390	102.7	105.8	0.970
S5	390	118.3	119.86	0.987
S6	390	65.33	59.99	1.08
S7	400	102.1	99.11	1.03
S8	490	89.76	93.96	0.955
S9	320	76.55	69.64	1.09
S10	390	82.12	79.36	1.034

FIG (6.6) COMPARISON OF THE TEST AND PREDICTED PERFORATION
 VELOCITY (HALDAR & MILLER FORMULA)

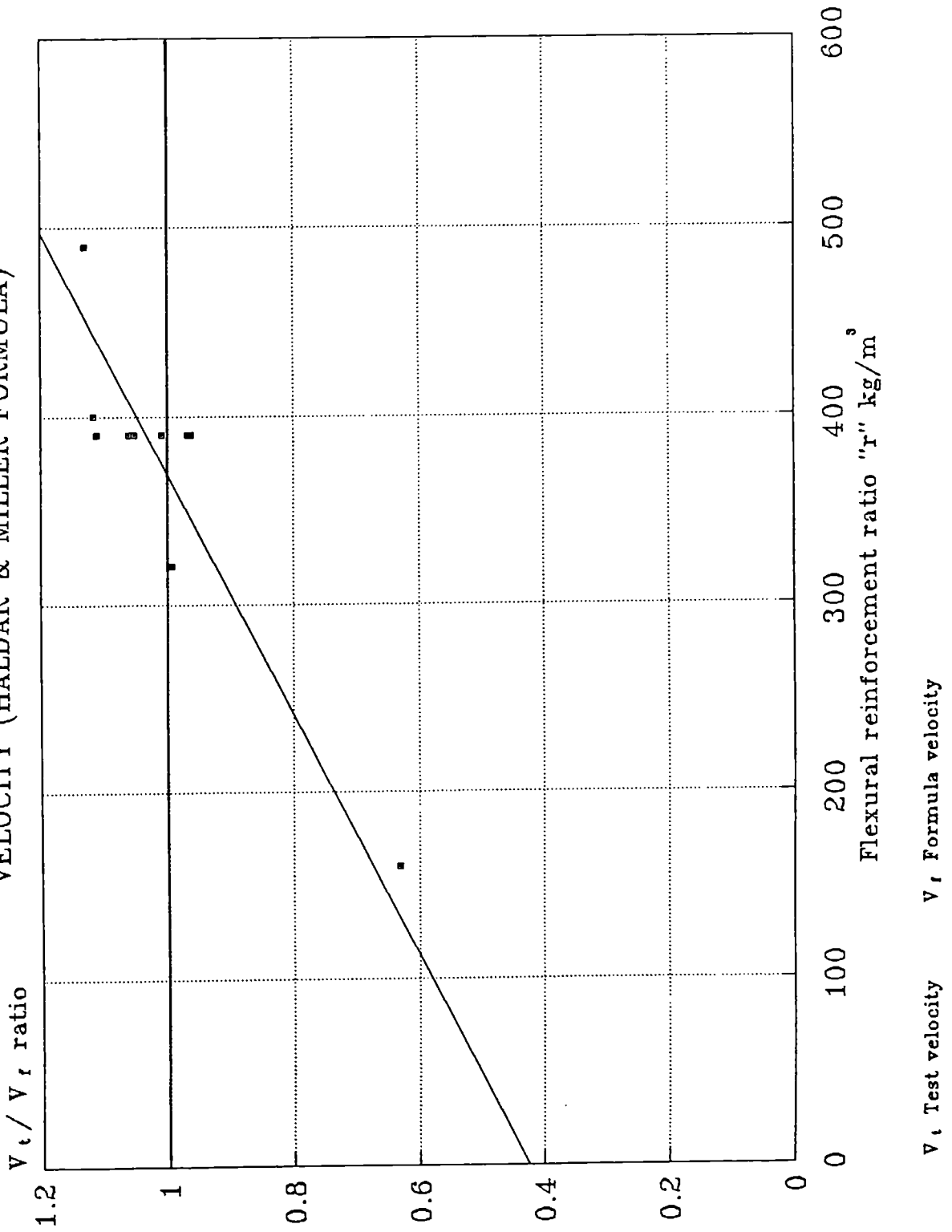


Table (6.9) Comparison of experimental results with corrected Haldar & Miller formula (perforation resistance)

Series No.	Flexural reinforcement ratio (kg/m ³)	Critical perforation velocity (m/sec.)		Test velocity formula velocity ratio
		Test	Formula with correction factor	
S1	160	54.11	57.61	0.94
S2	390	82.56	88.0	0.938
S3	390	91.15	93.16	0.978
S4	390	102.7	99.88	1.028
S5	390	118.3	109.75	1.078
S6	390	65.33	69.96	0.933
S7	400	102.1	95.77	1.066
S8	490	89.76	94.37	0.951
S9	320	76.55	71.02	1.077
S10	390	82.12	80.47	1.02

FIG (6.7) COMPARISON OF THE TEST AND PREDICTED PERFORMANCE VELOCITY (ADELI & AMIN FORMULA)

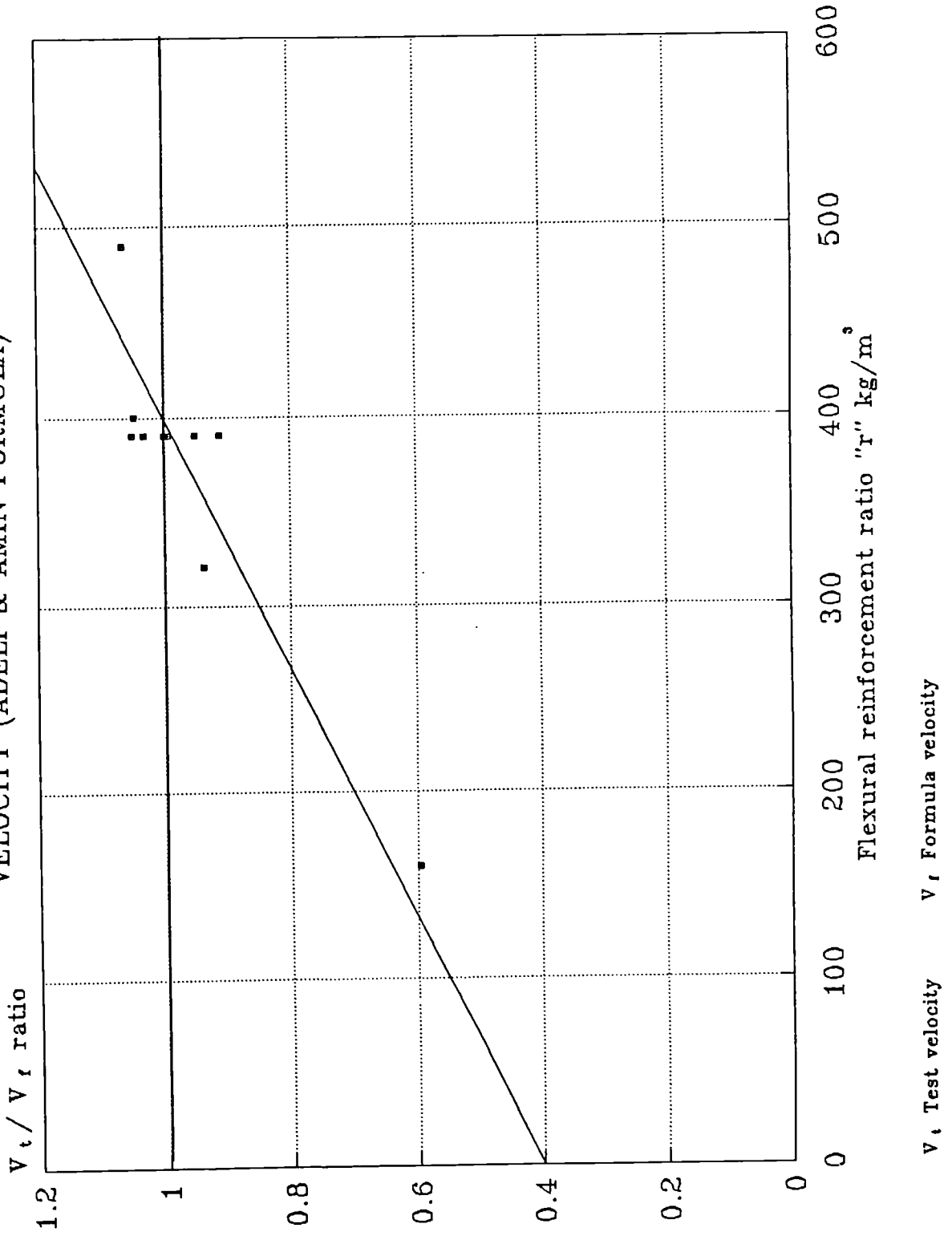


Table (6.10) Comparison of experimental results with corrected Adeli & Amin formula (perforation resistance)

Series No.	Flexural reinforcement ratio (kg/m ³)	Critical perforation velocity (m/sec.)		Test velocity formula velocity ratio
		Test .	Formula with correction factor	
S1	160	54.11	58.22	0.929
S2	390	82.56	89.26	0.925
S3	390	91.15	94.49	0.964
S4	390	102.7	101.18	1.015
S5	390	118.3	111.04	1.065
S6	390	65.33	62.41	1.046
S7	400	102.1	97.44	1.047
S8	490	89.76	95.75	0.937
S9	320	76.55	71.87	1.065
S10	390	82.12	81.48	1.007

Table (6.11) Experimental test results (scabbing resistance)

Series No.	Total percentage of reinforcement	Target thickness (mm)	Concrete compressive strength f_c' (cube) (N/mm ²)	Mass of missile (kg)	Diameter of missile (cm)	Critical scabbing velocity m/sec.
S1	1%	100	57.56	3.689	4.983	41.1
S2	2.5%	100	55.5	3.689	4.975	48.2
S3	2.5%	100	54.53	3.2	4.975	51.39
S4	2.5%	100	54.8	2.695	4.970	54.9
S5	2.5%	100	53.26	2.21	4.968	58.2
S6	2.5%	80	48.66	3.664	4.972	35.62
S7	2.5%	120	45.36	3.661	4.972	55.86
S8	3.1%	100	46.1	3.661	4.972	51.88
S9	2%	100	48.2	3.656	4.970	44.31
S10	2.5%	100	50.23	3.652	4.966	45.23

All the series have 4mm max. agg. size except S10 which had 2mm max. agg. size

slab thickness is defined as the thickness to just allow scabbing.

By considering the test results obtained from the S2, S6 and S7 series, it is possible to propose a formula which enables the slab thickness to be determined from the critical scabbing velocity. A regression analysis is carried out for these test results and the corresponding equation of slab scabbing thickness d_s as a function of the velocity V_{cs} may be obtained as follows

$$d_s = 3.467 V_{cs}^{0.877} \quad (6.11)$$

where d_s = target scabbing thickness (mm).

V_{cs} = critical scabbing velocity (m/sec).

By assuming that the thickness to prevent scabbing of the concrete increases with the missile mass, and reduces as the concrete compressive strength and missile diameter increase (9), then the scabbing thickness equation becomes

$$d_s = \frac{e}{0.1 (f'_c)^{e_4}} \cdot \frac{M^{e_2}}{D^{e_3}} \cdot V_{cs}^{e_5} \quad (6.12)$$

where M = missile mass (kg).

D = missile diameter (cm).

f'_c = concrete compressive strength (cube) (N/mm^2).

The constants e , e_2 , e_3 , e_4 and e_5 are experimentally determined. A value of 0.5 for e_4 is once more assumed. This value has been obtained from experimental work associated with high velocity missile impact (6). A value of 0.877 is used for e_5 and has been obtained from equation

(6.11). The general scabbing thickness equation becomes therefore

$$d_s = e_1 \cdot \frac{M^{e_2}}{(f'_c)^{0.5}} \cdot \frac{V_{CS}^{0.877}}{D^{e_3}} \quad (6.13)$$

In which e_1 is equal to $e/0.1$. In order to evaluate the constants in eq. (6.13), the following procedure is adopted. The velocity of the missile of mass 3.689 kg which cause scabbing of the concrete slab of thickness 100 mm is 48.2 m/sec (S2 test result from table (6.11)).

Using the S2 test result and substitution into eq (6.13) gives

$$100 = e_1 \cdot \frac{(3.689)^{e_2}}{(55.5)^{0.5}} \cdot \frac{(48.2)^{0.877}}{(4.975)^{e_3}} \quad (6.14)$$

Also using the S3 test result from table (6.11) substituting into eq. (6.13)

$$100 = e_1 \cdot \frac{(3.2)^{e_2}}{(54.53)^{0.5}} \cdot \frac{(51.39)^{0.877}}{(4.975)^{e_3}} \quad (6.15)$$

Dividing eq. (6.14) by eq. (6.15)

$$e_2 = 0.457$$

With the value of e_2 determined the value of e_3 can be found by using the test results of the S4 and S5 series from table (6.11) and the value of e_2 in eq. (6.13) to give

$$100 = e_1 \cdot \frac{(2.695)^{0.457}}{(54.8)^{0.5}} \cdot \frac{(54.9)^{0.877}}{(4.970)^{e_3}} \quad (6.16)$$

and

$$100 = e_1 \cdot \frac{(2.21)^{0.457}}{(53.26)^{0.5}} \cdot \frac{(58.2)^{0.877}}{(4.968)^{e_3}} \quad (6.17)$$

Dividing eq. (6.16) by eq. (6.17)

$$e_3 = 62.67$$

The value of e_1 can be determined by substituting the value of e_2 and e_3 into eq. (6.13) and substituting into eq. (6.11).

Thus

$$e_1 \cdot \frac{M^{0.457}}{(f'_C)^{0.5}} \cdot \frac{1}{D^{62.67}} = 3.467$$

$$\therefore e_1 = 3.467 \frac{(f'_C)^{0.5} D^{62.67}}{M^{0.457}} \quad (6.18)$$

The test results of series S2, S6 and S7 from table (6.11) can be used in eq. (6.18) to find the average value of e_1 which is found to be equal to 6.13×10^{44} and the proposed scabbing formula becomes

$$d_s = 6.13 \times 10^{44} \cdot \frac{M^{0.457}}{(f'_C)^{0.5}} \cdot \frac{V_{CS}^{0.877}}{D^{62.67}} \quad (6.19)$$

Table (6.12) shows the comparison of test and proposed scabbing formula velocities using the experimental data of all the series. The predicted critical scabbing velocity is most accurate when the flexural reinforcement ratio is 390 kg/m^3 which is to be expected. In order to improve the predicted critical scabbing velocity for the reinforcement quantities other than this ratio a correction factor will be proposed. The derivation of the correction factor has been discussed in section 6.2. For the determination of the critical scabbing velocity, the proposed correction factor is

$$0.5 \left(1 + \frac{r}{370} \right) \quad (6.20)$$

The factor has been obtained from a consideration of fig. (6.8), r being the flexural reinforcement ratio in kg/m^3 . The use of equations (6.19) and (6.20) to obtain the critical scabbing velocity is identical to the perforation case which has been explained. Table (6.13) summarises the measured and predicted values of the proposed critical scabbing velocity when the correction factor is included. The test results show a clear dependence of scabbing resistance on the quantity of flexural reinforcement.

The maximum aggregate size used in the concrete is also a factor influencing the critical scabbing velocity. The extent of the influence of aggregate size upon the critical scabbing velocity was not thoroughly investigated.

6.3.1 Evaluation Of Existing Empirical Formulae To Predict Critical Scabbing Velocity

The critical scabbing velocity of a missile impacting upon a reinforced concrete target can be estimated using the existing empirical formulae described in section 2.3. The data obtained from the current experimental programme can be

Table (6.12) Comparison of test and proposed formula velocities (scabbing resistance)

Series No.	Total percentage of reinforcement	Flexural reinforcement ratio (kg/m ³)	Critical scabbing velocity (m/sec.)		Test velocity formula velocity ratio
			Test	Formula	
S1	1%	160	41.1	57.81	0.711
S2	2.5%	390	48.2	50.48	0.955
S3	2.5%	390	51.39	53.81	0.955
S4	2.5%	390	54.9	54.93	0.999
S5	2.5%	390	58.2	58.23	0.999
S6	2.5%	390	35.62	34.9	1.02
S7	2.5%	400	55.86	53.26	1.048
S8	3.1%	490	51.88	43.66	1.188
S9	2%	320	44.31	43.55	1.017
S10	2.5%	390	45.23	42.12	1.073

FIG (6.8) COMPARISON OF THE TEST AND PROPOSED SCABBING VELOCITY

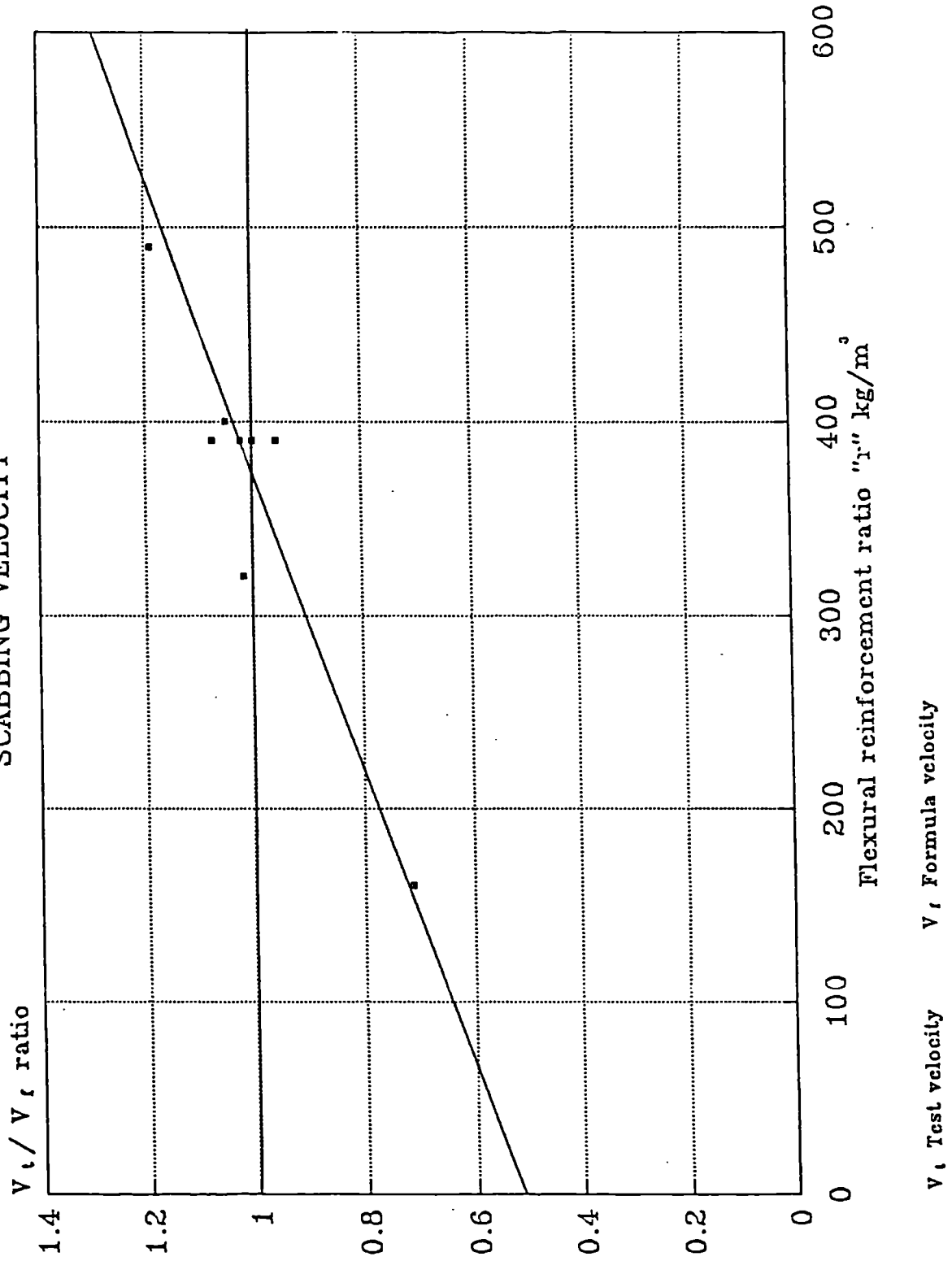


Table (6.13) Comparison of experimental results with the proposed formula predictions (scabbing resistance)

Series No.	Flexural reinforcement ratio (kg/m ³)	Critical scabbing velocity (m/sec.)		Test velocity formula velocity ratio
		Test	Formula with correction factor	
S1	160	41.1	41.4	0.992
S2	390	48.2	51.84	0.930
S3	390	51.39	55.26	0.930
S4	390	54.9	56.41	0.973
S5	390	58.2	59.80	0.973
S6	390	35.62	53.84	0.993
S7	400	55.86	55.42	1.008
S8	490	51.88	50.74	1.022
S9	320	44.31	43.6	1.016
S10	390	45.23	43.25	1.045

used with these formulae to determine their accuracy. Table (6.14) summarises the measured and calculated critical scabbing velocities using these formulae. Typical calculations to determine this velocity for one of the experimental series are given in appendix B.

It can be seen from table (6.15) and fig. (6.9) that only the Chang and Haldar & Miller formulae provide a critical scabbing velocity which is in close agreement to the experimental value. These formulae can be improved by adding a correction factor to allow for the variation of the quantity of flexural reinforcement in the target. The author has ignored other existing formulae because they are restricted in their range of applicability. The restrictions of these formulae have been discussed in section 6.2.1. Some further comments will be made

i. The Bechtel corporation and Adeli & Amin formulae have been developed for the prediction of damage to reinforced concrete targets with a thickness between 0.15 to 0.6 m.

ii. The Stone & Webster corporation formula has been developed for predicting a scabbing thickness of concrete target for a concrete compressive strength of between 20 to 30 N/mm².

The critical scabbing velocity given by Chang formula should be corrected by the coefficient, $0.2 \left(4 + \frac{r}{186}\right)$.

Where r is the flexural reinforcement ratio (kg/m³). This correction factor accounting for variation in the amount of flexural reinforcement is obtained from a consideration of fig (6.10) using the method described previously in section 6.2. Table (6.16) summarises the measured and the calculated

critical scabbing velocity when this correction factor is used.

The critical scabbing velocity given by the Haldar and Miller formula should be corrected by the coefficient, $0.427 (1.34 + \frac{r}{570})$, fig (6.11).

Table (6.17) summarises the measured and the calculated critical scabbing velocities.

Table (6.14) Measured and calculated critical scabbing velocities

Series No.	Flexural reinforcement ratio (kg/m ³)	Critical scabbing velocity (m/sec.)										
		1	2	3	4	5	6	7	8	9	10	11
S1	160	41.1	67.95	27.29	75.3	31.59	25.63	27.85	41.11	57.71	31.92	27.54
S2	390	48.2	85.0	27.02	74.28	31.0	25.63	27.58	40.18	57.3	31.64	26.85
S3	390	51.39	92.74	29.01	75.55	34.12	27.52	30.76	43.34	60.31	33.78	28.57
S4	390	54.9	102.98	32.05	93.32	39.31	30.0	32.71	53.24	65.76	36.89	30.91
S5	390	58.2	116.4	35.5	107.12	44.77	33.12	36.23	48.09	71.56	40.44	34.47
S6	390	35.62	75.36	19.04	59.9	17.47	18.4	19.33	26.73	41.32	23.18	-
S7	400	55.86	95.36	34.34	79.11	36.66	33.82	35.18	47.1	61.79	39.66	48.85
S8	490	51.88	85.59	25.76	69.4	25.87	25.73	26.29	36.2	51.71	30.3	24.94
S9	320	44.31	85.36	26.1	70.37	27.05	25.75	26.65	37.13	52.79	30.65	25.91
S10	390	45.23	85.36	26.44	71.51	28.21	25.76	26.96	38.05	55.93	30.98	26.5

Note: The "ACE" formula is not applicable because it gives negative results for all the test series

- 1 - Test result
- 2 - Modified petry formula
- 3 - "NDRC" formula
- 4 - "BRL" formula
- 5 - Bechtel corporation formula
- 6 - Stone and Webster corporation formula
- 7 - Kar formula
- 8 - Chang formula
- 9 - Haldar & Miller formula
- 10 - Hughes formula
- 11 - Adelli & Amin formula

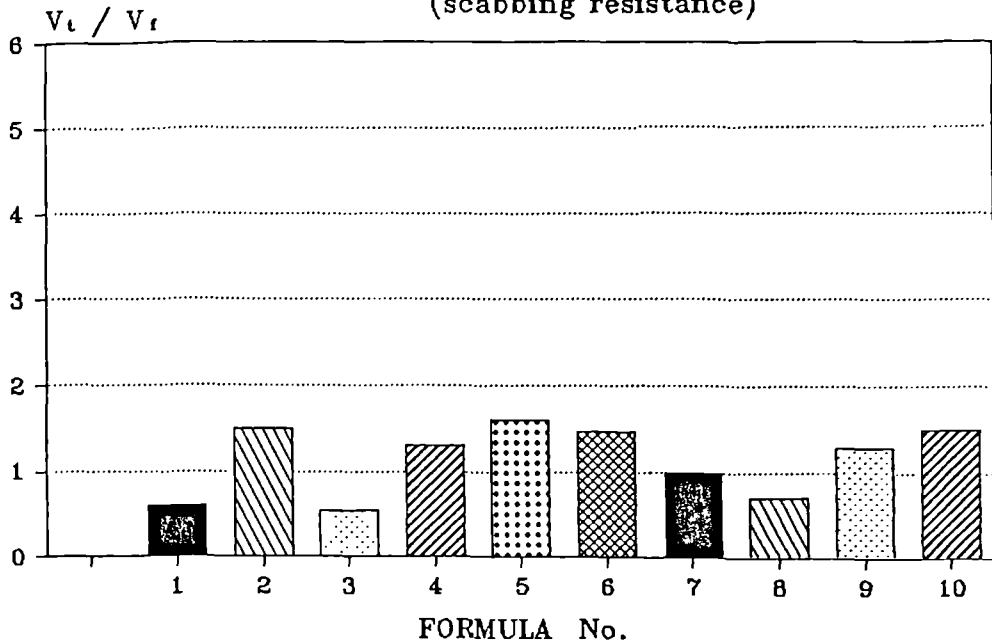
Table (6.15) Test velocity/formula velocity ratios (scabbing resistance)

Series No.	Total percentage of reinforcement	Flexural reinforcement ratio (kg/m ²)	measured/calculated critical scabbing velocity ratio									
			1	2	3	4	5	6	7	8	9	10
S1	1%	160	0.604	1.506	0.545	1.301	1.603	1.475	0.999	0.712	1.287	1.503
S2	2.5%	390	0.567	1.783	0.649	1.554	1.88	1.747	1.199	0.841	1.523	1.795
S3	2.5%	390	0.554	1.77	0.680	1.506	1.867	1.67	1.185	0.852	1.521	1.798
S4	2.5%	390	0.533	1.713	0.588	1.396	1.83	1.678	1.031	0.834	1.488	1.773
S5	2.5%	390	0.5	1.639	0.543	1.3	1.757	1.606	1.210	0.813	1.439	1.688
S6	2.5%	390	0.472	1.870	0.594	2.039	1.935	1.842	1.332	0.862	1.536	-
S7	2.5%	400	0.585	1.626	0.706	1.523	1.651	1.587	1.186	0.904	1.408	1.143
S8	3.1%	490	0.606	2.014	0.747	2.005	2.016	1.973	1.433	1.003	1.712	2.08
S9	2%	320	0.519	1.697	0.629	1.638	1.72	1.662	1.193	0.839	1.445	1.71
S10	2.5%	390	0.529	1.71	0.632	1.603	1.755	1.677	1.188	0.838	1.46	1.706

- 1 - Modified petry formula
- 2 - "NDRC" formula
- 3 - "BRL" formula
- 4 - Bechtel corporation formula
- 5 - Stone and Webster corporation formula

- 6 - Kar formula
- 7 - Chang formula
- 8 - Haldar & Miller formula
- 9 - Hughes formula
- 10 - Adell & Amin formula

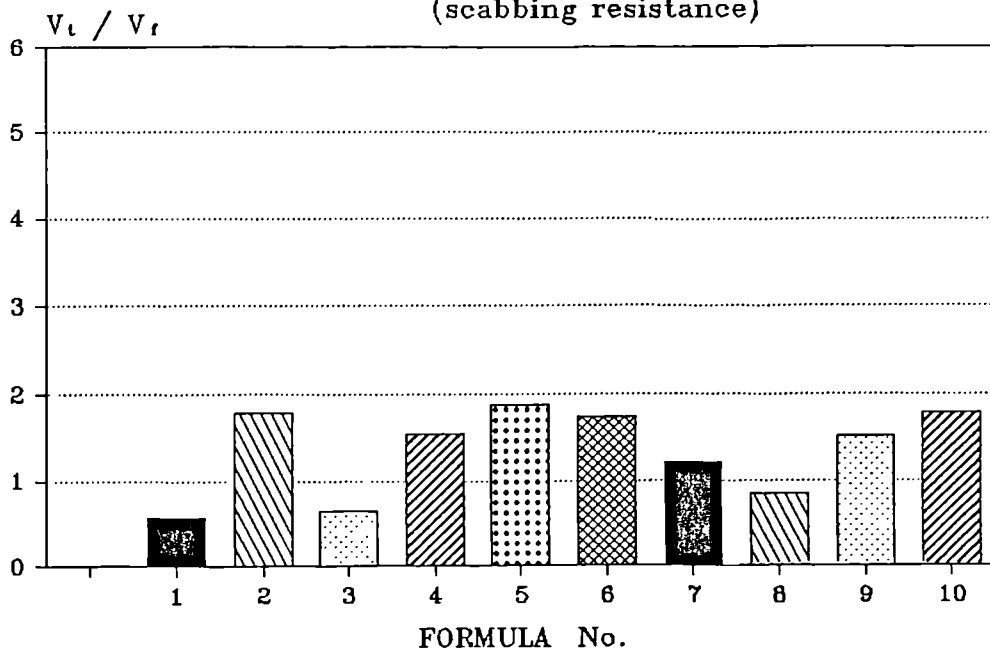
FIG (6.9a) TEST VELOCITY/FORMULA VELOCITY RATIOS
(scabbing resistance)



- | | |
|---------------------------|-----------------------------|
| 1-Modified Petry formula | 6-Kar formula |
| 2-NDRC formula | 7-Chang formula |
| 3-BRL formula | 8-Haldar and Miller formula |
| 4-Bechtel formula | 9-Hughes formula |
| 5-Stone & Webster formula | 10-Adeli & Amin formula |

The calculation uses the experimental data obtained during the S1 series

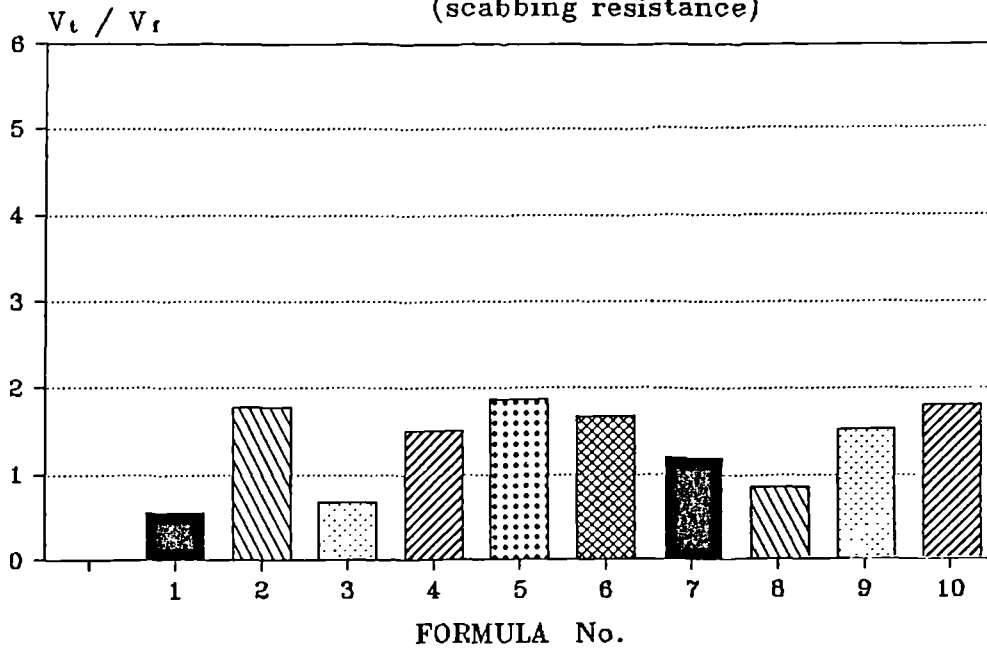
FIG (6.9b) TEST VELOCITY/FORMULA VELOCITY RATIOS
(scabbing resistance)



- | | |
|---------------------------|-----------------------------|
| 1-Modified Petry formula | 6-Kar formula |
| 2-NDRC formula | 7-Chang formula |
| 3-BRL formula | 8-Haldar and Miller formula |
| 4-Bechtel formula | 9-Hughes formula |
| 5-Stone & Webster formula | 10-Adeli & Amin formula |

The calculation uses the experimental data obtained during the S2 series

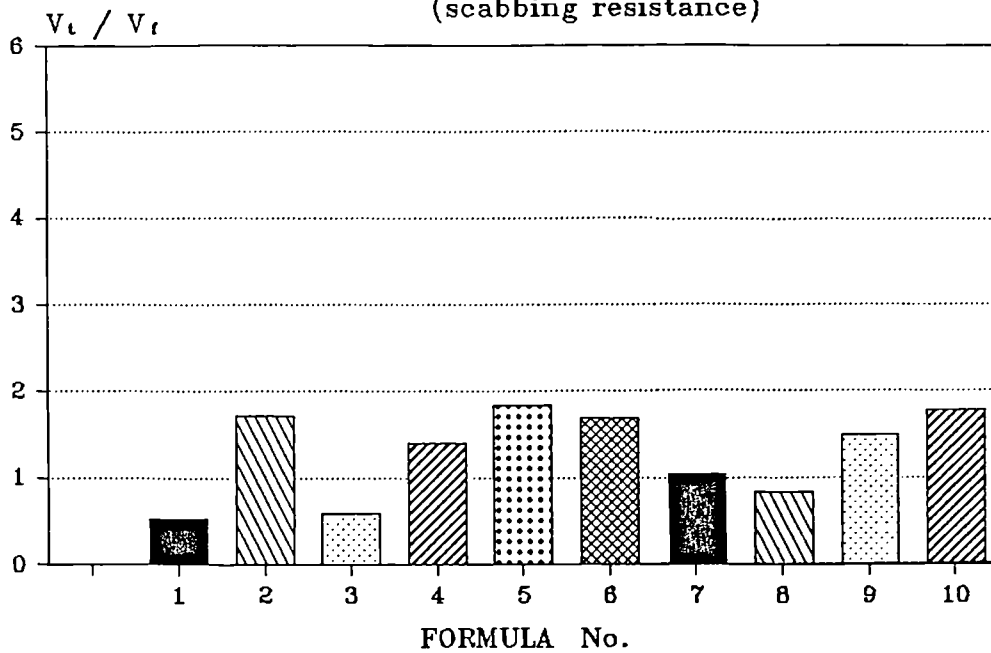
FIG (6.9c) TEST VELOCITY/FORMULA VELOCITY RATIOS
(scabbing resistance)



- | | |
|---------------------------|-----------------------------|
| 1-Modified Petry formula | 6-Kar formula |
| 2-NDRC formula | 7-Chang formula |
| 3-BRL formula | 8-Haldar and Miller formula |
| 4-Bechtel formula | 9-Hughes formula |
| 5-Stone & Webster formula | 10-Adeli & Amin formula |

The calculation uses the experimental data obtained during the S3 series

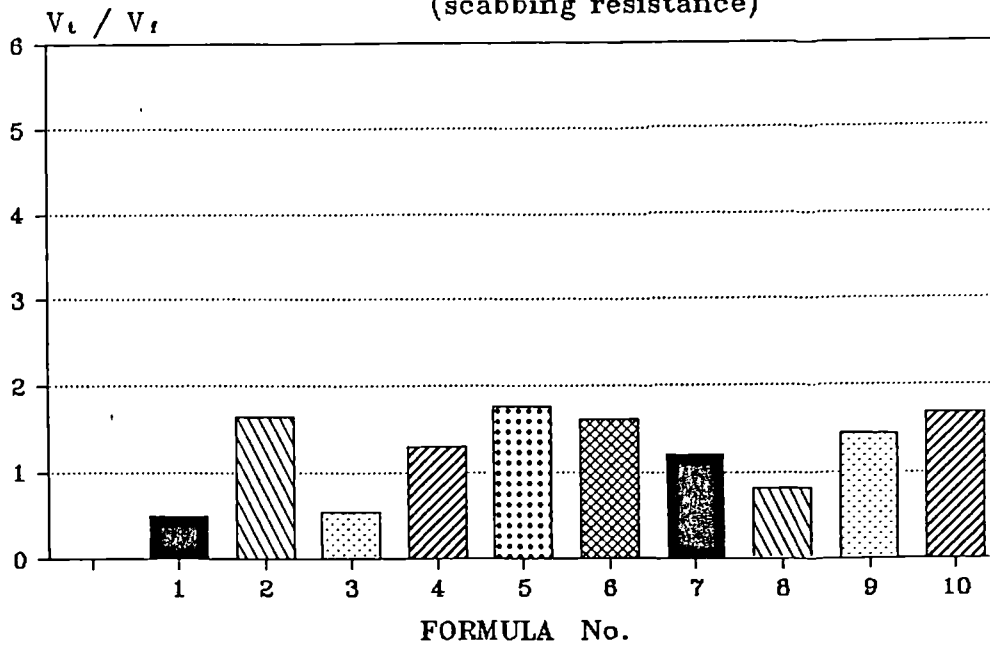
FIG (6.9d) TEST VELOCITY/FORMULA VELOCITY RATIOS
(scabbing resistance)



- | | |
|---------------------------|-----------------------------|
| 1-Modified Petry formula | 6-Kar formula |
| 2-NDRC formula | 7-Chang formula |
| 3-BRL formula | 8-Haldar and Miller formula |
| 4-Bechtel formula | 9-Hughes formula |
| 5-Stone & Webster formula | 10-Adeli & Amin formula |

The calculation uses the experimental data obtained during the S4 series

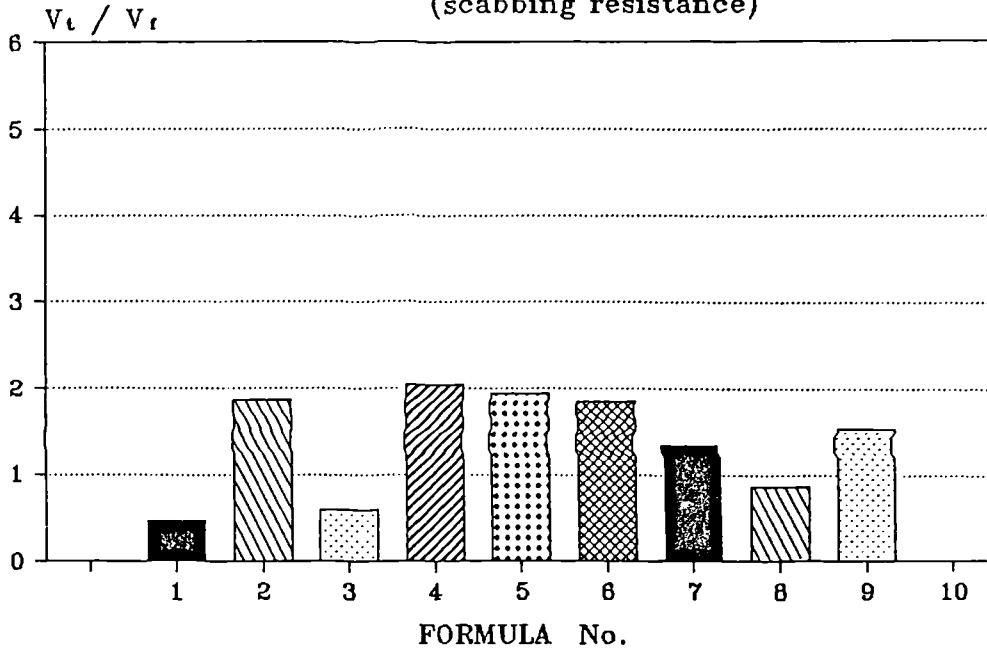
FIG (6.9e) TEST VELOCITY/FORMULA VELOCITY RATIOS
(scabbing resistance)



- | | |
|---------------------------|-----------------------------|
| 1-Modified Petry formula | 6-Kar formula |
| 2-NDRC formula | 7-Chang formula |
| 3-BRL formula | 8-Haldar and Miller formula |
| 4-Bechtel formula | 9-Hughes formula |
| 5-Stone & Webster formula | 10-Adeli & Amin formula |

The calculation uses the experimental data obtained during the S5 series

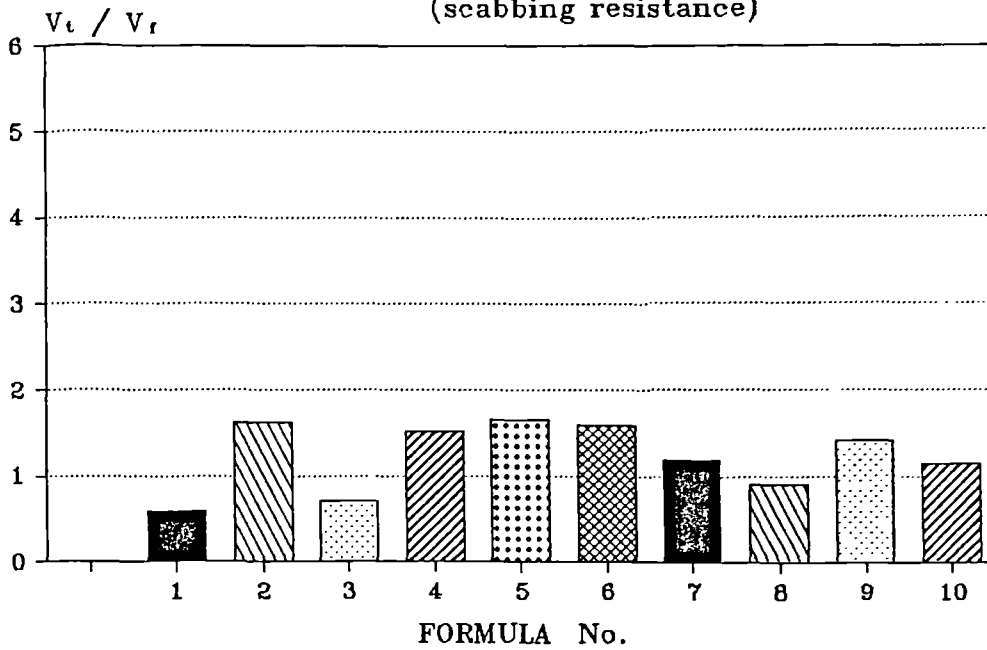
FIG (6.9f) TEST VELOCITY/FORMULA VELOCITY RATIOS
(scabbing resistance)



- | | |
|---------------------------|-----------------------------|
| 1-Modified Petry formula | 6-Kar formula |
| 2-NDRC formula | 7-Chang formula |
| 3-BRL formula | 8-Haldar and Miller formula |
| 4-Bechtel formula | 9-Hughes formula |
| 5-Stone & Webster formula | 10-Adeli & Amin formula |

The calculation uses the experimental data obtained during the S6 series

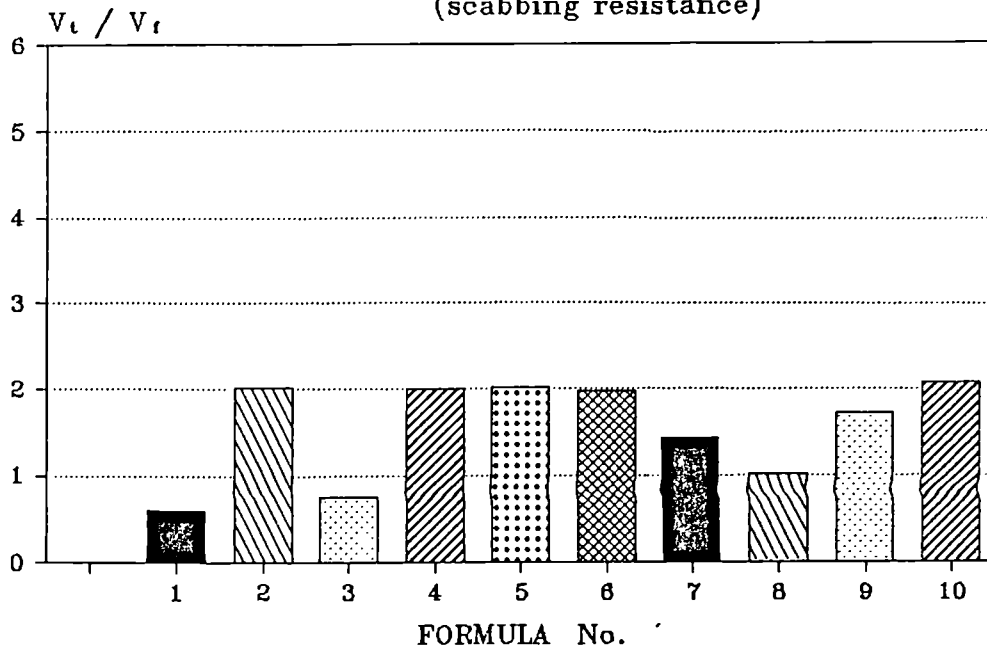
FIG (6.9g) TEST VELOCITY/FORMULA VELOCITY RATIOS
(scabbing resistance)



- | | |
|---------------------------|-----------------------------|
| 1-Modified Petry formula | 6-Kar formula |
| 2-NDRC formula | 7-Chang formula |
| 3-BRL formula | 8-Haldar and Miller formula |
| 4-Bechtel formula | 9-Hughes formula |
| 5-Stone & Webster formula | 10-Adeli & Amin formula |

The calculation uses the experimental data obtained during the S7 series

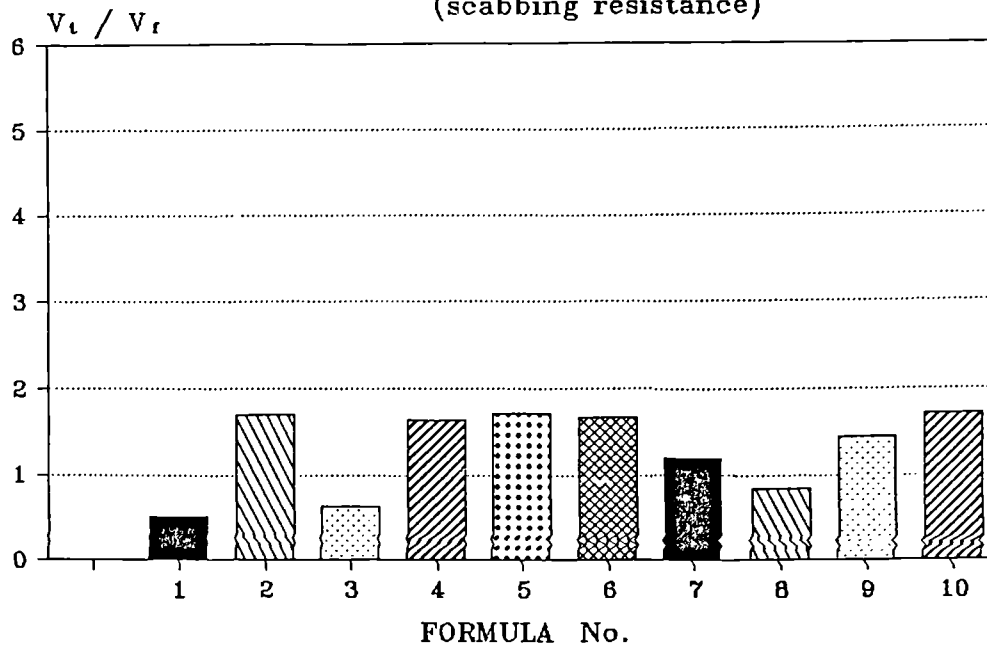
FIG (6.9h) TEST VELOCITY/FORMULA VELOCITY RATIOS
(scabbing resistance)



- | | |
|---------------------------|-----------------------------|
| 1-Modified Petry formula | 6-Kar formula |
| 2-NDRC formula | 7-Chang formula |
| 3-BRL formula | 8-Haldar and Miller formula |
| 4-Bechtel formula | 9-Hughes formula |
| 5-Stone & Webster formula | 10-Adeli & Amin formula |

The calculation uses the experimental data obtained during the S8 series

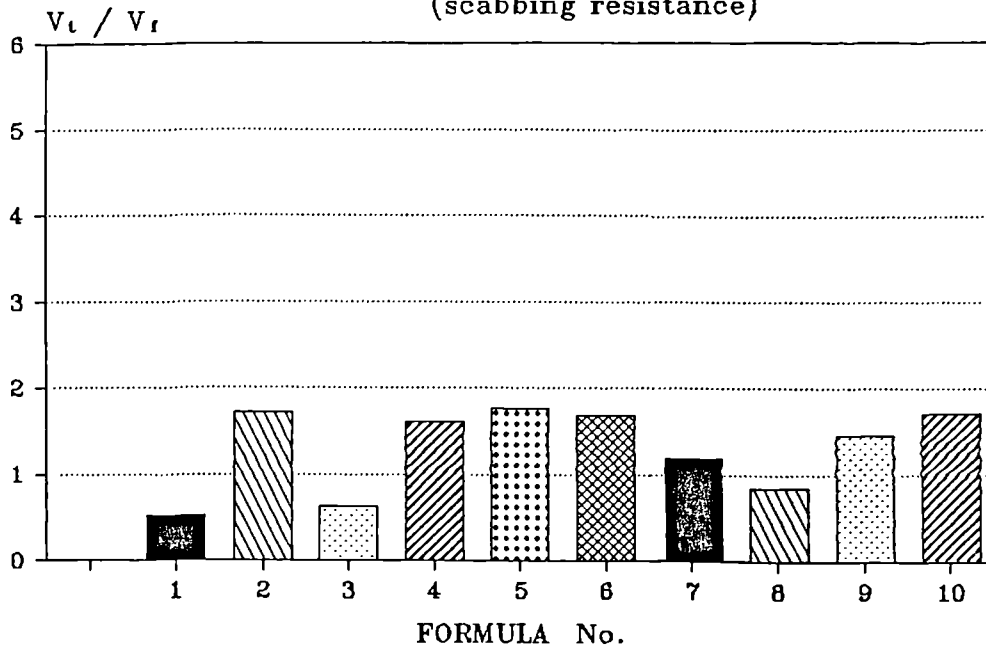
FIG (6.9i) TEST VELOCITY/FORMULA VELOCITY RATIOS
(scabbing resistance)



- | | |
|---------------------------|-----------------------------|
| 1-Modified Petry formula | 6-Kar formula |
| 2-NDRC formula | 7-Chang formula |
| 3-BRL formula | 8-Haldar and Miller formula |
| 4-Bechtel formula | 9-Hughes formula |
| 5-Stone & Webster formula | 10-Adeli & Amin formula |

The calculation uses the experimental data obtained during the S9 series

FIG (6.9j) TEST VELOCITY/FORMULA VELOCITY RATIOS
(scabbing resistance)



- | | |
|---------------------------|-----------------------------|
| 1-Modified Petry formula | 6-Kar formula |
| 2-NDRC formula | 7-Chang formula |
| 3-BRL formula | 8-Haldar and Miller formula |
| 4-Bechtel formula | 9-Hughes formula |
| 5-Stone & Webster formula | 10-Adeli & Amin formula |

The calculation uses the experimental data obtained during the S10 series

FIG (6.10) COMPARISON OF THE TEST AND FLEXUREL STRENGTH VELOCITY (CHANG FORMULA)

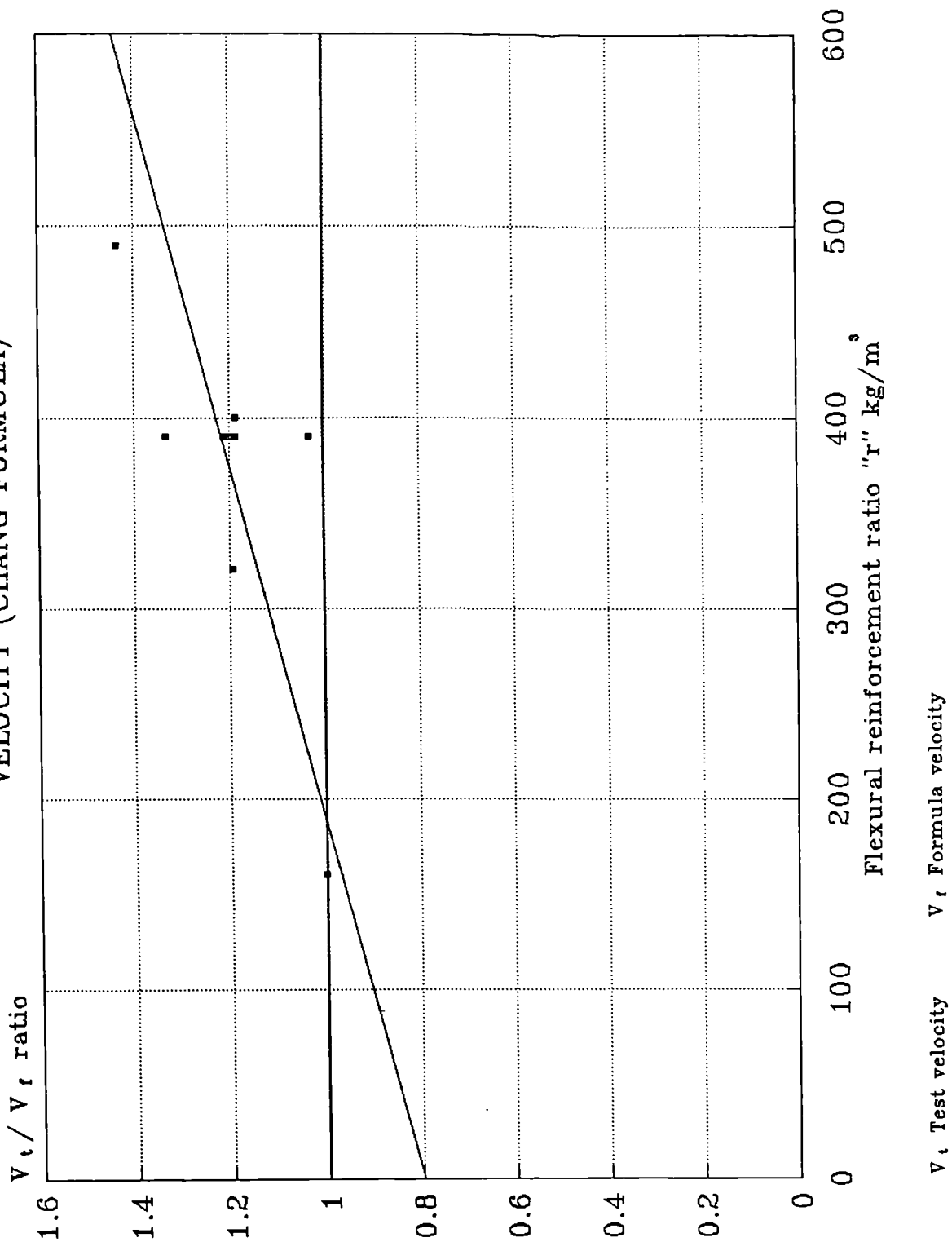


Table (6.16) Comparison of experimental results with corrected Chang formula (scabbing resistance)

Series No.	Flexural reinforcement ratio (kg/m ³)	Critical scabbing velocity (m./sec)		Test velocity formula velocity ratio
		Test	Formula with correction factor	
S1	160	41.1	39.96	1.028
S2	390	48.2	48.99	0.983
S3	390	51.39	52.84	0.972
S4	390	54.9	54.92	0.999
S5	390	58.2	58.63	0.992
S6	390	35.62	32.6	1.092
S7	400	55.86	57.93	0.964
S8	490	51.88	48.03	1.08
S9	320	44.31	42.48	1.043
S10	390	45.23	46.4	0.974

FIG (6.11) COMPARISON OF THE TEST AND PREDICTED SCABBING VELOCITY (HALDAR & MILLER FORMULA)

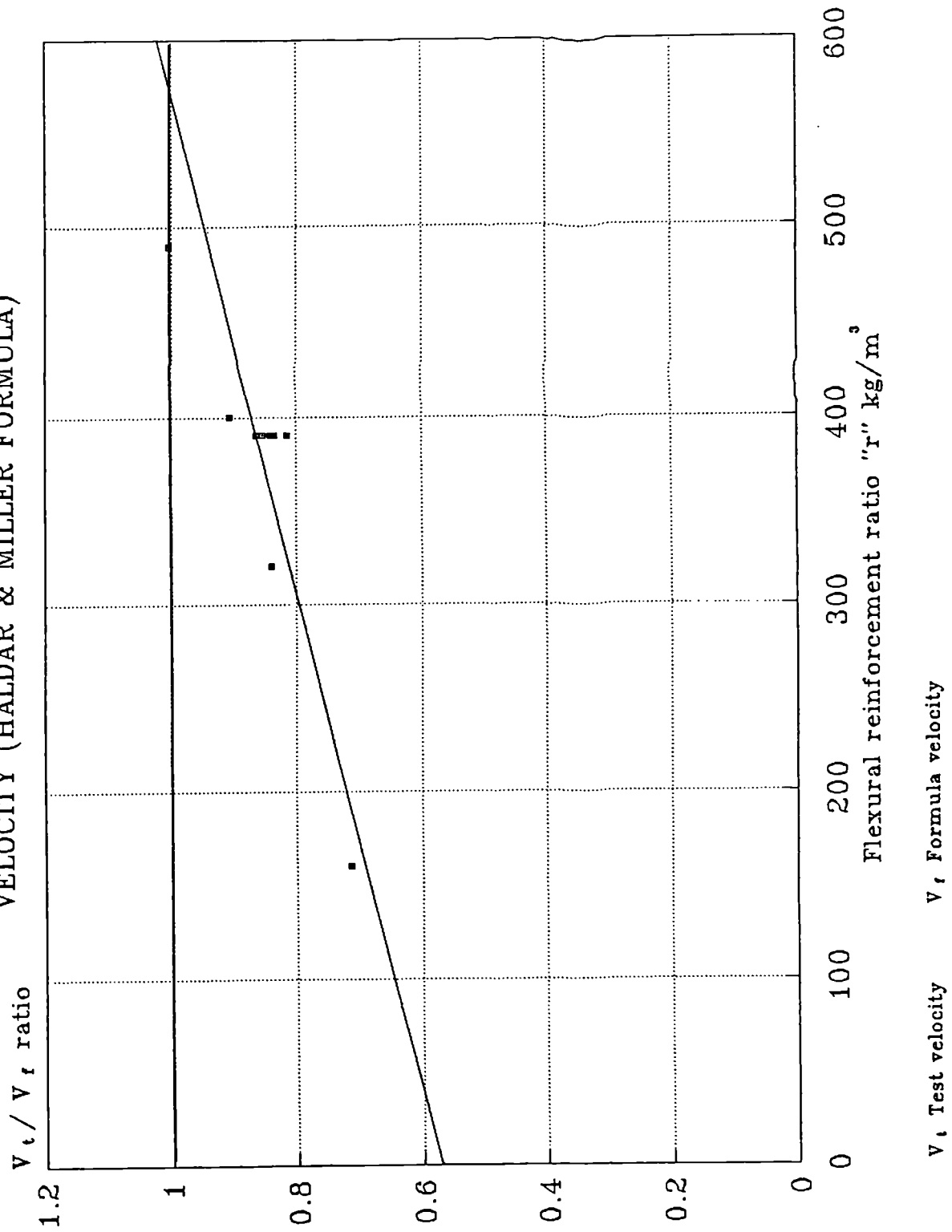


Table (6.17) Comparison of experimental results with corrected Haldar & Miller formula (scabbing resistance)

Series No.	Flexural reinforcement ratio (kg/m ³)	Critical scabbing velocity (m/sec.)		Test velocity formula velocity ratio
		Test	Formula with correction factor	
S1	160	41.1	39.93	1.029
S2	390	48.2	49.52	0.973
S3	390	51.39	52.13	0.985
S4	390	54.9	56.83	0.966
S5	390	58.2	61.85	0.941
S6	390	35.62	35.71	0.997
S7	400	55.86	53.87	1.036
S8	490	51.88	48.56	1.068
S9	320	44.31	42.86	1.033
S10	390	45.23	46.61	0.970

CHAPTER SEVEN

DISCUSSION

7.1 Perforation and Scabbing Resistance of the Target

Some authors incorrectly conclude from their test results involving under-reinforced structures, that reinforcement is of no influence upon the local effects of hard missile impact.

The objective of the current work was to establish an equation in which the level of flexural reinforcement was accounted for. Also, the influence of maximum aggregate size was to be established.

The results show the dependence of perforation resistance of the target upon the quantity of flexural reinforcement. Perforation resistance of the targets has been quantified in terms of the velocity at which the missile just perforates the target. This resistance is improved by increasing in the amount of reinforcement. There would appear no significant influence of varying the maximum aggregate size upon the perforation resistance.

The test results show that the scabbing resistance of the target depends upon the quantity of flexural reinforcement. Once again this resistance has been quantified in terms of the velocity at which the missile just causes scabbing of concrete from the back face of the target. The scabbing resistance increases as the amount of flexural reinforcement increases. Also, the maximum aggregate size used in the

concrete is a factor influencing the scabbing resistance. This influence, however, was not thoroughly investigated during the course of the experimental work.

7.2 Procedures Used for Determining the New Formulae

The proposed perforation and scabbing formulae were developed using the second method described in section 2.2. This method shows that the perforation or scabbing thickness could be empirically correlated with the missile properties if reliable and sufficient experimental results were available. The BRL formula, the Bechtel formula, Stone & Webster formula and "CEA-EDF" formula were based on the same concept.

The derivation of the New Formulae followed the steps used in the development of the Bechtel Corporation formula (9). Thus, the forms of equations (6.9) and (6.19) are similar to the Bechtel formula, but are applicable to different range of parameters.

7.3 Limitations of the Proposed Perforation and Scabbing Formulae

The proposed perforation and scabbing formulae have been developed as a direct result of the experimental work. The work which has examined a finite range of parameters. The application of these two formulae, therefore, has only validity with the range of the test parameters. Extrapolation outside this range is likely to predict inadequate results. In particular, the diameter of the missile is important since the development of the formulae is related to only one diameter (49.8 mm). For this reason the

powers of D are 45.5 and 62.67 in the proposed perforation and scabbing formulae respectively. It should be noted that these values are high and as a consequence the constant c_1 and e_1 are also very high.

The applications of the proposed perforation and scabbing formulae are limited to the following conditions.

- i) The formula are valid for a fully fixed edge concrete target impacted by a perpendicular hard missile.
- ii) The ratio between the flexural reinforcement mass in the target and the concrete volume is 0 kg/m^3 to 500 kg/m^3 .
- iii) The concrete compressive cube strength varies between 44 N/mm^2 to 57 N/mm^2 .
- iv) The slab thickness varies between 80 mm to 120 mm.
- v) The mass of the missile varies between 2 kg to 4 kg.

7.4 The Mechanisms of Scabbing and Perforation Damage Caused by the Missile Impact

The mechanism of scabbing and perforation damage may be described in the following way.

- i) For scabbing, similar damage was observed for all the slabs tested at the critical scabbing velocity. On impact, a compressive dilatational wave starts propagating into the slab. The compressive wave travels

in the slab at the speed of sound and if it encounters a free surface the wave will be reflected as a tensile wave causing scabbing of the back face of the slab (45) over a certain diameter. An average value of 200mm for all the series was observed. Whether this wave causes scabbing of the material depends upon the concrete tensile strength of the impacted slab and the loading generated on the slab because of this impact. The concrete situated between the back face and the nearest layer of steel reinforcement is reduced to small pieces and is ejected at a velocity which can be measured. The tests also show the missile penetration to be equal to a depth of 9.0 ± 1.0 mm.

- ii) For perforation, the missile velocity is higher than the scabbing velocity. The missile will penetrate the slab beyond the depth which causes scabbing at higher velocities, forming a cylindrical penetration hole with a diameter only slightly greater than the missile diameter. Further increase in velocity produces cracking of the concrete on the back face followed by ejection of concrete from this face. With increasing missile velocity, perforation of the slab will occur as the penetration hole extends through the slab thickness. A higher velocity will cause the missile to exit from the back face of the slab when the missile passes completely through the slab. In this case a neat round hole is observed where the nose of the missile struck.

The associated velocity is known as the perforation velocity. The front and rear reinforcement mesh is deformed and in some parts broken at the place of impact. It can be seen that the concrete is shattered into a conical plug shape.

Similar damage was evident for plain concrete specimen.

7.5 Comments on the Transient Displacement and Reaction Load Measurements

The measured transient displacement of the target shown in fig. (5.2) and fig. (5.4) confirm that the reduced circular area formed within the square target provided appropriate boundary conditions allowing symmetrical bending. The measurements also confirm that although missile perforation or penetration is a local phenomenon, some bending of the impacted structure around the impact zone should be allowed (32).

The transient displacement of the target at the critical perforation velocity shown in fig(5.2) confirms that:

- i- From the 0% reinforcement specimen (fig 5.2k), it can be seen that very low imposed energy occurs, thus the reinforcement, even at low percentage (fig 5.2a) is an essential agent in penetration resistance. The relatively small displacements are associated with the lack of ductility in the panel.
- ii- For the over-reinforced case (fig 5.2h) the initial recovery is very slow, corresponding with less level of reinforcement.

iii- The compressive strength of the concrete appears to have considerable influence on the pattern of recovery. This can be observed when a comparison between the fig(5.2b), fig(5.2g) and fig(5.2j) is made. With the low strength of concrete, the initial (start) recover point is well defined and followed by a brief period of rapid recovery turning into a recovery at a slower rate. This observation can be explained in the contribution of the steel reinforcement to the recovery process. The recovery in the concrete once the shape is largely recovered is at a much slower rate than that of the steel. With more balanced slabs, in terms of concrete strength and reinforcement, the phenomena do not appear to the same degree.

The transient displacement of the target at the critical scabbing velocity shown in fig(5.4) confirms that:

- i- The initial recovery according to the 205mm position transducer is extended in the case of the under-reinforcement slab (fig 5.4a).
- ii- The recovery in the case of the most over-reinforcement slab (fig 5.4h) is distinctly different for the general observation, in that the starting point of recovery is clearly defined.
- iii- The thicker slab has deformation over a wide area considering the 270mm position transducer and generally a faster rate of initial recover part the start point of recovery (fig (5.4f), fig (5.4d) and fig (5.4g))

iv- The total recovery time generally appears to be related to the total imposed kinetic energy, higher values having longer recovery periods. This could be explained by the assumption that there is a common strain energy disruption rate for the materials.

The equal distribution of reaction loads also demonstrates the symmetric nature of the experimental arrangement. Some of the results of the measurement of the variation of transient reaction load with time have been plotted in Chapter 5. It can be seen from these plots that the variation with time of the reaction load varies with the amount of specimen reinforcement and concrete compressive strength. From fig(5.1) and fig(5.3) the following conclusions have been drawn:

- i- An increase in the value of the maximum reaction load of the target at the critical perforation or scabbing velocities for increasing amounts of reinforcement at almost constant concrete compressive strength. This increase in the value is very clear when a comparison between the test results of the series S1 and S2 and between the series S8, S9 and S10 is made.
- ii- An increase in the value of the maximum reaction load of the target if the concrete compressive strength increased and the amount of reinforcement was constant. This result can be observed when a comparison between the test results of the series S2, S3, S4, S5 and S10 is made.

Table (6.1): Results for perforation resistance tests

Series No	Maximum reaction load (kN)	Total percentage of reinforcement	Concrete compressive strength f'_c (cube) (N/mm ²)
S1	35.35	1.0%	56.53
S2	104.70	2.5%	56.00
S9	73.20	2.0%	45.46
S10	81.94	2.5%	46.63
S8	99.03	3.1%	48.50
S2	104.70	2.5%	56.00
S3	104.60	2.5%	54.40
S4	106.09	2.5%	52.93
S5	102.61	2.5%	52.36
S10	81.94	2.5%	46.63

Table (6.2): Results for scabbing resistance tests

Series No	Maximum reaction load (kN)	Total percentage of reinforcement	Concrete compressive strength f'_c (cube) (N/mm ²)
S1	83.35	1.0%	57.56
S2	133.77	2.5%	55.50
S9	84.63	2.0%	48.20
S10	86.51	2.5%	50.23
S8	80.83	3.1%	46.10
S2	133.77	2.5%	55.50
S3	122.75	2.5%	54.53
S4	113.65	2.5%	54.80
S5	98.40	2.5%	53.26
S10	86.51	2.5%	50.23

CHAPTER EIGHT

CONCLUSIONS AND RECOMMENDATIONS FOR FUTURE WORK

A number of formulae which have been developed from experimental studies of impact phenomena are in use for assessing the impact performance of reinforced concrete targets. These formulae, however, do not take account of the amount of flexural reinforcement.

In the work reported in this thesis a series of experiments have been undertaken to investigate the effects of variations in the amount of flexural reinforcement in a concrete slab upon the critical perforation and the critical scabbing velocities. The influence of the maximum size of aggregate used in the concrete on the value of these velocities has been considered.

During the course of the experimental work, new empirical relationships have been proposed to determine the critical perforation and the critical scabbing velocity of hard missile impact upon reinforced concrete model slabs.

Some of the most appropriate of the existing perforation and scabbing formulae have been modified to account for the amount of flexural reinforcement.

This chapter presents the conclusions of the current work and discusses the limitations of the proposed formulae. Finally, recommendations for future work are proposed.

8.1 Conclusions

From the experimental programme carried out on reinforced concrete model slabs subjected to high velocity impact, the

following formulae have been developed:

The proposed perforation formula

$$d_p = 3.628 \times 10^{32} \frac{M^{0.456}}{(f'_c)^{0.5}} \cdot \frac{V_{cp}^{0.909}}{D^{45.5}} \quad \text{and}$$

The proposed scabbing formula

$$d_s = 6.13 \times 10^{44} \frac{M^{0.457}}{(f'_c)^{0.5}} \cdot \frac{V_{cs}^{0.877}}{D^{62.67}}$$

From these formula it is possible to calculate the critical perforation and scabbing velocities for a given range of experimental conditions.

The following two conclusions may be drawn from the application of these equations.

- i) The proposed perforation formula, which has been developed as a direct result of the experimental work incorporates the factor,

$$0.455 \left(1.2 + \frac{r}{408} \right)$$

to account for the amount of flexural reinforcement

where r is the flexural reinforcement ratio kg/m^3 .

The inclusion of this factor provides results which are in close agreement with the experimental values.

- ii) The proposed scabbing formula with the factor,

$$0.5 \left(1 + \frac{r}{370} \right)$$

predicted results which agree very closely with

the measured values.

Other significant conclusions follow:

- iii) The test results show the dependence of the critical perforation velocity upon the quantity of flexural reinforcement. There would appear to be no significant influence, however, of the maximum aggregate size upon this velocity.
- iv) By comparing the experimental results with the predictions of critical perforation velocity using existing empirical formulae enables a modification factor accounting for the amount of flexural reinforcement to be obtained. This has been done for the most appropriate formulae thus enabling a favourable comparison with experimental results. The modification factors may be summarised as follows.

	<u>modification factor</u>
Petry 1 formula	$0.58(0.724 + \frac{r}{444})$
"CED-EDF" formula	$0.4(1.5 + \frac{r}{338})$
Chang formula	$0.57(0.75 + \frac{r}{350})$
Halдар & Miller formula	$0.577(0.733 + \frac{r}{370})$
Adeli & Amin formula	$0.6(\frac{2}{3} + \frac{r}{400})$

- v) The test results show that the scabbing resistance depends upon the quantity of flexural reinforcement. Also, the maximum aggregate size used in the concrete is a factor influencing the critical scabbing velocity. The extent of the influence of aggregate size upon the critical scabbing velocity was not thoroughly investigated.

vi) By comparing the experimental results with the predictions of critical scabbing velocity using existing empirical formulae enables a modification factor accounting for the amount of flexural reinforcement to be obtained. This has been done for the most appropriate formulae thus enabling a favourable comparison with experimental results. The modification factors may be summarised as follows.

	<u>modification factor</u>
Chang formula	$0.2(4 + \frac{r}{186})$
Halдар & Miller formula	$0.427(1.34 + \frac{r}{570})$

vii) The proposed perforation and scabbing formulae have been developed as a direct result of the experimental work. The work which has examined a finite range of parameters. The application of these two formulae, therefore, has only validity within the range of the test parameters. Extrapolation outside this range is likely to predict inadequate results. Section 7.3 discusses the parametric limitation of the applications of the proposed perforation and scabbing formulae.

8.2 Recommendations for Future Work

The following recommendations are made for future work.

- i) Further tests outside the range of parameters reported in this thesis should enable the range of validity of the proposed perforation and scabbing formulae to be extended. In particular, the effect of varying the missile diameter should be investigated.
- ii) Since the maximum aggregate size used in the concrete is a factor influencing the critical scabbing velocity, some more tests should be carried out using a wide range of maximum aggregate size to investigate this influence thoroughly.
- iii) A test programme may be developed to study the effects of other parameter that influence the local damage in the target structural element, such as:
 - The geometry of the target.
 - The span/depth ratio of the target.
 - The hardness of the missile impacted upon the target.
 - The effect of the type of target support.
 - The inclination of the missile on the target
 - The inclusion of shear reinforcement and its variation in a concrete target and
 - Arrangement of reinforcement within the target.
- iv) The bulk of the hard missiles tested have been flat faced cylinders. The effects of both nose shape and cross-section, therefore, deserves investigation.
- v) All the targets used in experiments up to the present time have been flat and the performance of cylindrical

and domed reinforced concrete targets has yet to be investigated.

- vi) A series of experiments could be carried out on steel-concrete composite targets to quantify the effects of steel plate cladding on the perforation resistance. The steel plates might be attached to either the impacted or back face, or to both faces.

REFERENCE

1. Eibl, J.
"Behaviour of critical regions under missile impact".
Interassociation Symposium - Concrete Structures
Under Impact and Impulsive Loading - Introductory
Report, Berlin (West), June 2-4, 1982, pp.(113-128).

2. Haldar, A. and Miller, F.J.
"Penetration depth in concrete for non-deformable
missile". Nuclear Engineering and Design, vol. 71,
1982, pp.(79-88).

3. Haldar, A., Hatami, M. and Miller, F.J.
"Concrete structures penetration depth estimation".
ASCE, Structural Division, vol. 109, No.1, January
1983, pp.(245-250).

4. Kennedy, R.P.
"A review of procedures for analysis and design of
concrete structures to resist missile impact effects".
Nuclear Engineering and Design, vol. 37, 1976,
pp.(183-203).

5. Adeli, H. and Amin, A.M.
"Local effects of impactors on concrete structures".
Nuclear Engineering and Design, vol. 88, 1985,
pp.(301-317).

6. National Defence Research Committee
"Effects of Impact and Explosion"
Summary Technical Report of Division 2, Vol. 1,
Washington, D.C., 1946.

7. Slitter, G.E.
"Assessment of empirical concrete impact formulas".
ASCE Structural Division, vol. 106, No. ST5, May 1980,
pp.(1023-1045).

8. Chelapati, C.V., Kennedy, R.P. and Wall, I.B.
"Probabilistic assessment of aircraft hazard for
nuclear power plants". Nuclear Engineering and
Design, vol. 19, 1972, pp.(333-364).

9. Rotz, J.V.
"Results of missile impact tests on reinforced
concrete panels". Second ASCE, Speciality Conference
on Structural Desing of Nuclear Plant Facilities,
vol. 1, New Orleans, Louisiana, December 1975,
pp.(720-730).

10. "Structural analysis and design of nuclear plant
facilities". ASCE - Manuals and Reports on
Engineering Practice, No. 58, 1980.

11. Gueraud, R., Sokolovsky, A., Kavyrchine, M. and Astruc, M.
"Study of the perforation of reinforced concrete slabs by rigid missiles", Part 1.
Nuclear Engineering and Design, vol. 41, 1977,
pp.(91-102).
12. Fiquet, G. and Dacquet, S.
"Study of the perforation of reinforced concrete slabs by rigid missiles", Part 2.
Nuclear Engineering and Design, vol. 41, 1977,
pp.(103-120).
13. Goidstein, S. and Berriaud, C.
"Study of the perforation of reinforced concrete slabs by rigid missiles", Part 3.
Nuclear Engineering and Design, vol. 4, 1972,
pp.(121-128).
14. Berriaud, C., Verpeaux, P., Jumet, P., Avet-FlanCARD,
R. and Perrot, J.
"Concrete wall perforation by rigid missile".
Interassociation Symposium-Concrete Structures
Under Impact and Impulsive Loading - Proceedings,
Berlin (West), June 2-4, 1982, pp.(358-367).

15. Kar, A.K.
"Design for tornado - generated missiles and aircraft impact".
American Nuclear Society, Thermal - Reactor Safety Meeting Idaho, Sunvall, July 31 - August 5, 1977, pp.(451-466).
16. Kar, A.K.
"Local effects of tornado - generated missiles".
ASCE, Structural Division, vol. 104, ST5, May 1978, pp.(809-816).
17. Kar, A.K.
"Impact load for tornado - generated missiles".
Nuclear Engineering and Design, vol. 47, 1978, pp.(107-114).
18. Kar, A.K.
"Impactive effects of tornado missiles and aircraft".
ASCE, Structural Division, vol. 105, No. ST11, November 1979, pp.(2243-2260).
19. Kar, A.K.
"Loading time history for tornado - generated missiles".
Nuclear Engineering and Design, vol. 51, 1979, pp.(487-493).

20. Kar, A.K.
"Projectile penetration into buried structures".
ASCE, Structural Division, vol. 104, No. ST1,
January 1978, pp.(125-139).
21. Burdette, E.G.
"Projectile penetration into buried structures".
ASCE, Structural Division, vol. 105, No. ST2,
February 1979, pp.(454-457).
22. Berriaud, C.
"Local behaviour of reinforced concrete walls under
missile impact".
4th International Conference on Structural Mechanics
in Reactor Technology (SMIRT), San Francisco,
California, August 1977, Paper J. 7/9.
23. Kavyrehine, M. and Astruc, M.
"Study on the perforation of reinforced concrete slabs
by rigid missiles".
International Seminar on Extreme Load Conditions and
Limit Analysis Procedure for Structural Reactor
Safeguards and Containment Structures (ELCALAP),
Berlin, Germany, September 1975, Paper S 2/4.
24. Deyen, P.
"Perforation of reinforced concrete slabs by rigid
missiles".
ASCE, Structural Division, vol. 106, No. ST7, July
1980, pp.(1623-1642).

25. Chang, W.S.
"Impact of solid missiles on concrete barriers".
ASCE, Structural Division, vol. 107, No. ST2,
February 1981, pp.(257-271).

26. Haldar, A.
"Impact of solid missiles on concrete barriers".
ASCE, Structural Division, vol. 107, No. ST11,
November 1981, pp.(2307-2309).

27. Haldar, A. and Miller, J.
"Local effects evaluation of concrete structures".
Interassociation Symposium - Concrete Structure
Under Impact and Impulsive Loading - Proceeding,
Berlin (West), June 2-4, 1982, pp.(345-357).

28. Haldar, A. and Hamieh, H.A.
"Local effect of solid missiles on concrete
structures".
ASCE, Structural Division, vol. 110, No. ST5,
May 1984, pp.(948-960).

29. Hughes, G.
"Hard missile impact on reinforced concrete".
Nuclear Engineering and Design, vol. 77, 1984,
pp.(23-35).

30. Williams, A.
"The bearing capacity of concrete over a limited area".
Technical Report No. 526, Cement and Concrete Association, London, U.K., August 1979.
31. Barr, P., Carter, P.G., Howe, W.D. and Neilson, A.J.
"An experimental investigation of the effects of reinforcement quantity and geometry on the perforation resistance of concrete panels to impacts by rigid missiles.
Contributions from Atomic Energy Establishment - Winfrith to the 6th (SMIRT) Conference 1981, AEEW-M 1866, pp.(68-81).
32. Barr, P., Carter, P.G., Howe, W.D. and Neilson, A.J.
"Replica scaling studies of hard missile impacts on reinforced concrete".
Interassociation Symposium - Concrete Structures Under Impact and Impulsive Loading - Proceedings, Berlin (West), June 2-4, 1982, pp.(329-344).
33. Reinhardt, H.W.
"Testing and monitoring techniques for impact and impulse loading of concrete structures".
Interassociation Symposium - Concrete Structures Under Impact and Impulsive Loading - Introductory Report, Berlin (West), June 2-4, 1982, pp.(65-87).

34. Davies, I.
"Damaging effects from the impact of missiles against reinforced concrete structures".
Nuclear Energy, vol. 19, No.3, June 1980,
pp.(199-205).
35. Skov, K. and Olesens, S.O.
"Impact resistance of reinforced and prestressed concrete members"
State of the art Report, RILEM, Technical Committee 21-11, vol. 8, No.44, 1975, pp. 116-125.
36. B.S. 5242 Part 1: 1987
"Tubes for fluid power cylinder barrels"
British Standards Institution.
37. B.S. 18: 1987
"Tensile testing of metals"
British Standards Institution.
38. B.S. 12: 1978
"Ordinary and rapid-hardening Portland Cement"
British Standards Institution.
39. B.S. 410: 1986
"Test sieves"
British Standards Institution.

40. B.S. 882: 1983
"Aggregates from natural sources for concrete"
British Standards Institution.

41. B.S. 1881 Part 120: 1983
"Testing Concrete"
British Standards Institution.

42. B.S. 1881 Part 116: 1983
"Testing concrete"
British Standards Institution.

43. B.S. 1881 Part 117: 1983
"Testing Concrete"
British Standards Institution.

44. Minitab Project
The Pennsylvania State University.
U.S.A., Nov. 1982.

45. Johnson, W.
"Impact strength of materials"
Edward Arnold, London, 1972.

APPENDIX A

Calculation of The Critical Perforation Velocity of The missile Using The Existing Empirical Formulae Described in Section 2.3.

The calculation uses the experimental data obtained during the S2 series. The following data is relevant

S2 has 390 kg/m^3 of flexural reinforcement and 4mm max. agg. size

d_p	= slab thickness	= 100 mm	= 3.937 in
W	= wt. of missile	= 3.689 kg	= 8.1328 lb
D	= dim. of missile	= 49.72 mm	= 1.957 in
V_{cp}	= critical perforation velocity (test)	= 82.56 m/sec.	= 270.8 ft/sec.
f'_c	= concrete compressive strength (cylinder)	= 44.8 N/mm ²	= 6496 psi
f_r	= concrete tensile strength	= $7.5\sqrt{f'_c}$	= 4.1688 N/mm ² = 604.48 psi
ρ	= density of concrete	= 2257 kg/m ³	

1. Modified Petry Formula

$$d_p = 2 X_p$$

$$= 24 \cdot k_p \cdot A_p \log_{10} \left(1 + \frac{V^2}{215000} \right)$$

where

$$k_p = 0.00284 \quad \text{for special reinforcement}$$

$$A_p = \frac{W}{\text{area of missile}} = 389.34 \text{ lb/ft}^2$$

$$3.937 = 24 (0.00284) 389.34 \log\left(1 + \frac{V^2}{215000}\right)$$

$$\therefore V_{cp} = 259.58 \text{ ft/sec.}$$

$$79.14 \text{ m/sec.}$$

2. Army Corps of Engineers Formula

$$\frac{d_p}{D} = 1.32 + 1.24 \frac{X_p}{D} \quad 1.35 \leq \frac{X_p}{D} \leq 13.5$$

$$\frac{3.937}{1.957} = 1.32 + 1.24 \frac{X_p}{D}$$

$$\frac{X_p}{D} = 0.5578$$

$$\frac{X_p}{D} = \frac{282}{D^{2.785}} \frac{W}{f_c^{0.5}} \frac{V^{1.5}}{1000^{1.5}} + 0.5$$

$$0.5578 = \frac{282 (8.1328) V^{1.5}}{(1.957)^{2.785} (6496)^{0.5} (1000)^{1.5}} + 0.5$$

$$V^{1.5} = 416.71$$

$$V_{cp} = 55.79 \text{ ft/sec.}$$

$$= 17 \text{ m/sec.}$$

3. Modified National Research Committee Formula

$$\frac{d_p}{D} = 3.19 \left(\frac{X_p}{D}\right) - 0.718 \left(\frac{X_p}{D}\right)^2 \quad \frac{X_p}{D} \leq 1.35$$

$$\frac{3.937}{1.957} = 3.19 h - 0.718 h^2 \quad h = \frac{X_p}{D}$$

$$h^2 - 4.4429 h + 2.8 = 0$$

$$h = \frac{-B \pm \sqrt{B^2 - 4AC}}{2A}$$

$$\therefore h = 0.76 \quad \text{or} \quad h = 3.68$$

$$\text{use } h = 0.76 \quad h \leq 1.35$$

$$h = \frac{X_p}{D} = \left(\frac{4 k k_1 W V^{1.8}}{D(1000D)^{1.8}} \right)^{0.5}$$

$$\text{where } k = 0.72 \quad \text{and} \quad k_1 = \frac{180}{\sqrt{f_c'}} = 2.2333$$

$$(0.76)^2 = \frac{4 (0.72) (2.2333) 8.1328}{1.957 (1000 \times 1.957)^{1.8}} V^{1.8}$$

$$V^{1.8} = 18176.148$$

$$V_{cp} = 232.48 \text{ ft/sec.}$$

$$= 70.88 \text{ m/sec.}$$

4. The Ballistic Research Laboratory Formula

$$\frac{d_p}{D} = \frac{427 W V^{1.33}}{D^{2.8} (f_c')^{0.5} (1000)^{1.33}}$$

$$\frac{3.937}{1.957} = \frac{427 (8.1328) V^{1.33}}{(1.957)^{2.8} (6496)^{0.5} (1000)^{1.33}}$$

$$V^{1.33} = 2990.08$$

$$V_{cp} = 410.48 \text{ ft/sec.}$$

$$= 125.14 \text{ m/sec.}$$

5. Commissariata a L'Energie Atomique Electricite de France

$$V = 1.3 (\sigma_c)^{0.5} \rho^{0.16666} \left(\frac{D \cdot d_p^2}{M} \right)^{0.6666}$$

$$= 1.3 (44.8 \times 10^6)^{0.5} (2257)^{0.16666} \left(\frac{(0.04972)(0.1)^2}{3.689} \right)^{0.6666}$$

$$V_{cp} = 82.84 \text{ m/sec.}$$

6. Kar Formula

$$\frac{d_p - a}{D} = 3.19 \frac{X_p}{D} - 0.718 \left(\frac{X_p}{D} \right)^2 \quad \frac{X_p}{D} \leq 1.35$$

$$\frac{3.937 - 0.078}{1.957} = 3.19 \frac{X_p}{D} - 0.718 \left(\frac{X_p}{D} \right)^2$$

$$h^2 - 4.4429h + 2.746 = 0 \quad h = \frac{X_p}{D}$$

$$h = 0.742 \text{ or } h = 3.7$$

$$\text{use } h = 0.742 = \frac{X_p}{D}$$

$$\frac{X_p}{D} = \left[\frac{4 k k_1}{D} \left(\frac{E}{E_m} \right)^{1.25} \frac{W V^{1.8}}{(1000D)^{1.8}} \right]^{0.5} \quad \frac{X_p}{D} \leq 2$$

$$\text{where } k = 0.72, k_1 = 2.2333 \text{ and } \left(\frac{E}{E_m} \right)^{1.25} = 0.9367$$

$$(0.742)^2 = \frac{4(0.72)(2.2333)}{1.957} (0.9367) \frac{8.1328 V^{1.8}}{(1000 \times 1.957)^{1.8}}$$

$$V^{1.8} = 18496.17$$

$$V_{cp} = 234.74 \text{ ft/sec.}$$

$$= 71.56 \text{ m/sec.}$$

7. Degen Formula

$$\frac{d_p}{D} = 2.2 \frac{X_p}{D} - 0.3 \left(\frac{X_p}{D}\right)^2 \quad \frac{X_p}{D} \leq 1.52$$

$$\frac{3.937}{1.957} = 2.2h - 0.3h^2 \quad h = \frac{X_p}{D}$$

$$h^2 - 7.333h - 6.7058 = 0$$

$$h = 1.07 \quad \text{or} \quad 6.26$$

uses $h = 1.07 = \frac{X_p}{D}$

$$\frac{X_p}{D} = \left(\frac{4 k k_1 W V^{1.8}}{D(1000D)^{1.8}} \right)^{0.5} \quad \frac{X_p}{D} \leq 2.0$$

$$(1.07)^2 = \frac{4(0.72)(2.2333)(8.1328)}{1.957(1000 \times 1.957)^{1.8}} V^{1.8}$$

$$V^{1.8} = 36028.17$$

$$V_{cp} = 340 \text{ ft/sec.}$$

$$= 103.65 \text{ m/sec.}$$

8. Chang Formula

$$d_p = \left(\frac{200}{V}\right)^{0.25} \left(\frac{MV^2}{D f_c}\right)^{0.5}$$

$$3.937 = \left(\frac{200}{V}\right)^{0.25} \left(\frac{(12)(8.1328)V^2}{(32.2)(1.957)(6496)}\right)^{0.5}$$

$$V_{cp} = 277.5 \text{ ft/sec.}$$

$$= 84.6 \text{ m/sec.}$$

9. Halder & Miller Formula

$$\frac{d_p}{D} = 3.19 \left(\frac{X_p}{D}\right) - 0.718 \left(\frac{X_p}{D}\right)^2$$

$$\frac{X_p}{D} \leq 1.35$$

$$\frac{3.937}{1.957} = 3.19h - 0.718h^2$$

$$h = \frac{X_p}{D}$$

$$h^2 - 4.4429h + 2.8 = 0$$

$$h = 0.76 \quad \text{or} \quad 3.68$$

use $h = 0.76 = \frac{X_p}{D}$

$$\frac{X_p}{D} = -0.0308 + 0.2251 I$$

$$0.3 \leq I \leq 4.0$$

$$I = 3.513$$

$$I = \frac{12 \times 0.72}{32.2} \cdot \frac{W V^2}{D^3 f_c'}$$

$$3.513 = \frac{12 \times 0.72}{32.2} \cdot \frac{8.1328 V^2}{(1.957)^3 (6496)}$$

$$V_{cp} = 279.96 \text{ ft/sec.}$$

$$= 85.35 \text{ m/sec.}$$

10. Hughes Formula

$$\frac{d_p}{D} = 3.6 \frac{X_p}{D}$$

$$\frac{d}{D} = 3.5$$

$$\frac{3.937}{1.957} = 3.6 \frac{X_p}{D}$$

$$\therefore \frac{X_p}{D} = 0.55882$$

$$\frac{X_p}{D} = 0.19 k' I'/S$$

$$= 0.19 k' \frac{MV^2}{fr.D^3} \cdot \frac{1}{1 + 12.3 \ln \left(1 + 0.03 \frac{MV^2}{fr.D^3} \right)}$$

$$0.55882 = (0.19)(1) \frac{(8.1328)12 V^2}{(32.2)(604.48)(1.957)^3} \cdot$$

$$\frac{1}{1 + 12.3 \ln \left(1 + \frac{0.03 (8.1328)12 V^2}{(32.2)(604.48)(1.957)^3} \right)}$$

$$4396.5 = V^2 \frac{1}{1 + 12.3 \ln \left(1 + 2.00693 \times 10^{-5} V^2 \right)}$$

$$V_{cp} = 172.2 \text{ ft/sec.}$$

$$= 52.5 \text{ m/sec.}$$

11. Adeli & Amin Formula

$$\frac{d_p}{D} = 0.906 + 0.3214 I - 0.0106 I^2$$

$$\frac{3.937}{1.957} = 0.906 + 0.3214 I - 0.0106 I^2$$

$$I^2 - 30.32 I + 104.31 = 0$$

$$I = 3.46 \text{ or } I = 26.36$$

use $I = 3.96$

$$I = \frac{k W V^2}{g D^3 f_c'}$$

$$3.96 = \frac{(0.72) (8.1328) 12 V^2}{(32.2) (1.957)^3 (6496)}$$

$$V_{cp} = 297.24 \text{ ft/sec.}$$

$$= 90.62 \text{ m/sec.}$$

APPENDIX B

Calculation of The Critical Scabbing Velocity of The Missile using The Existing Empirical Formulae described in section 2.3.

The calculation uses the experimental data obtained during the S5 series. The following data is relevant.

S5 has 390 kg/m³ of flexural reinforcement and 4 mm max. agg. size.

d _s = slab thickness	= 100 mm	= 3.937 in
W = wt. of missile	= 2.21 kg	= 4.872 lb
D = dim. of missile	= 49.68 mm	= 1.956 in
V _{CS} = critical scabbing velocity (test)	= 58.2 m/sec.	= 190.9 ft/sec.
f _c ' = concrete compressive strength (cylinder)	= 42.6 N/mm ²	= 6178.16 psi
f _r = concrete tensile strength	= 7.5 √f _c '	= 4.065 N/mm ² = 589.51 psi

1. Modified Petry Formula

$$d_s = 2.2 X_p$$

$$= 2.2 (12) k_p A_p \log \left(1 + \frac{V^2}{215000} \right)$$

where

$$k_p = 0.00284 \quad \text{for special reinforcement}$$

and

$$A_p = \frac{W}{\text{area}} = \frac{4.872}{\text{area}} = 233.475 \text{ lb/ft}^2$$

$$3.937 = 2.2 (12) (0.00284) (233.475) \log \left(1 + \frac{V^2}{215000} \right)$$

$$\therefore V_{CS} = 381.82 \text{ ft/sec.}$$

$$= 116.4 \text{ m/sec.}$$

2. Modified National Research Committee Formula

$$\frac{d_s}{D} = 7.91 \left(\frac{X_p}{D} \right) - 5.06 \left(\frac{X_p}{D} \right)^2$$

$$\frac{X_p}{D} \leq 0.65$$

$$\frac{d_s}{D} \leq 3$$

$$\frac{3.937}{1.956} = 7.91 h - 5.06 h^2$$

$$h = \frac{X_p}{D}$$

$$\therefore h^2 - 1.5632 h + 0.3977 = 0$$

$$h = \frac{-B \mp \sqrt{B^2 - 4AC}}{2A}$$

where

$$A = 1 \quad B = -1.5632 \quad \text{and} \quad C = 0.3977$$

$$\therefore h = 0.3199 \quad \text{or} \quad h = 1.2433$$

use $h = 0.3199$

$$\frac{X_p}{D} = \left[\frac{4 k k_1 W V^{1.8}}{D(1000D)^{1.8}} \right]^{0.5}$$

$$\frac{X_p}{D} \leq 2.0$$

where

$$k = 0.72 \quad \text{and} \quad k_1 = \frac{180}{\sqrt{f_c}} = 2.29$$

$$(0.3199)^2 = \frac{4 (0.72) (2.29) 4.872}{1.956 (1000 \times 1.956)^{1.8}} V^{1.8}$$

$$\therefore V_{CS} = 116.43 \text{ ft/sec.}$$

$$= 35.5 \text{ m/sec.}$$

3. The Ballistic Research Laboratory Formula

$$d_s = 2 d_p$$

$$= (2) \frac{427 W D V^{1.33}}{D^{2.8} f_c^{0.5} (1000)^{1.33}}$$

$$3.937 = \frac{854 (4.872) V^{1.33}}{(1.956)^{1.8} (6178.16)^{0.5} (1000)^{1.33}}$$

$$V_{CS} = 351.38 \text{ ft/sec.}$$

$$= 107.12 \text{ m/sec.}$$

4. Bechtel Corporation Formula

$$d_s = 15.5 \frac{W^{0.4} V^{0.5}}{f_c^{0.5} D^{0.2}}$$

$$3.937 = \frac{15.5 (4.872)^{0.4}}{(6178.16)^{0.5} (1.956)^{0.2}} V^{0.5}$$

$$V_{CS} = 146.86 \text{ ft/sec.}$$

$$= 44.77 \text{ m/sec.}$$

5. Stone & Webster Formula

$$d_s = \left(\frac{W V^2}{C} \right)^{\frac{1}{3}}$$

$$3.937 = \left(\frac{4.872 V^2}{942.3} \right)^{\frac{1}{3}}$$

$$V_{CS} = 108.64 \text{ ft/sec.}$$

$$= 33.12 \text{ m/sec.}$$

6. Kar Formula

$$b \left(\frac{d_s - a}{D} \right) = 7.91 \frac{X_p}{D} - 5.06 \left(\frac{X_p}{D} \right)^2$$

$$\frac{X_p}{D} \leq 0.65$$

$$\frac{a}{D} \leq 3$$

where

$$b = \left(\frac{E}{E_m} \right)^{0.2} = 1.0102 \quad \text{and} \quad a = 4 \text{ mm} = 0.078 \text{ in}$$

$$1.0102 \left(\frac{3.937 - 0.078}{1.956} \right) = 7.91 h - 5.06 h^2 \quad h = \frac{X_p}{D}$$

$$\therefore h^2 - 1.5632 h + 0.3938 = 0$$

$$\therefore h = 0.3157 \quad \text{or} \quad h = 1.2475$$

uses $h = 0.3157$

$$\frac{X_p}{D} = \left[\frac{4 k k_1}{D} \left(\frac{E}{E_m} \right)^{1.25} \frac{W V^{1.8}}{(1000D)^{1.8}} \right]^{0.5}$$

where

$$\left(\frac{E}{E_m} \right)^{1.25} = 0.9384$$

$$(0.3157)^2 = \frac{4 (0.72) (2.29)}{1.956} (0.9384) \frac{(4.872) V^{1.8}}{(1000 \times 1.956)^{1.8}}$$

$$\therefore V_{CS} = 118.86 \text{ ft/sec.}$$

$$= 36.23 \text{ m/sec.}$$

7. Chang Formula

$$d_s = 1.84 \left(\frac{200}{V}\right)^{0.13} \frac{(M V^2)^{0.4}}{D^{0.2} f_c'^{0.4}}$$

$$3.937 = 1.84 \left(\frac{200}{V}\right)^{0.13} \frac{\left(\frac{(4.872)(12)V^2}{32.2}\right)^{0.4}}{(1.956)^{0.2} (6178.16)^{0.4}}$$

$$80.346 = \left(\frac{200}{V}\right)^{0.13} (0.1513 V^2)^{0.4}$$

$$V_{CS} = 142.16 \text{ ft/sec.}$$

$$= 43.34 \text{ m/sec.}$$

8. Halder & Miller Formula

$$\frac{d_s}{D} = 3.3437 + 0.0342 I \quad 21 \leq I \leq 385$$

$$I = \frac{12}{32.2} \cdot \frac{k W V^2}{D^3 f_c'}$$

$$\frac{3.937}{1.956} = 3.3437 + 0.034 I$$

The value of I will be negative, therefore the indirect method to estimate the critical scabbing velocity (28) will be used.

$$\frac{d_s}{D} = 7.91 \left(\frac{x_p}{D}\right) - 5.06 \left(\frac{x_p}{D}\right)^2$$

$$\frac{x_p}{D} \leq 0.65$$

$$\frac{d_s}{D} \leq 3$$

$$\frac{3.937}{1.956} = 7.91 h - 5.06 h^2$$

$$h = \frac{x_p}{D}$$

$$h^2 - 1.5632 h + 0.3977 = 0$$

$$h = 0.3199 \quad \text{or} \quad h = 1.2433$$

uses $h = 0.3199$

$$\frac{x_p}{D} = -0.0308 + 0.2251 I \qquad 0.3 \leq I \leq 4.0$$

$$0.3199 = -0.0308 + 0.2251 I$$

$$I = 1.558$$

$$= \frac{W}{g} \frac{k}{D^3} \frac{V^2}{f_c'}$$

$$1.558 = \frac{12 (4.872)}{32.2} \cdot \frac{0.72}{(1.956)^3} \cdot \frac{1}{6178.16} V^2$$

$$V_{CS} = 234.7 \text{ ft/sec}$$

$$= 71.56 \text{ m/sec.}$$

9. Hughes Formula

$$\frac{d_s}{D} = 5.0 \frac{x_p}{D} \qquad \frac{x_p}{D} < 0.7$$

$$\frac{3.937}{1.956} = 5.0 \frac{x_p}{D}$$

$$\frac{x_p}{D} = 0.40255$$

$$\frac{x_p}{D} = 0.19 k' I'/S$$

$$= 0.19 k' \frac{M \cdot V^2}{fr \cdot D^3} \cdot \frac{1}{1 + 12.3 \ln(1 + 0.03 \frac{M \cdot V^2}{fr \cdot D^3})}$$

$$0.40255 = (0.19) (1) \frac{(4.872) (12) V^2}{(32.2) (589.51) (1.956)}$$

$$\frac{1}{1 + 12.3 \ln(1 + 0.03 \frac{(4.872) (12) V^2}{(32.2) (589.51) (1.986)^3})}$$

$$5147.91 = V^2 \frac{1}{1 + 12.3 \ln(1 + 1.234685 \times 10^{-5} V^2)}$$

$$\therefore V_{CS} = 132.65 \text{ ft/sec.}$$

$$= 40.44 \text{ m/sec.}$$

10. Adeli & Amin Formula

$$\frac{d_s}{D} = 1.8685 + 0.04035 I - 0.0114 I^2 \quad 0.3 \leq I \leq 21$$

$$\frac{3.937}{1.956} = 1.8685 + 0.4035 I - 0.0114 I^2$$

$$I^2 - 35.394 I + 12.656 = 0$$

$$I = 0.3615 \text{ or } I = 35.0325$$

use $I = 0.3615$

$$I = \frac{k W}{g D^3 f_c'} V^2$$

$$0.3615 = \frac{(0.72) (4.872) 12}{(32.2) (1.956)^3 (6178.16)} V^2$$

$$V_{CS} = 113.07 \text{ ft/sec.}$$

$$= 34.47 \text{ m/sec.}$$